Université Aboubekr Belkaïd Tlemcen

جامعة أبو بكر بلقايد

DYNAMIC SOIL-FLUID-STRUCTURE INTERACTION APPLIED FOR CONCRETE DAM

Presented by

Amina Tahar Berrabah

This Thesis was submitted in Partial Fulfillment of the Requirements for the Doctorate Degree in Civil Engineering

Examination committee

Hanachi Nasreddine	Professor	chairman	Tizi Ouzou University Rector
Djafour Mustapha	Professor	Examiner	Tlemcen University
Khelidj Abdelhafid	Professor	Examiner	Nantes University
Zendagui Djawad	Doctor	Examiner	Tlemcen University
Bekkouche Abdelmalek	Professor	Supervisor	Ain Temouchent University center
Belharizi Mohamed	Doctor	Supervisor	CRIL Technology Paris

2012

Acknowledgment

I would like to express my sincere gratitude to my advisors, Professor **Bekkouche.A** and Doctor **Belharizi.M** for their continuous support, guidance and constructive suggestions throughout this research.

I would like to extend my sincere thanks to my advisory committee: Professor **Djafour.M**, Professor **Hanachi.N**, Professor **Khelidj.A** and Doctor **Zendagui.D** for their valuable comments and helpful recommendations.

Dedication

This work is dedicated to:

My dear **parents**

Doctor **Errouane miloud**

And

Zazoua Soufiane

Table of contents

Chapter 8 : Three Dimensional Modal Behaviour of Dam Reservoir Foundation System using ANSYS

Abstract

The construction of new dams as well as the evolution and improvement of existing ones create an important need of developing modern tools and design methods allowing for taking into account realistically and completely the dam-reservoir-foundation system interaction.

The seismic design of concrete dams implies several difficulties to estimate the dam's dynamic stress, the response of the dam-reservoir-foundation system interaction and the assessment of the impact regarding the parameters involved.

The current work examines the effect of foundation representation, reservoir water modeling and Rayleigh's viscous damping on the dynamic response of the dam-reservoir-foundation system. This study is achieved using ANSYS, one of the leading commercial finite elements software worldwide.

Three approaches have been adopted to investigate the dynamic behavior and the interaction phenomenon of the dam-foundation system:
- Dam alone,
- Dam and foundation without consideration of its mass,
- Dam and foundation with its mass taken into account.

The dam-reservoir and foundation-reservoir interfaces have been modeled using the following assumptions:

1- Interface modeling with coupling equations,
2- Interface modeling by contact elements,
3- Interface modeling by added masses.

The third method consists in splitting the water reservoir's mass in a great number of small added masses, using the 'surf' elements available via the ANSYS code library (added masses approach). The calculations take into account the hydrostatic pressure of the water reservoir. The results of all three methods are then compared.

These analyses results have been used to carry on a parametric study. They allowed for understanding the effect of the above mentioned parameters on the dynamic behavior of Brezina's concrete arch dam, located in Elbayadh in Algeria and chosen as a case study in this work.

Key words:
ANSYS code, Interaction foundation-fluid-structure, concrete dam, contact element, coupling equations

Résumé

La construction des nouveaux barrages, l'évolution et l'amélioration des ouvrages déjà existants, nécessitent des outils modernes et méthodes de conception adaptées qui permettent de prendre en compte d'une manière réaliste et exhaustive l'interaction de l'ensemble du système barrage, réservoir d'eau et sol de fondation environnante.

La conception sismique des barrages en béton est associée à des difficultés pour évaluer aussi bien les contraintes dynamiques du barrage, la réponse de l'interaction de l'ensemble de l'ouvrage barrage - réservoir d'eau - fondation ainsi que l'estimation de l'impact des divers paramètres associés.

La présente étude démontre l'influence de la fondation, la modélisation de l'eau et l'amortissement proportionnel visqueux de Rayleigh sur la réponse dynamique de l'ensemble du système barrage - réservoir d'eau - fondation. L'étude est réalisée avec le code industriel américain éléments finis ANSYS.

Trois configurations ont été examinées pour étudier le comportement dynamique et appréhender le phénomène d'interaction fondation - barrage :

-barrage seul,

-barrage avec fondation environnante sans tenir compte de sa masse,

- barrage avec fondation environnante en tenant compte de sa masse.

Les interfaces barrage - réservoir d'eau et fondation - réservoir d'eau ont été modélisées en utilisant les approches suivantes :

1- Modélisation de l'interface par des équations de couplage,
2- Modélisation de l'interface par des éléments de contact,
3- Modélisation par masse ajoutée.

La troisième méthode consiste à répartir la masse du réservoir d'eau sous forme de masse ajoutée en utilisant les éléments ' surf ' disponibles dans la bibliothèque des éléments d'ANSYS (approche des masses ajoutées). La pression hydrostatique du réservoir d'eau est prise en compte dans les calculs. Les résultats des trois méthodes sont comparés.

Les résultats d'analyse ont été utilisés pour mener une étude paramétrique. Ils ont permis de comprendre l'effet des paramètres cités ci-dessus sur le comportement dynamique du barrage voûte de Brézina, situé à El bayadh en Algérie, choisi comme étude pour mener ce travail.

Key words:

Code ANSYS, Interaction fondation-fluide-structure, Barrage en Béton, élément de contact, équations de couplage

ملخص

بناء سدود جديدة وكذلك التطور وتحسين القائم منها خلق حاجة مهمة لتطوير الأدوات الحديثة وأساليب تصميم والسماح للاخد بعين الاعتبارالتفاعل السد- الخزان- قاعدة.

التصميم الزلزالي للسدود الخرسانية يعني عدة صعوبات لتقدير الإجهاد الديناميكي للسد، استجابة لنظام التفاعل سد- الخزانة-أساس وتقييم تأثير مختلف المعايير المرتبطة.

العمل الحالي يدرس تأثيرالقاعدة, تمثيل خزان المياه والتخميد اللزج لرايلي على الاستجابة الديناميكية للنظام سد- خزان-قاعدة.

تمت الدراسة باستخدام برنامج و هو واحدة من أبرز البرمج في جميع أنحاء العالم.

,وقد اعتمدت ثلاثة نهج للتحقيق في السلوك الديناميكي وظاهرة التفاعل بين السد و القاعدة:
- السد وحده،
- السد و القاعدة دون النظر في كتلته،
- السد و القاعدة مع كتلته تؤخذ بعين الاعتبار.

الواجهات سد - خزان الماء و القاعدة- خزان الماء تم تمثيلهم باستخدام الافتراضات التالية
تمثيل الواجهة باستخدام معادلات الاقتران

تمثيل الواجهة باستخدام عناصر الاتصال
تمثيل الواجهة باستخدام الكتل المضافة

الأسلوب الثالث هو توزيع الوزن من خزان للمياه في شكل كتل المضافة باستخدام العنصر

واستخدمت نتائج التحليل لإجراء دراسة حدودية لفهم تأثير المعلمات المذكورة أعلاه على السلوك الديناميكي لسد بريزينا الدى يقع في الجزائر.

:الكلمات الرئيسية

رمز ، التفاعل السد- الخزان- قاعدة، سد بلخرسانة ، عنصر الاتصال،معادلات الاقتران

List of Figures

List of Tables

INTRODUCTION

Introduction

Most civil engineering structures are elements of much larger systems, called the overall system, containing several other system components. When subjected to transient loads, these structures interact with the other components of the overall system such that a continuous transfer of energy is established between them. The effects of interaction on the dynamic behavior of these structures are determined by the mechanical properties of all the components of the overall system, the interaction mechanism and the type of dynamic loading. Dams belong exactly to this category of structures. They interact with the foundation rock and with the reservoir. The kind and intensity of the interaction depends on the physical processes that occur at the interfaces of the dam with the foundation rock and the reservoir (Glauco Feltrin, 1997).

Usually we speak of weak or strong interaction depending on whether the interaction has little or large effects on the behavior of the structure being analyzed. This classification has obvious implications for the modeling. In the case of weak interaction, we may neglect the interaction effects in the analysis without serious consequences for the accuracy. In contrast, strongly interacting structures impose a sophisticated modeling of the interaction effects in order to capture the relevant features of the response. In many cases, say for moderate interaction, simple models may yield very good results. However, their range of application is usually limited (Glauco Feltrin, 1997).

A class of interaction problems requiring special methods for its analysis is that involving overall systems which are much larger in size than the structure itself. Typical examples are foundations resting on rock or soil or dams interacting with the reservoir and the foundation rock. The size of the overall system is so large that its direct modeling, e.g. with finite elements, is virtually impossible because of the tremendous effort needed to compute a solution. In addition, usually engineers are mainly interested on the response of the structure and its close neighborhood so that an accurate modeling is only needed for a small subdomain of the overall system (Glauco Feltrin, 1997).

It is now generally known that the foundation soil significantly affects the dynamic response of gravity dam; (A. Bayraktar et al. 2005). Dam safety during and after an earthquake is an area of current concern. The failure of a dam during an earthquake may be catastrophic in terms of loss of life and financial loss (K. Hatami, 1997). Dam response is then governed by the interplay between the characteristics of the soil, the dam itself and the input motion. Soil-structure interaction (SSI), as this phenomenon has become known, has been of research interest for the past 30 years (D. Pitilakis et al. 2008).

In the literature, *four* different earthquake input mechanisms are used to consider the effect of local soil conditions on the earthquake response of dam – foundation interaction systems (A. Bayraktar et al. 2005): the standard rigid-base model, the massless-foundation model, the deconvolved-base-rock model, and the free-field dam-foundation interface model (P. Leger et al. 1989). In the massless foundation model, absence of mass makes the foundation rock as a spring, i.e., only the flexibility of the foundation rock is taken into account. Theoretically, to take advantage of the dam's geometrical characteristics and loading conditions, most structural analyses performed on the dam-foundation soil system are based on the 2D plane strain assumption.

Concrete dams do not possess high structural damping compared to other civil engineering structures. Due to the effect of the adjacent reservoir, however, there are other sources of damping present in a dam-reservoir-foundation system. The *added damping* due to the radiation of waves in the unbounded upstream direction of the reservoir and due to the absorption of incoming waves at the reservoir bottom may result in significant reduction in the response of a concrete dam under earthquake excitation. In addition to the radiation of refracted waves from the bottom of the reservoir, the foundation of the dam allows for the radiation of energy waves from the vibrating dam to the far field (K. Hatami, 1997). The main energy loss mechanism currently assumed in the analysis of concrete dams is viscous damping (T. O. Florin *et al*. 2010). Equivalent viscous damping constants have been determined experimentally. Shaking tests using low-level excitations have been performed on concrete dams throughout the world, and a damping ratio of 2 to 5 percent of the critical damping have been reported, (K.J. Dreher et al. 1980). However, a damping ratio as high as 10 percent of the critical damping has been measured during higher levels' excitations. Therefore, a damping ratio of 2 to 10 percent appears reasonable for most concrete dams (K.J. Dreher et al. 1980).

It is well known that real modes, which are obtained assuming free natural vibrations without damping, can be used as a modal base in a modal superposition analysis, e.g. a spectrum analysis, where damping is small. However, for structures exhibiting significant viscous damping, for example a damping ratio of 5 percent, real modes might not be appropriate. In this case complex modes should be employed instead.

The analysis of dams is a complex problem due to the dam-reservoir and dam-foundation interaction. In addition to the static water pressure, the dam undergoes dynamic forces from the reservoir when the system is subjected to earthquake ground motion. The magnitude of this additional hydrodynamic force is quite significant and may lead to crack initiation and propagation in the dam even under a moderately strong seismic event (K. Hatami, 1997).

In the literature, three approaches can be used to represent the hydrodynamic effect of the fluid: *added mass* approach, *Lagrangian* approach and *Eulerian* one. For the added mass approach, the dynamic effect of the reservoir is modeled as masses applied at the upstream dam face. However, in the Eulerian approach the displacements are the variables in the structure and the pressures are the variables in the fluid, hence a special purpose computer program is required to obtain the solution of the coupled systems. In the Lagrangian approach the behavior of the fluid and structure is expressed in terms of displacements. For that reason, compatibility and equilibrium are automatically satisfied at the nodes along the interfaces between the fluid and structure. This makes Lagrangian displacement-based fluid finite elements very desirable; they can be readily incorporated into a general purpose computer program for structural analysis, since special interface equations are not required.

One of the important steps in dam-reservoir-fluid interaction study consists in modeling the reservoir–dam and reservoir–foundation interfaces. At the interfaces the normal components of the displacements of the reservoir–dam and reservoir–foundation interfaces have to be continuous (A. Bayraktar et al. 2005). In the literature this condition can be accomplished by using coupling equations at reservoir–dam and reservoir–foundation interfaces. A short and almost axially rigid truss element in the normal direction of the interfaces also represents a solution for this condition (A. Bayraktar et al. 2005).

Another approach is exposed in the present thesis to model the reservoir–dam and reservoir–foundation interfaces, concerning the use of contact elements at the location of these interfaces.

ANSYS is one of the leading commercial finite element programs in the world and can be applied to a large number of applications in engineering. It performs linear and nonlinear analyses; nevertheless it is not specialized for SSI analysis. The first objective of the present work is to focus this finite elements code on the structural dynamic analysis of foundation-fluid-structure interaction problems, whereas the second one is to examine the combined effect of foundation and reservoir water on the seismic response of a concrete gravity dam. The special emphasis of the study concerns the effects of the contact at the dam-foundation interface and the effects of hydrodynamic pressure on the seismic response of concrete dam using different approaches for fluid-structure interaction as well as for the foundation-structure fluid interface.

In order to achieve the above mentioned objectives, a numerical study was conducted using finite elements ANSYS code for “Brezina” concrete gravity arch dam, chosen as a case study.

The first part of the work deals with the foundation-structure interaction problem using a direct method. Dynamic analyses were performed for the dam being object of the study, under three generated records and three foundation modeling assumptions (mass foundation model, massless foundation model and fixed support foundation). In the same axis, a parametric study was performed to view the effect of damping ratio on the modal response of the dam using the damped modal analysis and the undamped one.

The second part consists in incorporating the hydrodynamic effect of reservoir water assuming different levels’ values. A special emphasis was done on modeling the fluid-foundation and also the fluid-dam upstream face interfaces. Two assumptions were adopted to model the interfaces; the coupling equations and the contact elements available in ANSYS finite elements code. An important application takes place in the present work, regarding the modeling of “*added mass approach*” using “*Surf Element*” available in ANSYS library.

This thesis is structured as follows:

Introduction

Chapter 1: Soil Structure Interaction Phenomenon

Chapter 2: Fluid Structure Interaction Phenomenon

Chapter 3: Structural Dynamic Capabilities of ANSYS

Chapter 4: Dam Description, Generation of Data Base, and Inputs

Chapter 5: Dynamic foundation Structure Interaction Study using ANSYS

Chapter 6: Undamped and Damped Modal Response of Dam Foundation Interaction using ANSYS

Chapter 7: Two-Dimensional (2D) Modal and Transient Behavior of Dam Reservoir Foundation System using ANSYS

Chapter 8: Three-Dimensional Modal Behavior of Dam Reservoir Foundation System using ANSYS

General Conclusion

And of course, as in any other work, this thesis finishes by a general conclusion.

CHAPTER 1

Soil Structure Interaction Phenomenon

CHAPTER 1

Soil Structure Interaction Phenomenon

1.1 Introduction to Soil–Structure Interaction Phenomenon

The response of a structure during an earthquake depends on the characteristics of the ground motion, the surrounding soil, and the structure itself. For structures founded on rock or very stiff soils, the foundation motion is essentially that which would exist in the soil at the level of the foundation in the absence of the structure and any excavation; this motion is denoted the *Free field ground motion***.** For soft soils, the foundation motion differs from that in the free field due to the coupling of the soil and structure during the earthquake. This interaction results from the scattering of waves from the foundation and the radiation of energy from the structure due to structural vibrations. Because of these effects, the state of deformation (particle displacements, velocities, and accelerations) in the supporting soil is different from that in the *free field***.** As a result, the dynamic response of a structure supported on soft soil may differ substantially in amplitude and frequency content from the response of an identical structure supported on a very stiff soil or rock (Johnson et all, 2003). Structural response is then governed by the interplay between the characteristics of the soil, the structure and the input motion. Soil structure interaction (SSI), as this phenomenon has become known, has been of research interest for the past 30 years (D. Pitilakis et al, 2008).

Compared with the counterpart fixed-base system, SSI has two basic effects on structural response (D. Pitilakis et al, 2008):

- Firstly, the SSI system has an increased number of degrees of freedom and thus modified dynamic characteristics;
- Secondly, a significant part of the vibration energy of the SSI system may be dissipated either by radiation waves, emanating from the vibrating foundation-structure system back into the soil, or by hysteretic material damping in the soil. The result is that SSI systems have longer natural periods of vibration than their fixed-base counterparts.

Some codes practice for seismic design report that any lengthening of the natural period of vibration will be beneficial for the seismic response of the structure. However, SSI effects can give rise to an increased structural response in certain seismic and soil environments, depending mostly on the design response spectrum at the site.

Moreover, the simplification ignores the fact that a structure experiencing SSI is not subjected to the free-field ground motion. Instead, the input motion depends on the properties of the foundation soil and the dynamic characteristics of the superstructure.

Analysis method for SSI that were developed in the late 1960s and 1970s are still in use today, although much enhanced by latter day advanced in information technology and numerical processing.

Eurocode 8, Part 5 (2008) specifies that the effects of dynamic soil-structure interaction (DSSI) shall be taken into account where P-delta (2^{nd} order) effects are significant, for structures with massive or deep-seatd foundations (such as bridge abutments and gravity

walls, piles, diaphragms and caissons), for slender tall structures and for structures supported on very soft soil, with average shear wave velocity less than 100m/s (Srbulov, 2008).

1.2 Types of Dynamic Soil Structure Interaction

Two types of dynamic soil structure interaction are commonly referred to in the literature:

1.2.1 Kinematic Interaction

It is caused by inability of a foundation to follow ground motion due to greater foundation stiffness in comparison with ground stiffness. In effect, stiff foundation filters high frequency ground motion to an average translational and rotational foundation motion. Average values are smaller than the maximum values and therefore "kinematic" interaction is beneficial except if averaged motion results in significant rotation rocking of a foundation (Srbulov, 2008).

1.2.2 Inertial Interaction

It is caused by the existence of structural and foundation masses. Seismic energy transferred into a structure is dissipated by material damping and radiated back into ground causing superposition of incoming and outgoing ground waves. As a result, the ground motion around a foundation can be attenuated or amplified, depending on variety of factors.

The most important factor in determining the response is the ratio between the fundamental period of a foundation and the fundamental period of adjacent ground in the free field. The ratio of unity indicates resonance condition between foundation and its adjacent ground, which is to be avoided. Considerable research, involving analytical, numerical and experimental modeling, has produced a variety of techniques for the evaluation of the interaction (Srbulov, 2008).

Analyses of inertial interaction effects predict the variations of first-mode period and damping ratio between the actual "flexible-base" case and a fictional "fixed-base" case. The flexible-base modal parameters can be used with a free field response spectrum to evaluate design base shear forces for the structure. The analyses for kinematic interaction predict frequency dependent transfer function amplitudes relating foundation and free field motions Wang Jiachun, 2005).

1.3 Methods of Analysis of Dynamic Soil Structure Interaction Phenomenon

Modeling and analysis of dynamic soil structure interaction during earthquakes have gone through various stages, but always in two distinct directions, that is, the direct method and the substructure method, depending on the modeling method for the soil around the structure. (Wang Jiachun, 2005).

1.3.1 Direct Method (Global Method)

In a direct method, the soil and structure are included within the same model and analyzed in a single step (Wang Jiachun, 2005). It solves the dynamic equation in its matrix form as:

$$\underline{M}\ddot{\underline{U}} + \underline{C}\dot{\underline{U}} + \underline{K}\underline{U} = -\underline{M}\underline{I}\ddot{u}_g \tag{1.1}$$

Where:

$\underline{U}$: Represent the system relative displacements vector with respect to the base,

$\underline{I}$: Influence vector, indicates $\ddot{u}_g$ sollicitation direction,

$\underline{M}, \underline{C}, \underline{K}$: System mass, damping and stiffness matrix respectively.

$\ddot{u}_g$: Horizontal component of ground acceleration.

The solution outline using global method is illustrated in Figure 1.1 and follows the steps below:

First step: The design seismic motion is known at soil surface, in free field;

Second step: The motion is calculated at the bottom model base, which is located at a sufficient depth so that the presence of the structure at the surface will not affect this motion. This step is known as *seismic motion deconvolution*;

Third step: The deconvoluted motion is uniformly imposed at the soil-structure system base and the response is calculated by solving Eq. (1.1).

Because the assumptions of superposition are not required, true nonlinear analyses are possible. However, results from nonlinear analyses can be quite sensitive to poorly defined parameters in the soil constitutive model, and the analyses remain quite expensive from a computational standpoint. Hence, direct SSI analyses are more commonly performed using equivalent linear methods to approximate the effects of soil nonlinearity (Wang Jiachun, 2005).

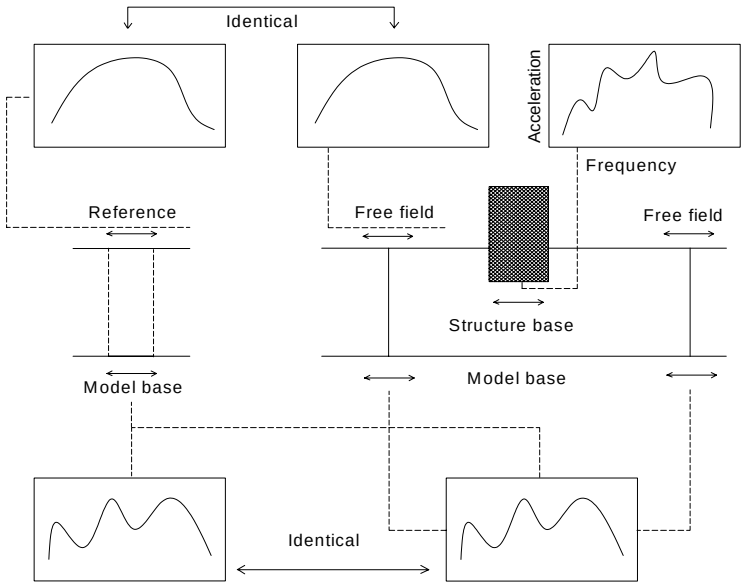

Figure 1.1: Solution outlines using global method.

To activate the SSI within a computer program it is only necessary to identify the foundation mass in order that the loading is not applied to that part of the structure. Most structural analysis computer programs automatically assign seismic loading to all mass degrees of freedom within the computer model and cannot solve the SSI problem. This lack of capability has motivated the development of the massless foundation model which allows the correct seismic forces to be applied to the structure. However, the inertia forces within the foundation material are neglected.

1.3.2 Substructure Method (Multistep Method)

Substructuring techniques is particulary popular. Based on the decomposition of the complete soil foundation structure domain to several subdomains, the solution of the initially complex problem can be very fast and easy to implement. However, methods using

substructuring rely on the principle of superposition and, consequently, are limited to either the linear elastic or the viscoelastic domain (D. Pitilakis et al, 2008).

The envisaged substructures are constituted by the soil on one hand and the structure on the other, as indicated in Figure 1.2. Equilibrium equations are written for each subsystem, and then compatibility conditions at the interface, continuity of displacement, and stress vector are satisfied.

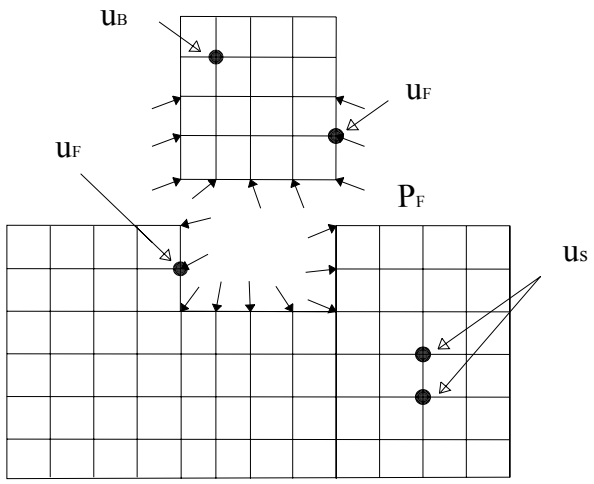

Figure 1.2: Substructure method scheme.

As mentioned earlier, ground motions that are not influenced by the presence of structures are called *free field motions*. When structures are present, the structure interacts with the soil through a process referred to as soil-structure interaction (SSI). SSI has little effect on the response of some systems and a large effect on the response of others. SSI effect is of most significance for stiff and/or heavy structures supported on relatively soft soils. For soft and/or light structures founded on stiff soils, SSI effect is generally small (Kramer, 1996).

1.4 Soil Structure Interaction Modeling

For SSI problems, the dynamic behavior of the foundation-superstructure system can be modeled using either the finite element method (FEM) or equivalent mass-spring dashpots models. The soil, in contrast, can be modeled by the FEM or, utilizing both the theory of integral equations and Green's functions, by the boundary element method (BEM).

1.4.3 Viscoelastic foundation rock model

In this approach, the stiffness and damping characteristics of foundation-structure interaction in a viscoelastic half plane (2-D) or half space (3-D) model are described by the impedance function. Mathematically, an impedance function is a matrix that relates the forces (i.e., shear, thrust, and moment) at the base of the structure to the displacements and rotations of the foundation relative to the free field. The terms in an impedance function are complex and frequency dependent with the real component representing the stiffness and inertia of the foundation and the imaginary component characterizing the radiation and material damping (V. Saouma, 2006).

1.4.2 Massless finite element foundation model

The effects of dam-foundation interaction can most simply be represented by including, in the finite element idealization, foundation rock or soil region above a rigid horizontal boundary. The response to the earthquake excitation applied at the rigid base (bedrock) is then computed by the standard procedures. Such an approach, however, can lead

to enormous foundation models where similar materials extend to large depths and there is no obvious ”rigid” boundary to select as a fixed base. Although the size of foundation model can be reduced by employing viscous or transmitting boundaries to absorb the wave energy radiating away from the dam, such viscous boundaries are not standard features of the general-purpose structural analysis programs.

These difficulties can be overcome by employing a simplified massless foundation model, in which only the flexibility of the foundation rock is considered while its inertia and damping effects are neglected. The size of a massless foundation model need not be very large so long as it provides a reasonable estimate of the flexibility of the foundation rock region. A foundation model that extends one dam height in the upstream, downstream, and downward directions usually suffices in most cases. Unlike the homogeneous viscoelastic half plane model described previously, this approach permits different rock properties to be assigned to different elements, so that the variation of rock characteristics with depth can be considered (ex : foundation mass soil). The massless foundation model also permits the earthquake motions recorded on the ground surface to be applied directly at the fixed boundaries of the foundation model. This is because in the absence of wave propagation, the motions of the fixed boundaries are transmitted to the base of the dam without any changes (V. Saouma, 2006).

It should be pointed out that numerical modeling of dynamic soil structure interaction is still in its course of development. The various current models are no longer restricted only in the time or the frequency domain alone. Techniques used to establish numerical models are not restricted to be finite element method or boundary element method. On the contrary, all these are always incorporated with one and another, and some new analysis techniques have been introduced into the problem, such as a coupling model of finite elements and scaled boundary finite elements, and a coupling model of finite elements, boundary elements, infinite elements and infinite boundary elements (Wang Jiachun, 2005).

1.5 Earthquake Input Mechanisms for SSI Problems

In the literature, *four* different earthquake input mechanisms are used to consider the effect of local soil conditions on the earthquake response of structure – foundation interaction systems (A. Bayraktar et al, 2005):

- ✓ *The standard rigid- base input model*: the earthquake motion applied to the base of the soil layer by foundation rock is an accelerogram that had been recorded previously by a strong motion seismograph located at the soil surface.
- ✓ *The massless-foundation input model*: for this model, the rigid base rock input motions are transmitted instantaneously through the foundation rock to the base of the structure, without any wave propagation effects. These assumptions neglect the interaction effects due to radiation damping of the infinite mass rock and the non-uniform input motions along the foundation base.

It is clear that the motions occurring at the base of soil layer cannot be identical to those recorded at its free surface which means that the two cited models are deficient. Overcoming this deficiency can be done, either by the deconvolution of the free-field surface record which represents the third earthquake input mechanisms (*the deconvolved-base-rock input model*), or by employing a formulation of the analysis procedure that applies the recorded accelerogram as a free –field input which is the forth earthquake input mechanisms (*the free-field structure-foundation interface input model*).

1.6 Material Nonlinearity

With SSI analysis there are two kinds of nonlinearities. The first one which has received most attention from researchers and practicing engineers, and is associated with the nonlinear behavior of the soil. The second is associated with the partial separation (uplift) of the foundation from the soil mass, resulting from the inability of the soil to resist tension. Soil is the most complicated engineering material, especially when considering the effects of seismic and dynamic loading (M. Kutanis et al, 2000).

A number of recent researches have provided insights into the seismic response characteristics of structures. Application of system identification techniques to measure earthquake response data for structures has indicated that structure foundations and the surrounding soil constitute a strongly coupled system. The dynamic behavior of the structure foundations and the surrounding soil has a first order influence on the dynamic response of the structure. Analysis of measured strong motion response data has also indicated that local nonlinear behavior of soil can result in significant nonlinear global behavior of the entire system, even when the structure remains linear. However, the different boundary assumption may lead to erroneous results, and the different codes result in different analysis results (Wang Jiachun, 2005).

For seismic analysis of such high arch dams to resist strong earthquakes, it is necessary to consider some important factors: (1) complete interaction effects between the dam and the rock foundation; (2) nonlinearities of the dam with contraction joint opening during the extreme ground motions (Z. Chuhan et al, 1998). Some state of the art procedures dealing with seismic analysis of arch dams assume a truncated massless rock foundation and apply the design earthquake input at the rigid base beneath the truncated rock foundation. These assumptions neglect the interaction effects due to radiation damping of the infinite mass rock and the non-uniform input motions along the canyon. With regard to the nonlinear behaviour of arch dams, the most important nonlinearity is initiated by the contraction joint opening during strong ground motions. This phenomenon often occurs in the upper portion of a dam where the largest tensile stresses up to 5-6 Mpa are expected to occur in the arch direction for moderately strong earthquake motion (Z. Chuhan et al, 1998)

1.7 Numerical Analysis procedures for dynamic soil structure interaction problems:

For a long time, modeling of dynamic soil structure interaction was carried out in the frequency domain, which restricted the analysis of the soil structure system to be linear. Nonlinearity of the soil was taken into account only in an approximate manner through equivalent linear analysis procedure in which dynamic soil parameters were adjusted in accordance with the peak or the average strain during iterative solutions of the system in frequency domain, whereas the structure had to be assumed to be linear. To address this problem, the direct method went into the time domain, using well-established procedure of structural dynamics. But, at this stage, the direct method still could not model the energy radiation effect, whereas the substructure method, which remained in the frequency domain, could model this phenomenon very well. In response, there began in the direct method the development of "transmitting boundaries", such as the early "viscous boundary" proposed by Lysmer, J. etc, and then the various kinds of "consistent boundaries" (Wang Jiachun, 2005).

More recent researches of dynamic soil structure modeling tend to be concentrated in the time domain, not only because the problem of nonlinearity can be better simulated in the time domain than in the frequency domain, but also that the typical structural analyst is not accustomed to working in the frequency domain; its natural approach is to consider the sequence of developments from one time to the next that is to apply the time domain concept (Wang Jiachun, 2005).

1.8 Domain Boundaries

Finite element model is able to treat soil domains of arbitrary layer geometry and accommodate material nonlinearity, anisotropy and inhomogeneity, but does not satisfy the radiation-towards-infinity condition at the boundaries, a phenomenon inherent in SSI. Special boundary conditions have to be introduced to simulate the unbounded nature of the soil medium.

Modeling of domain boundaries is one of the biggest problems in dynamic SSI. Because of limited computational resources the computational domain needs to be small enough so that it can be analyzed in a reasonable amount of time. By limiting the domain however an artificial boundary is introduced. As an accurate representation of the soil-structure system this boundary has to absorb all outgoing waves and reflect no waves back into the computational domain. The general purpose of these"transmitting boundaries" is to avoid the reflection of waves emanating from the structure and the adjacent soil. Some more recent "transmitting boundaries" are frequency dependent and made the direct method enter the frequency domain again and ready to model the hysteretic nature of soil damping (Wang Jiachun, 2005).

Many numerical methods or techniques have been developed to solve this problem, such as transmitting boundaries of different kinds, boundary elements, and infinite elements and their coupling procedures (M. Kutanis et al, 2000).

In numerical simulation of soil structure interaction, usually only a finite region of the problem domain is discretized and analyzed to save computational cost. Two important characteristics that distinguish the dynamic soil-structure interaction system from other general dynamic structural systems are the unbounded nature and the nonlinearity of the soil medium. Generally, when the numerical dynamic soil-structure interaction models are established, radiation of dynamic energy into the unbounded soil, the hysteretic nature of soil damping, separation of the soil from the structure, other inherent nonlinearities of the soil and the structure should be taken into account.

If no special boundary treatment is used to prevent outwardly radiating waves from reflecting from the boundary of computational region, errors will be introduced into the results. In order to model this problem using computational simulation procedure, two main difficulties should be taken into consideration: transmitting boundary conditions and soil structure interface (Wang Jiachun, 2005).

- *Fixed or free*

By fixing all degrees of freedom on the domain boundaries any radiation of energy away from the structure is made impossible. Waves are fully reflected and resonance frequencies can appear that don't exist in reality. The same happens if the degrees of freedom on a boundary are left *free*, as at the surface of the soil.

A combination of free and fully fixed boundaries should be chosen only if the entire model is large enough and if material damping of the soil prevents reflected waves to propagate back to the structure.

- *Absorbing Lysmer Boundaries*

A way to eliminate waves propagating outward from the structure is to use *Lysmer boundaries*. This method is relatively easy to implement in a finite element code as it consists of simply connecting dash pots to all degrees of freedom of the boundary nodes and fixing them on the other end (Figure 1.3).

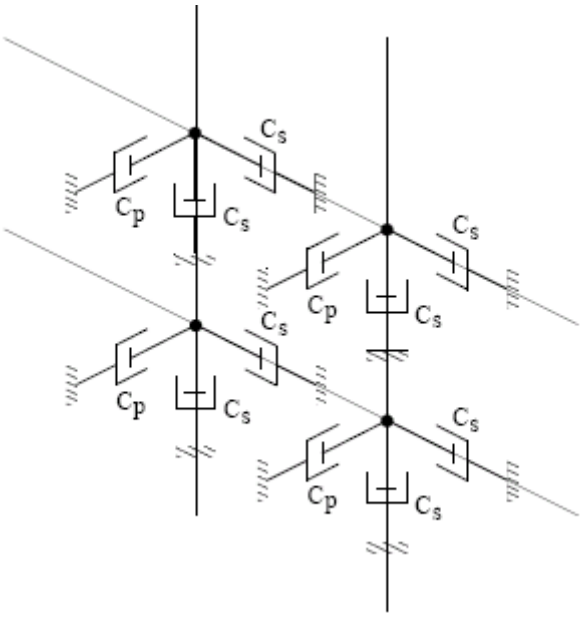

Figure 1.3: Absorbing boundary consisting of dash pots connected to each degree of freedom of a boundary node.

Lysmer boundaries are derived for an elastic wave propagation problem in a one dimensional semi-infinite bar. It can be shown that in this case a dash pot specified appropriately has the same dynamic properties as the bar extending to infinity.

The damping coefficient C of the dashpot equals:

$$C = A\rho c \tag{1.2}$$

Where A is the section of the bar, ρ is the mass density and c the wave velocity that has to be selected according to the type of wave that has to be absorbed (shear wave velocity c_s or compressional wave velocity c_p).

In a 3D or 2D model the angle of incidence of a wave reaching a boundary can vary from almost 0^o up to nearly 180^o. The lysmer boundary is able to absorb completely only those under an angle of incidence of 90^o. Even with this type of absorbing boundary a large number of reflected waves are still present in the domain. By increasing the size of the computational domain the angles of incidence on the boundary can be brought closer to 90^o and the amount of energy reflected can be reduced (Ismail et al, 2000).

- *Infinite elements*

The infinite element type can also be used as transmitting boundary condition in place of traditional ones (dashpots) (Ismail et al, 2000).

The advantages of infinite elements can be summarized as:

- ✓ Unlike a dashpot element, an infinite element does not require calculations of coefficients, which require knowledge of detailed soil properties and mesh geometry. The infinite element offers a slight improvement in the regularity of the wave absorbing characteristics computed in the idealized cases examined, and infinite elements radiation damping performance is reliable (Wang Jiachun, 2005).
- ✓ For 2D problems, one infinite element can replace four dashpot elements and, for 3D problems up to twelve dashpot elements, which reduces the total number of elements in the model achieving significant economy in the case of large models.

- ✓ Unlike a dashpot, the infinite element is more manageable and accessible.
- ✓ Infinite Elements radiation damping performance for Rayleigh waves is reliable.

1.9 Some Existing Studies on Soil Structure Interaction phenomena

Chopra & Zhang (1991) developed an analytical procedure considering hydrodynamic effects to determine the response history of earthquake-induced sliding of a rigid or flexible dam monolith supported without bonding on a horizontal rock surface. Their results indicated that this approximate procedure, which has been widely used in estimating the deformations of embankment dams, cannot provide accurate estimates of the concrete dam sliding displacement, as its precision can only be used to approximate the order of magnitude. In addition, base sliding was shown to be more important than rocking of the dam for the cases considered.

An important result of Chopra & Zhang (1991) was that, even if the ground motion contains spikes of downstream acceleration large enough to initiate tipping, the influence of the resulting rocking of the dam on its sliding motion is negligible. Thus, the rocking motion may be ignored when evaluating the sliding response. This observation is valid, provided that the dam is directly founded on rock. Conversely, it can be unrealistic when the dam is founded on a compliant soil layer. Usually when soft soils are encountered, embankment dams are more preferable than concrete dams. However, in certain situations, the local site conditions may not permit the construction of embankment dams, and the construction of a concrete dam is unavoidable. If a concrete dam is constructed on a soft soil layer, sliding effects are trivial and the rocking response is progressively increased. Inadequate results are available for this issue, thus, further research is needed to cope with the aforementioned cases.

A shaking table study of concrete dam monoliths was performed by Donlon & Hall (1991). The three small-scale concrete gravity dam models examined showed good performance, which is attributed to the favourable crack orientations that can be attributed to sliding failure resistance in each case. Plizzari et al. in 1991 presented results of centrifuge modeling of concrete gravity dams. Among the types of dam models tested in the centrifuge there was a concrete dam which was cast on a rock foundation, so that failure was expected to occur along the damfoundation interface. Using water for upstream loading ensured that uplift pressure inside the crack was maintained. Comparison of the experimental data with numerical fracture mechanics-based finite-element solutions showed an excellent consistency of the results.

Mir & Taylor (1995) performed a series of shaking table tests to assess the possible failure mechanisms of medium to low height dams which were subjected to simple motions and artificial earthquake excitations. The hydrodynamic pressure was simulated using Westergaard's added mass approach. Although the main failure mechanism was observed to be base cracking, after the full crack development at the interface, a tendency of the models to slide and rock was observed in some cases.

In any case, to obtain realistic estimates of the base sliding displacement for a dam, it is necessary to include the effects of dam-foundation interaction. Dam foundation interaction generally reduces the amount of base sliding and the earthquake response of a gravity dam, primarily due to increased energy dissipation. The assumption of rigid foundation can overestimate the base sliding displacement significantly compared to more realistic estimates obtained from including dam foundation interaction, particularly for tall dams. Chavez & Fenves (1995) conducted finite element analyses for a dam monolith. The monolith was modeled using plane stress finite elements with linear elastic material properties, while the base of the dam was assumed rigid. The foundation layer was idealized as a homogeneous,

isotropic and viscoelastic half-plane. The main finding of this study was that the accumulated sliding displacement is influenced by the duration, the amplitude and the characteristics of the free-field ground motion. Sliding is more pronounced when the duration and the amplitude get higher. Moreover, sliding increases when the ground motion has several significant cycles. In addition, sliding displacements are strongly dependent on the value of the coefficient of friction. This dependency decreases for shorter dams and for dams founded on a flexible foundation layer.

The dynamically induced sliding characteristics of a typical low height gravity dam monolith cracked at its base was examined in a series of dynamic slip tests on a concrete gravity dam model, conducted on a shaking table by Mir & Taylor (1996). A comparison of the observed displacements with those calculated via the popular Newmark's sliding block method indicated that the latter gives conservative estimates of seismic induced sliding of gravity dams.

The foundation on rock, which is usually modeled as being bonded with the dam, has been considered to behave linearly elastically (Akköse et al. 2008 a, b, Bilici et al. 2009), or visco-elastically (Aznárez et al. 2006). Nonlinear base sliding behavior has been examined by Chopra & Zhang (1991), where the concept of critical acceleration is used to study the horizontal base displacements of rigid and flexible dams. This type of behavior was also studied by Danay & Adeghe (1993), where an empirical formula was developed to estimate the sliding displacement of a concrete gravity dam using statistical methods. In all the aforementioned studies the rocking displacement (rotation) of the dam is considered negligible when it is free to slip horizontally. Nevertheless, the rocking motion can significantly reduce the normal stresses at the base of the dam, which contribute to its sliding resistance. The sliding displacement has proved to decrease in the case of compliant foundation (Chavez & Fenves, 1995). For this reason, various possibilities of dam foundation interface de-bonding have been considered (Javanmardi et al. 2005, Arabshahi & Lotfi, 2008), whereas energy dispersion in infinite foundation has been studied by Du et al. (2007).

Three examples were used by Chongbin.Z in 1998 to show how engineering practice soil structure interaction problems are solved using the infinite elements method:

The first example was about a three dimensional multi-storey frame structure with a plate foundation resting on a rock medium which was considered to investigate the effect of foundation flexibility on the dynamic response of a structure with the soil-structure interaction included. The frame structure was modelled using 3D frame elements, while the plate and the near field of the rock mass were modelled using the thick plate elements and solid elements respectively. To reflect the wave propagation between the near and far fields, the far field of the rock mass was modelled using 3D infinite element. The plate foundation was considered both flexible and rigid so that the related results can be compared with each other. It was observed that when the frame is subjected to a horizontal movement induced by the dynamic load on the plate, the maximum value of the displacement difference within each storey of the frame structure occurs in the ground storey of the frame for both rigid and flexible plate foundations. This implies that the safety of the columns in the ground storey is the controlling factor in the seismic design of the frame structures. In addition, the flexibility of the plate foundation has a significant effect on the displacement response of the ground storey of the frame structure**.**

The second example was about a coupled method of finite and infinite elements which was investigated for solving the dynamic behaviour of a retaining wall. The near field of this problem consists of the retaining wall, the backfill soil and part of the natural soil, while the far field was comprised of the rest of the natural soil and the base rock mass. Finite elements and dynamic infinite elements are used to model the near and far fields of the natural soil and

rock mass respectively. It was concluded that the configuration of a retaining wall may affect significantly the amplification factor of the retaining wall to an input earthquake.

However the third example was about a typical embankment dam with either a central clay core or an upstream inclined concrete apron, where the dam and the near field of its foundation medium were modelled using finite elements, but the far field was modelled using dynamic infinite elements. It was observed that the resonant frequencies of the system with an upstream inclined concrete apron are different from those of the system with a central clay core because the concrete apron is much stiffer than the central clay core. However, since the thickness of the inclined concrete apron was not profound although it deserves being considered in the analysis. In terms of the amplification factors of the system due to different impervious members, it has recognized that the types of impervious members have a significant influence on the dynamic response of the system in the low frequency range of excitation. The reason for this is that the material damping of the system plays a considerable role in the dynamic response of the system for low frequency excitation.

The effect of both the dam-canyon interaction and the local nonlinearity of the contraction joint opening between the dam monoliths on the response of high arch dams were considered by Z. Chuhan et al in 1998 and combined by into one program. The substructuring technique was employed, thus the equilibrium iteration involved only the degrees of freedom in nonlinear substructure. The Big Tujunga arch dam, located in Big Tujunga canyon, Los Angele country, California was chosen as an engineering example. 3D boundary elements (BEs) and infinite boundary elements (IBEs) were used for discretization of the canyon, taking into account the irregular geometrical conditions in the near field of the canyon. The effects of reservoir water can be viewed as added mass by finite elements and attached to dam-fluid interface. The impedance of the canyon rock were transformed into discrete parameters and attached to the dam-canyon interface. The remaining task was to solve the equations of motion of the dam body which includes linear elastic cantilevers and a set of nonlinear contraction joints. 3D nonlinear joint element was used to model the nonlinear contraction joints of dam. The earthquake ground motion used in the analysis in the lake Hughes No.12 record obtained during the 1971 San Fernando earthquake having a maximum peak acceleration of 0.6g. Time step Δt of 0.01 sec was used although Δt of 0.005sec was also examined to verify the convergence of the response. Dynamic analysis was first conducted for linear analysis assuming the contraction joints were closed. Nonlinear analysis was then performed allowing for the opening of the contraction joints. Both linear and nonlinear analyses are performed using massless and infinite mass foundation for comparison. It had been concluded that the effects of contraction joint opening of arch dams on the response are significant and that the effects of canyon radiation due to the infinite mass foundation are also significant on both linear and nonlinear responses of dams.

W. Shiming et al in 1998**,** analyzed vibration impedance function of raft and pill foundations on layered media with 3D model consisting of special beam, column and panel elements. The authors presented superstructure-foundation-soil 3-D dynamic interaction equations and corresponding program with substructure method. The results were compared for commonly used frame and frame-shear wall structures on different subsoil, different types of foundation and different input of seismic waves. The results show variation of vibration period of structure, displacement, stresses under consideration of interaction.

The control effectivness of Tuned Mass damper (TMD) device was studied by L. Menglin et al in 1998 for high rising building rested on the soft soil, subjected to seismic excitation. Two approaches, random analysis in frequency domain and determinative analysis in time domain, were applied for evaluating the effects of soil-structure interaction (SSI) on the dynamic response of the structure with TMD device. The shear buildings with (LxL)

square cross-section, rested on half space, were selected for illustration. As well as two types of structure's base foundation, surface foundation and group piles foundation, were taken in consideration respectively. The TMD device was installed at the building top. Its damping ratio was designed as 8% and mass was equal to 2% of the first modal mass of the building. El centro and San Fernando earthquake records were selected as the horizontal seismic input.

The numerical cases studied gave the following several results:

- ✓ The function of TMD control to suppress the seismic response of the building is weakened by the soil structure interaction with decrease of the shear wave velocity of the soil. The stronger interaction between the soil and the structure, the more reduction of the TMD control effectiveness.
- ✓ If the high-rising building with higher modal damping, for example 5% in reinforced concrete structure, is rested on soft soil, TMD technique is not available to control the seismic response of the building efficiently.
- ✓ If the soil is not very soft and damping of the building is small, for example about 1% or 2% in the steel structure, TMD control can still be applied to reduce the seismic response of the building. However, the frequency of the TMD device has to be designed to equal approximately to the fundamental frequency of the soil structure system rather than the fundamental frequency of the structure without considering the SSI effect.

Cases studies of the structure seismic response on the campus of the University of Mississippi by Ismail and all in 2000, have highlighted the importance of interaction between structure foundations and soil deposits. Two different ABAQUS models have been used to study this problem, one with dashpots and the other with Infinite Element. In this problem a sinusoidal dynamic displacement history has first been applied to an assumed rigid interface surface between the soil and footing and the interaction forces at the edge of both models have been determined. Second an earthquake load of moderate intensity has been applied from underneath, and a displacement history at one of the interface nodes has been calculated for each model. It had been concluded that responses of both models were almost the same in both models, which gave a positive impression about using the Infinite Elements as transmitting boundary conditions.

Evaluating the interaction of Soil -Structure system subjected to a seismic load is an important step in any dynamic analysis. One of the most important problems in this kind of analysis is the local nonlinear behavior between the soil and the structure foundation. For this reason, Ismail et al. in 2000, used one of the contact-surface modeling procedures available in the commercial software package, ABAQUS, which is the Master-Slave technique. In this technique, the model was divided into two submodels one called the Master and the other called the Slave. The two sub-models interact along a user-defined contact surface. By virtue of this surface, it is not necessary to have compatibility of the meshes at the interface. By using the standard sub-structural approach, the program determined the displacement for the Master nodes on the contact surface, then the Slave ones. It was concluded that contact surface technique is well suited to handle the Soil-Structure Interaction problem. It can successfully capture the most important local nonlinear behaviors at the soil-structure interface. Two practical cases of seismic loading, a gravity retaining wall and a rectangular spread footing for a building column have been introduced.

M. Kutanis et al. in 2000 presented an idealized 2-dimensional plain strain finite element seismic soil-structure interaction (SSI) analysis based on a substructure method by using original software developed by the authors. The accelerogram (E-W component) for the Erzincan earthquake of 1992 was employed as the horizontal ground motion applied to the analysis model and scaled to have different peak accelerations: 0.15g, 0.3g and 0.45g. In

another case for a different site soil with a shear wave velocity of 200, 300 and 500 m/s, a linear SSI analysis was performed. To investigate the effects of soil-structure interaction with each input motion level, the following cases were studied:

- ✓ Neglecting the effect of soil-structure interaction, i.e. assuming the structure being fixed at its base, the soil was assumed to be completely rigid and only the superstructure was considered for analysis.
- ✓ Linear soil-structure interaction analysis.
- ✓ Nonlinear soil-structure interaction analysis.

In the analysis, the radiation condition was fully accounted for, the soil plasticity was modeled with the Von Mises failure criterion, basemat uplift was not considered, and the action of gravity was not taken into consideration. It had been shown that:

- ✓ At the 0.15g acceleration, the level linear and nonlinear responses are coincident, but, as the acceleration level increases nonlinear response becomes significant.
- ✓ Fixed base analysis gives somewhat greater displacements.
- ✓ As the shear wave velocity of the soil increases the response decreases.

Cheng H.C and al. in 2003, were investigated the effects of soil-structure interaction on the dynamic response of a soil-structure system. A model with a simple structure supported on elastic half space is used to derive a factor noted as F_{SSI} that can completely represent the effects of soil-structure interaction. This factor characterizes the altering of predominant frequency and damping ratio of the system when compared to the conventional rigid-base type structural analysis. Based on that, an equivalent fixed base (EFB) model, which takes the effects of soil-structure interaction into account, was constructed. Field test results were used to verify the applicability of the proposed equivalent fixed base (EFB) model.

D. Pitilakis et al, in 2008 provided an insight into the numerical simulation of soil-structure interaction (SSI) phenomena studied in a shaking table facility. The shaking table test was purposely designed to confirm the ability of the numerical substructure technique to simulate the SSI phenomenon. A model foundation-structure system with strong SSI potential was embedded in a dry bed of sand deposited within a purpose designed shaking-table soil container. The experimental system was subjected to a strong ground motion. The numerical simulation of the complete soil-foundation-structure system was conducted in the linear viscoelastic domain using substructure approach. Significant increases in damping were recorded in both laboratory experiment and numerical simulations. Both stiffness decrease and damping increase lead to a decrease of the acceleration forces at the top of the structure, while the vibration cycles were reduced significantly in number and increases in period. The principal effects of the SSI were attested in both the laboratory experiments and the numerical solution.

M. Yahyai et al in 2008 evaluated the effect of Soil-Structure Interaction (SSI) on seismic behavior of two adjacent 32 story buildings such as time period, base shear and displacements. The interaction effects were investigated for variable distance between the two buildings. Three types of soil such as soft clay, sandy gravel and compacted sandy gravel were considered for this study. The result obtained showed that the Structure-Soil-Structure Interaction effects causes the time period increasing of buildings and considering of this effect often causes increasing the base shear and displacements and these increasing depends on the distance of two adjacent buildings. The Soil-Structure Interaction effects changes the maximum lateral displacement up to three times to without considering the Soil-Structure Interaction effects and the applying base shear up to two times to without considering the Soil-Structure Interaction effects.

A 3D discrete element model was proposed by J.V. Lemos et in 2008 for the dynamic behaviour analysis of Cabril dam taking into account the contraction joints effect. The dam study was performed for different water levels. The water effect in the dam dynamic response was evaluated by the analysis of the natural frequencies variation. Numerical and experimental results are compared. The numerical analysis was based on two types of numerical models: i) a 3D finite element model, which was used in the analysis of the dam assumed as a continuous structure (without joints); ii) a discrete element model, which made it possible to consider the contraction joints of the dam and their non-linear behaviour. The hydrodynamic interaction is represented on both types of software by adding masses to the upstream face of the dam, which are calculated by Westergaard's hypothesis.

1.10 Conclusion

In this chapter an overview about the elements of soil structure interaction effect and the different methods used to take into account this phenomenon have been presented, also some works and not all works done in the past have been discussed.

In the next chapter, the fluid domain will be introduced in our discussion field to get an interaction between three elements instead two only; we talk about soil-fluid-structure interaction phenomenon.

CHAPTER 2

Fluid Structure Interaction Phenomenon

CHAPTER 2

Fluid Structure Interaction Phenomenon

2.1 Introduction to Fluid–Structure Interaction Phenomenon

The distress of a concrete dam is affected by several parameters, such as the compressibility of the impounded water, the various dynamic interactions which can be incorporated in the general term “dam-reservoir-foundation interaction”, the possible existence of a sedimentary material at the bottom of the reservoir, the effect of surface (sloshing) waves, and the selection of an appropriate upstream boundary condition to represent the infinite extent of the reservoir in the upstream direction. The impact of these factors has been investigated in the past by many researchers analytically, numerically, or even experimentally as it will be briefly discussed in the sequence. The main scope of this chapter is to present the most commonly used analytical and numerical methods for the evaluation of the seismic distress and response of concrete dams and their interaction with the retained water and the foundation soil layer.

2.2 Different Approaches used to Model the Fluid–Structure Interaction Phenomenon

In order to cope with fluid-structure interaction problems, three approaches have been developed in the past: the added mass approach; the Eulerian approach and the Lagrangian approach.

2.2.1 The added mass approach:

The modeling of interaction effects in the field of earthquake analysis of dams has a long tradition. The first to study these types of problem was Westergaard in 1933. He considered the problem of fluid-structure interaction of a two-dimensional dam-reservoir system subjected to horizontal earthquake ground motion. The dam was assumed to be rigid and the reservoir was supposed to be semi-infinite and of constant depth. With analytical methods he derived the pressure distribution in the fluid at the dam-reservoir interface. His finding was that the interaction forces are proportional to the acceleration of the earthquake ground motion such that they may be approximated by a mass density distributed parabolically over the height of the dam. This technique is called added mass approach (Glauco Feltrin, 1997).

The added mass approach of Westergaard allows modeling an important effect of fluid-structure interaction which is in close agreement with more elaborated models. Because of the additional mass, the eigen frequencies of the coupled dam-reservoir system relevant for the earthquake response of the dam are significantly lower than those of the dam alone. However, the added mass approach doesn’t consider any radiation damping so that energy dissipation is only due to the structural damping of the dam. Nevertheless, because of its simplicity, it has been one of the most frequently used models for the numerical analysis of dams in engineering practice (Glauco Feltrin, 1997).

2.2.2 Eulerian approach:

Since in this approach the displacements are the variables in the structure and the pressures are the variables in the fluid, a special purpose computer program is required for the solution of the coupled systems.

a. Dam-reservoir interaction

In the Eulerian-based FEM approaches the variables describing the response of the fluid are the pressures, the velocities, or the velocity potentials. The hydrodynamic pressure distribution in the reservoir is governed by the pressure wave equation. Assuming that water is linearly compressible and neglecting its viscosity, the small-amplitude irrotational motion of water is governed by the two dimensional wave equations:

$$\nabla^2\phi(x,y,t)=\frac{1}{V_p{}^2}\ddot{\phi}(x,y,t) \tag{2.1}$$

The relations between pressure p, the velocity vector {v} and the velocity potential ϕ are as follows:

$$\{v\}=\nabla\phi \tag{2.2}$$

$$p=-\rho\dot{\phi} \tag{2.3}$$

The velocity potential distribution within each finite element is represented in terms of nodal parameters $\bar{\phi}$ by:

$$\phi=[N]\{\bar{\phi}\} \tag{2.4}$$

For the case of an earthquake excitation at the dam-reservoir boundary the boundary condition usually imposed is:

$$\frac{\partial p(x,y,t)}{\partial n}=-\rho a_n(x,y,t) \tag{2.5}$$

Where ρ is the density of water, p is the pressure given by (2.3) and $a_n(x,y,t)$ is the component of acceleration on the boundary along the direction of the inward normal n. According to finite element method formulation, equation (2.1) results in the following matrix form:

$$[G]\{\ddot{P}\}+[H]\{P\}=\{F\} \tag{2.6}$$

Where the terms of the matrices are given by the following relations:

$$G_{ij}=\sum G_{ij}^e,\ H_{ij}=\sum H_{ij}^e,\ F_i=\sum F_i^e \tag{2.7}$$

$$G_{ij}^e=\frac{1}{V_P^2}\int_{A_e} N_iN_j\,dA \tag{2.8}$$

$$H_{ij}^e=\int_{A_e}\left(\frac{\partial N_i}{\partial x}\frac{\partial N_j}{\partial x}+\frac{\partial N_i}{\partial y}\frac{\partial N_j}{\partial y}\right)dA \tag{2.9}$$

$$F_i^e=\int_{S_e} N_i\frac{\partial P}{\partial n}\,ds \tag{2.10}$$

In which A_e denotes the element's area and s_e is the prescribed length along the boundary of each finite element.

b. Impact of compliant reservoir bottom

Usually, an absorbing boundary condition is imposed at the reservoir-bottom interface. It has been observed that the existence of compliant soil (or sediments) on the bottom of the reservoir has significant effect on the seismic distress and response of a concrete gravity dam. The soft soil layers do not behave as totally reflective boundaries like rigid rock, and there exists dynamic interaction between the reservoir and the underlying soil.

As far as the reservoir bottom is concerned, the following boundary conditions (Li et al. 1996, Küçükarslan et al. 2005) are considered appropriate:

$$\frac{\partial p}{\partial n} = -\rho a_n - \bar{q}\frac{\partial p}{\partial t} \tag{2.11}$$

Where $\bar{q}$ is a damping coefficient which characterizes the effects of the reservoir bottom materials given by:

$$\bar{q} = \frac{1-a_b}{c(1+a_b)} \tag{2.12}$$

And :

$$a_b = \frac{1-\dfrac{\rho V_P}{\rho^r V^r}}{1+\dfrac{\rho V_P}{\rho^r V^r}} \tag{2.13}$$

ρ^r and V^r denote the density and longitudinal velocity of the material comprising the reservoir bottom, respectively. To incorporate the reservoir bottom effect into the finite element solution, Eq. (2.6) is rewritten as follows:

$$[G]\{\ddot{P}\}+[C]\{\dot{P}\}+[H]\{P\}=\{F\} \tag{2.14}$$

$[C]$ is the diagonal damping matrix, and its terms contain the damping coefficient $\bar{q}$.

c. Truncation boundary conditions

To simulate infinite upstream direction, the reservoir is usually separated into a small region adjacent to the dam, called near-field reservoir and the far-field reservoir which extends from the upstream boundary of the near-field reservoir to infinity, or any other physical boundary existent in real conditions. Whenever the far-field reservoir is neglected for computational reasons, the boundary imposed at the upstream direction of the near-field reservoir is called truncation boundary. The boundary condition imposed at the truncation boundary while calculating the near-field reservoir is of critical importance, as the computational domain is significantly reduced compared to the initial reservoir configuration.

Various approaches of describing the boundary conditions if the far-field is truncated are available in the literature:

- The Sommerfeld radiation condition for the truncated surface is given by (Küçükarslan et al. 2005):

$$\frac{\partial p}{\partial n} = -\frac{\dot{p}}{V_p} \tag{2.15}$$

- The Sharan's boundary condition (Sharan, 1985):

$$\frac{\partial p}{\partial n} = -\frac{\pi}{2h} p - \frac{1}{V_p} \dot{p} \tag{2.16}$$

- The far-boundary condition (Maity & Bhattacharyya, 1999):

$$\frac{\partial p}{\partial n} = -\frac{p}{h} Z \tag{2.17}$$

Where :

$$Z = -\frac{\sum_{k=1}^{\infty} \frac{(-1)^{k+1}}{2k-1} e^{-f_k x} \cos(\lambda_k y)}{\sum_{k=1}^{\infty} \frac{(-1)^{k+1}}{(2k-1) f_k} e^{-f_k x} \cos(\lambda_k y)} \tag{2.18}$$

In which

$$f_k = \sqrt{\lambda_k^2 - \left(\frac{\omega}{V_p}\right)^2} \tag{2.19}$$

And :

$$\lambda_k = \frac{(2k-1)\pi}{2h} \tag{2.20}$$

Notice that the above boundary conditions can be imposed for compressible fluids. If the reservoir is assumed incompressible, V_P becomes infinite and the various boundary conditions degenerate into their incompressible counterparts (Küçükarslan 2003, Fan & Li 2008).

d. Free surface (sloshing) waves

The sloshing oscillations are characterised by the presence of gravity surface waves, which behave in a different manner than the acoustic waves. Gravity waves are non-conservative and their velocity depends on their wavelength. It has been shown (Taylor, 1981) that for most concrete gravity dams free-surface waves are negligible. However, in cases where the duration of the excitation is long, the surface wave effect has to be taken into account by imposing an appropriate boundary condition at the free surface of the reservoir. The effects of surface waves (or sloshing waves) of the retained water have been neglected repeatedly in the past (Saini et al. 1978, Sharan 1985, Tsai & Lee 1991, Ghaemian & Ghobarah 1998, 1999, Küçükarslan 2005, Maity 2005, etc.). In such cases the pressure along the free surface is assumed to be equal to zero:

$$p = 0 \tag{2.21}$$

Nevertheless, in some more recent studies sloshing effects are considered by imposing the following boundary condition (Maity & Bhattacharyya 2003, Gogoi & Maity 2007) at the free surface:

$$\ddot{p} + g\frac{\partial p}{\partial y} = 0 \tag{2.22}$$

Moreover, sloshing waves have been studied rigorously for the design of liquid storage tanks and tuned liquid dampers against dynamic loading. In these cases, advanced boundary conditions have been developed to take realistically into account sloshing phenomena.

e. Effect of reservoir sediments

Cheng in 1986 examined the effect of the existence of sediments at the bottom of the reservoir, where the sediment was modelled as a poroelastic material. It was found that for a modest amount of sediment and slight desaturation of pore water, significant changes in the hydrodynamic response curves can be observed.

2.2.1 Lagrangian approach:

In this approach the behavior of the fluid and structure is expressed in terms of displacements. For that reason, compatibility and equilibrium are automatically satisfied at the nodes along the interfaces between the fluid and structure. This makes a Lagrangian displacement based fluid finite element very desirable; it can be readily incorporated into a general purpose computer program for structural analysis, because special interface equations are not required.

a. Dam-reservoir interaction

In the Lagrangian finite element procedures the equations of motion of the fluid are obtained using energy principles, contrary to the Eulerian approach, where the governing equations are solved in the discretized domain. In the former approach fluid is assumed to be linearly elastic, inviscid and irrotational. For a general three-dimensional fluid, stress–strain relationships can be written in matrix form as follows:

$$\begin{Bmatrix} p \\ p_x \\ p_y \\ p_z \end{Bmatrix} = \begin{bmatrix} C_{11} & 0 & 0 & 0 \\ 0 & C_{22} & 0 & 0 \\ 0 & 0 & C_{33} & 0 \\ 0 & 0 & 0 & C_{44} \end{bmatrix} \begin{Bmatrix} \varepsilon_v \\ w_x \\ w_y \\ w_z \end{Bmatrix} \tag{2.23}$$

Or

$$\{p\} = [C_f]\{\varepsilon\} \tag{2.24}$$

p is the mean pressure, C_{11} is the bulk modulus of the water (C_{11}=K), εv is the volumetric strain, p_x, p_y, p_z are the rotational pressures C_{22}, C_{33}, C_{44} are constraint parameters and w_x, w_y, w_z are rotations about the x, y, z axes, respectively. As the irrotational condition is generally not verified a priori, it must be imposed.

Otherwise the solution may be corrupted by spurious modes and the frequency analysis may result to a number of zero-frequency modes. To impose this condition, the constraint parameters C_{22}, C_{33}, C_{44} are taken approximately 10 to 1000 times greater than C_{11} (Parrinello & Borino, 2007). Using the finite element approximation the total strain energy of the fluid system may be written as:

$$\Pi_e = \frac{1}{2}\{U_f\}^T [K_f]\{U_f\} \tag{2.25}$$

Where $\{U_f\}$ and $[K_f]$ are the nodal displacement vector and stiffness matrix of the fluid system, respectively. Moreover, $[K_f]$ is calculated by summation of the stiffness matrices of the fluid elements:

$$[K_f] = \sum K_f^e \tag{2.26}$$

In which the stiffness matrix of each element is obtained as:

$$K_f^e = \int_{V_e} [B_f^e]^T [C_f][B_f^e] dV_e \tag{2.27}$$

Where $[B_f^e]$ is the strain-displacement matrix of the element. An important characteristic of fluid systems is the ability to displace without volume changes.

This movement is known as sloshing waves in which the displacement is in vertical direction. The increase in potential energy of the system due to the free surface motion can be written as:

$$\Pi_s = \frac{1}{2}\{U_{sf}\}^T [S_f]\{U_{sf}\} \tag{2.28}$$

Where

$$[S_f] = \sum S_f^e \tag{2.29}$$

$$S_f^e = \rho g \int_{A_e} \{\bar{h}_s\}^T \{\bar{h}_s\} dA_e \tag{2.30}$$

$\{\bar{h}_s\}$ is a vector consisting of interpolation functions of the free surface fluid element and $\{U_{sf}\}$ is the vertical nodal displacement vector.

Finally, the kinetic energy of the fluid system can be written as:

$$T = \frac{1}{2}\{\dot{U}_f\}^T [M_f]\{\dot{U}_f\} \tag{2.31}$$

Where:

$$[M_f] = \sum M_f^e \tag{2.32}$$

$$M_f^e = \rho \int_{V_e} [\overline{H}]^T [\overline{H}] dV_e \tag{2.33}$$

$[\overline{H}]$ is a matrix consisting of interpolation functions of the fluid element and

$\{\dot{U}_f\}$ is the nodal velocity vector of the fluid. Equations (2.25), (2.28) and (2.31) are combined and using the Lagrange's equation (Clough & Penzien, 1993):

$$\frac{\partial}{\partial t}\left(\frac{\partial T}{\partial q_i}\right) - \frac{\partial T}{\partial q_i} + \frac{\partial \Pi_t}{\partial q_i} = Q_i \tag{2.34}$$

The following set of equations is obtained:

$$\left[M_f\right]\left\{\ddot{U}_f\right\}+\left[K^*{}_f\right]\left\{U_f\right\}=\left\{R_f\right\} \tag{2.35}$$

Where $\left[K^*{}_f\right]$, $\left\{\ddot{U}_f\right\}$ and $\left\{R_f\right\}$ are system stiffness matrix that includes the free surface stiffness, nodal acceleration vector and time-varying nodal force vector for the fluid system, respectively. In addition, qi and Qi represent the generalized coordinate and force, respectively.

The total potential energy results from addition of strain energy and the potential energy due to surface waves: $\Pi_t = \Pi_e + \Pi_s$. Along the dam-reservoir boundary continuity of displacements is imposed, i.e. the nodal displacement of the reservoir

is equal to the nodal displacement of the dam:

$$\left\{U_n^-\right\}=\left\{U_n^+\right\} \tag{2.36}$$

where U_n is the normal component of the interface displacement. Eventually, the coupled matrix differential equations are extracted, which describe the motions of the dam and the retained water.

b. Truncation boundary condition

In the case of a displacement–based formulation, the boundary conditions described for the Eulerian case cannot be utilized to represent infinite reservoir domain in the upstream direction. When the waves present are merely acoustic, the Sommerfeld condition reproduces efficiently the outgoing-waves problem. However, a fluid dynamic problem involving free surface is characterized by the contemporaneous presence of acoustic and gravity (sloshing) waves. The acoustic waves are characterized by propagation velocity independent of the exciting frequency, whereas the sloshing waves are dispersive and their velocity depends on frequency and water depth. The gravity wave velocity is given by:

$$V_s = \lambda_s f \tag{2.37}$$

Where:

$$f = \sqrt{\frac{g}{2\pi\lambda_s}\tanh\left(\frac{2\pi h}{\lambda_s}\right)} \tag{2.38}$$

In which λ_S is the sloshing wavelength and h the depth of the reservoir. It is evident that the sloshing wave velocity depends on the wavelength, and consequently on the frequency. Therefore, the Sommerfeld boundary condition is inadequate to handle problems which involve acoustic and sloshing wave propagation.

An accurate non-reflecting boundary condition was initially proposed by Higdon in1994. This boundary condition can be used with both pressure- and displacement- formulated problems. The Sommerfeld condition can be considered as the first approximation of this more general non-reflecting boundary condition.

Assuming that the x-axis is normal to the truncation boundary, for a generic variable field $\phi(x, y)$ (displacement, pressure, etc.) Higdon's absorbing boundary of order J is defined as:

$$\left[\prod_{j=1}^{J}\left(\partial t + c_j \partial x\right)\right]\phi(x, y) = 0 \tag{2.39}$$

For the imposition of the Higdon boundary condition Eq. (2.39) is applied to both displacement components ux and uy. An exact response is obtained if the set J of parameters cj contains all possible wave speeds for the examined problem (Parrinello & Borino, 2007).

2.3 Some Existing Studies On Soil-fluid-Structure Interaction

The methods used for the analysis of concrete dams under earthquake loading range from the simple pseudo-static method initially proposed by Westergaard in 1931 to advanced numerical methods that include not only the well-known FEM, BEM and FEM-BEM hybrid numerical approaches, but methods utilizing semidiscrete hyperelements. In between these two extreme categories there exist some other methods, such as the Fenves & Chopra (Fenves & Chopra, 1984) refined pseudo-static method (the so-called "equivalent lateral force method") and the methodology suggested by the US Corps of Engineers (2007). The method proposed by Westergaard assumes that the hydrodynamic effect on a rigid dam is equivalent to the inertial force resulting from a mass distribution added on the dam body. The refined pseudo-static method suggested by Fenves & Chopra takes into account the influence of the dam response on the foundation distress, as the latter is considered flexible. The guidelines of US Corps of Engineers recommend that if high tensile stresses develop at the base of the dam then a finite element analysis may have to be conducted to incorporate the variation of the natural period due to cracking at the base. Whenever the aforementioned assumptions are not satisfied, then the engineer has to carry out sophisticated numerical simulations of the whole dam structure and its interaction with the foundation and the retained water.

The added mass concept is fundamental in seismic concrete dam design. Although it seems a rather simplified procedure, it is often utilized in cases where the computational cost of simulating the whole dam-reservoir model is unaffordable. Nevertheless, such cases are very common in engineering practice, since dam–foundation interface non-linearities are usually present and need to be included in the analysis (Arabshahi & Lotfi, 2008, Du et al. 2007). The most characteristic cases are base sliding and uplifting, in which dam-foundation interface elements increase the computational cost. In these studies the hydrodynamic effects of the reservoir were simulated as added masses on the dam. A plasticdamage model for earthquake analysis of concrete dams was developed by Lee & Fenves (1998), in which emphasis was given on the advanced constitutive model. Moreover, the inclusion of the reservoir domain requires a huge computational effort, thus, the added mass approach was implemented. The effect of monolith interaction on the overall dynamic response of concrete gravity dams was investigated by Ghobarah et al. (1994). In that study the monoliths are represented by beam elements connected by shear links. The effect of hydrodynamic interaction is considered as added mass to the dam structure. Therefore, it is evident that the added-mass approach is vital for the evaluation of complicated dam geometries, for dams comprised by individual monoliths, or in cases in which the dam foundation interaction is associated with substantial non-linearities, as the computational cost of the solution is greatly reduced.

The finite difference method for fluid field and the finite element method (isoparametric four-node quadrilateral finite element) for the pine flat dam response were used by B.F.Chen in 1996 to calculate the nonlinear hydrodynamic pressure on dam faces and the corresponding structural dynamic responses of the dam. Both analyses with and without surface waves and convective accelerations were made. Four earthquake records were adopted as exciting ground motions. The results include rigid horizontal dam motion, flexible horizontal dam motion and flexible dam motion under simultaneous action of vertical and horizontal ground motions. The hydrodynamic force coefficient on a rigid dam face was be predicted by the formula $C_F=0.525\ a_h + a_v$ where a_h and a_v are the ratio of the horizontal and vertical components, respectively, of the ground acceleration to the acceleration due to

gravity.The characteristics of the relationships between the hydrodynamic force coefficient, the rise of the water surface and the time history of the ground motion were studied.

It was being seen that:

- The flexibility of the dam could significantly increase the hydrodynamic force coefficient, especially due to the horizontal and vertical ground acceleration exciting simultaneously.
- The vibration of the dam face and the vertical component of the ground acceleration do not affect either the magnitude or the shape of the profiles of the rise of the water surface at the dam face.
- The effects of surface wave and nonlinear convective acceleration of the fluid could be neglected in the dynamic structural analysis of concrete gravity dam.
- Evaluation of the rise of the water surface still is necessary.

F.Guan et al in 1997 proposed a hybrid Numerical for the dynamic frequency domain response of the earth dams resting on a multi-layered foundation. A new technique was described to determine the frequency dependent added masses and loads contributed by the reservoir at the inclined upstream dam face. For the reservoir-dam interaction a green function was developed and the influence matrices are determined using the Garlerkin weighted residual method. The developed technique did not involve any discretization of the reservoir beyond the dam face. For the soil-structure interaction, the impedance of the multi-layered foundation was obtained using the layer transfer matrix and the dam was modelled by finite elements. An interface function was defined using interpolating functions to maintain equilibrium of the interface forces and the displacement compatibility at the interface nodes. Numerical results, including transient responses of the earth dam at La Villita (Mexico) to the S90W El Centro earthquake ground motion (1940), were presented to illustrate the modelling of reservoir-dam and soil-dam interaction. The damping ratios in both fluid and solid were assumed to be 5% in the analyses.

The performance of four different dam-reservoir finite element models, suitable for direct time domain analysis of the earthquake response of concrete gravity dams including dynamic fluid-structure interaction was investigated by B. Tiliouine et al in 1998. Namely, these models are respectively: 1) the standard rigid dam-incompressible water model, 2) the flexible dam-incompressible water model, 3) the rigid dam-compressible water model and 4) the flexible dam-compressible water model. First, the discrete system of finite element equations resulting from a Galerkin variational formulation of the governing equations of the pressure and displacement fields was established for each model. Then, the distribution of the dynamic pressure coefficient at the upstream face of a typical concrete gravity dam and the hydrodynamic pressure time histories at its base, derived from the application of the four fluid-structure models have been determined. linearly elastic properties were assumed for the material of the dam and the water of the reservoir. The motion of the dam-reservoir system was considered as two dimensional and restricted to small amplitudes. The fluid was assumed to be inviscid and extends to infinity in the upstream direction. However, the effects of surface waves, water compressibility, dam flexibility, radiation damping at the upstream boundary of the reservoir and the slope of the upstream dam wall were considered. It was choosen to retain a pressure field for the representation of the fluid action and a displacement field for the description of the dam behavior. The dam and the reservoir domains, were thus modeled separately and it was demonstrated that the dynamic interaction forces linking the two subsystems at the dam-water interface were caused by hydrodynamic pressures from the fluid region acting on the upstream face of the dam, and the structural accelerations at the interface acting in turn on the reservoir.

A study of seismic behaviour of a high arch dam with dynamic interaction with reservoir and foundation based on the wave propagation in a non-uniform and local non-linear medium by using an explicite finite element method with transmitting boundaries was presented by C. Houqun et al in 1998. The calculated Xiawan arch dam is located in the upper reach of the Lanchuang Rviver in Yunnan province. It is a parabolical double curvature dam of 292m high. Its design earthquake intensity was IX degree with a horizontal peak acceleration of 0.308g, while the vertical peak acceleration was 2/3 of the horizontal one. Only the most important fault located 76m apart from the dam heel was considered in the analysis. A nonlinear constitutive relation with Druker-Prager cap model was adopted for this fault. A finite element mesh automatically generated in the program and the dam foundation system was modelled by 1364 8-node 3D solid elements. For simplicity, the dam reservoir interaction was considered through added mass with neglect the compressibility of the reservoir water. The acceleration recorded at rock foundation during and after shock of Tangshan earthquake in 1976 with its peak acceleration scaled to one half of the design values were used as the incident s and p waves in the analysis. For comparison, three alternatives of input, with one streamwise component, one cross-stream component, and all three components simultaneously were applied respectively. In order to reveal the effect of the fault, three foundation models were analyzed separately. They are: Model without fault, Model with fault of linear property and Model with fault of non linear property.

J. Nasserzare et al, in 2003 were developed a procedure which can be used to identify the natural frequencies and natural modes in vacuum of an Arch-Dam from forced vibration testing data of partially filled reservoir. The effect of hydrodynamic pressure was removed by using an efficient algorithm. To verify the procedure, a simple structure was substituted for the dam with known properties in vacuum. Then a thin SSSF-plate was considered as the retaining wall representing of the dam and a sub-structuring technique was used with regard to a three dimensional linear compressible inviscid fluid body. The calculated resonance in the illustrated example replaces the resonance which in practical in-situ has been measured. Also the effect of the wave absorption at the bottom and bank of the reservoir was considered. The hydrodynamic pressure of the reservoir was calculated using boundary element method. The results which derived by solving an inverse problem, were compared with the exact analytical responses of the plate.

Dam-water, dam-foundation rock and dam-water foundation rock interactions on the linear and nonlinear responses of a selected arch dam to earthquake ground motion were investigated by M. Akkose et al in 2004. The hydrodynamic effects on the dynamic response of a selected arch dam were examined by modeling water in the reservoir with 8-noded Lagrangian fluid finite elements. The element including compressible behavior and surface sloshing motion of the fluid has been coded and incorporated into a general-purpose computer program, NONSAP. The step-by-step integration was used to solve the dynamic equations of motion. The El-Centro N-S component of the Imperial Valley earthquake, on May 18, 1940, has been used as the ground motion. The response of the dam was characterized by crest displacements and envelopes of maximum tensile stresses. As conclusions:

- Hydrodynamic effects considerably affect the linear and nonlinear responses of the dam to earthquake ground motion.
- The step-by-step integration technique may be efficient in the linear and nonlinear analyses of the response of arch dams to earthquake ground motion and water in the reservoir can be successfully represented by 3-dimensional 8-noded Lagrangian fluid elements.
- Both the hydrodynamic and the foundation flexibility effects significantly increase the linear and nonlinear responses of the dam to earthquake ground motion.

- The effects of dam-water interaction on the linear and nonlinear responses of the dam to earthquake ground motion are qualitatively similar to those for rigid and flexible foundations.
- The hydrodynamic effects influence the distribution of the maximum tensile stresses on the upstream and downstream faces of the dam similarly, whether the foundation rock is flexible or rigid.

- Dam-water interaction has more influence on the response of the dam with a flexible foundation than on that of the dam on a rigid foundation in both linear and nonlinear analyses.
- A large portion of the upstream and downstream faces of the dam is affected by the excessive tensile stresses due to hydrodynamic effects for both the linear and the nonlinear analyses.

Numerical models for the analysis of the water sloshing in a tank during the impact with the ground have been developed by M. Anghileri et al in 2005 and validated using experimental data. The standard approach to the study of an event consists of developing a numerical model utilising experimental data. When these data are not available, it is necessary to perform appropriate tests. Therefore, in 1998, at Dipartimento di Ingegneria Aerospazial (DIA) of the Plitecnico di Milano, an intensive test programme was performed in order to collect data regarding the impact of a filled tank with the ground. It was being stated that the full FE approach is appropriate for structure design development whereas the coupled analysis using the SPH model of the water is appropriate for the design verification and that the coupled analysis using the Eulerian and ALE models of the water remain still reasonable for specific problems where, for instance, the presence of the air has a deep influence on the results.

N. Bouaanani et al in 2004 presented some results regarding the dynamic behaviour of concrete dams with ice-covered reservoirs using a mathematical formulation. The method was programmed and incorporated to a finite element code specialized for the seismic analysis of concrete dams using substructure method. The Outardes 3 gravity dam was chosen as a model for this numerical study. A parametric study where the dam alone, ice–dam, and ice–dam–reservoir systems were successively studied was carried out to evaluate the influence of various factors on the dynamic behaviour of the ice–dam–reservoir system. Main features of this influence were emphasized and discussed in a parametric study through the analysis of: (i) acceleration frequency response curves at the dam crest, (ii) hydrodynamic frequency response curves inside the reservoir, and (iii) the hydrodynamic pressure distribution on the upstream face of the dam. Both the dam and the ice cover were modelled by quadrilateral isoparametric finite elements, including incompatible displacement modes to ensure a better shear behaviour. At the ice–reservoir interface, the derivation of boundary condition includes the effect of possible damping at the ice–reservoir interface represented by the viscous damping term β. The reservoir and the ice cover extend to infinity in the upstream direction. However, finite element modelling of the ice cover requires the definition of a boundary condition at its far upstream end. Ideally, this condition must take account of the friction of the ice cover at the reservoir border and allow for energy dissipation at this location using appropriate impedance functions. This effect could also be simulated with a reasonable degree of accuracy by truncating the ice cover at a given distance from the dam face and finding the adequate transmitting boundaries. These questions were difficult to address, because of the complexity of the dynamic behaviour of the ice cover and its interaction with the reservoir border, which was associated with the lack of related experimental evidence. For this reason it was assumed that the ice cover was clamped at its far upstream end, due to the small

deformations induced in the ice cover during the in-situ dynamic tests. To account for energy dissipation in the system, a hysteretic damping factor ηs = 3.0% was considered, corresponding to a viscous damping ratio ξs = 1.5%. The hyrodynamic pressure inside the ice-covered reservoir was defined by the authors of this article as the sum of an infinite number of reservoir modes. In practice, this sum has to be truncated at a finite number N_w, small enough to reduce computational time and large enough to include all reservoir modes contributing significantly to the overall dynamic response within the frequency range considered. It was been clearly concluded that: The ice cover affects the dynamic response of the ice–dam–reservoir system, the ice cover influences the shape of the frequency response curves and produces additional resonant modes with more less pronounced peaks, with amplitudes generally lower than those obtained for the dam without ice cover and that the ice cover causes the hydrodynamic pressure to increase in the vicinity of the ice-reservoir interface and to diminish closer to the reservoir bottom.

An algorithm for the analysis of coupled dam-reservoir systems was presented by D. Maity et al, 2005. The complete system had been considered to be composed of two sub-systems, namely, the reservoir and the elastic dam. The water was considered inviscid and compressible and the equations of motion were expressed in terms of the pressure variable alone. Structural damping of the dam material and the radiation damping of the water have been accounted for in the analysis. The solution of the coupled system was accomplished by solving the two sub-systems separately with the interaction effects at the dam-reservoir interface enforced by a developed iterative scheme. Non-divergent pressure and displacement fields were obtained simultaneously through a limited numbers of iterations. The method was computationally economical, stable and capable of taking into account the arbitrary geometry of the systems and may be applied for practical application. The parametric study of the coupled system showed the importance of water height of the reservoir and the material property of the dam.

A. Bayraktar et al in 2005 were examined the effect of the base rock characteristics on the stochastic dynamic response of dam-reservoir-foundation systems subjected to earthquake forces using the Lagrangian approach. The dam object of this study was Sariyar concrete gravity dam constructed on the river Sakarya, which is located 120 km to the northwest of Ankara, Turkey. The S16E component recorded on the Pacoima dam during the San Fernando earthquake in 1971 was selected as a ground motion. For this purpose, three different earthquake input mechanisms were used as: the standard rigid-base input model, the massless-foundation input model and the deconvolved-base-rock input model. The deconvolved accelerogram of the ground motion was calculated by using the computer program SHAKE91, which is based on the one dimensional wave propagation theory. The fluid was assumed to be inviscid. The normal components of the displacements of the reservoir dam and reservoir foundation interfaces were to be continuous. This condition was accomplished by using short and axially almost rigid truss element in the normal direction of the interfaces. Since the extent of the reservoir was large, it was necessary to truncate the reservoir at a sufficiently large distance from the dam. A length of reservoir equivalent to three times its depth was appropriate for adequate representation of hydrodynamic effects on the dam. The nodes representing the extreme side of the reservoir were free to displace in the vertical direction only. The depth of the foundation was taken as much as the depth of the reservoir. Plane strain conditions are taken into account in the calculations. The dam material was assumed to be linear-elastic, homogeneous and isotropic. A damping ratio of 5% was assumed for the coupled system. Surface sloshing, volume change and rotational frequencies occur in the modal analysis of fluids when the Lagrangian approach is used, so the selection of the mode number in the modal analysis based on the Lagrangian approach is very important. The

number of surface sloshing modes, which varies with the finite element model of the reservoir, becomes very high and takes place in the first range of the frequency table. The effects of these modes on the behaviour of the dams are very little. Therefore, the first 30 modes are taken into account this study. It had been concluded that:

- The mean of the maximum values of the displacements, stresses and hydrodynamic pressures obtained using the deconvolved-base-rock input model is smaller than those of the others two models.
- The standard rigid-base input model introduces very significant amplification in the response quantities of interest.
- It was also thought that the standard rigid-base input model is inadequate to evaluate the dynamic response of dam-reservoir-foundation interaction systems subjected to random load.
- The massless-foundation input model, although not as accurate as the deconvolved-base-rock input model, can be used for practical analyses.

A new method for seismic analysis of containers in three-dimensional space was introduced by M.R. Kianoush et al in 2006, in which the effects of both impulsive and convective components and their corresponding damping are accounted for in time domain. A case study was performed to investigate the behaviour of a concrete rectangular container under the effects of horizontal and vertical ground motions using the scaled earthquake components of the 1940 El-Centro earthquake record. Two dimensional behaviour of the tank was assumed. The results of the study were compared with those obtained using the current practice and those determined from finite element (FE) analysis based on a lumped mass model. The results of the FE analysis with the equivalent added masses and rigid walls were in good agreement with those from the current practice. Compared with the proposed method, however, the current practice overestimates the response of the container. Also, the vertical excitation leads to a significant response in the container, but combining the effects of horizontal and vertical excitations reduces the response of the structure in the considered system. A 1 m strip of the tank wall was modeled to simulate the two-dimensional behavior of the system. It was assumed that the tank rests on a rigid foundation and the effect of soil–structure interaction was ignored. It was also assumed that the tank was anchored at its base and the effect of uplift pressures was not considered. It was been showed that the proposed staggered displacement method can be successfully used in the analysis of rectangular structures for containing liquid.

R. Livaoglu et al in 2006 presented a review of simplified seismic design procedures for elevated tanks and the applicability of general-purpose structural analyses programs to fluid–structure–soil interaction problems for these kinds of tanks. Ten models were evaluated by using mechanical and finite-element modelling techniques. An added mass approach for the fluid–structure interaction, and the massless foundation and substructure approaches for the soil–structure interactions were presented. The applicability of these ten models for the seismic design of the elevated tanks with four different subsoil classes were emphasized and illustrated. It was concluded that single lumped-mass models underestimate the base shear and the overturning moment.

Reservoir water level effects on nonlinear dynamic response of arch dams were investigated by M. Akkose et al in 2008. The nonlinear behaviour of dam concrete was idealized as elasto-plastic using the Drucker–Prager model. Instead of the nonreflective boundary condition, the reservoir length was selected as three times of the reservoir depth to consider the damping effect arising from the propagation of pressure waves in the upstream direction. Foundation rock was assumed to be linearly elastic and represented by eight-noded three-dimensional solid elements up to a certain distance from the dam. To avoid reflection of

the outgoing waves, these elements were assumed to be massless. One hundred and sixty-four three-dimensional elements were used in the finite element mesh of the foundation rock. The fluid was assumed to be linearly elastic, inviscid and irrotational. The bulk modulus and mass density of the fluid are taken as 0.207×10^7 kN/m^2 and 1000 kg/m^3, respectively. 512 eight-noded three-dimensional fluid elements were used to represent the water in the reservoir. The rotation constraint parameters of the fluid about each Cartesian axis were taken as 1000 times of the bulk modulus. The optimum value of the rotation constraint parameter changes with the properties of material and it can be a different value for various problems. The parameter should be as high as necessary to enforce the rotational constraint but small enough to avoid causing numerical ill-conditioning in the assembled stiffness matrix. This parameter is generally taken as 100 times of the bulk modulus in two-dimensional fluid–structure problems. But, it was taken as 1000 times of the bulk modulus in three-dimensional fluid–structure problems due to the mentioned reasons. The fluid was only able to transmit normal forces to both solid (canyon sides) and structure (dam) boundaries. This is because of its inviscid nature. The slip condition at the solid–fluid interface can be modelled by the use of constraint relations, interface elements or short and axially almost rigid link (truss) elements in the normal direction of the interface.

At the interface of the reservoir–canyon, one node, which corresponds to the canyon side, of the link element was completely restrained (grounded), whereas the other is capable of moving in the translational directions. At the interface of the dam–reservoir, each of nodes of the link element allows translational motions. The length and the elasticity modulus of the truss elements were taken as 0.001m and 2×10^{16} kN/m^2, respectively .

Nonlinear dynamic analyses of the selected arch dam are performed according to the assumption that the dam is subjected to uniform ground motion along the dam–foundation interface. The El-Centro N–S record of Imperial Valley earthquake, on May 18, 1940, measured on a rock-like surface, was chosen as the ground motion (PEER: Pacific Earthquake Engineering Research Center, 2005). The record was applied to the coupled systems in the upstream–downstream direction (y-direction). In the analysis only the first 6.5 s of the earthquake was considered. The time step increment is chosen was 0.001 s for the integration.

Initial (static) stresses and displacements can have strong effects on the nonlinear dynamic response. Therefore, static analysis of the dam–water–foundation rock system under self-weight and the hydrostatic pressure was carried out to establish the initial condition for dynamic analysis. Subsequently, the linear and nonlinear dynamic analyses of the system were performed. Water levels in the reservoir were considered as 40, 60, 80, 100 and 120m to investigate the water level effects on the nonlinear dynamic response of the selected arch dam.

It was concluded that reservoir water level effects must be considered in the elasto-plastic analysis of arch dams to earthquake ground motion. The Drucker–Prager elasto-plastic model can overcome the problem and predict realistic distribution and levels of stresses in the dam body. It was thought that the elasto-plastic analyses of arch dams are very important for the determination of the plastic regions in the dam body.

A 3D discrete element model was proposed by J.V. Lemos et in 2008 for the dynamic behaviour analysis of Cabril dam taking into account the contraction joints effect. The results obtained with this 3D discrete element model were compared with the results obtained from a 3D finite element model assuming the structural continuity. The dam study was performed for different water levels. The water effect in the dam dynamic response was evaluated by the analysis of the natural frequencies variation. Numerical and experimental results were compared. The numerical analysis was based on two types of numerical models: i) a 3D finite element model, which was used in the analysis of the dam assumed as a continuous structure

(without joints); ii) a discrete element model, which made it possible to consider the contraction joints of the dam and their non-linear behaviour. The hydrodynamic interaction was represented on both types of software by adding masses to the upstream face of the dam, which were calculated by Westergaard's hypothesis.

Two approaches were studied by B. Poursartip et al, in 2008 for modal analysis of concrete arch dams in time domain. The results of these investigations were compared against the direct approach which was envisaged as an exact method. The decoupled modal approach relies on independent modes of the dam and the reservoir, and coupled modal approach, which employs mode shapes of coupled system. An asymmetric eigenvalue problem was required to be solved to calculate the coupled modes, which makes the programming very complicated. However, in the decoupled modal approach, a symmetric eigenvalue problem was employed which was resulted by elimination of asymmetric parts of the initial equation. The mode shapes extracted through this problem were utilized to calculate the response. The analysis of Shahid Rajaee concrete arch dam was considered as a controlling example, and the number of required mode shapes for an accurate analysis was compared for these two modal approaches.

A semi-analytical procedure for solution of dam-reservoir interaction in the fundamental mode shape was described by P. Marcelo et al in 2009. The fundamental frequency was solved using a generalized coordinate approach mixed with a wave equation analytical solution for a flexible boundary, resulting in a coupled system equilibrium frequency equation. Pressure field in the fluid domain and fluid added mass were obtained upon the solution of this equation. Results indicate good agreement between finite element solution for the coupled system and the resulting fluid added mass solution. This methodology provides a useful resource for solution of the coupled system and can be readily applied in dam engineering problems.

Hydrodynamic pressures induced due to seismic forces and Fluid-Structure Interaction (FSI) were evaluated by H. Shariatmadar et al in 2009. The interaction of reservoir water-dam structure and foundation bed rock were modeled using the ANSYS computer program. The analytical results obtained from over twenty 2D finite element modal analysis of concrete gravity dam show that the accurate modeling of dam-reservoir-foundation and their interaction considerably affects the modal periods, mode shapes and modal hydrodynamic pressure distribution.

2.4 Conclusion

This chapter is dedicated to the fluid structure interaction phenomenon, it comports the different approaches used to model the mutual reaction between the fluid and the structure. A list of some works done in this axe of research has been presented and detailed. The next chapter will be offered to a one of the first finite element code in the word which is ANSYS, and which will be used in the following chapters of this thesis.

CHAPTER 3

Structural Dynamic Capabilities of ANSYS

CHAPTER 3

Structural Dynamic Capabilities of ANSYS

3.1 Introduction

The finite element method (FEM) is the most popular simulation method to predict the physical behaviour of systems and structures. Since analytical solutions are in general not available for most daily problems in engineering sciences numerical methods have been evolved to find a solution for the governing equations of the individual problem. Although the finite element method was originally developed to find a solution for problems of structural mechanics it can nowadays be applied to a large number of engineering disciplines in which the physical description results in a mathematical formulation with some typical differential equations that can be solved numerically.

Much research work has been done in the field of numerical modelling during the last twenty years which enables engineers today to perform simulations close to reality. Nonlinear phenomena in structural mechanics such as nonlinear material behaviour, large deformations or contact problems have become standard modelling tasks. Because of a rapid development in the hardware sector resulting in more and more powerful processors together with decreasing costs of memory it is nowadays possible to perform simulations even for models with millions of degrees of freedom.

ANSYS provides finite element solutions for several engineering disciplines like statics, dynamics, heat flow, fluid flow, electromagnetics and also coupled field problems. The ANSYS user is able to run simulations for linear and nonlinear problems in engineering where structural nonlinearities may occur due to nonlinear material behaviour, large deformations or contact boundary conditions.

With this chapter, we give an overview of the present capabilities of ANSYS in the field of structural dynamics. A general classification of dynamical calculation disciplines will be provided. The algorithms that are available with ANSYS code are discussed together with their typical applications. Considering the time integration method for transient problems we emphasize implicit and explicit solution capabilities of ANSYS. Furthermore, we focus on algorithms that reduce the solution time of dynamical calculations significantly. Two methods will be discussed in detail: First of all, to determine the natural frequencies of very large models where typically solid elements are used ANSYS provides an algorithm called Powerdynamics Method which shows quite good results when comparing the solution time with other classical algorithms. In addition, the QR Damped Method is introduced which enables the user to model non-proportional damping not only in a modal analysis but also in a transient and harmonic analysis when based on the modal superposition technique. Again this results in less computation time. We also will mention how damping can be modelled in ANSYS.

3.2 Problems of Structural Dynamics - Numerical Methods in ANSYS

Here we give a general overview of typical problems in structural dynamics. Based on d'Alemberts principle and due to the discretization process of a continuous structure with finite elements the following equation of motion can be derived:

$$\underline{M}\ddot{\underline{U}} + \underline{C}\dot{\underline{U}} + \underline{K}\underline{U} = f(t) \tag{3.1}$$

$\underline{M}, \underline{C}, \underline{K}$: System mass, damping and stiffness matrix respectively.

The vectors of nodal accelerations, velocities and displacements are $\ddot{U}, \dot{U}$ and U

$f(t)$ is the vector of applied forces. Dynamical equilibrium is obtained if equation (3.1) holds for all times « t ».

All problems in structural dynamics can be formulated based on the above equation of motion (Eq. 3.1). A coarse classification is obtained by taking different representations for the time varying applied forces. For this classification Figure 3.1 presents a diagram where several analysis types of structural dynamics are listed according to the representation of the applied load.

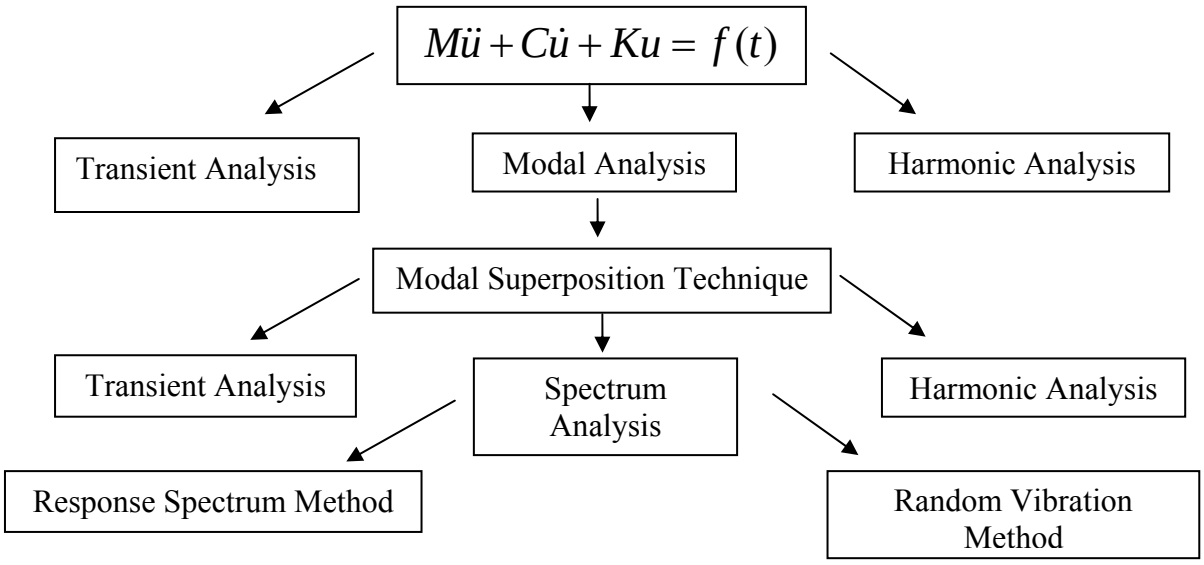

Figure 3.1 : Classification of Problems in Structural Dynamics

Furthermore, a structural analysis that accounts for damping has to be distinguished from an analysis where damping is neglected. Finally, since not every engineering application results in the formulation of symmetric system matrices we should further distinguish between analyses with symmetric and unsymmetric matrices.

In the following sections we briefly describe the different analysis types mentioned in the above Figure 3.1. We also discuss present solution algorithms of ANSYS and describe practical applications for each type of dynamic analysis.

3.3 Modal Analysis

A modal analysis is used to determine the vibration characteristics of a structure while it is being designed. Hence, the goal of a modal analysis is determining the natural frequencies and mode shapes. The right hand side of the equation of motion (3.1) is considered to be zero, i.e. $f(t) = 0$. A modal analysis can also be taken as a basis for other more detailed dynamic analyses such as a transient dynamic analysis, a harmonic analysis or even a spectrum analysis based on the modal superposition technique. The modal analysis is a

linear analysis. Any nonlinearity which may have been specified by the user is ignored. However, prestress effects may be considered.

3.3.1 Solution Algorithms for a Modal Analysis and Typical Applications

In a mathematical sense the computation of natural frequencies and mode shapes is equivalent with the solution of an eigenvalue problem. Depending on the presence of damping and the form of the resulting system matrices the numerical effort to solve the eigenvalue problem may vary. However, ANSYS provides a lot of different eigenvalue solvers. Many of them are designed for special application purposes and it is important to know which eigenvalue solver best suits the physics of the individual problem. Therefore, we will give an overview of all eigensolvers which are currently available in ANSYS together with typical applications.

a. Systems without damping and symmetric matrices:

In many engineering applications damping effects are neglected and the system matrices are symmetric. For those problems ANSYS provides the following eigensolvers:

- Block Lanczos Method
- Subspace Method
- Reduced Method
- Powerdynamics Method

The Block Lanczos Method is a very efficient algorithm to perform a modal analysis for large models. It is a fast and robust algorithm and used for most applications as the default solver.

The Subspace Method was popular in earlier years since very little computer resources were necessary to perform a modal analysis. However, compared with the Block Lanczos Method the Subspace Method is fast for small models but solution time increases as soon as larger models are considered.

The Reduced Method is also an old eigensolver which works with reduced matrices in order to minimize the number of dynamic degrees of freedom. Master degrees of freedom have to be chosen which represent the dynamic response of the system as accurately as possible. Neither the Subspace Method nor the Reduced Method are popular today.

The Powerdynamics Method is a special algorithm based on the Subspace Method. During the Subspace Algorithm linear systems of equations have to be solved. For this purpose, ANSYS provides several equation solver. Typical solver for problems in structural mechanics are the Sparse Solver, the Frontal Solver and the Pre-conditioned Conjugate Gradient Solver (PCG-Solver). Each of these equation solver has its special characteristics. By default the Subspace Method as mentioned above uses the Frontal Solver to obtain the first natural frequencies of a structure. This solver works efficiently for small models of up to 50,000 active degrees of freedom. However, if models consist mainly of solid elements with more than 50,000 active degrees of freedom, the Subspace Method combined with the PCG-Solver should be the preferred solution method. In ANSYS the combination of the Subspace Method together with the PCG-Solver is called Powerdynamics Method. For large models of up to 10,000,000 degrees of freedom, this method significantly reduces solution time. Another characteristic of the Powerdynamics Method is the lumped mass matrix formulation. In a lumped mass approach, the mass matrix is diagonal since the mass is considered concentrated at the nodes. Note that the Subspace Method is the only eigensolver in ANSYS where the user has the option to specify the equation solver.

b. Systems without damping and unsymmetric matrices:

Some engineering applications in which structural damping is ignored may lead to unsymmetric system matrices. In those cases the ANSYS user can take advantage of the following eigensolver called:

• Unsymmetric Method

In fact, this method uses a Lanczos algorithm to solve the resulting unsymmetric eigenvalue problem which is commonly encountered in fluid-structure-interaction problems. For example if interest lies in the natural frequencies of a steel ring which is submerged in a compressible fluid the matrices are unsymmetric and the user has to apply the Unsymmetric Method as an appropriate eigensolver.

c. Damped systems with symmetric matrices:

If damping is considered and the system matrices are symmetric, the user can choose the following eigensolver to calculate damped natural frequencies of a structure:

• QR Damped Method

The QR Damped Method typically consists of two parts: First, the Block Lanczos Method mentioned earlier in this section is used to compute the solution of the undamped system. Hence, all natural frequencies and mode shapes will be calculated for zero damping. Note that the Block Lanczos Method ignores the damping matrix even if it is set up by the program.

In a second step, the equation of motion now including the damping matrix is transformed with the matrices of undamped mode shapes into the modal subspace. This procedure is identical with the first step of the modal superposition technique which will be discussed in the next subsection. After some further mathematical manipulations an extended eigenvalue problem can be formulated. The resulting eigenvalues of this problem are complex. Each real part of an eigenvalue physically represents the damping coefficient multiplied with the undamped natural frequency of the considered mode whereas the imaginary part consists of the damped natural frequency itself.

Let us briefly summarize the main properties of the QR Damped Method as an eigensolver: Damped natural frequencies are computed as well as modal damping coefficients of each mode. However, the effects of damping are not considered for the computation of the resulting mode shapes which simply means that only undamped mode shapes are obtained. Furthermore, we should mention that the QR Damped Method gives reasonable results only if undercritical damping is specified. Considering the solution speed the QR Damped Method shows a better performance especially when compared with the Damped Method which will be discussed next.

d. Damped systems with symmetric/unsymmetric matrices:

Let us assume damping is considered and the resulting damping matrix is either symmetric or unsymmetric. For such applications ANSYS provides the eigensolver called:

• Damped Method

This method accounts for the damping matrix for the formulation of the considered eigenvalue problem. From a mathematical point of view this results in a so called quadratic eigenvalue problem. The obtained eigenvalues are again complex. The real part physically represents the product of the modal damping coefficient and the undamped natural frequency. The imaginary part, however, obtains the damped natural frequency.

In contrast to the QR Damped Method the effect of damping is also considered for the computation of mode shapes which has the consequence that all mode shapes are obtained in a complex form. Therefore, the dynamic response in each mode consists of a real and an imaginary part.

In summary, we note that the Damped Method computes the damped natural frequencies and the real and imaginary parts of each mode shape. Considering solution time, the Damped Method works less efficiently compared with the QR Damped Method described above.

Finally, we discuss in which engineering discipline a symmetric damping matrix is obtained and in which case the damping matrix appears as an unsymmetric one. The modal analysis of damped systems which are at rest leads in general to a symmetric formulation of the resulting damping matrix. Different possibilities to model the effect of damping will be summarized later on in this paper. However, if a modal analysis of a spinning structure has to be performed the effect of the resulting gyroscopic forces has to be included. Indeed these effects are physically comparable with structural damping and therefore a so called gyroscopic matrix has to be set up. In the equation of motion (Eq. 3.1) it typically occurs at the same position where usually the damping matrix can be found. It should be noted that for problems involving such rotordynamic stability this gyroscopic matrix is usually unsymmetric. Hence, the Damped Method has to be chosen to perform the analysis.

3.3.2 Modal Superposition Technique for Problems in Structural Dynamics

At this stage we would like to describe briefly the modal superposition technique since it is based on a modal analysis which has been discussed so far in this chapter. Many solution disciplines of structural dynamics require a transient or harmonic analysis that can be performed efficiently when the modal superposition technique is used. Also remember the fact that the spectrum analysis always uses the modal superposition as a basic concept.

We refer to Figure 3.1 where the important role of the modal superposition technique is shown in context with classical solution disciplines of structural dynamics. The basic idea of the modal superposition technique is to describe the dynamic response of a structure by a linear combination of its first n undamped mode shapes. This can be formulated as :

$$\mathrm{U}(\mathrm{t}) = \sum_{\mathrm{i}=1}^{\mathrm{n}} \varphi_{\mathrm{i}} . \mathrm{y}_{i}(t) = \phi . \mathrm{y}(\mathrm{t}) \tag{3.2}$$

where φ_{i} denotes the undamped mode shape of mode i and $y_i(t)$ is its modal coefficient. In the columns of the modal matrix ϕ, we find the n undamped mode shapes φ_{i} and the vector $y(t)$ consists of the n modal coefficients $y_i(t)$. By substituting equation (3. 2) into the equation of motion (3.1) and further pre-multiplying with the transposed modal matrix ϕ^T we obtain:

$$\phi^T M \phi . \ddot{y}(t) + \phi^T C \phi . \dot{y}(t) + \phi^T K \phi . y(t) = \phi^T . f(t) \tag{3.3}$$

Since the undamped mode shapes are orthogonal with respect to the mass and stiffness matrix, (3.3) is decoupled and represents n equations each describing a generalized single degree of freedom model in the modal subspace. Strictly speaking, a set of decoupled equations is only achieved if the damping matrix is proportional to the total mass and/or the total stiffness matrix. This kind of damping is often called proportional or Rayleigh damping. If non-proportional damping is specified, for example by using discrete damping elements, the above equation (3.3) is coupled.

It should be mentioned again that based on equation (3.3) a transient and harmonic analysis or even a spectrum analysis can be performed quite efficiently since for these three analysis disciplines just the right hand side will be different.

If equation (3.3) is decoupled for example in case of Rayleigh damping the solution speed increases rapidly. However, if non-proportional damping is specified it may also be convenient to work in the modal subspace since all system matrices are reduced to the order $n \times n$ independently of the form of the resulting damping matrix.

To sum up, we notice that working in the model subspace always reduces the original dimension of the considered problem. Consequently, we obtain better performance in terms of solution time.

3.4 Transient Dynamic Analysis

A transient dynamic analysis is a technique which is used to determine the time history dynamic response of a structure to arbitrary forces varying in time. On the right hand side of equation (3.1) any function for the load vector may be specified, i.e. $f(t) = f(t)$. This type of analysis yields the displacement, strain, stress and force time history response of a structure to any combination of transient or harmonic loads.

To obtain a solution for the equation of motion (3.1) a time integration has to be performed. In the literature, several time integration algorithms are discussed in detail. They can be broadly classified into implicit and explicit methods. Considering the stability of these two types of integration methods we notice that implicit methods are usually unconditionally stable which means that different time step sizes can be chosen without any limitations originating from the method itself.

Explicit methods on the other hand are only stable if the time step size is smaller than a critical one which typically depends on the largest natural frequency of the structure. Due to the small time step necessary for stability reasons explicit methods are typically used for short-duration transient problems in structural dynamics.

Since both types of time integration methods are available with the ANSYS product family we will discuss them below in more detail. We will also mention typical applications for both methods.

3.4.1 Implicit Time Integration and its Typical Application

The implicit time integration algorithm in ANSYS is the Newmark method. The stability of this method is controlled by two parameters that are set up by default so that the scheme is unconditionally stable and the effect of numerical damping is minimized. Applying the Newmark method to the equation of motion (3.1) results in a linear system of equation for each time step. Since the stiffness matrix appears on the left hand side it must be inverted in each time step in the incremental solution process. Since its inversion is computationally expensive especially for highly nonlinear problems the implicit solution technique in ANSYS is always a good choice to solve a transient analysis if the problem is not crucially dominated by nonlinearities.

To solve a transient analysis ANSYS provides different solution options which will be discussed according to their importance and computational efficiency in more or less detail:

- Full Method
- Reduced Method
- Modal Superposition Method

The Full Method does not reduce the dimension of the considered problem since original matrices are used to compute the solution. As a consequence it is simple to use, all kinds of nonlinearities may be specified, automatic time stepping is available, all kinds of loads may be specified, masses are not assumed to be concentrated at the nodes and finally all results are computed in a single calculation. The main disadvantage of the Full Method is the fact that the required solution time will increase with the size of the considered model.

The Reduced Method originates from earlier years. Because of the reduced system matrices which are used to solve the transient problem, this method has an advantage when compared with the Full Method with respect to the required solution time. However, the user has to specify master degrees of freedom which represent the dynamic behaviour as good as possible. The only nonlinearity which can be specified is node-to-node contact via a gap condition. However, automatic time stepping is not possible. Consequently, this method is not very popular any more since all its disadvantages do not really compensate the advantage of lower costs in solution time.

The Modal Superposition Method usually reduces the dimension of the original problem as well since the transient analysis is finally performed in the modal subspace which has the dimension of the number of mode shapes used for the superposition. The main advantage is again the reduction of solution time. It turns out that this method is actually the most efficient one compared with the other two. The accuracy just depends on the number of mode shapes used for the modal superposition. Even if a few modes shapes are taken the requested solution time might still be less when compared with the Full and the Reduced Method. Contact can be applied using the gap condition we mentioned in the discussion of the Reduced Method. The time step has to be chosen as constant which means that automatic time stepping is not available for this method. It should also be noted that a modal analysis has to be performed before the transient problem can be solved with the modal superposition technique. Hence, the solution process consists basically of two analyses, the modal analysis and the transient analysis in the modal subspace. Since for most problems in structural dynamics the natural frequencies of a structure are of interest this is not really a disadvantage. Summing up, using the modal superposition technique for a transient analysis reduces not only solution time, but the user also obtains information about the natural frequencies and the undamped mode shapes, respectively.

Comparing the above solution options the Modal Superposition Method is the most powerful method considering the required solution time. However, it cannot handle nonlinearities. The Full Method requires more time to finish the analysis but can handle nonlinearities.

3.4.2 Explicit Time Integration and its Typical Application

ANSYS also provides the possibility to perform an explicit transient analysis. ANSYS/LS-DYNA as a product of the ANSYS family combines the LS-DYNA explicit finite element solver with the powerful pre- and postprocessing capabilities of ANSYS.

As an explicit time integration algorithm, LS-DYNA uses a central difference scheme. Similarly as the implicit Newmark method linear systems of equation have to be solved in each time step. However, the stiffness matrix will appear on the right hand side during the solution process and therefore does not need to be inverted in each step. For this reason ANSYS/LS-DNYA can handle highly nonlinear problems in transient dynamics very well. Fast solution capabilities are provided for short-time large deformation dynamics, quasi-static problems with large deformations and multiple nonlinearities and also for complex contact/impact problems. For highly nonlinear transient problems the product ANSYS/LS-DYNA might be the better choice compared with ANSYS in its implicit version.

Because of the small time step which has usually to be taken for stability reasons in ANSYS/LS-DYNA long-time transient problems might run inefficiently with this code and ANSYS in its implicit form could be a better choice.

With ANSYS/LS-DYNA, the user can perform the complete preprocessing in ANSYS, obtain the explicit dynamic solution via LS-DYNA and review the results using again the ANSYS postprocessing tools the user might be already familiar with. It is also possible to transfer geometry and result information between ANSYS and ANSYS/LS-DYNA to perform a sequential implicit-explicit/explicit-implicit analysis, such as required for a drop test or a springback analysis.

3.5 Harmonic Response Analysis

Any sustained cyclic load will produce a sustained cyclic response in a structure which is often called a harmonic response. The harmonic response analysis solves the equation of motion (3.1) for linear structures undergoing steady-state vibrations. All loads and displacements vary sinusoidally with the same known frequency although not necessarily in phase. The use of a complex notation allows a compact and efficient description of the problem. For the function of applied force on the right hand side of the equation of motion (Eq. 3.1) the following expression is used, i.e :

$$f(t) = f_{max} . e^{i(\Omega t + \Psi)} \tag{3.4}$$

In this formulation f_{max} represents the amplitude of the force, Ω denotes the imposed circular frequency measured in radians/time and Ψ stands for the force phase shift which is measured in radians.

As for the transient dynamic analysis ANSYS provides several solution options to solve a harmonic response analysis which will be discussed more or less in detail according to their immediate meaning:

- Full Method
- Reduced Method
- Modal Superposition Method

Note that the same three solution methods which are available for the transient dynamic analysis are provided to perform a harmonic response analysis. Since the mean characteristics of these methods have been already explained earlier we will not repeat them at this stage. All discussed advantages and disadvantages remain the same if the above methods are applied to a harmonic response analysis. Some features which are typical for these methods when used in the harmonic response analysis are discussed as follows.

One feature of the Full Method which should be mentioned here is the capability of handling unsymmetric matrices which occur in problems of fluid-structure-interaction or rotordyamics. However, considering the solution time the Reduced Method and the Modal Superposition Method will still provide better performance, but cannot handle unsymmetric matrices.

The Reduced Method and the Modal Superposition Method have the capability to take into consideration the effects of pre-stressing within a harmonic analysis. With the general improvement in solution time this turns out as an advantage when compared with the Full Method. Nevertheless, the Modal Superposition Method itself shows the best performance when observing the solution time.

3.6 Spectrum Analysis

A spectrum analysis is a dynamical calculation discipline in which the results of a modal analysis are used together with a well-known spectrum to calculate certain quantities in the structure like displacements and stresses for example. A spectrum is simply a graph of a spectral quantity like the acceleration versus frequency that captures the intensity and frequency content of time-history loads.

The spectrum analysis is often used instead of a transient dynamic analysis to determine the response of structures due to random or time-dependent loading conditions such as earthquakes, wind loads, ocean wave loads, jet engine thrusts, rocket motor vibrations and so on. Contrary to a transient analysis a spectrum analysis does not calculate the dynamic answer for the whole considered time range where the dynamic forces have been acting. Rather a conservative estimation for the maximum response of a certain quantity like the displacements or stresses is obtained from this type of analysis.

To discuss further aspects of a spectrum analysis we should distinguish the deterministic way of consideration from the non-deterministic one. Up to now each analysis type has been of a deterministic nature since the load function has been always a clearly defined one. This assumption holds for the most engineering applications of today. Strictly speaking, dynamic loads appear quite often to be statistical in nature and hence a non-deterministic probabilistic consideration could be even more suitable. In the following two subsections we provide detailed information about the deterministic response spectrum analysis and the non-deterministic random vibration analysis.

3.6.1 Deterministic Response Spectrum Analysis

For the deterministic response spectrum analysis the following types of spectra are available in ANSYS and we will try to explain their main characteristics as follows:

• Response Spectrum

Single-point Response Spectrum

Multi-point Response Spectrum

• Dynamic Design Analysis Method

A response spectrum represents the response of a single degree of freedom system to a time-history loading function. It is a graph of response versus frequency where the response might be a displacement, velocity, acceleration, or even a force. In a single-point response spectrum analysis you specify one response spectrum curve at a set of points in the model, such as at all supports. On the other hand, in a multi-point response spectrum analysis you specify different spectrum curves at different sets of points.

The dynamic design analysis method is a technique used to evaluate the shock resistance of shipboard equipment. The technique is essentially a response spectrum analysis in which the spectrum is obtained from a series of empirical equations and shock design tables provided in the U.S. Naval Research Laboratory Report NRL-1396.

3.6.2 Non-deterministic Random Vibration Analysis

For the non-deterministic random vibration analysis the following type of spectrum is used in ANSYS:

• Power Spectral Density (PSD)

PSD is a statistical measure defined as the limiting mean-square value of a random variable. It is used in a random vibration analysis in which the instantaneous magnitudes of

the response can be specified only by a probability distribution function that shows the probability of the magnitude taking a particular value. A PSD is a statistical measure of the response of a structure to random dynamic loading conditions. It is a graph of the PSD value versus frequency where the PSD may be a displacement PSD, velocity PSD, acceleration PSD, or a force PSD. Mathematically spoken, the area under a PSD-versus-frequency curve is equal to the variance that is simply the square of the standard deviation of the response.

Similarly to the response spectrum analysis a random vibration analysis may be single-point or even multi-point. In a single-point random vibration analysis you specify one PSD spectrum at a set of points. In a multi-point random vibration analysis, you specify different PSD spectra at different points.

3.7 Various Possibilities to Model the Effect of Damping in ANSYS

In nature, every dynamic process is subjected to the effect of damping. A totally undamped vibration actually does not exist in reality. In ANSYS, there are several possibilities available to model the effect of structural damping. The aim of this chapter is to give an overview of currently existing damping models of ANSYS. Since not every kind of damping can be applied in each solution method that is available for the different calculation disciplines, we have to discuss which damping model can be used in which solution method.

Assuming that the damping matrix in the equation of motion (3.1) is set up directly and no transformation into the modal subspace is performed the following formulation can be given taken from:

$$C = \underbrace{\alpha.M + \beta.K}_{1} + \underbrace{\sum_{i=1}^{NMAT} \beta_i.K_i}_{3} + \underbrace{\beta_c.K}_{3} + \underbrace{\sum_{j=1}^{NEL} C_j}_{4} \tag{3.5}$$

The first term in equation (3.5) represents the well-known Rayleigh damping. Clearly, this part of the damping matrix is proportional to the total mass and stiffness matrix of the system. Damping which is proportional to the total mass matrix is often called « α » damping whereas damping proportional to the total stiffness matrix is often called « β » damping. The second term describes material dependent damping since the element stiffness matrices covering the same material properties are just multiplied by a constant factor. If just one material is used the second term is actually identically with « β » damping. The third term is only used in a full or reduced harmonic response analysis and will therefore be discussed later. The fourth term of equation (3.5) describes damping due to the presence of discrete damping elements.

We describe below which kind of damping can be used considering the different dynamic calculation methods mentioned in this paper so far:

3.7.1 Modal analysis including damping

In a modal analysis, the user can apply Rayleigh damping as well as material dependent damping. Furthermore, discrete damping elements can be used. The available eigensolver for this purpose can be the Damped Method or the QR Damped Method. These eigensolver have been already characterized in detail together with typical applications. We should mention again that the QR Damped Method reduces the required solution time for a damped modal analysis significantly when compared with the Damped Method.

3.7.2 Transient dynamic analysis including damping

In a transient dynamic analysis that is performed using the Full or the Reduced Method, Rayleigh damping can be specified as well as material dependent damping. Discrete damping elements may also be used.

3.7.3 Harmonic response analysis including damping

Considering the harmonic response analysis solved by the Full or Reduced Method the user is not just able to specify Rayleigh damping, material dependent damping or even make use of discrete damping elements. With the third term of equation (3.5) it is also possible to specify a constant damping ratio regardless of each natural frequency. Remember that the damping ratio is defined as the ratio between the actual damping and the critical damping itself. The specified damping ratio for the harmonic response analysis is internally used to get the stiffness matrix multiplier β_c appearing in equation (3.5) which further depends on each imposed exciting frequency.

3.7.4 Performing a dynamical analysis in the modal subspace including damping

It has been mentioned earlier that a transient dynamic analysis or a harmonic response analysis can be solved much more efficiently considering the required solution time if they are performed in the modal subspace so that the modal superposition technique can be applied.

We have also mentioned that a spectrum analysis cannot be performed without modal superposition. Remember that the basis of the modal superposition technique is the decoupling process of the equation of motion (3.3) into generalized single degree of freedom models.

This decoupling process only works properly if Rayleigh damping is specified which finally results in a modal damping ratio depending on the parameters « α » and « β ». Additionally, a constant modal damping ratio for all modes and an individual damping ratio for each mode can be specified when working in the modal subspace independently of « α » and « β ». This results in the following formulation for the total modal damping ratio which is taken from :

$$\xi_i = \underbrace{\frac{\alpha}{2.\omega_i} + \frac{\beta.\omega_i}{2}}_{1} + \underbrace{\xi}_{2} + \underbrace{\xi_{mi}}_{3} \tag{3.6}$$

In equation (Eq. 3.6) the first term represents « α » and « β » damping. The second one describes the constant modal damping ratio used for all modes and the third term represents the individual modal damping ratio which can be prescribed for each single mode differently.

It has been mentioned already that it is quite convenient to perform a dynamic analysis in the modal subspace since the dimension of the problem is reduced according to the number of mode shapes you consider. However, the modal superposition technique in its classical form cannot take into account the effects of non-proportional damping, i.e. when material dependent damping is used or discrete damping elements are present. In such a case the decoupling process of the resulting damping matrix does not work properly.

Nevertheless, if the user wants to apply non-proportional damping but also likes to take advantage of working in the modal subspace ANSYS provides a special method to do this. The modal analysis has to be done by using the QR Damped Method as an eigensolver. Every kind of non-proportional damping can be considered further in a transient, harmonic or in a spectrum analysis when performed in the modal subspace. Hence, the QR Damped

Method does not just reduce the solution time in a modal analysis it also enables the user to work in the modal subspace with non-proportional damping which results again in a better performance considering the solution speed.

3.8 ANSYS Contact Capabilities

Contact problems fall into two general classes: rigid-to-flexible and flexible-to-flexible. In rigid-to-flexible contact problems, one or more of the contacting surfaces are treated as rigid (i.e., it has a much higher stiffness relative to the deformable body it contacts). In general, any time a soft material comes in contact with a hard material, the problem may be assumed to be rigid-to-flexible. The other class, flexible-to-flexible, is the more common type. In this case, both (or all) contacting bodies are deformable. An example of a flexible-to-flexible contact is bolted flanges.

ANSYS supports five contact models: node-to-node, node-to-surface, surface-to-surface, line-to-line, and line-to-surface. Each type of model uses a different set of ANSYS contact elements and is appropriate for specific types of problems.

To model a contact problem, you first must identify the parts to be analyzed for their possible interaction. If one of the interactions is at a point, the corresponding component of your model is a node. If one of the interactions is at a surface, the corresponding component of your model is an element: either a beam, shell, or solid element. The finite element model recognizes possible contact pairs by the presence of specific contact elements. These contact elements are overlaid on the parts of the model that are being analyzed for interaction. The different contact elements that ANSYS uses, and procedures for using them, are described in the remaining chapters of ANSYS guides.

At this stage we will present sorface-to-surface contact element which will be used in the thesis work.

3.8.1 Surface-to-Surface Contact Elements

ANSYS supports both rigid-to-flexible and flexible-to-flexible surface-to-surface contact elements. These contact elements use a "target surface" and a "contact surface" to form a contact pair.

- The target surface is modeled with either TARGE169 or TARGE170 (for 2-D and 3-D, respectively).
- The contact surface is modeled with elements CONTA171, CONTA172, CONTA173, and CONTA174.

To create a contact pair, assign the same real constant number to both the target and contact elements. You can find more details on defining these elements and their shared real constant sets in "Surface-to-Surface Contact".

These surface-to-surface elements are well-suited for applications such as interference fit assembly contact or entry contact, forging, and deep-drawing problems. The surface-to-surface contact elements have several advantages over the node-to-node element CONTA175. These elements:

- Support lower and higher order elements on the contact and target surfaces (in other words, corner-noded or midside-noded elements).
- Provide better contact results needed for typical engineering purposes, such as normal pressure and friction stress contour plots.

- Have no restrictions on the shape of the target surface. Surface discontinuities can be physical or due to mesh discretization.

Using these elements for a rigid target surface, you can model straight and curved surfaces in 2-D and 3-D, often using simple geometric shapes such as circles, parabolas, spheres, cones, and cylinders. More complex rigid forms or general deformable forms can be modeled using special preprocessing techniques.

Surface-to-surface contact elements are not well-suited for point-to-point, point-to-surface, edge-to-surface, or 3-D line-to-line contact applications, such as pipe whip or snap-fit assemblies. You should use the node-to-surface, node-to-node, or line-to-line elements in these cases. You also can use surface-to-surface contact elements for most contact regions and use a few node-to-surface contact elements near contact corners.

The surface-to-surface contact elements only support general static and transient analyses, buckling, harmonic, modal or spectrum analyses, or substructure analyses.

3.9 Conclusion

In this chapter, we have given an overview of the present capabilities of ANSYS in the field of structural dynamics. Various computation disciplines have been discussed together with available algorithms of ANSYS. Considering the solution speed of eigenvalue problems we have focused on a few quite powerful eigenvalue solvers available in ANSYS especially the QR Damped Method and the Powerdynamics Method that decrease the required solution time significantly. In addition, we have mentioned that this algorithm is able to perform a transient, harmonic and also a spectrum analysis quite efficiently in the modal subspace even if non-proportional damping is modelled.

It is important to note that the totality of this chapter is taken from the course of Erke Wang and Thomas Nelson (2001) about Ansys applicability.

CHAPTER 4

Dam Description, Generation of Data Base, and Inputs

CHAPTER 4

Dam Description, Generation of Data Base, and Inputs

4.1 Introduction

This section is dedicated to « Brezina » case study dam description, different materials properties and the different elements used in the modeling of dynamic foundation-fluid-dam interaction by ANSYS finite element code.

4.2 Dam Description

The concrete gravity arch dam of Brezina is located in El Beyadh at the west of Algeria. It transmits part of its actions to both sides of the valley through arching effect, whereas the bottom part acts on the foundation.

The dam is 60 m high, its maximum arch length is 78.5 m and its thickness varies from 5m at the crest to 36.3 m at the foundation level. Figure 4.1 shows Brezina concrete arch dam location, and Figure 4.2 illustrates its actual geometry.

Figure 4.1: Location of Brezina Concrete Arch Dam in Algeria map.

Figure 4.2: Brezina concrete arch dam.

Figure 4.3 and Table 4.1 present the geometrical characteristics used to model Brezina dam.

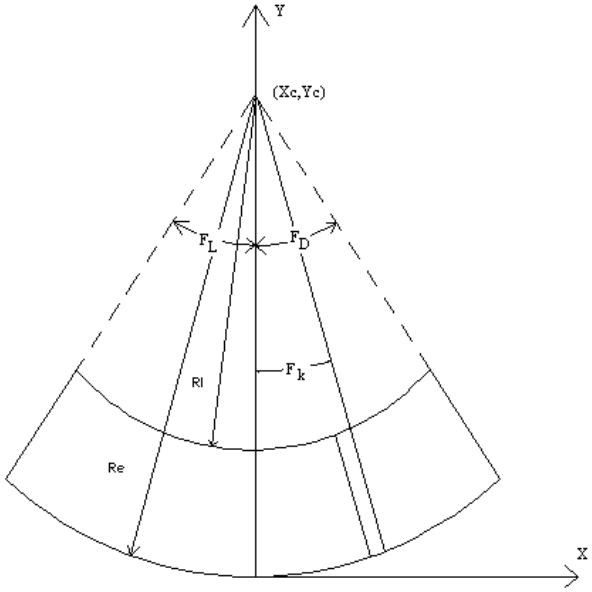

Figure 4.3: Geometrical characteristics of Brezina dam.

Elevation	Re	RI	F_L	F_D	X_c	Y_c
m	m	m	degree	degree	m	m
910	67.8	62.8	34.7	34.7	0	67.8
900	67.8	56.8	34.7	34.7	0	67.8
890	65	50.8	33	34.7	0	67.8
880	65	44.8	31	34.7	0	67.8
870	65	28.7	23	20	0	67.8
860	65	28.7	13	15	0	67.8
850	65	28.7	1.5	5	0	67.8

Table 4.1: Geometrical characteristics of Brezina dam.

The material properties used for the next applications are summarized in Table 4.2 for concrete dam and foundation rock, and in Table 4.3 for reservoir water respectively. :

Material	Young's Modulus (N/m^2)	Poisson's ratio	Density (kg/m^3)
Concrete dam	28.5e+09	0.2	2500
Foundation rock	14.5e+09	0.25	2100

Table 4.2: Material properties of Brezina concrete dam and its rock foundation

Compressibility Modulus (N/m^2)	Poisson's Ratio	Density (kg/m^3)	Viscosity
2.068E+09	0.49	1000	0.001

Table 4.3 : Reservoir water properties

4.3 Dam-foundation rock finite element Geometry

The dam-foundation rock system is investigated using 2D finite element models in one hand and 3D finite element models in the other hand.

4.3.1 2D finite element Geometry:

For the 2D finite element representation, two models are used; the first one represent the dam only (without surrounding rock), however the second on represent the dam with adjacent rock.

PLANE 42 is used for 2-D modeling of solid structures. The element can be used either as a plane element (plane stress or plane strain) or as an axisymmetric element. The element is defined by four nodes having two degrees of freedom at each node: translations in the nodal x and y directions. The geometry, node locations, and the coordinate system for this element are shown in Figure 4.4, The element input data includes four nodes, a thickness (for the plane stress option only) and the orthotropic material properties.

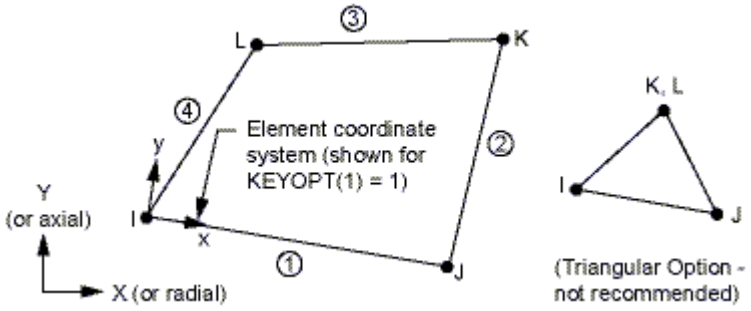

Figure 4.4: PLANE 42 Geometry (ANSYS help, version 2011)

Another 2D finite element is used to model the cylindrical tank in chapter 8; it is about SHELL 181 sketched in figure 4.5. SHELL 181 is suitable for analyzing thin to moderately-thick shell structures. It is a 4-node element with six degrees of freedom at each node: translations in the x, y, and z directions, and rotations about the x, y, and z-axes. (If the membrane option is used, the element has translational degrees of freedom only). The degenerate triangular option should only be used as filler elements in mesh generation.

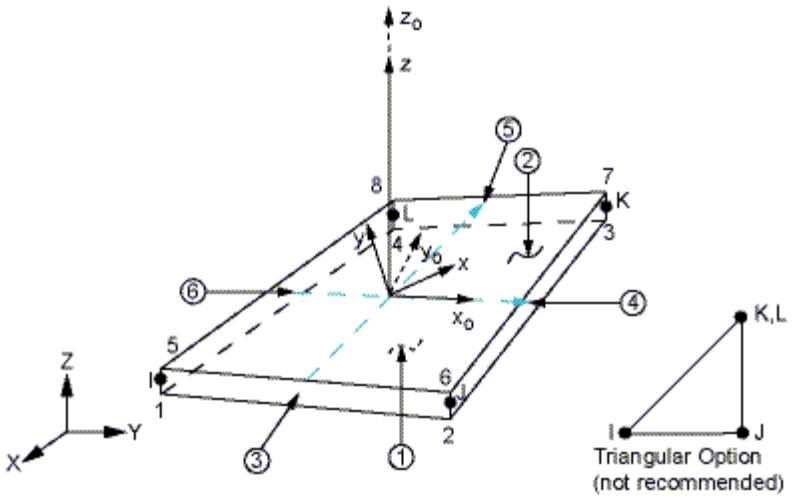

x_o = Element x-axis if ESYS is not provided.

x = Element x-axis if ESYS is provided.

Figure 4.5: SHELL 181 Geometry (ANSYS help, version 2011)

4.3.2 3D finite element Geometry:

As for the 2D finite element representation, the 3D one also contains two models: the dam without rock foundation model and the dam with adjacent rock foundation model.

SOLID185 is used for the 3-D modeling of solid structures. It is defined by eight nodes having three degrees of freedom at each node: translations in the nodal x, y, and z directions. The element has plasticity, hyperelasticity, stress stiffening, creep, large deflection, and large strain capabilities. It also has mixed formulation capability for simulating deformations of nearly incompressible elastoplastic materials, and fully incompressible hyperelastic materials. Figure 4.6 shows SOLID185 element geometry.

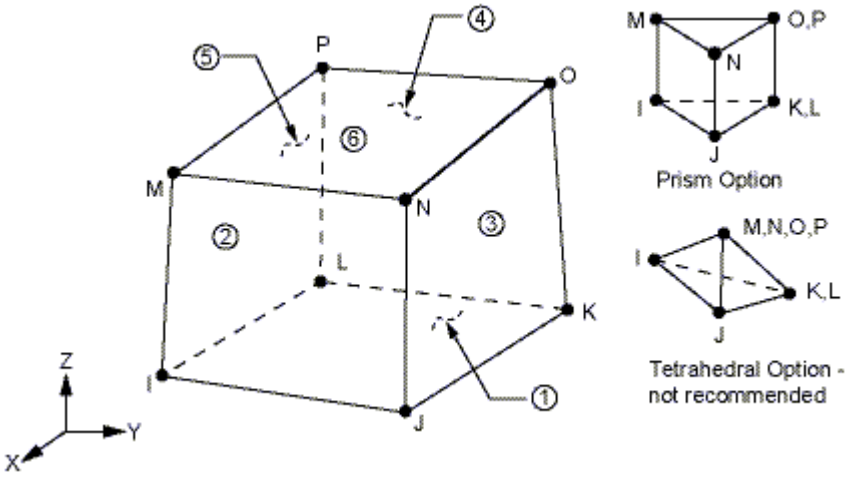

Figure 4.6: SOLID185 Geometry (ANSYS help, version 2011)

4.4 Fluid finite element models

To model the fluid two, approaches are chosen, in the first one the fluid is modeled as added mass which represent *added mass* approach using *surf element* available in ANSYS Library, however in the second approach, the reservoir is modeled by fluid element already available in ANSYS Library. Depending on the finite element model kind which means if the

model is in two dimensions (2D) or three dimensions (3D), two fluid elements are used; the FLUID 79 (for 2D modeling) and FLUID80 (for 3D modeling).

4.4.1 SURF153 (for 2D modeling)

SURF153 may be used for various load and surface effect applications. It may be overlaid onto a face of any 2-D structural solid element.

The geometry, node locations, and the coordinate system for this element are shown in Figure 4.7.

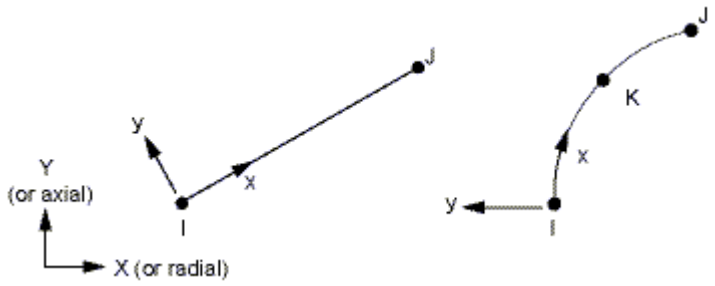

Figure 4.7: SURF153 Geometry (ANSYS help, version 2011)

The element is defined by two or three node points and the material properties. The element x-axis is along to the I-J line of the element. The mass calculation uses the density (material property DENS, mass per unit volume) and the real constant ADMSUA, the added mass per unit area. The stiffness matrix calculation uses the in-plane force per unit length (input as real constant SURT) and the elastic foundation stiffness using pressure-per-length (or force-per-length-cubed) units (input as real constant EFS). The foundation stiffness can be damped, either by using the material property DAMP as a multiplier on the stiffness or by directly using the material property VISC.

4.4.2 SURF154 (for 3D modeling)

SURF154 may be used for various load and surface effect applications. It may be overlaid onto an area face of any 3-D element. The element is applicable to 3-D structural analyses. Various loads and surface effects may exist simultaneously. The geometry, node locations, and the coordinate system for this element are shown in Figure 4.8. The element is defined by four to eight nodes and the material properties.

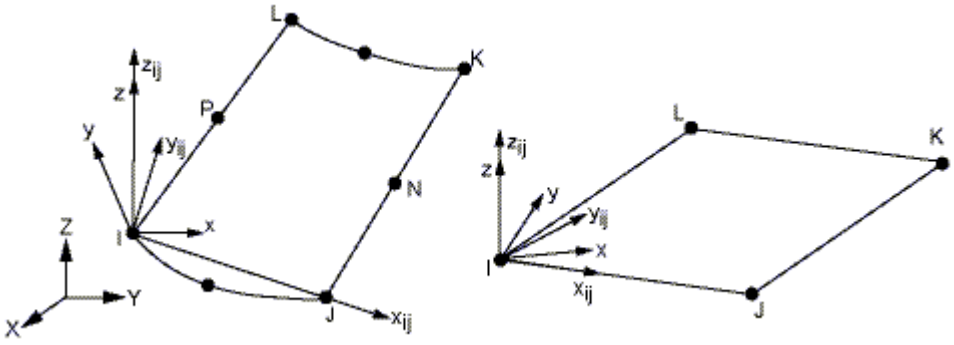

Figure 4.8: SURF154 Geometry (ANSYS help, version 2011)

The mass calculation uses the density (material property DENS, mass per unit volume) and the real constant ADMSUA, the added mass per unit area. The stiffness matrix calculation uses the in-plane force per unit length (input as real constant SURT) and the elastic foundation stiffness using pressure-per-length (or force-per-length-cubed) units (input

as real constant EFS). The foundation stiffness can be damped, either by using the material property DAMP as a multiplier on the stiffness or by directly using the material property VISC.

4.4.3 FLUID 79 (for 2D modeling)

FLUID79 is a modification of the 2-D structural solid element (PLANE42). The fluid element is used to model fluids contained within vessels having no net flow rate. The fluid element is particularly well suited for calculating hydrostatic pressures and fluid/solid interactions. Acceleration effects, such as in sloshing problems, as well as temperature effects, may be included. The fluid element is defined by four nodes having two degrees of freedom at each node: translation in the nodal x and y directions. The element may be used in a structural analysis as a plane element or as an axisymmetric ring element. The geometry, node locations, and the coordinate system for this element are shown in Figure 4.9.

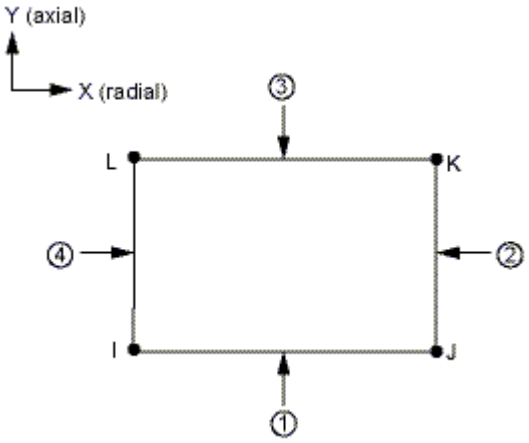

Figure 4.9: FLUID79 Geometry (ANSYS help, version 2011)

The element input data includes four nodes and the isotropic material properties. EX, which is interpreted as the "fluid elastic modulus", should be the bulk modulus of the fluid. The viscosity property (VISC) is used to compute a damping matrix for dynamic analyses.

4.4.4 FLUID80 (for 3D modeling)

FLUID80 is a modification of the 3-D structural solid element (SOLID45). The fluid element is used to model fluids contained within vessels having no net flow rate. The fluid element is particularly well suited for calculating hydrostatic pressures and fluid/solid interactions. Acceleration effects, such as in sloshing problems, as well as temperature effects, may be included.

The geometry, node locations, and the coordinate system for this element are shown in Figure 4.10.

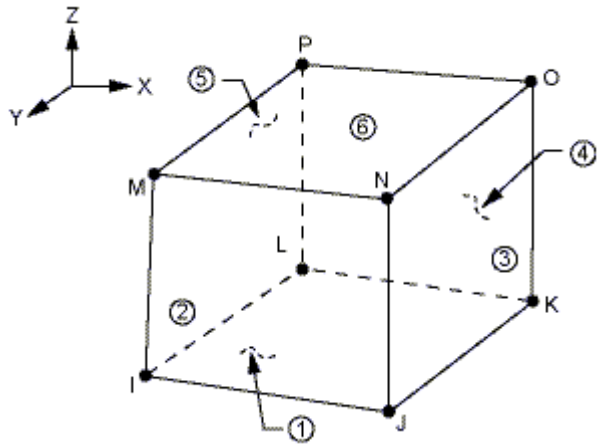

Figure 4.10: FLUID80 Geometry (ANSYS help, version 2011)

4.5 Interfaces finite element Geometry

Also in the next applications two contact elements type will be used depending already on whether the modeling is in two dimensions (2D) or in three dimensions (3D); we talk about CONTA172 (for 2D models) and CONTA174 (for 3D models).

4.5.1 CONTA172 (for 2D models)

CONTA172 is used to represent contact and sliding between 2-D "target" surfaces (TARGE169) and a deformable surface, defined by this element. The element is applicable to 2-D structural and coupled field contact analyses. It has the same geometric characteristics as the solid element face with which it is connected (Figure 4.11). Contact occurs when the element surface penetrates one of the target segment elements (TARGE169) on a specified target surface. Coulomb and shear stress friction is allowed. This element also allows separation of bonded contact to simulate interface delamination.

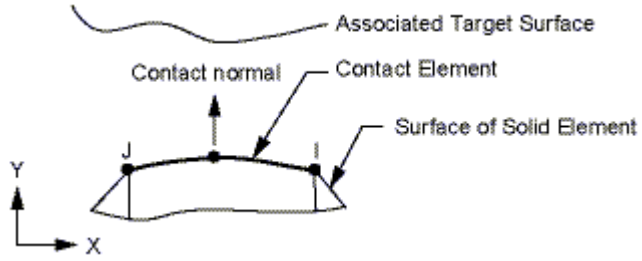

Figure 4.11: CONTA172 Geometry (ANSYS help, version 2011)

4.5.2 CONTA174 (for 3D models)

CONTA174 is used to represent contact and sliding between 3-D "target" surfaces (TARGE170) and a deformable surface, defined by this element. The element is applicable to 3-D structural and coupled field contact analyses. This element is located on the surfaces of 3-D solid or shell elements with mid-side nodes. It has the same geometric characteristics as the solid or shell element face with which it is connected (Figure 4.12). Contact occurs when the element surface penetrates one of the target segment elements (TARGE170) on a specified target surface. Coulomb and shear stress friction is allowed.

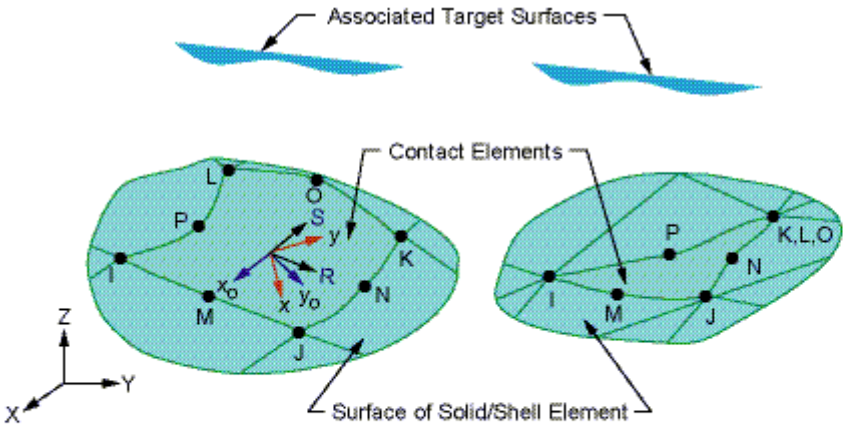

R = Element x-axis for isotropic friction

x_o = Element axis for orthotropic friction if **ESYS** is not supplied (parallel to global X-axis)

x = Element axis for orthotropic friction if **ESYS** is supplied

Figure 4.12: CONTA174 Geometry (ANSYS help, version 2011)

4.6 Conclusion

All elements discussed in this chapter will be used in the next chapters, where the case study dam will be modelized by Ansys finite element code.

CHAPTER 5

Dynamic foundation Structure Interaction Study using ANSYS

CHAPTER 5

Dynamic foundation Structure Interaction Study using ANSYS

5.1 Introduction

The effect of the surrounding rock foundation, as depicted by the foundation-structure interaction phenomenon, on the dynamic behavior of Brezina concrete gravity arch dam described in chapter 4 is investigated in the present one using “Direct method”. Both modal and transient analyses are performed for this dam using ANSYS finite element code.

The results of these analyses constitute a data base for a parametric study that treats the effect of the rock-structure interaction, the mass of rock foundation, and the viscous damping ratio on the dynamic behavior of Brezina concrete arch dam under three different generated synthetic earthquake excitations (Armouti, N.S. 2004) (with a peak ground acceleration equal to 0.2g).

It is important to note that the water effect is not taken into account in the present chapter. It is the target of the next chapters.

5.2 Finite Element Meshing of Brezina Concrete Arch Dam without foundation and Dam with Adjacent foundation Using ANSYS Software

The dam-foundation system is investigated using three 3D finite element models. The first model or dam alone, neglecting the foundation, represents the dam only, which is clamped at its base on the foundation (Figure 5.1). The second model or dam-massless foundation, represents the dam and the adjacent foundation but the foundation’s mass is neglected. The foundation is also clamped at its base (Figure 5.2). Lastly, the third model or dam-foundation with foundation mass, is similar to the second one, except that the mass of the foundation is taken into account (Figure 5.2). These finite elements models are created using the finite element commercial package, ANSYS, with a mapped meshing (Ansys theory manual, 2011). The finesse of the mesh has been determined by performing a convergence analysis (mesh sensitivity).

The first model, i.e., dam alone, possesses 972 quadratic solid elements (SOLID185) and 1378 nodes (Figure 5.1). The second and third model (with the foundation) exhibits 16252 quadratic solid elements and 19035 nodes (Figure 5.2).

The length and width of the foundation, along the global X and Y axis, respectively, are taken to be 150m, while its depth, along the Z direction, is taken to be 100 m. These sizes are chosen so that the applied boundary condition will not affect the modal responses of the dam.

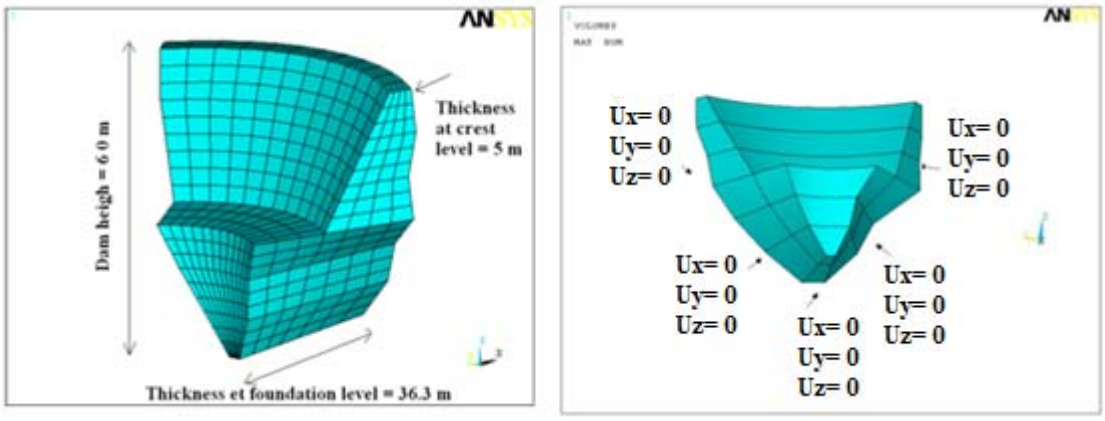

Figure 5.1 : 3D finite element model of Brezina arch dam without adjacent foundation and boundary conditions.

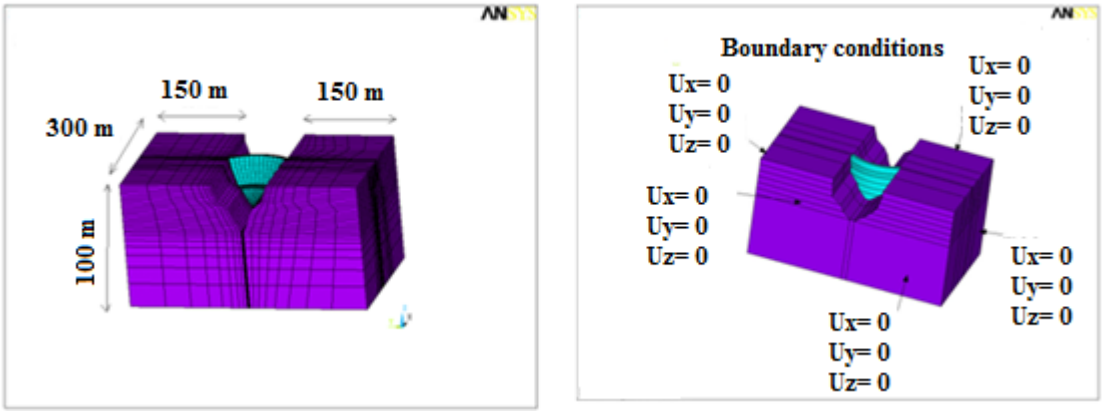

Figure 5.2: 3D finite element model of Brezina arch dam with adjacent foundation and boundary conditions.

5.3 Methodology

For each input motion (each generated record), the following cases are investigated:

- Neglecting the effect of dam-foundation interaction, i.e. assuming the structure as being fixed at its base, the foundation is assumed to be completely rigid (the modulus of elasticity is infinite).
- Linear dam-foundation interaction analysis assuming massless foundation (neglecting the inertial effect of foundation) having a modulus of elasticity equals to a half of the dam modulus of elasticity.
- Linear dam-foundation interaction analysis while allowing for the mass of the foundation (taking into account the inertial effect of the foundation) the foundation modulus of elasticity is taken as half of the dam concrete modulus of elasticity.
- All the analyses above are repeated for different earthquake records applied in x direction, and for different damping ratios (2%, 5% and 10%).

5.4 Generation of Data Base

5.4.1 Introduction

Earthquakes and consequently acceleration time histories are characterized by their randomness and their dependency on many factors that are also random such as: site

condition, earthquake source-to-site distance, earthquake magnitude, source-mechanism characteristics and others.

Using actual earthquake records in the design of earthquake-resistant structures does not always suit the actual conditions in terms of the above cited factors. Additionally, actual records do not cover all areas nor predict future earthquakes that may occur.

The resort is to develop synthetic acceleration time histories based on theoretical models that reflect the specified conditions.

5.4.2 Synthetic Earthquakes

Armouti (2004) developed a computer program named GNREQ for generation of synthetic earthquakes; this program is used in the present thesis to generate the required earthquake records. The program generates synthetic records to represent randomness of the earthquakes and to include site characteristics in the generation process such characteristics are given in terms of dominant ground frequency ω_g, ground damping ratio ζ_g and equivalent earthquake duration T_n.

The maximum duration of synthetic earthquakes is selected to 15 seconds and the corresponding circular frequency is 60 rad/second, these values are adopted because they are sufficient to express the earthquake effects, additional ground excitations are minimal at the end of these periods.

The site characteristic of the foundation of Brezina dam is rock and hence, its dominant ground frequency ω_g, ground damping ratio ζ_g, equivalent earthquake duration T_n, may be assigned according to Table 5.1 (Armouti, 2004).

foundation type	ω_g	ζ_g	T_n
Rock	8π	0.6	10

Table 5.1: Site condition parameters (Armouti, 2004).

Three artificial earthquakes are generated for rock foundation of Brezina arch dam using three different identified random numbers initializers as: 17962, 16454 and 18124 (the peak ground acceleration is maintained the same at 0.2 g). These three acceleration time histories are presented in Figure 5.3, Figure 5.4 and Figure 5.5 respectively.

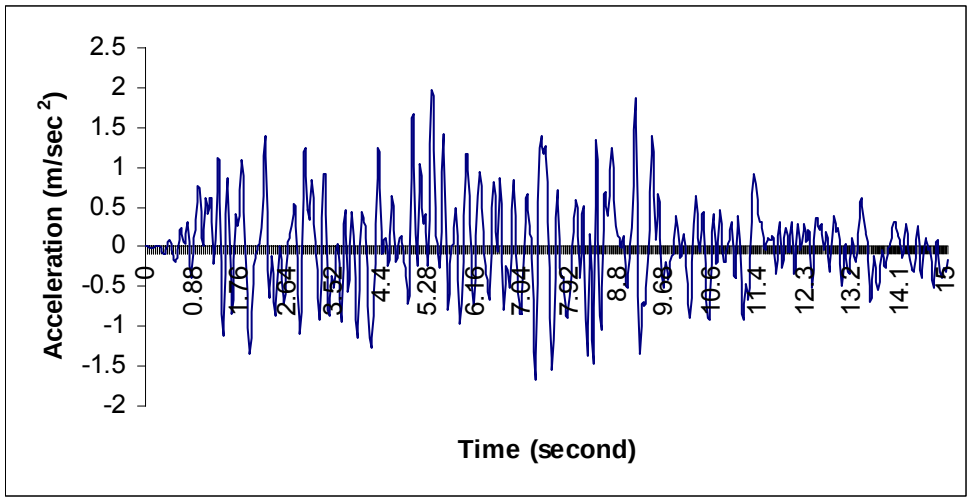

Figure 5.3: Acceleration time history for random number initializer equals to 17962 (PGA=0.2g).

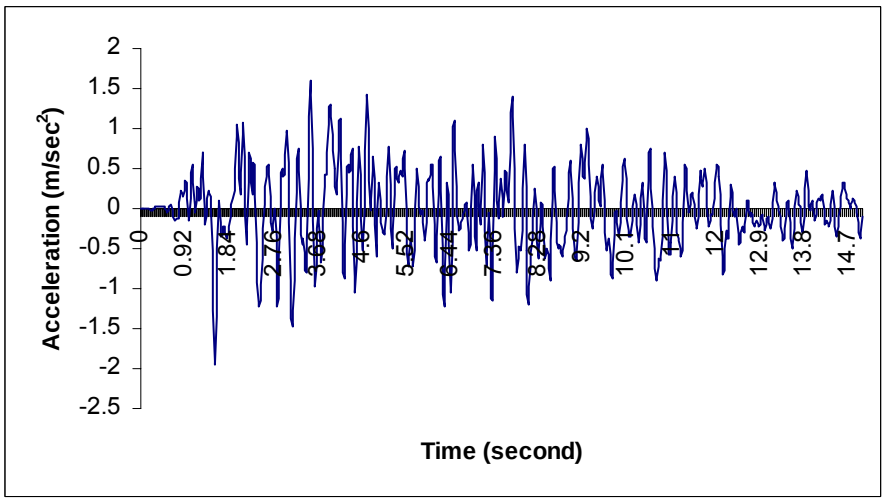

Figure 5.4: Acceleration time history for random number initializer equals to 16454 (PGA=0.2g).

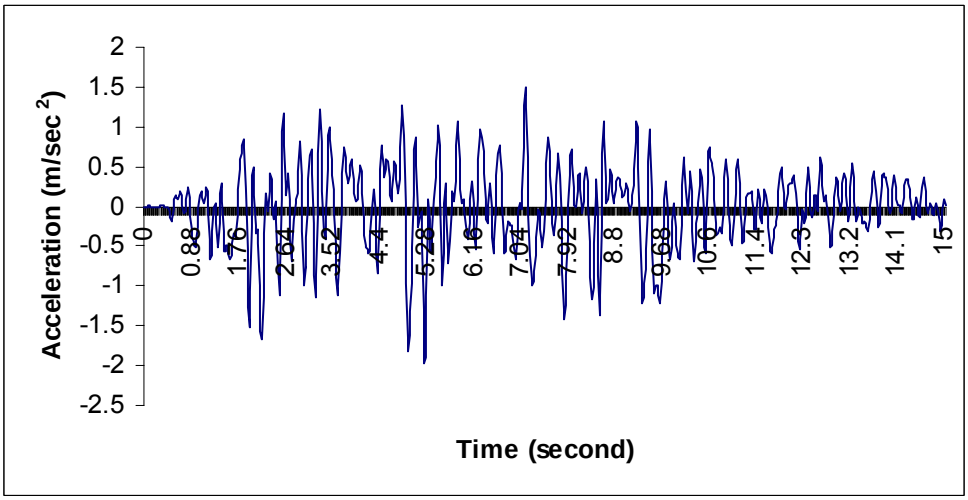

Figure 5.5: Acceleration time history for random number initializer equals to 18124 (PGA=0.2g)

5.5 Record Deconvolution Using Shake Program

As mentioned above, two models will be adopted for Brezina concrete arch dam. In the first one, analyses will be performed without considering the adjacent foundation, while in the second model the dam foundation is taken into account.

The second step of direct method procedure for studying SSI consist of calculating the motion at the bottom model base (which is chosen at a sufficient depth so that the presence of a structure at surface can not affect this motion), which means the necessity to do the deconvolution of the above generated synthetic earthquakes at the bottom model level. This process is to be achieved by Shake computer program but because the dam object of the present study is built on rock, the deconvoluted records are similar (with a very little variation) to the generated ones, because rock is reliable in transmitting seismic waves.

5.6 Dam Damping Ratios

Viscous damping is the damping of choice in many cases for describing the response of single degree of freedom dynamic systems. One of the main reasons for selecting viscous damping is associated with the fact that this damping is the most amenable for solving the dynamic equilibrium differential equation. When these concepts are extended to multiple degree of freedom systems, serious shortcomings come into play, because there is no such a clear relationship between the physical phenomena and its mathematical modelling (L. E. Garcia et al, 2003).

A multi-degree of freedom system with viscous damping under ground motion is described by the following equilibrium equations:

$$\underline{M}\ddot{\underline{U}} + \underline{C}\dot{\underline{U}} + \underline{K}\underline{U} = -\underline{M}\underline{I}\ddot{u}_g \qquad (5.1)$$

The force exerted by a viscous damper is proportional to the relative velocity between the two ends of the damper. The procedure to obtain the elements of the damping matrix $[C]$ is by imposing a unit velocity to one degree of freedom at a time, while maintaining the velocity of all other degrees of freedom in zero. The internal forces exerted in all degrees of freedom of the structure by the dampers affected by the unit velocity of the selected degree of freedom compose the column of the damping matrix corresponding to the selected degree of freedom (L. E. Garcia et al, 2003).

$$[C] = \begin{bmatrix} c_{1,1} & c_{1,2} & .... & c_{1,n} \\ c_{2,1} & c_{2,2} & .... & c_{2,n} \\ . & . & & . \\ . & . & & . \\ c_{n,1} & c_{n,2} & .... & c_{n,n} \end{bmatrix} \qquad (5.2)$$

Limitation in current knowledge about damping of structural materials, or structural members built with these materials; make the described procedure difficult to apply in most practical cases. The procedure generally involves approximations based on experimentally measured damping on structures that somewhat resemble the structure under study. These procedures generally employ what is called *modal damping*. Modal damping is based on the principle that the damping matrix can be uncoupled by the vibration modes obtained from the mass and stiffness properties. This means that matrix $[C]$ when pre-multiplied by $[\Phi]^T$ and post-multiplied by $[\Phi]$ turns into a diagonal matrix:

$$[\Phi]^T[C][\Phi]=[2\xi_i\omega_i] \tag{5.3}$$

In Eq. (5.3) $[2\zeta_i\omega_i]$ is a diagonal matrix and ζ_i is the viscous damping associated with mode « i ». This type of damping in which the damping matrix is uncoupled by the vibration modes obtained only from mass and stiffness matrices $[M]$ and $[K]$, is known as *classic damping*. However, we have to be careful that under this premise, the main property of the damping matrix is the possibility of being uncoupled by the computed modes, a mathematical property that has little relation to the physical phenomena (L. E. Garcia et al, 2003).

By stating that the damping matrix is a linear combination of mass $[M]$ and stiffness matrix $[K]$, where α and β are constants:

$$[C]=\alpha[M]+\beta[K] \tag{5.4}$$

The damping matrix can be uncoupled to produce the following result:

$$[\Phi]^T[C][\Phi]=\alpha[\Phi]^T[M][\Phi]+\beta[\Phi]^T[K][\Phi]=\alpha[I]+\beta[\omega^2]=[\alpha+\beta\omega_i^2] \tag{5.5}$$

Where $[\alpha+\beta\omega_i^2]$ is a diagonal matrix and each one of the terms of the diagonal corresponds to $2\xi_i\omega_i$. Then the damping coefficient ζ_i for each uncoupled equation is:

$$\xi_i=\frac{\alpha}{2\omega_i}+\frac{\beta\omega_i}{2} \tag{5.6}$$

Where:

α: Alpha damping or mass damping.

β: Beta damping or stiffness damping.

This type of damping is known as *Rayleigh damping*, and correspond to a particular case of the classic damping. From Eq. (5.6) it is evident that damping is a function of the corresponding mode frequency, being thus different for each mode. If we know experimentally obtained values for damping in two modes, say « r »and « s », it is possible to state two simultaneous equations from which we can solve for α and β:

$$\begin{Bmatrix}\xi_r\\ \xi_s\end{Bmatrix}=\frac{1}{2}\begin{bmatrix}\frac{1}{\omega_r} & \omega_r\\ \frac{1}{\omega_s} & \omega_s\end{bmatrix}\begin{Bmatrix}\alpha\\ \beta\end{Bmatrix} \tag{5.7}$$

If the damping coefficients of two modes are equal $(\xi=\xi_r=\xi_s)$, solution of the simultaneous equations leads to:

$$\begin{Bmatrix}\alpha\\ \beta\end{Bmatrix}=\frac{2\xi}{\omega_r+\omega_s}\begin{Bmatrix}\omega_r\omega_s\\ 1\end{Bmatrix} \tag{5.8}$$

Figure 5.6 shows the relationship between damping and frequency. Cases of damping being proportional only to the mass and proportional only to stiffness are also shown in the same figure.

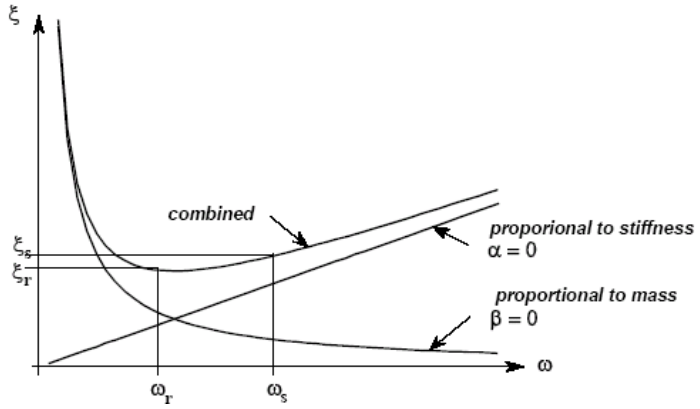

Figure 5.6: Relationship between damping and frequency for Rayleigh's damping (L. E. Garcia et al, 2003).

It is convenient to take ω_r as the value of the fundamental frequency and ω_s as the frequency corresponding to the last of the upper modes that significantly contribute to the response. This way the first mode and mode « s » will have exactly the same damping, and all modes in between will have somewhat smaller similar values and the modes with frequencies larger than ω_s will have larger damping values thus reducing their contribution to response (L. E. Garcia et al, 2003).

In many practical structural problems, alpha damping (or mass damping) may be ignored $(\alpha = 0)$ (it is specified only for bodies which resist to wind or for submarine applications) (Ansys theory manual, 2011). In such cases, β can be evaluated from known values of ξ_i and ω_i, as:

$$\beta = \frac{2\xi_i}{\omega_i} \tag{5.9}$$

5.7 Integration Time Step

For the time integration techniques, there is an important concept named "integration time step" noted Δt which is defined as the temporal increment from one temporal point to another.

The accuracy of the transient dynamic solution depends on the integration time step: the smaller the time step, the higher the accuracy. A time step that is too large will introduce error that affects the response of the higher modes (and hence the overall response). A time step that is too small will waste computer resources. To calculate an optimum time step, the following guidelines should be considered (Ansys theory manual, 2011):

- ✓ Resolve the response frequency. The time step should be small enough to resolve the motion (response) of the structure. Since the dynamic response of a structure can be thought of as a combination of modes, the time step should be able to resolve the highest mode that contributes to the response. For the Newmark time integration scheme, it has been found that using approximately twenty points per cycle of the highest frequency of interest results in a reasonably accurate solution. That is, if f is the frequency (in cycles/time), the integration time step (ITS) is given by

$$ITS = \frac{1}{20f} \tag{5.10}$$

Smaller ITS values may be required if acceleration results are needed (Ansys manual, version 11).

- ✓ Resolve the applied load-versus-time curve(s). The time step should be small enough to "follow" the loading function. The response tends to lag the applied loads, especially for stepped loads. Stepped loads require a small ITS at the time of the step change so that the step change can be closely followed. ITS values as small as Eq. 2.2 may be needed to follow stepped loads (Ansys theory manual, 2011).

$$ITS = \frac{1}{180f} \tag{5.11}$$

- ✓ Resolve the wave propagation. If you are interested in wave propagation effects, the time step should be small enough to capture the wave as it travels through the elements (Ansys theory manual, 2011)

$$ITS \le \frac{\Delta x}{3c} \tag{5.12}$$

Δx : Element size

$$\Delta x \le \frac{L}{20} \tag{5.13}$$

L : The structure length along the waves direction.

c : Elastic wave velocity.

$$c = \sqrt{\frac{E}{\rho}} \tag{5.14}$$

E : Young's modulus.

ρ : Mass density.

For transient dynamic analysis which is the present study type Eq. 2.1 is the more important (Ansys theory manual, 2011).

5.8 Recaptulation

At first, seismic free field input motion at ground surface is determined. This is achieved by analyzing the unexcavated virgin foundation in the absence of the structure.

The free field motion will be calculated using the power spectral density for the foundation. To carry out this step, computer program GNREQ is utilized (Armouti, N.S, 2004).Then the deconvolution of this motion is carried out using the computer program "Shake".

In the second step the rock foundation-structure behavior is assumed linear.

In the third step, the analysis of the foundation-structure system under the action of ground motion determined in the first step; and using the linear foundation-structure behavior assumed in second step, the analysis is carried out using ANSYS (Saeed Moaveni 1999).

The analysis is carried out for different damping ratios, using two assumptions of rock foundation (mass and massless foundation), and two values of foundation modulus of elasticity, infinite value (rigid base), and half the modulus of elasticity of the dam (Table 4.2).

It is important to note that for each case of analysis named above, modal analysis must be done to calculate the fundamental frequency and consequently to calculate the value of structural damping β from the assumed damping ratio using Eq.(5.9). The results are tabulated, presented graphically, analyzed and compared.

5.9 Dynamic Analysis and Parametric Study

5.9.1 Modal Analysis

The five lowest natural frequencies and the corresponding effective masses and participation factors of Brezina dam without foundation, Brezina dam with massless foundation, and Brezina dam with mass foundation are presented in Table 5.2, Table 5.3, and Table 5.4, respectively.

Mode	Frequency (Hz)	Effective mass (Kg)	Participation factor
1	12.42	0.3078e+08	5548.5
2	18.56	219.850	-14.827
3	24.83	0.2918e+08	-5402.2
4	26.53	0.1062e+08	3259.9
5	27.80	38388.0	-195.93

Table 5.2: The first ten natural frequencies of the dam without foundation.

Mode	Frequency (Hz)	Effective mass (Kg)	Participation factor
1	9.334	0.5948e+08	7712.6
2	13.67	872.768	-29.543
3	14.28	0.3305e+08	5749.5
4	16.27	59275.8	-243.47
5	16.78	0.3838e+08	-6195.4

Table 5.3: The first ten natural frequencies of the dam with massless foundation.

Mode	Frequency (Hz)	Effective mass (Kg)	Participation factor
1	6.48	0.10664e+08	-3265.6
2	6.90	112.840	-10.623
3	7.40	33858.1	184.01
4	7.83	0.52358e+10	72359.
5	8.57	0.16137e+10	-40172.

Table 5.4: The first ten natural frequencies of the dam with mass foundation.

Table 5.2, shows that frequencies are very important; vary between 12.42 Hz and 27.80 Hz, which implies that the dam is very rigid, this is obvious as the dam is fixed end.

From Tables 5.3 and 5.4, it is clear that for the case of dam with massless foundation, the frequencies are much greater than those for the case of the dam with mass foundation. This is due to the fact that the mass matrix is located at the denominator in the frequency formula, thus decreasing the mass leads to increased the frequency and vice versa.

5.9.2 Transient Analysis

A transient analysis using full Newmark method is performed for the three models representing Brezina concrete arch dam using ANSYS finite element code. Three generated records are used having the same peak ground acceleration (0.2 g) and different random numbers initializers and assuming three values of viscous damping (three values of structural damping β).

Using Eq. (5.11) leads to an integration time step equals to 0.005 but after a sensitivity analysis and because of the huge size of the output file and also the long duration of the run operation a time step of 0.01 second is judged sufficient.

It is important to denote that the results of the transient analysis are presented below for one synthetic earthquake record having an initialized number of 17962 but these results remain applicable for the three other generated earthquakes having initialized numbers of 16454 and 18124.

a. Displacements Comparison

Figure 5.7, Figure 5.8, and Figure 5.9 represent the displacement contours in x direction for the dam without foundation, dam with massless foundation, and dam with mass foundation respectively subjected to the first generated record of random number initializer of 17962 with a damping ratio equal to $\xi = 0.05$.

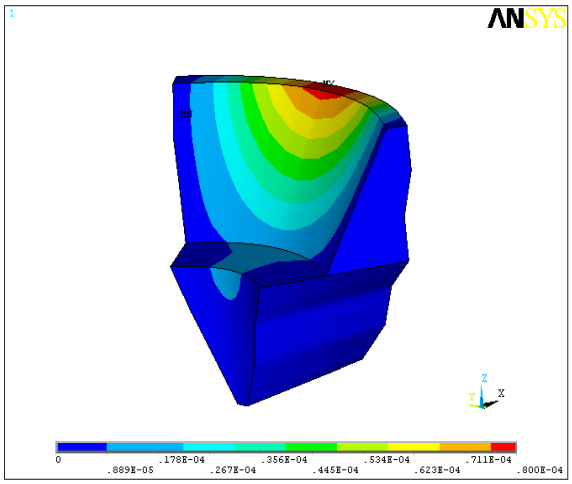

Figure 5.7: Nodal displacement contours (m) in x direction for dam without foundation for $\xi = 0.05$ and random number initializer of 17962

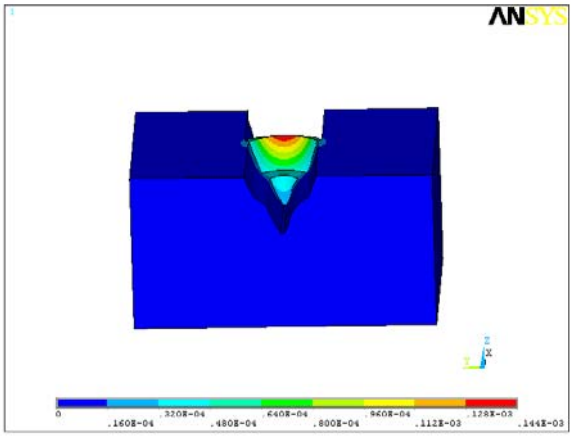

Figure 5.8: Nodal displacement contours (m) in x direction for dam with massless foundation for $\xi = 0.05$ and random number initializer of 17962

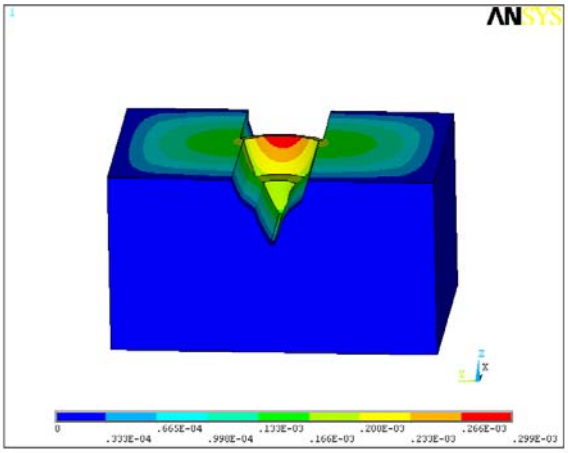

Figure 5.9: Nodal displacement contours (m) in x direction for dam with mass foundation for $\xi = 0.05$ and random number initializer of 17962.

It is important to note that the maximum displacements in the dam structure occur at the same nodes for the case of the dam without foundation and the dam with foundation. For example the maximum displacement in x direction occurs at node 123 located at the middle

crest of the dam without foundation in the downstream face, which is the node 339 in the case of dam with foundation (the same results are obtained in Y and Z direction).

Figure 5.10, Figure 5.11, and Figure 5.12 represent a comparison of the displacements for the crest part of the dam structure in x, y, and z directions for the three studied cases (dam without foundation, dam with massless foundation, and dam with mass foundation) for viscous damping ratio equal to $\xi = 0.05$ and generated record of random number initializer of 17962.

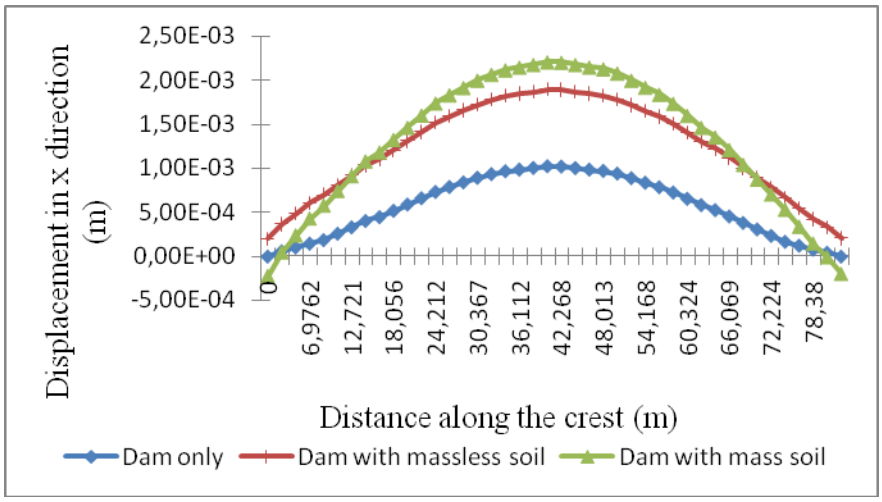

Figure 5.10: Displacements in x direction along the crest for the three studied cases for $\xi = 0.05$ and random number initializer of 17962.

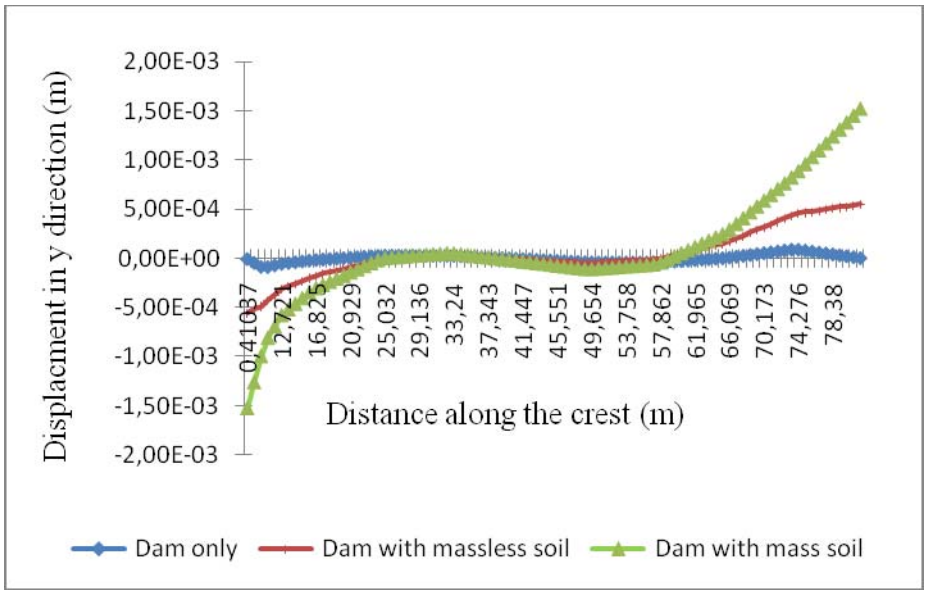

Figure 5.11: Displacements in y direction along the crest for the three studied cases for $\xi = 0.05$ and random number initializer of 17962.

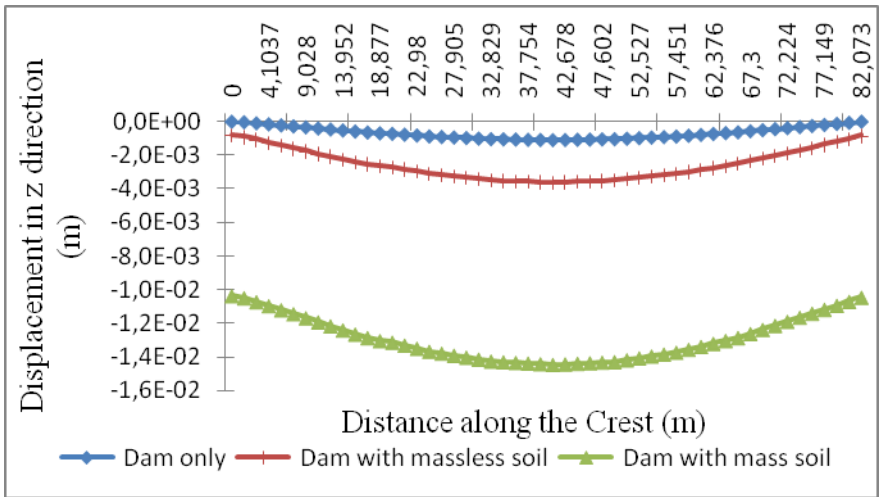

Figure 5.12: Displacements in z direction along the crest for the three studied cases for $\xi = 0.05$ and random number initializer of 17962.

From these figures two observations can be made:

The first one is that the case of the dam with foundation leads to more displacements amplitude than the case of the dam without foundation, where the foundation is modeled by fixed end supports. This is due to the presence of the foundation which gives more flexibility to the dam body to displace.

The second observation is that displacements are larger when the foundation mass is considered than for the case of massless foundation. The results of modal analysis can be used to interpret this observation; Table 5.3 and Table 5.4 show that frequencies for the case of dam with mass foundation are less than those for the case of dam with massless foundation which means that the periods and, consequently, the displacements of the first case are greater than those for the second case. This is not enough to take conclusions. For design purposes, stresses are of great interest.

b. Stress Variation

As for the displacement contours, the maximum stresses in the dam structure occur at the same nodes for the case of the dam without foundation and the dam with foundation.

Since the response of the dam is complex, the maximal stresses obtained are represented for the two essential parts of the upstream face of the dam: the central zone with its cantilever effect and the crest with its arch effect.

Figure 5.13, Figure 5.14, Figure 5.15, and Figure 5.16 represent a comparison of the maximal stresses in x, y, z direction as well as Von Mises stress respectively for the three studied cases; dam without foundation, dam with massless foundation, and dam with mass foundation.

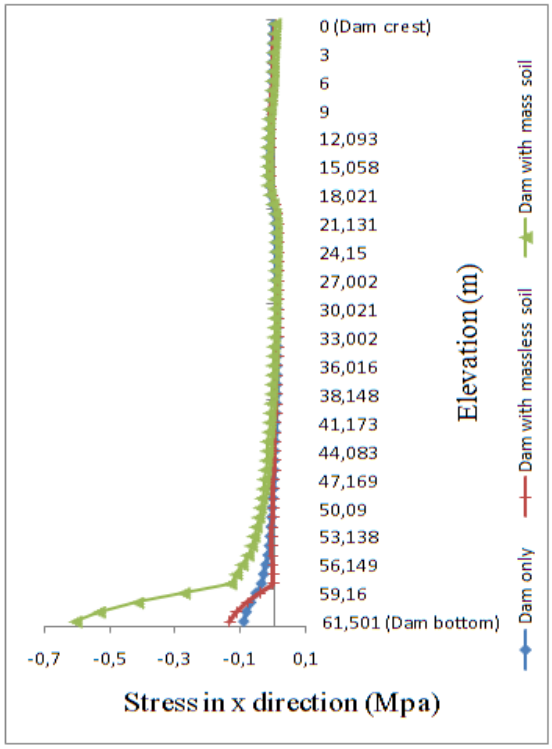

Figure 5.13: Variation of stresses in x direction in the central part of the dam for the three cases studied for $\xi = 0.05$ and random number initializer of 17962

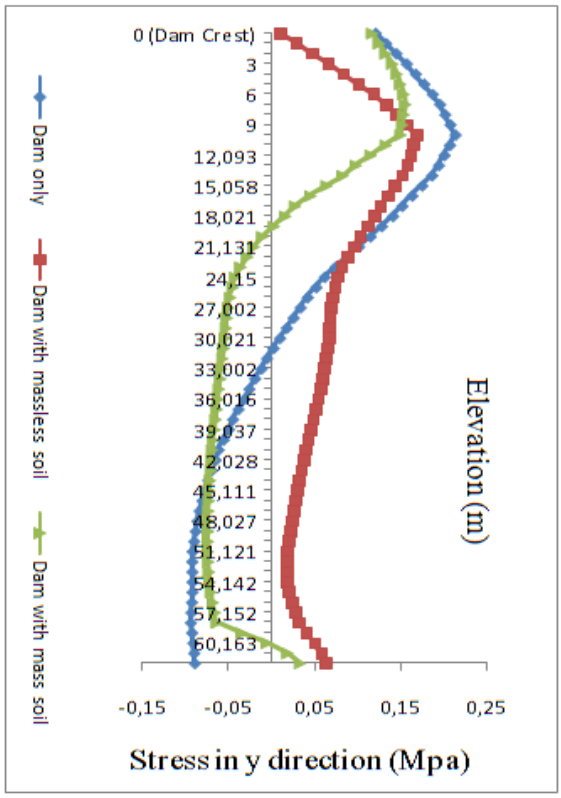

Figure 5.14: Variation of stresses in y direction in the central part of the dam for the three cases studied for $\xi = 0.05$ and random number initializer of 17962

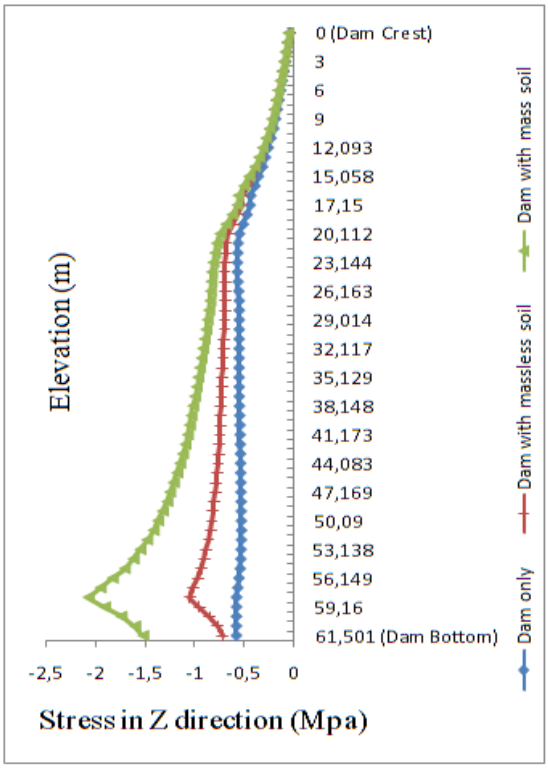

Figure 5.15: Variation of stresses in z direction in the central part of the dam for the three cases studied for $\xi = 0.05$ and random number initializer of 17962.

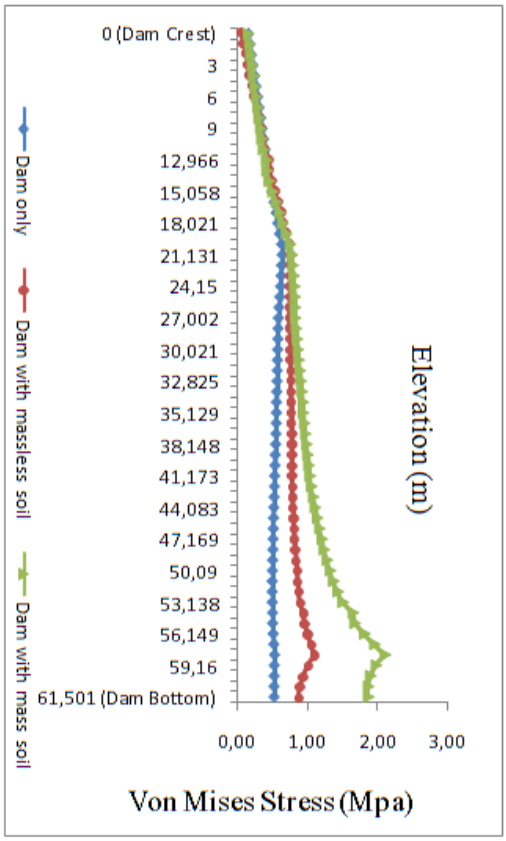

Figure 5.16: Variation of Von Mises stresses in the central part of the dam for the three cases studied for $\xi = 0.05$ and random number initializer of 17962.

It can be seen from the previous three figures that the presence of foundation develops more stresses in the dam body compared with the case of dam without foundation, furthermore, when the foundation is modeled as mass foundation, the same results are obtained along the crest part of the dam for the three cases studied.

c. Effect Of Viscous Damping On Displacement And Stress For The Three Cases Studied

The present study shows that damping ratio has a very small effect on the dynamic behavior of the dam without foundation, the dam with massless foundation, and the dam with mass foundation, where the stresses increase with decreasing the damping ratio which is obvious.

5.10 Discussion of Results and conclusion

From this parametric study, the following conclusions can be drawn:

- ✓ The case of the dam with foundation is more conservative; it develops more displacement amplitude and more stresses than the case of dam without foundation.
- ✓ The case of the dam with mass foundation is more conservative than the dam with massless foundation.
- ✓ The damping ratio has a very small effect on the dynamic behavior of the dam without foundation, the dam with massless foundation, and the dam with mass foundation, where the stresses increase with decreasing the damping ratio which is obvious.

To interpret the first two results, response spectra (maximum accelerations as function of the natural periods of vibration) which excite the natural periods of the three models need to be compared. In this study, response spectra are constructed using customized program RESSPEC (Armouti, N.S, 2004). Figure 5.17 depicts the response spectra for the first record having an initializer number of 17962 for the three damping ratios (2%, 5% and 10%) which excite the natural periods of the dam (for the three studied cases).

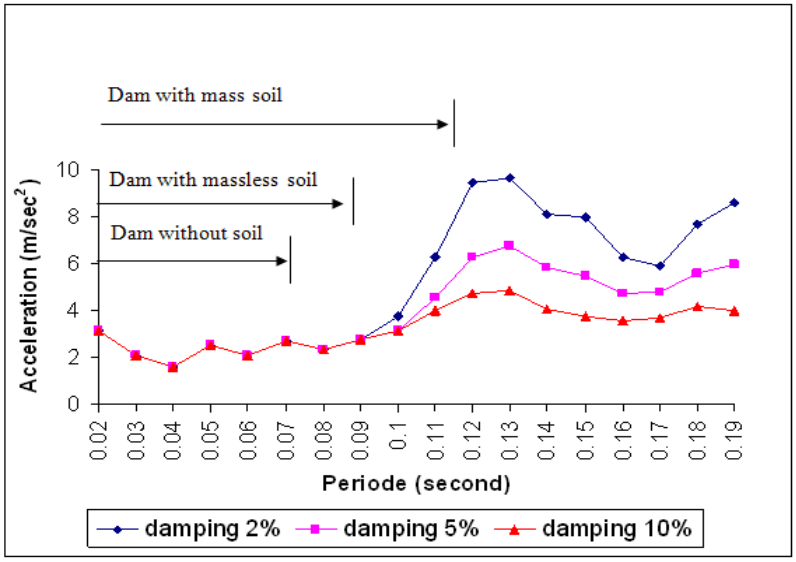

Figure 5.17: Response spectrum for the record of initializer number of 17962 at different damping ratios.

From Figure 5.17, it is clear that the spectral accelerations that excite the dam without foundation is smaller than that with foundation (both mass and massless foundation) which means that neglecting the foundation is not safe in term of design.

The dam with foundation is more excited than the dam without foundation, which justifies the difference of stresses and displacement for the different cases studied. This is due to the fact that the modulus of elasticity of the rock foundation for the case of dam with foundation is less than the modulus of elasticity of the rock foundation for the case of dam without foundation where the foundation is modeled as a fixed support (which means that the modulus of elasticity is infinite).

Adding the foundation to the dam leads to a change in the system dynamic properties (natural frequencies) and consequently a change in its total response. This is known as the foundation-structure interaction. The foundation with its properties (which are totally different from those of the dam) affect the dam and vice versa.

The presence and the behavior of the rock foundation have an important effect on the dynamic response of the dam structure. This response depends on the dynamic properties of the dam itself, the rock foundation and the excitation (record).

Taking the mass of the rock foundation into account proved to be more conservative than ignoring it. Since *Brezina* dam is embedded in rock, the foundation mass surrounding the dam will participate in the interaction by its inertial force exerted on the dam, and consequently, the interaction effect becomes more pronounced than the case where the foundation is considered massless (the foundation inertial effect is ignored).

CHAPTER 6

Undamped and Damped Modal Response of Dam Foundation Interaction using ANSYS

CHAPTER 6

Undamped and Damped Modal Response of Dam Foundation Interaction using ANSYS

6.1 Introduction

In this chapter, modal undamped and damped responses of the Brezina concrete arch dam taking into account structure interaction effect, are determined using the finite elements commercial packages ANSYS. It is well known that real modes, which are obtained assuming free natural vibrations without damping, can be used as a modal base in a modal superposition analysis, e.g. a spectrum analysis, where damping is small. However, for structures exhibiting significant viscous damping, for example a damping ratio of 5 percent, real modes might not be appropriate. In this case complex modes should be employed rather (Ansys theory manual, 2011).

To the best of the authors' knowledge, consideration of the foundation with its mass in the dam-foundation modeling has been the subject of a few work; and by taking into account the damping ratio, even fewer papers can be found in the literature.

6.2 Mode extraction methods

Two mode extraction methods are used here to extract the mode shapes and the complex natural frequencies for the system object of the present study; the Block Lanczos method and the QR damped one (Ansys theory manual, 2011).

6.2.1 block lanczos method

The block lanczos method is applied for any free, undamped system where equations of motion can be written as (Ansys theory manual, 2011):

$$[M]\{\ddot{x}\}+[K]\{x\}=0 \tag{6.1}$$

Where it is assumed that the motion is harmonic:

$$\{x_i\}=\{\phi_i\}e^{j\ \omega_i t} \tag{6.2}$$

The equations of motion can then be written as:

$$\left(-\omega_i{}^2[M]+[K]\right)\{\phi_i\}e^{j\omega_i t}=0 \tag{6.3}$$

ω_i : The eigenvalue (frequency value)

The eigenvalue problem posed above is solved in order to obtain the natural frequencies and mode shapes of the system.

6.2.2 The QR damped eigenvalue method

The QR damped eigenvalue extraction method provides significant speed improvements over the older damped method for modal analyses involving damping.

If damping is added, the equations of motion are (Ansys theory manual, 2011):

$$[M]\{\ddot{x}\}+[C]\{\dot{x}\}+[K]\{x\}=0 \tag{6.4}$$

And the behavior is expressed by complex eigenvectors and eigenvalues:

$$\{x_i\}=\{\phi_i \pm \upsilon_i\}e^{(\sigma_i \pm \omega_i j)t} \tag{6.5}$$

In the above cases, $(\sigma_i \pm \omega_i j)t$ express both a time-decay term as well as the damped, free vibration term. $e^{\sigma_i t}$ represents the time decay if σ_i is negative, which is representative of stable systems. On the other hand, if σ_i is positive, this indicates unbounded exponential increase in amplitude and represents an unstable system. The $e^{\omega_i j t}$ term is the damped, free vibration term similar to an undamped system as noted above.

$(\sigma_i \pm \omega_i j)$ represents the complex eigenvalue.

σ_i is the real part of the eigenvalue.

ω_i is the imaginary part of the eigenvalue.

$\{\phi_i \pm \upsilon_i\}$ represents the complex eigenvector.

On the other hand, the complex eigenvectors represent the mode shapes. In certain cases, the various nodes (DOF) in the system may be out of phase with one another. As a result, the real and imaginary values can be used to determine the actual response of the system.

To understand better when the nodes (DOF) may be out of phase with one another, it is instructive to look at the damping matrix. If proportional (Rayleigh) damping is used, the damping matrix can be expressed as a linear combination of the mass and stiffness matrices (Ansys theory manual, 2011) (T. O. Florin et al, 2010):

The equations of motion result in only complex eigenvalues, not complex eigenvectors.

$$[M]\{\ddot{x}\}+[C]\{\dot{x}\}+[K]\{x\}=0 \tag{6.6}$$

$$\left(\left(-\omega_i^{\,2}+\alpha\omega_i j\right)[M]+\left(1+\beta\omega_i j\right)[K]\right)\{\phi_i\}=0 \tag{6.7}$$

However, for non-proportional damping, the damping matrix $[C]$ cannot be simplified in this manner. Thus, the eigenvectors and eigenvalues solved for are complex. This means that the nodes (DOF) will be out of phase with one another (Ansys theory manual, 2011).

6.3 Aim of investigation

The goal of this study is to examine the effect of the presence of foundation on the modal unpamped and the modal damped dynamic response of Brezina concrete arch dam using ANSYS finite element code. To achieve these objectives the following cases are studied:

(1) Neglecting foundation-structure interaction effect; assuming the dam as being fixed at its base which means that the is assumed being completely rigid (the modulus of elasticity is infinite);

(2) Linear -structure interaction using the direct method; while allowing for the mass of the foundation (taking into account the inertial effect of the foundation);

(3) Linear -structure interaction using already the direct method; assuming massless foundation (neglecting the inertial effect of the foundation).

Some group of structure-sub interaction problems can be successfully modeled as 2D phenomenon however there is a group of problems, which requires full 3D modeling e.g. concrete arch dam, which is the case of the present study. To achieve the modal damped analysis three damping coefficients are assumed; 2%, 5% and 10%.

6.4 Definition of some parameters used in the modal analysis and given by Ansys code

6.4.1 Participation factor

The participation factor for a given excitation is given as:

$$P_{fi} = \{\phi\}_i^T [M]\{D\} \tag{6.8}$$

Where:

P_{fi} : Participation factor for the ith mode.

$\{D\}$: vector describing the excitation direction

$\{\phi\}_i$: Eigenvector normalized using equation [16]

$\{\phi\}_i^T$: Normalized Eigenvector transpose.

6.4.2 Effective mass

The effective mass in a given direction is defined by:

$$M_{ei} = \frac{P_{fi}^{\ 2}}{\{\phi\}_i^T [M]\{\phi\}_i} \tag{6.9}$$

M_{ei} : The effective mass for the i^{th} mode

With:

$$\{\phi\}_i^T [M]\{\phi\}_i = 1 \tag{6.10}$$

It is important to note that in ANSYS code the frequencies are normalized by default with respect to the mass but it is also possible to normalize it with respect to the unity.

6.4.3 Total effective mass

The total masse effective is:

$$M_{e\ total} = \sum M_{ei} \tag{6.11}$$

$M_{e\ total}$: The total effective mass.

6.4.4 Ratio

The ratio is defined as:

$$Ratio = \frac{P_{fi}}{P_{fi\ max}} \tag{6.12}$$

$P_{f\,i\ max}$: The maximal participation factor.

6.4.5 Modal damping ratio

The modal damping ratio α_i is given by:

$$\alpha_i = \frac{\sigma_i}{\sqrt{\sigma_i^2 + \omega_i^2}} \tag{6.13}$$

6.4.6 Cumulative mass fraction

The cumulative mass fraction is given by:

$$\text{cumulative mass fraction} = \sum \frac{M_{e\,i}}{M_{total}} \tag{6.14}$$

M_{total} : Total mass of the system

6.5 ANSYS validation for the modal damped and undamped analyses methods

6.5.1 Modal undamped analysis applied for mass spring system

A modal undamped analysis is performed for a simple mass-spring system having as properties:

k=3,8 N/m

m=0.15 kg

The analytical results and the one given by ANSYS are presented in Table 6.1:

Analytical results						
Mode	Frequency (HZ)	Period (sec)	P_{fi}	Ratio	M_{ei} (kg)	Cumulative mass fraction (kg)
1	0.801	1.248	0.387	1	0.150	1
Results given by ANSYS code						
Mode	Frequency (HZ)	Period (sec)	P_{fi}	Ratio	Mei(kg)	Cumulative mass fraction (kg)
1	0.801	1.248	0.387	1	0.150	1

Table 6.1: Analytical and ANSYS modal results for a mass-spring system

6.5.2 Modal damped analysis applied for mass spring system

A damped analysis is also performed for the same system with a damping coefficient (mass-spring-damper system) equal to:

c=0,6 kg/sec

Both analytical and results given by ANSYS are presented in Table 6.2:

Analytical results								
Mode	Frequency (real part)	Frequency (im part) (HZ)	Period (sec)	P_{fi}	Ratio	Mei (kg)	Cumulative mass fraction (kg)	α_i
1	-0,318	0,735	1,360	0.274	1	0.75e-01	1	0,397
Results given by ANSYS code								
Mode	Frequency (real part)	Frequency (im part) (HZ)	Period (sec)	P_{fi}	Ratio	Mei (kg)	Cumulative mass fraction (kg)	α_i
1	-0.318	0.735	1.360	0.274	1	0.75e-01	1	0.397

Table 6.2: Analytical and ANSYS modal results for a mass-spring-damper system

It is clear from Table 6.1 and Table 6.2 that ANSYS results are in a perfect agreement with analytical ones.

6.5.3 Undamped modal analysis results

This section covers the detailed undamped modal responses of the Brezina arch dam-foundation system, which is presented briefly in section 5.9.1. The same finite elements models used in chapter 5 are conserved for the present one (figure 5.1 and figure 5.2). The modal responses are calculated using the Block Lanczos method (Ansys theory manual, 2011). Reported quantities are the first natural mode frequencies and the corresponding participation factor, Pfi along X direction, its ratio to the maximum participation factor, Ratio and effective mass, Mei. Table 6.3, Table 6.4 and Table 6.5 list these quantities for the dam alone, dam with massless , and dam- with mass, respectively (results are along X direction). The number of modes reported is such that the ratio of the cumulative effective mass to the total mass reaches a minimum of 0.9 along each of the three, X, Y and Z directions. Quantities along Y and Z direction are omitted herein.

The fundamental mode is defined as the one that involves the maximum mass, i.e., the most dominant mode having a ratio, *Ratio* of one for the direction considered (here along *X* direction).

Mode	Frequency (Hz)	P_{fi}	Ratio	Mei (Kg)
1	12.42	5548.5	1.00000	0.3078e+08
2	18.56	-14.827	0.00267	219.850
3	24.83	-5402.2	0.97363	0.2918e+08
4	26.53	3259.9	0.58753	0.1062e+08
5	27.80	-195.93	0.03531	38388.0
6	30.37	-1909.8	0.34419	0.3647e+07
7	33.17	-143.98	0.02595	20730.7
8	35.86	190.59	0.03435	36323.9
9	38.56	4063.6	0.73238	0.1651e+08
10	44.41	-1961.4	0.35350	0.3847e+07
11	44.74	1253.8	0.22596	0.1571e+07
12	46.51	331.38	0.05972	109814.
13	48.04	1684.0	0.30349	0.2835e+07
14	49.02	-836.08	0.15068	699027.
15	51.22	160.33	0.02889	25706.9
16	51.46	-1437.2	0.25902	0.2065e+07
17	53.00	-2126.5	0.38326	0.4522e+07

Table 6.3: Dam alone first undamped natural frequencies in *X* direction.

Mode	Frequency (Hz)	P_{fi}	Ratio	Mei (Kg)
1	9.334	7712.6	1.00000	0.5948e+08
2	13.67	-29.543	0.00383	872.768
3	14.28	5749.5	0.74546	0.3305e+08
4	16.27	-243.47	0.031567	59275.8
5	16.78	-6195.4	0.8032	0.3838e+08

Table 6.4: Dam with massless first undamped natural frequencies in *X* direction.

Mode	Frequency (Hz)	P_{fi}	Ratio	Mei (Kg)
1	6.48	-3265.6	0.04513	0.10664e+08
2	6.90	-10.623	0.00014	112.840
3	7.40	184.01	0.00254	33858.1
4	7.83	72359.	1.00000	0.52358e+10
5	8.57	-40172.	0.55516	0.16137e+10
6	8.81	-493.93	0.00682	243963.
7	9.16	-36506.	0.50451	0.13327e+10
8	9.74	-12211.	0.16875	0.14911e+09
9	9.83	-941.21	0.01300	885870.
10	10.04	-4659.5	0.06439	0.21711e+08
11	10.065	-33267.	0.45975	0.11067e+10
12	10.57	-202.47	0.00279	40992.7
13	10.72	3511.3	0.04852	0.12329e+08
14	11.64	0.9712	0.00001	0.943311
15	11.70	10302.	0.1423	0.1061e+09
16	11.94	995.11	0.0137	990249.
17	12.15	33474.	0.4626	0.1120e+10

Table 6.5: Dam- with mass first undamped natural frequencies in *X* direction.

As expected, the highest frequencies are obtained from the dam alone model (Table 6.3) while the lowest ones are due to the dam- with mass (Table 6.5). Qualitatively, these results can be explained with the single degree of freedom mass-spring system for which the circular frequency is:

$$\omega = \sqrt{\frac{k}{m}} \tag{6.15}$$

where *k* is the stiffness of the spring and *m* the mass (Shabanna,1995). With respect to the dam alone model, the dam-massless has the same total mass, but is globally less rigid since the 's Young's modulus is almost half the value of that of the concrete dam (Table 4.2), thus from Eq.6.15, lower frequencies are obtained from the latter model. Also, between the dam-massless and dam- with mass, the global stiffness is identical but the total mass is evidently larger for the dam- with mass, hence, again from Eq. (6.15), lower frequencies are obtained from the latter model. It is worth noting that the position of the fundamental mode is unchanged from the dam alone to the dam-massless model (mode number one of Table 6.3 and Table 6.4), while it switches to the fourth position when the mass of the is taken into account (Table 6.5).

In terms of numerical values, the dam alone shows much higher frequencies than that of the dam-massless (12.42 Hz compared to 9.334 Hz for the first mode). This latter's frequencies, in turn, are also much higher than that of the dam- with mass (6.48 Hz for the first mode). These results are depicted for the first 5 modes in Figure 6.1. Table 6.6 summarizes the frequencies decrease between the three models for the first 5 modes. The calculations performed highlight the need to model the foundation as a deformable structure, and to take into account its mass.

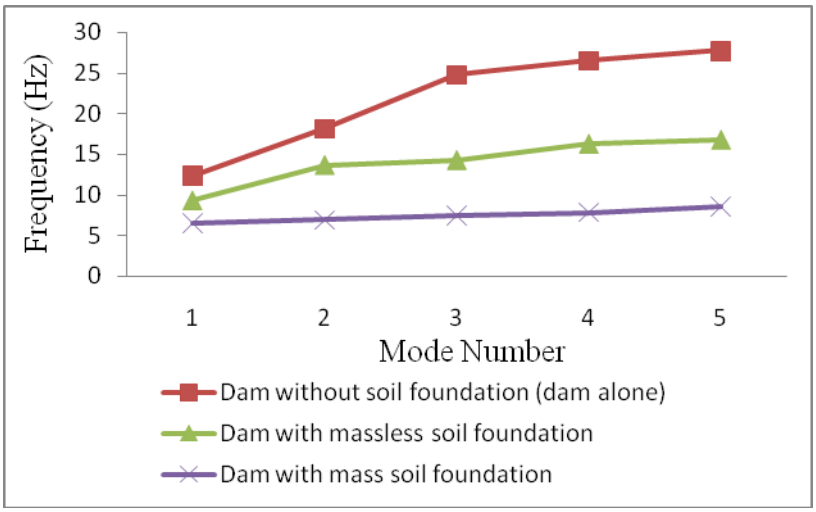

Figure 6.1: Undamped first 5 frequencies for the three models.

Mode	Dam-massless /Dam alone (%)	Dam- with mass /Dam alone (%)	Dam- with mass /Dam-massless (%)
1	24,85	47,80	30,54
2	26,30	62,79	49,52
3	42,46	70,18	48,18
4	38,64	70,45	51,84
5	39,62	69,15	48,91

Table 6.6: Frequencies decrease (%) between the three models

6.6 Damped modal analysis results

In this section, damped modal responses of the Brezina arch dam-foundation system are investigated. Recall that the free damped vibration equations (Reddy, 2002) are

$$M\ \ddot{x} + C\ \dot{x} + K\ x = 0 \tag{6.16}$$

where M, C and K is the mass, damping and stiffness matrix, respectively; $x, \dot{x}, \ddot{x}$ is the displacement, velocity and acceleration vector, respectively. Herein, viscous damping is assumed to be of the Raleigh form (R. Priscu et al. 1982):

$$C = \alpha\ M + \beta\ K \tag{6.17}$$

where α, β are constants refereed to as mass and stiffness damping, respectively. From Eq. 6.17), the following relation can easily be established:

$$\xi_i = \frac{\alpha}{2\omega_i} + \frac{\beta\omega_i}{2} \tag{6.18}$$

where ξ_i is the viscous damping ratio to critical damping for mode i, and ω_i the corresponding circular frequency. The mass damping α, which is important for bodies resisting to wind or for submarine applications (ANSYS Theory Manual, 2011), is neglected herein. Hence, assuming $\alpha = 0$, Eq. 6.18 is reduced to

$$\beta = \frac{2\xi_i}{\omega_i} \tag{6.19}$$

which yields β for given ξ_i and ω_i. Searching harmonic solutions, and making use of the Raleigh damping assumption Eq. 6.17 with $\alpha = 0,$ Eq. 6.16 becomes:

$$\left[(1 + j\omega\beta)K - \omega^2 M\right] x_0 = 0 \tag{6.20}$$

where j is the unit complex number, $j^2 = -1$ and x_0 the modal vector.

For the parametric study conducted herein, the viscous damping ratio ξ will be 2%, 5% and 10%, while ω_i will be the circular frequency of the fundamental mode (that involves the largest effective mass). The damped modal responses are calculated using the QR damped method (ANSYS Theory Manual, 2011). Reported quantities are the first eigenvalues in terms of imaginary part, ω_i, and real part, σ_i, the corresponding participation factor along X direction, P_{fi}, the ratio to the maximum participation factor, *Ratio*, the effective mass, *Mei*, and the modal damping ratio, γ_i . Recall that the imaginary part ω_i of the eigenvalue ρ_i is the frequency whereas the real part σ_i of ρ_i is the damping related quantity for mode *i*. The modal damping ratio, γ_i, is

$$\gamma_i = \sigma_i / \sqrt{\sigma_i^{\,2} + \omega_i^{\,2}} \tag{6.21}$$

Table 6.7, Table 6.8 and Table 6.9 list these modal quantities for the dam alone, dam-massless , and dam- with mass, respectively. The input damping ratio ξ is 2% ($\xi = 0.02$). Firstly, these results show that the frequencies are almost identical, but very slightly lower, as compared to that of the undamped modes for each model studied, e.g. 12.42 Hz from Table 6.3 and 12.41Hz from Table 6.7. These findings are not surprising. Consider the mass-damper-spring single degree of freedom system for which the circular frequency is

$$\omega = \frac{\sqrt{4km - c^2}}{2m} \tag{6.22}$$

where k is the stiffness of the spring, m the mass and c the damper (A.A. Shabana, 1995). It is assumed that the system is far from over damped so that in the above equation, $4km - c^2 > 0$. Eq. 6.22 shows that the frequency is always lower than that of the mass-spring system, and that the two frequencies are almost identical if the damping c is small enough, i.e., if the system is only moderately damped. This is obviously the case for the 3D dam- models under study. The second remark worth noting is the negative values of σ_i, indicating that the dam- system is stable. This is expected as the analogy can be made again with the simple system for which

$$\sigma = -\frac{c}{2m} \tag{6.23}$$

It should be noted that under the Raleigh damping assumption with $\alpha = 0,$ the damping c, in the above mass-damper-spring system, becomes $c = \beta\ k$. Recall that σ and ω are the real and imaginary part, respectively, of the roots of the characteristic equation (A.A Shabana, 1995). Lastly, Table 6.7 shows that adding damping to the dam- system switches the fundamental mode. For example, mode number five is now the fundamental mode for the dam alone (Table 6.7) while without damping, the fundamental mode is number one (Table 6.3).

For $\xi = 0.02,$ Figure 6.2 depicts the frequencies decrease from the dam alone to the dam- with mass model for the first 5 modes, and Figure 6.3 illustrates the decrease of the damping

related quantity α_i . Like the comments made in the preceding section, qualitatively, the frequencies decrease between the three models can be explained from Eq. 6.22. Also, from Eq. 6.23 and $c = \beta\ k$, the damping decrease, in absolute value, from the dam alone to the dam- with mass model is obvious. Finally, this decrease in percentage is summarized in Table 6.10 and Table 6.11.

Mode	Im part ω_i (Hz)	R part, σ_i	P_{fi}	Ratio	Mei (kg)	γ_i
1	12,41	-0,251	19,267	0,01331	371,23	2,017E-02
2	18,55	-0,560	-0,071	0,00005	5,09E-03	3,015E-02
3	24,81	-1,002	-8,933	0,00617	79,804	4,034E-02
4	26,51	-1,143	-601,100	0,41524	361323	4,310E-02
5	27,77	-1,255	1447,600	1	2,10E+06	4,516E-02
6	30,34	-1,499	-1305,700	0,90195	1,70E+06	4,934E-02

Table 6.7: Dam alone first natural damped frequencies, viscous damping ξ = 2%.

Mode	Im part ω_i (Hz)	R part, σ_i	P_{fi}	Ratio	Mei (kg)	γ_i
1	9,33	-0,188	1240,4	0,01337	1,54E+06	2,01E-02
2	13,67	-0,403	1,2709	0,00001	1,61521	2,95E-02
3	14,28	-0,440	-741,23	0,00799	549425	3,08E-02
4	16,27	-0,571	-50129	0,54016	2,51E+09	3,51E-02
5	16,78	-0,607	92804	1,00000	8,61E+09	3,62E-02
6	22,63	-1,107	-83822	0,90322	7,03E+09	4,88E-02

Table 6.8: Dam with massless first natural damped frequencies, viscous damping ξ = 2%.

Mode	Im part ω_i (Hz)	R part, σ_i	P_{fi}	Ratio	Mei (kg)	γ_i
1	6,48	-0,107	4453,6	0,00055	1,98E+07	1,66E-02
2	6,90	-0,122	812,13	0,00010	659548	1,76E-02
3	7,40	-0,140	-1,20E+05	0,01493	1,45E+10	1,89E-02
4	7,84	-0,157	-8,05E+06	1,00000	6,49E+13	2,00E-02
5	8,57	-0,188	5,73E+06	0,71113	3,28E+13	2,19E-02

Table 6.9: Dam- with mass first natural damped frequencies, viscous damping ξ = 2%.

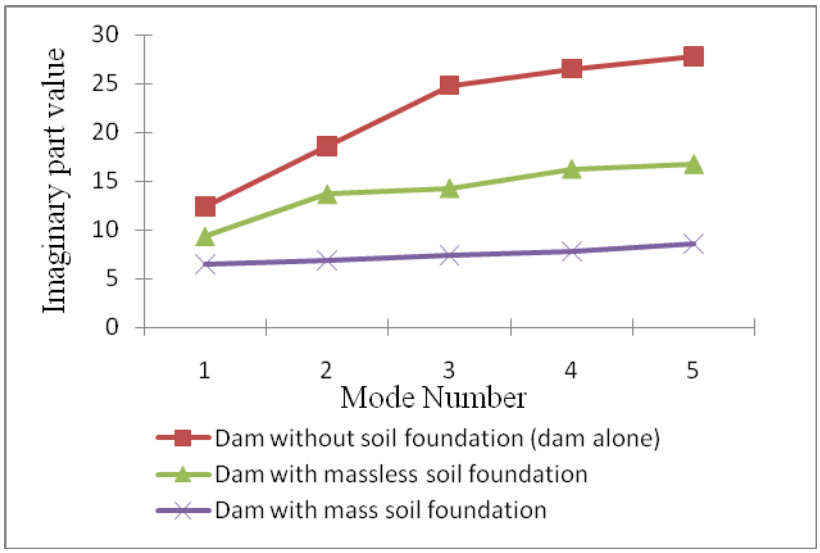

Figure 6.2: Damped first 5 frequencies for the three models, viscous damping ξ = 2%.

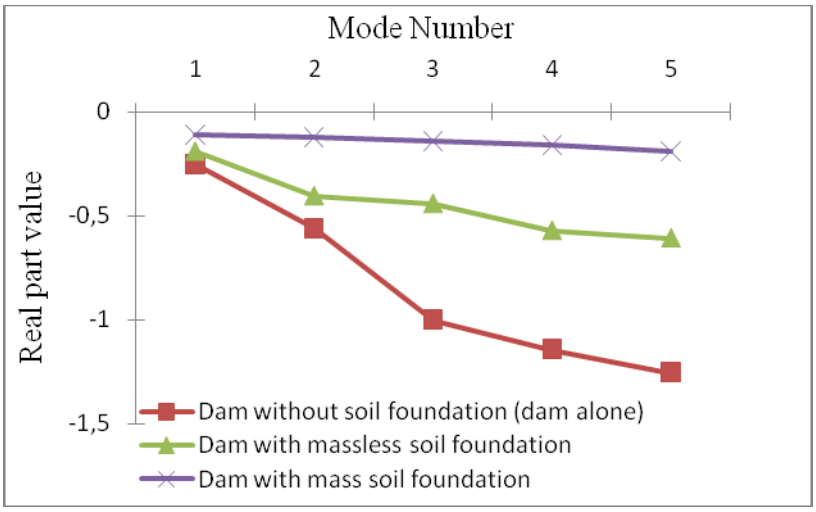

Figure 6.3: First 5 damping related quantities for the three models**,** viscous damping ξ = 2%.

Mode	Dam-massless /Dam alone (%)	Dam- with mass /Dam alone (%)	Dam- with mass /Dam-massless (%)
1	24,85	47,80	30,54
2	26,30	62,79	49,51
3	42,44	70,17	48,17
4	38,62	70,43	51,83
5	39,60	69,13	48,89

Table 6.10: Frequencies decrease (%) between the three models, viscous damping ξ = 2%.

Mode	Dam-massless /Dam alone (%)	Dam- with mass /Dam alone (%)	Dam- with mass /Dam-massless (%)
1	25,07	57,16	42,83
2	27,93	78,23	69,80
3	56,07	86,02	68,18
4	50,05	86,27	72,52
5	51,63	85,04	69,07

Table 6.11: Damped related quantities in absolute values decrease (%) between the three models, viscous damping ξ = 2%.

Similar results for the input damping ratio ξ of 5% and 10% are reported in Tables 6.12-6.14 and Tables 6.17-6.19, respectively. From these results, same comments as for ξ = 2% can be made although the differences in frequencies are slightly more pronounced with respect to that of the undamped modes: the larger the damping ratio, the bigger the differences. This is clearly supported by Eq. 6.22. Figures 6.4-6.5 and Figures 6.6-6.7 depict the frequency and damping related quantity decrease between the three models for $\xi = 0.05$ and $\xi = 0.1,$ respectively. Tables 6.15-6.16 and Tables 6.20-6.21 summarize theses evolutions in percentage.

Mode	Im part ω_i (Hz)	R part, σ_i	P_{fi}	Ratio	Mei (kg)	γ_i
1	12.40	-0.625	-38.605	0.01331	1490.36	0.503e-01
2	18.50	-1.396	0.143	0.00005	0.204e-01	0.503e-01
3	24.70	-2.499	17.899	0.00617	320.386	0.752e-01
4	26.37	-2.853	1204.4	0.41524	0.145e+07	0.752e-01
5	27.62	-3.132	-2900.5	1.000	0.841e+07	0.100
6	30.14	-3.740	2616.1	0.90195	0.684e+07	0.100

Table 6.12: Dam alone first natural damped frequencies, viscous damping ξ = 5%.

Mode	Im part ω_i (Hz)	R part, σ_i	P_{fi}	Ratio	Mei (kg)	γ_i
1	9.32	-0.468	457.64	0.01336	209432.	0.501e-01
2	13.64	-1.005	0.46888	0.000014	0.219844	0.734e-01
3	14.24	-1.096	-273.46	0.00798	74781.7	0.767e-01
4	16.21	-1.423	-18494.	0.54016	0.342e+09	0.874e-01
5	16.71	-1.513	34238.	1.00000	0.117e+10	0.901e-01
6	22.49	-2.758	-30924.	0.90322	0.956e+09	0.121

Table 6.13: Dam with massless first natural damped frequencies, viscous damping ξ = 5%.

Mode	Im part ω_i (Hz)	R part, σ_i	P_{fi}	Ratio	Mei (kg)	γ_i
1	6.47	-0.268	229.81	0.0005	52811.6	0.413e-01
2	6.89	-0.304	41.906	0.0001	1756.11	0.440e-01
3	7.39	-0.349	-6204.3	0.015	0.3849e+08	0.472e-01
4	7.82	-0.391	-0.415e+06	1.000	0.1726e+12	0.499e-01
5	8.56	-0.469	0.295e+06	0.711	0.8733e+11	0.546e-01

Table 6.14 Dam- with mass first natural damped frequencies, viscous damping ξ = 5%.

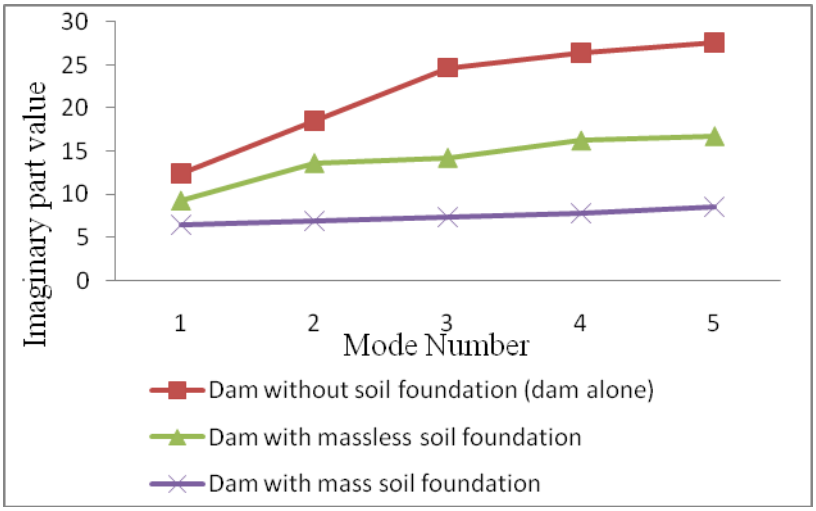

Figure 6. 4: First 5 damped frequencies for the three models, viscous damping ξ = 5%.

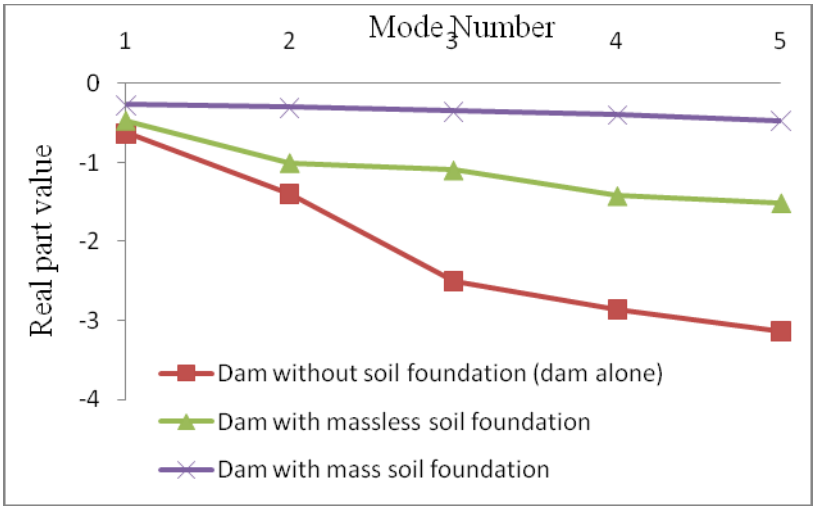

Figure 6.5: First 5 damped related quantities for the three models**,** viscous damping ξ = 5%.

Mode	Dam-massless /Dam alone (%)	Dam- with mass /Dam alone (%)	Dam- with mass /Dam-massless (%)
1	24,85	47,78	30,52
2	26,29	62,72	49,43
3	42,33	70,06	48,08
4	38,52	70,32	51,72
5	39,48	69,00	48,78

Table 6.15: Frequencies decrease (%) between the three models, viscous damping ξ = 5%.

Mode	Dam-massless /Dam alone (%)	Dam- with mass /Dam alone (%)	Dam- with mass /Dam-massless (%)
1	25,14	57,13	42,73
2	27,99	78,21	69,75
3	56,11	86,010	68,12
4	50,09	86,26	72,47
5	51,67	85,023	69,01

Table 6.16: Damped related quantities in absolute values decrease (%) between the three models, viscous damping ξ = 5%.

Mode	Im part , ω_i (Hz)	R part, σ_i	P_{fi}	Ratio	Mei (kg)	γ_i
1	12.35	-1.250	-35.469	0.013	1258.08	0.10
2	18.34	-2.792	0.1314	0.00004	0.172e-01	0.15
3	24.32	-4.999	16.445	0.0061	270.452	0.201
4	25.91	-5.706	1106.6	0.4152	0.1224e+07	0.215
5	27.08	-6.264	-2664.9	1.000	0.71019e+07	0.225
6	29.44	-7.480	2403.6	0.901	0.57774e+07	0.246

Table 6.17: Dam alone first natural damped frequencies, viscous damping ξ = 10%.

Mode	Im part , ω_i (Hz)	R part, σ_i	P_{fi}	Ratio	Mei (kg)	γ_i
1	9.28	-0.930	-171.52	0.013366	29420.3	0.997e-01
2	13.53	-1.998	-0.17574	0.000014	0.308e-01	0.146
3	14.12	-2.181	102.49	0.007987	10505.1	0.152
4	16.03	-2.830	6931.6	0.540160	0.480e+08	0.173
5	16.51	-3.009	-12832.	1.00	0.164e+09	0.179
6	21.98	-5.485	11591.	0.903	0.134e+09	0.242

Table 6.18: Dam with massless first natural damped frequencies, viscous damping ξ = 10%.

Mode	Im part ω_i (Hz)	R part, σ_i	P_{fi}	Ratio	Mei (kg)	γ_i
1	6.46	-0.536	-642.87	0.0005	413279.	0.826e-01
2	6.87	-0.608	-117.23	0.0001	13742.5	0.8807e-1
3	7.37	-0.699	17356.	0.0149	0.3012e+09	0.9444e-01
4	7.79	-0.783	0.11625e+07	1.0000	0.1351e+13	0.9998e-01
5	8.52	-0.938	-0.8267e+06	0.7111	0.6834e+12	0.1093

Table 6.19: Dam- with mass first natural damped frequencies, viscous damping ξ = 10%.

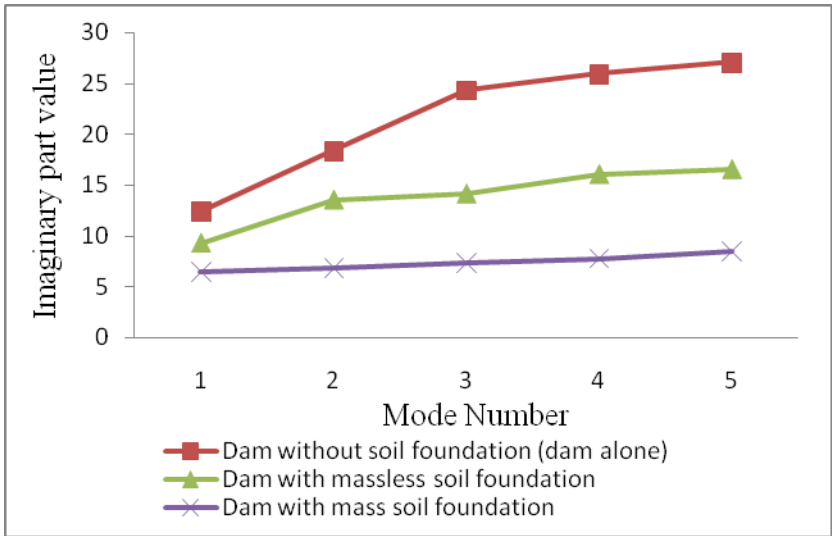

Figure 6.6: Damped first 5 frequencies for the three models, viscous damping ξ = 10%.

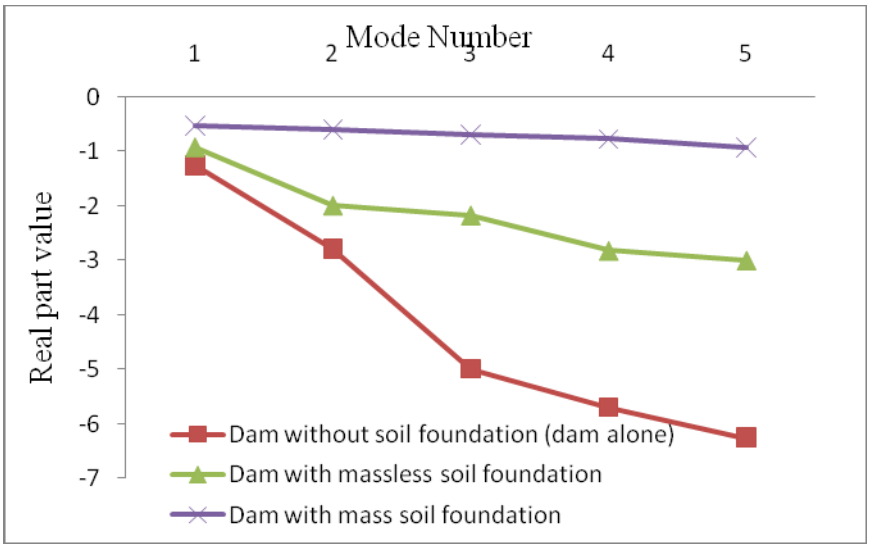

Figure 6.7: First 5 damped related quantities for the three models**,** viscous damping ξ = 10%.

Mode	Dam-massless /Dam alone (%)	Dam- with mass /Dam alone (%)	Dam- with mass /Dam-massless (%)
1	24,84	47,72	30,43
2	26,25	62,51	49,17
3	41,94	69,69	47,80
4	38,13	69,89	51,34
5	39,03	68,53	48,38

Table 6.20: Frequencies decrease (%) between the three models, damping ξ = 10%.

Mode	Dam-massless /Dam alone (%)	Dam- with mass /Dam alone (%)	Dam- with mass /Dam-massless (%)
1	25,57	57,13	42,40
2	28,42	78,21	69,57
3	56,37	86,01	67,93
4	50,38	86,26	72,31
5	51,95	85,02	68,83

Table 6.21: Damped related quantities in absolute value decrease (%) between the three models, viscous damping ξ = 10%.

Influences of the viscous damping ratio ξ on the frequencies and the damping related quantity are summarized in Figures 6.8-6.9 and Tables 6.22-6.23 for the dam without model, Figures 6.10-6.11 and Tables 6.24-6.25 for the dam with massless model, and Figures 6.12-6.13 and Tables 6.26-6.27 for the dam- with mass model.

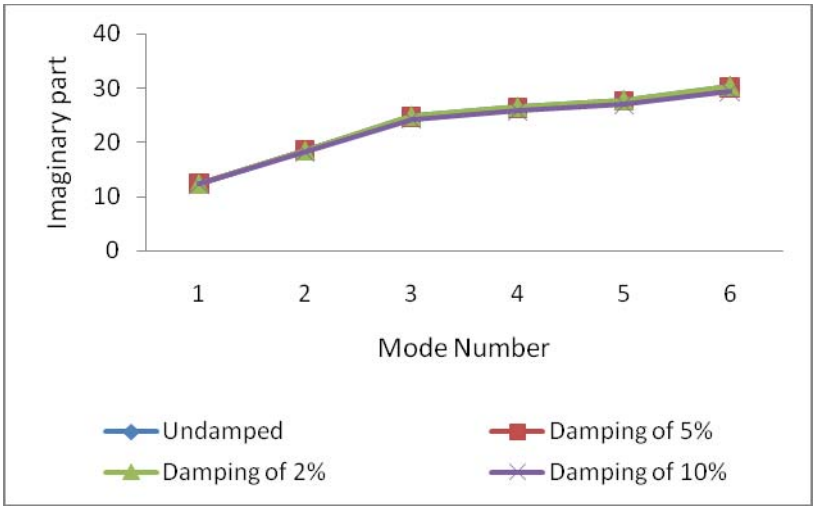

Figure 6. 8: Influence of viscous damping ξ on the frequencies for the dam alone model.

Mode	Undamped	Damping of 2%	Damping of 5%	Damping of 10%
1	12,42	12,41	12,40	12,35
2	18,56	18,55	18,50	18,34
3	24,83	24,81	24,70	24,32
4	26,53	26,50	26,37	25,91
5	27,80	27,77	27,62	27,08
6	30,37	30,34	30,14	29,44

Table 6.22: Influence of viscous damping ξ on the frequencies for the dam alone model.

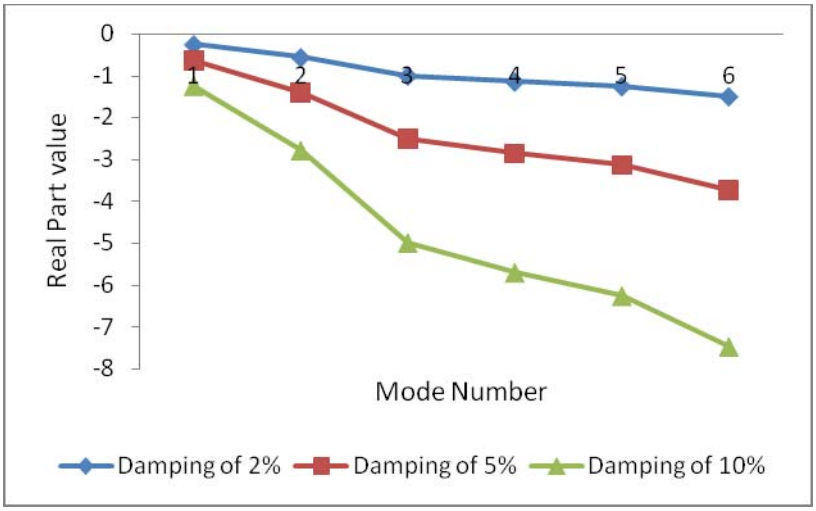

Figure 6.9: Influence of viscous damping ξ on the damping related quantities for the dam alone model.

Mode	Damping of 2%	Damping of 5%	Damping of 10%
1	-0,250	-0,625	-1,250
2	-0,559	-1,396	-2,792
3	-1,001	-2,499	-4,999
4	-1,143	-2,853	-5,706
5	-1,255	-3,132	-6,264
6	-1,499	-3,740	-7,480

Table 6.23: Influence of viscous damping ξ on the damping related quantities for the dam alone model.

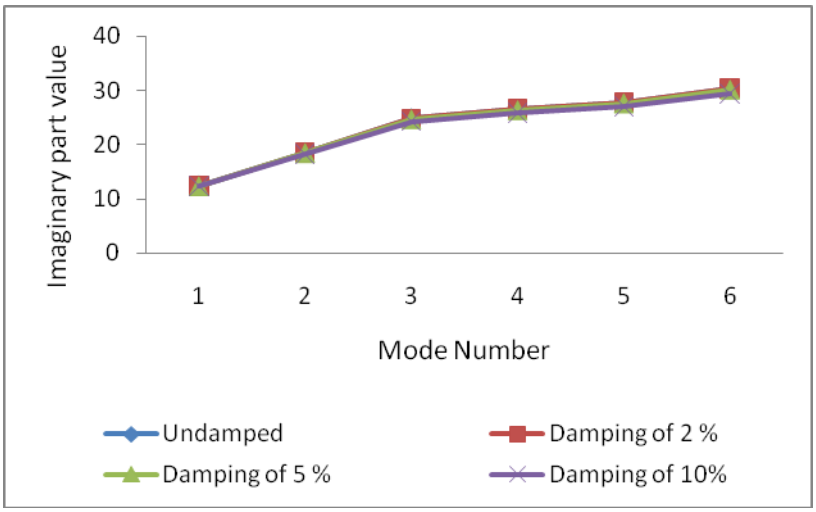

Figure 6.10: Influence of viscous damping ξ on the frequencies for the dam with massless model.

Mode	Undamped	Damping of 2%	Damping of 5%	Damping of 10%
1	9,33	9,33	9,32	9,28
2	13,67	13,67	13,64	13,53
3	14,28	14,28	14,24	14,12
4	16,27	16,26	16,21	16,03
5	16,78	16,77	16,71	16,51
6	22,66	22,63	22,49	21,98

Table 6.24: Influence of viscous damping ξ on the frequencies for the dam with massless model.

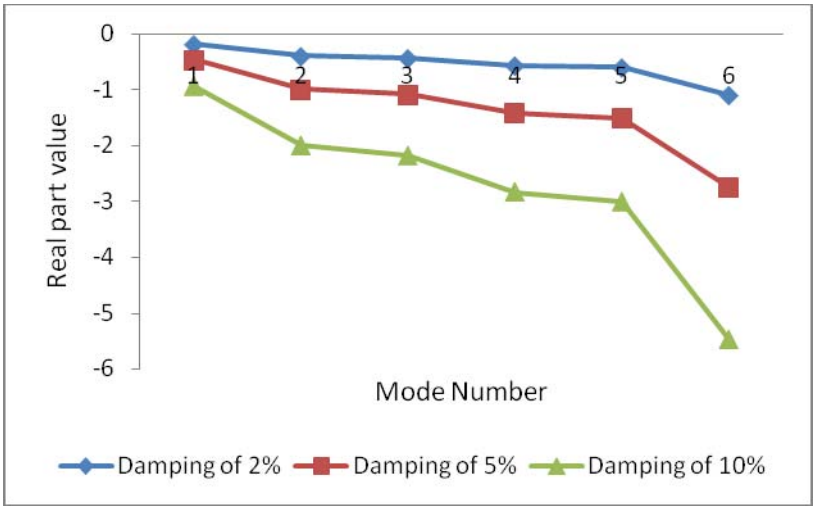

Figure 6.11: Influence of viscous damping ξ on the damping related quantities for the dam with massless model.

Mode	Damping of 2%	Damping of 5%	Damping of 10%
1	-0,187	-0,468	-0,930
2	-0,403	-1,005	-1,998
3	-0,440	-1,096	-2,181
4	-0,571	-1,423	-2,830
5	-0,607	-1,513	-3,009
6	-1,106	-2,758	-5,485

Table 6.25: Influence of viscous damping ξ on the damping related quantities for the dam with massless model.

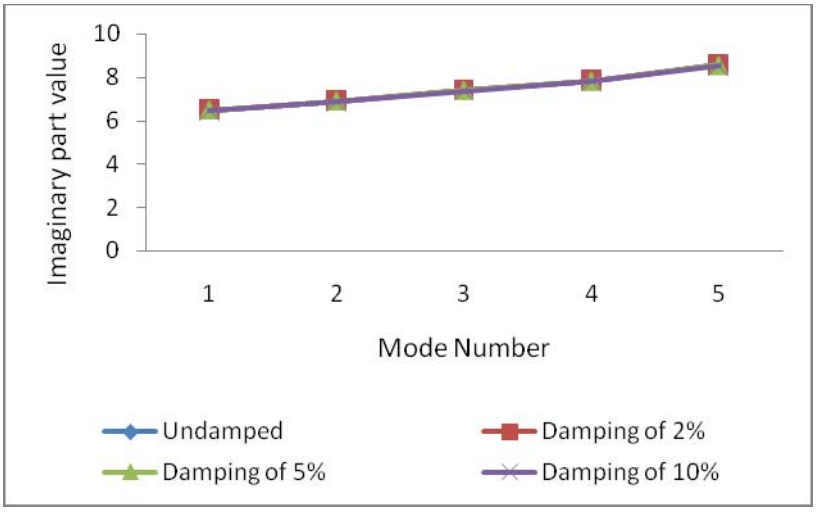

Figure 6.12: Influence of viscous damping ξ on the frequencies for the dam- with mass model.

Mode	Undamped	Damping of 2%	Damping of 5%	Damping of 10%
1	6,48	6,48	6,47	6,46
2	6,90	6,90	6,89	6,87
3	7,40	7,40	7,39	7,37
4	7,83	7,83	7,82	7,79
5	8,57	8,57	8,56	8,52

Table 6.26: Influence of viscous damping ξ on the frequencies for the dam- with mass model.

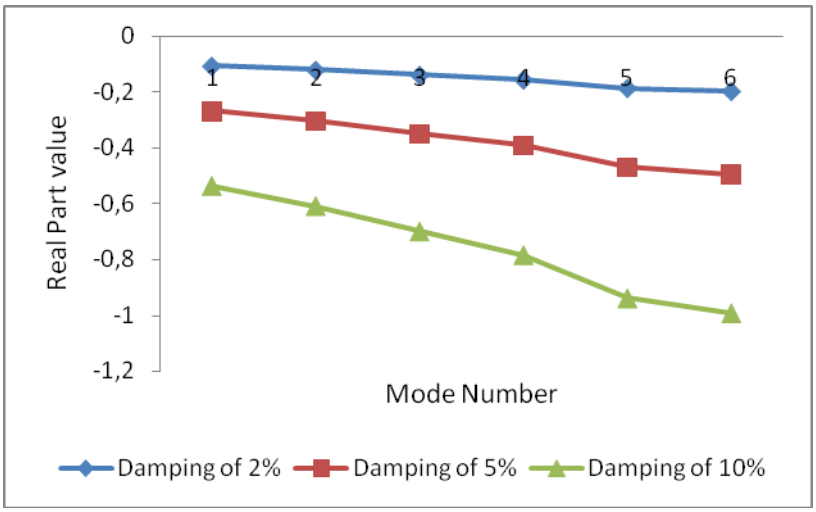

Figure 6.13: Influence of viscous damping ξ on the damping related quantities for the dam- with mass model.

Mode	Damping of 2%	Damping of 5%	Damping of 10%
1	-0,107	-0,268	-0,536
2	-0,121	-0,304	-0,608
3	-0,140	-0,349	-0,699
4	-0,156	-0,391	-0,783
5	-0,187	-0,469	-0,938
6	-0,198	-0,495	-0,991

Table 6.27: Influence of viscous damping ξ on the damping related quantities for the dam- with mass model.

Quantitatively, results reported in this section point out, again, the importance of taking into account the with its mass. For any of the damping ratio under study, the dam alone shows significantly higher frequencies than that of the dam-massless . This latter's frequencies are also much higher than that of the dam- with mass. The damping values calculated are also much lower in absolute value from the dam- with mass than that from the other two models. The results reported also show that adding only a small damping ratio, e.g. $\xi = 0.02$, to the dam- model reduces the number of modes needed to obtain 90% of the system's total mass. For example, for the undamped dam alone model, 17 modes are needed to reach 91.73 % of the total mass, whereas for its damped counterpart with $\xi = 0.02$, 6 modes are sufficient to reach 96.9 % of the total mass. This feature is of practical importance as it reduces the CPU time for a further analysis based on the modal superposition method such as a spectrum analysis or a modal superposition transient response analysis.

6.7 Conclusions

Modal responses of the Brezina dam-foundation system are calculated using the finite element software, *ANSYS*. The following conclusions are drawn based on the numerical experiments conducted herein:

For the study of the dam- system, the foundation should be modeled as a deformable structure with its mass taken into account. The natural frequencies of either undamped or damped modes are much lower from the dam- with mass than that from the dam alone, and

significantly lower than that from the dam-massless model. Modeling the with its mass also affects the mode shape by changing the fundamental mode position.

Likewise, for any of the damping ratio under study, the damping related values calculated are significantly lower, in absolute value, from the dam- with mass than that from the dam-massless , and much lower than that from the dam alone model.

Adding only a small damping ratio of 2% to the dam- model reduces the number of modes needed, as compared to the undamped model, to obtain 90% of the system's total mass. This is of practical importance as it reduces the CPU time for a further analysis based on the modal superposition method, such as a modal superposition transient response analysis, which will be undertaken following the present work.

CHAPTER 7

Two Dimensional (2D) Modal and Transient Behaviour of Dam-Reservoir-Foundation System using ANSYS

CHAPTER 7

Two Dimensional (2D) Modal and Transient Behaviour of Dam-Reservoir-Foundation System using ANSYS

7.1 Introduction

Gravity dams are fluid – structure – foundation interaction problems. It is obvious that the foundation and water reservoir affect the dynamic characteristics (especially modal frequencies) and consequently the dynamic response of gravity dams during earthquakes. A parametric study is performed in the present chapter to view the combined effect of foundation, water reservoir presence, fluid-dam and fluid-foundation interfaces modeling on both modal and transient behaviour of "Brezina" concrete dam.

Two assumptions are adopted to model the fluid reservoir using Ansys finite element code; the fluid finite element (representing the Lagrange approach) and the surface element (representing the *added masses* approach).

Two assumptions are also performed to model the dam-fluid and the foundation- fluid interfaces: the contact elements and the coupling equations. Also three approaches are adopted to investigate the foundation-dam interaction phenomenon: the fixed support foundation, the massless foundation and the mass foundation.

7.2 Constraint Equations and Boundary Conditions

The equations of motion for a fluid system have the similar form to that of the structure when the Lagrangian approach is used. But requires a different sensitivity to determine interface condition of the coupled system.

In order to satisfy the continuity conditions between the fluid and solid media at the boundaries, the nodes at the common lines of the fluid element and the plane elements are constrained to be coupled in the normal directions of the interfaces, while relative movements are allowed to occur in the tangential directions, this is implemented by two methods:

First: by the use of contact elements available in the ANSYS software (CONTA 172);

Second: by attaching the coincident nodes at the common lines between the fluid element (representing the fluid reservoir) and the plane elements (representing either the dam or the foundation system) in the normal direction.

Another approach is modeled here using *surface element* available in Ansys library to represent water reservoir using the added masses approach. The water mass is applied uniformly on the container face plus the hydrostatic pressure, the *surface element* (SURF 153) is characterized by its length and its thickness, these two properties depends on both water level and the contact length between the fluid and the container.

7.3 Ansys Validation

The model is to be developed from the elements available in the ANSYS software, the validity of the software via the fluid-structure interaction problem is judged by an example about a rectangular liquid container for the two approaches of fluid-structure interfaces modeling (coupling equations and contact elements). The geometry and the finite element model of the rectangular liquid container are given by Figure 7.1.

The liquid in an open container can oscillate at discrete natural frequencies. The liquid sloshing, at the lowest of these frequencies is of concern in this study; since the container natural sloshing frequency is to be tuned to the structure system natural frequency.

Water properties are given by Table 4.3 however for the container is characterized by a Elastic modulus of 3e+10N/m^2,a Poisson's ratio of 0.23 and a Density about 2500 kg/ m^3: 200 FLUID79 finite elements are used to model the fluid container; however, 228 PLANE 42 finite elements are used to model the container itself. This later is constrained (fixed) at its base.

Two approaches are adopted for the fluid-container interfaces modeling:

First: by coupling the coincident nodes at these interfaces in the normal direction only,

Second, by modeling these interfaces using contact elements available in Ansys code library considering the container as target elements (TARGE 169) and water as contact elements (CONTA 172) (view figure 4.10).

Another approach is applied here to model the fluid instead the fluid finite elements, it is the added masses approach using the element "*surf*" already available in Ansys code Library. The water mass is applied uniformly on the container faces plus the hydrostatic pressure, the surface finite element "SURF 153" is characterized by its length and its thickness, these two properties depends on both water level and the contact length between the fluid and the container.

From the linear wave theory, the natural frequencies of the first sloshing modes are calculated as follows (Robert D. Blevins, 2001):

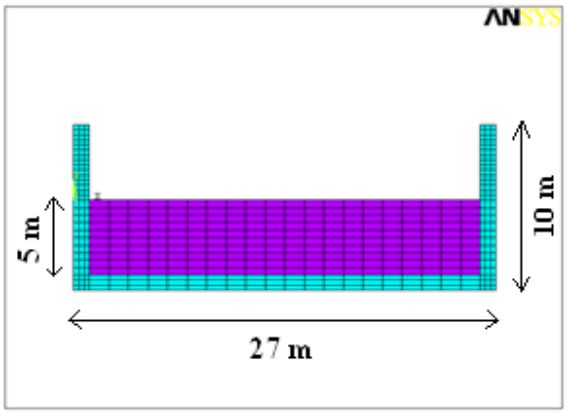

Figure 7.1: Reservoir finite element model

$$f_i = \frac{1}{2}\sqrt{\frac{g}{\pi}}\sqrt{\frac{i}{a}tanh\frac{\pi h i}{a}} \tag{7.1}$$

Where:

g= Acceleration due to gravity;

h= Depth of liquid in basin;

a= Basin length;

i= 0, 1, 2….etc

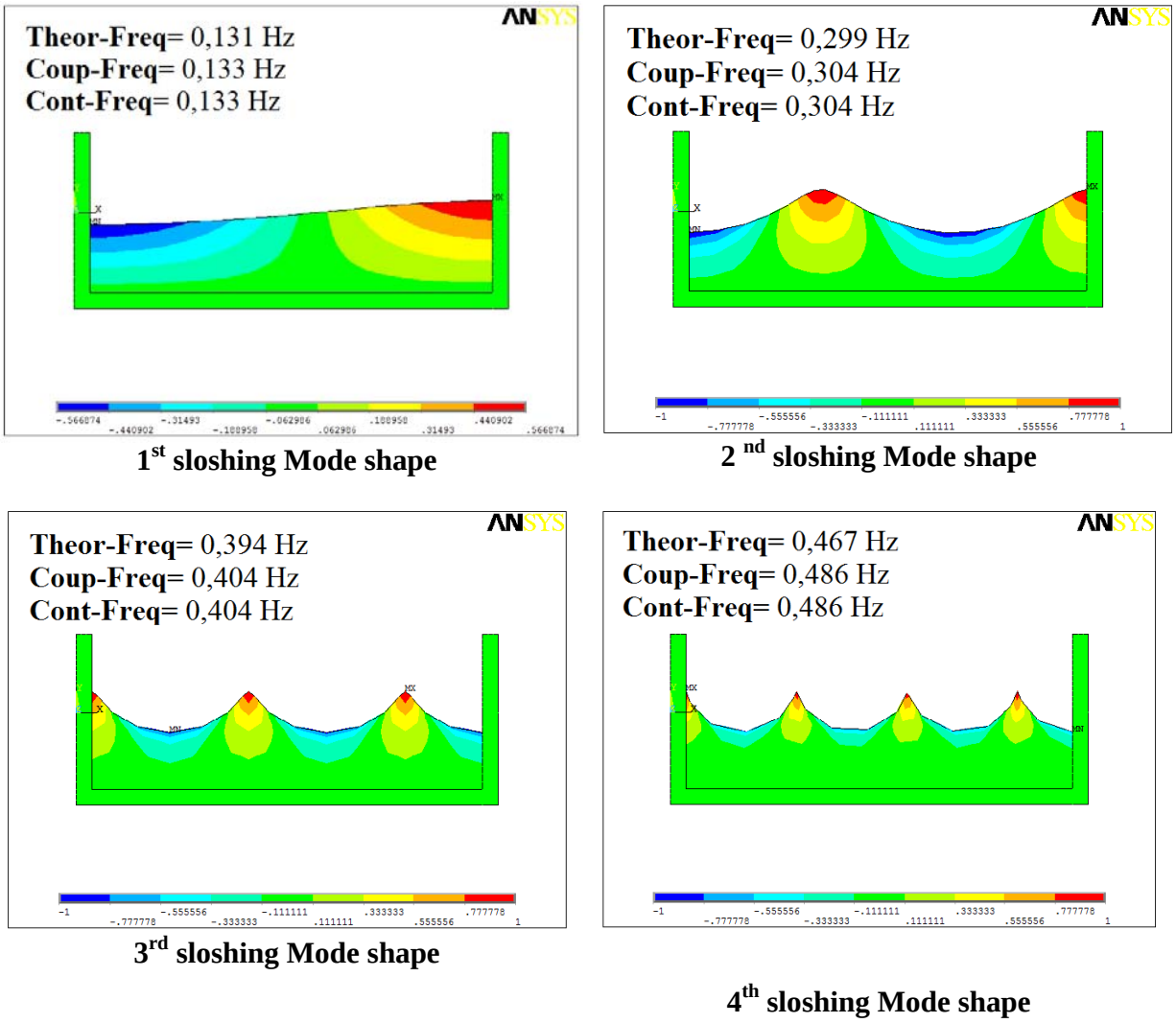

Figure 7.2: The four first sloshing mode shapes for the rectangular container example

Mode Number	Theoretical frequency (Hz)	Interface fluid-container modeled using *coupling equations*		Interface fluid-container modeled using *contact elements*	
		Frequency (Hz)	M_{ei} (kg)	Frequency (Hz)	M_{ei} (kg)
1	0,131	0,133	89368,1	0,133	89368,1
2	0,299	0,304	5378,17	0,304	5378,17
3	0,394	0,404	1076,58	0,404	1076,58
4	0,467	0,486	326,539	0,486	326,539

Table 7.1: The first four sloshing modal frequencies with their corresponding effective masses for coupling and contact interfaces approaches.

Figure 7.2 sketches the four first sloshing modes shapes for the rectangular container example, while Table 7.1 shows the consistence of the results between the theoretical and the finite element modeling (for the two approaches of fluid-container interface modeling).

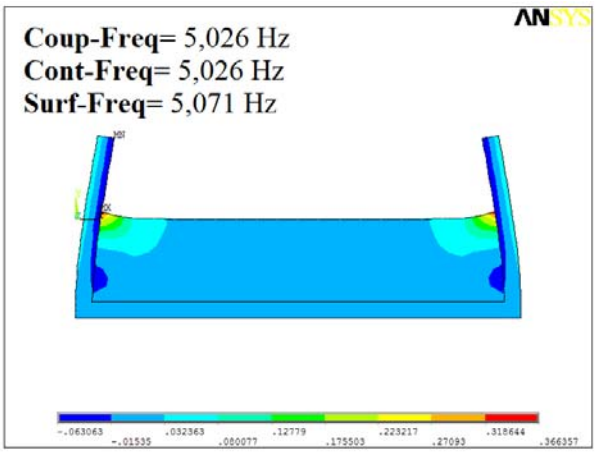

1st coupled Mode shape

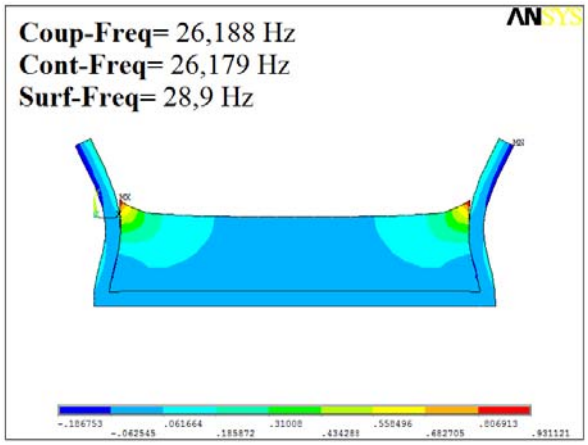

2nd coupled Mode shape

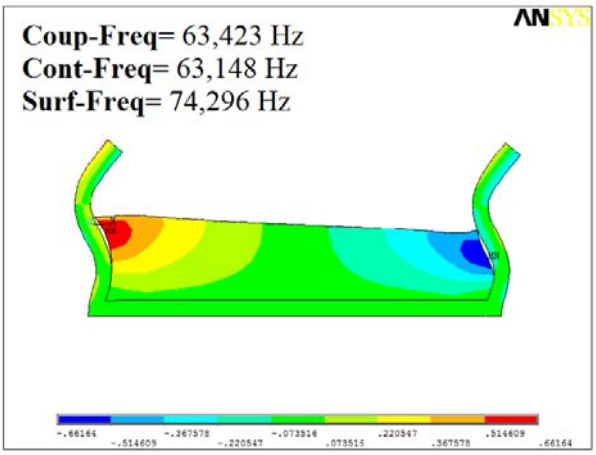

3rd coupled Mode shape

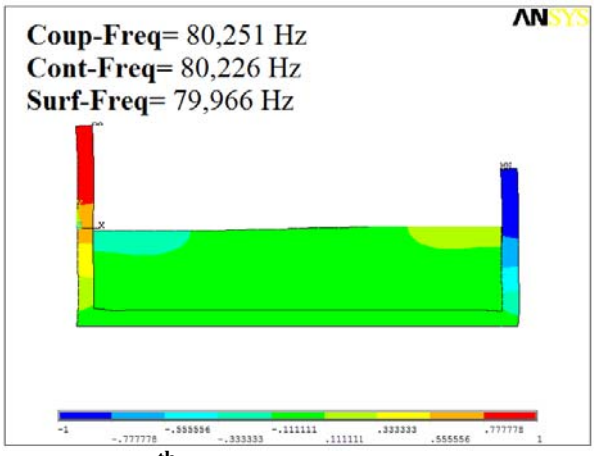

4th coupled Mode shape

Figure 7.3: The four first coupled mode shapes for the rectangular container.

Mode Number	Interface fluid-container modeled using *coupling equations*		Interface fluid-container modeled using *contact elements*		Added masses approach	
	Coupled frequency (Hz)	Ratio	Coupled frequency (Hz)	Ratio	Coupled frequency (Hz)	Ratio
1	5.026	0.679	5,026	0,679	5.071	1
2	26.188	0.5169	26,179	0,517	28.900	0.609
3	63.423	0.299	63,148	0,298	74.296	0.284
4	80.251	0.024	80,226	0,023	79.966	0.230

Table 7.2: The first four coupled modal frequencies for coupling and contact interfaces approaches.

Table 7.2 represents the four first values of coupled modes shapes for the container example for the two approaches used to model the fluid-container interface; coupling equations and contact elements. However, figure 7.3 sketches these frequencies. The table 7.2 shows a good consistence of the results for the two fluid-container interface approaches. Modeling the fluid-container interface using coupling equations or contact elements leads to the same results of coupled system frequencies.

7.4 Materials And Methods

The objective of this chapter is to study the effects of dam-reservoir-foundation interaction on modal behaviour of "Brezina" gravity dam. It is important to note that this dam is named Arch dam but it has no arch effect in it behaviour, for this reason plane strain behaviour is considered for the medium cross section. Hence, 2-D finite element models are created using ANSYS program. Water is also treated as compressible fluid. For simplicity, no absorption is considered at reservoir bottom. Material properties of the concrete dam structure, the foundation, and reservoir water are given in table 4.2 and table 4.3 respectively.

Since the extent of the reservoir is large, it is necessary to truncate the reservoir at a sufficiently large distance from the dam. A length of reservoir equivalent to three times its depth is appropriate for adequate representation of hydrodynamic effects on the dam, a length of 150 m on each side in X direction is judged sufficient after doing a sensitivity analysis, and the same length is chosen as extension of foundation (in X direction). The nodes representing the extreme side of the reservoir are free to displace in the vertical direction only. The depth of the foundation is taken as 100 m. Plane strain conditions are taken into account in the calculations.

The dam material is assumed to be linear-elastic, homogeneous and isotropic.

A two dimensional (2D) finite element model with 1521 nodes and 1394 plane elements (PLANE 42) is used to model Brezina dam with surrounding foundation.

A two dimensional (2D) finite fluid element model with 273 nodes and 240 plane elements (FLUID 79) is used to model the reservoir water for the first assumption; however for the second one; where the reservoir water is modeled as added masses, 42 surface elements (SURF 153) are used. The water mass is applied uniformly on the upstream face of the dam plus the hydrostatic pressure, the surface element (SURF 153) is characterized by its length and its thickness, these two properties depends on both water level and the contact length between the fluid and the system (dam- foundation system).

It is important to note that the number of elements used to model the reservoir water depends on the water level.

As mentioned above, two approaches are used to model the interfaces (fluid-dam and fluid–foundation):

First one: using contact elements;

Contact elements generated by ANSYS software are applied at the interfaces fluid-concrete dam and fluid- foundation, considering the foundation and the dam as target elements (TARGE 169) and water as contact elements (CONTA 172) (view figure 4.10).

Second: using coupling equations; by coupling the interface nodes in the normal direction only and let it free in all other directions.

Three assumptions of foundation models are suggested using the direct method; the fixed support foundation, the mass foundation to take into account the inertial effect of the foundation and the massless foundation to neglect it.

Figure 7.4 sketches the dam with fixed support without water and the dam with fixed support with full reservoir water. However, Figure 7.5 sketches dam with foundation without water and dam with foundation and full reservoir water.

To investigate the modal behaviour of the dam, twelve different cases are taken as follow:

- ✓ Dam with fixed support; Empty reservoir, named "*Fixed-Empty*";
- ✓ Dam with fixed support; Full reservoir; fluid-dam and fluid- foundation interfaces modeled by contact elements named "*Fixed-contact*";
- ✓ Dam with fixed support; Full reservoir; fluid-dam and fluid- foundation interfaces modeled by coupling equations, named "*Fixed-coupling*";
- ✓ Dam with fixed support; Full reservoir; fluid modeled as added masses named "*Fixed-surf*";
- ✓ Dam with massless foundation; Empty reservoir, named "*Massless-Empty*";
- ✓ Dam with massless foundation; Full reservoir; fluid-dam and fluid- foundation interfaces modeled by contact elements named "*Massless-contact*";
- ✓ Dam with massless foundation; Full reservoir; fluid-dam fluid- interface foundation modeled by coupling equations, named "*Massless-coupling*";
- ✓ Dam with massless foundation; Full reservoir; fluid modeled as added masses, named "*Massless-surf*";
- ✓ Dam with mass foundation; Empty reservoir, named "*Mass-Empty*";
- ✓ Dam with mass foundation; Full reservoir; fluid-dam and fluid- foundation interfaces modeled by contact elements, named "*Mass-contact*";
- ✓ Dam with mass foundation; Full reservoir; fluid-dam and fluid- foundation interfaces modeled by coupling equations, named "*Mass-coupling*";
- ✓ Dam with mass foundation; Full reservoir; fluid modeled as added masses, named "*Mass-surf*";

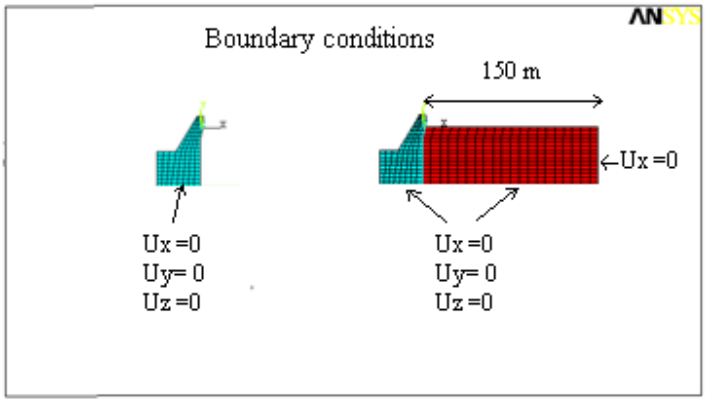

Figure 7.4: Finite element modeling of dam-reservoir interaction (foundation modeled as fixed support)

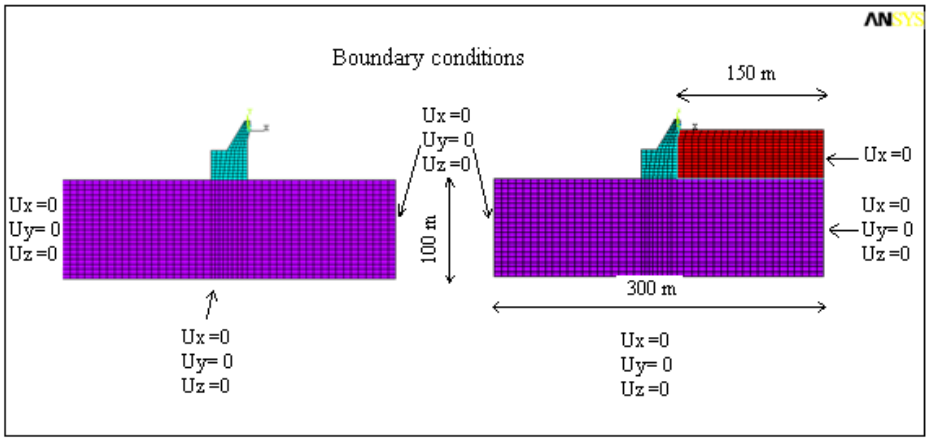

Figure 7.5: Finite element modeling of dam reservoir foundation interaction (foundation modeled as mass foundation / massless foundation)

7.5 Modal Analyses of dam-fluid-foundation systems

Modal analyses are performed for dam-fluid-foundation models presented in section 7.4 using Block Lanczos extraction method available in Ansys finite element code. Results of these analyses are then summarized and discussed in this section, starting by sloshing modes and then the coupled modes frequencies of systems.

7.5.1 Sloshing mode frequencies of dam-fluid-foundation systems

The first four sloshing mode shapes are presented in figure 7.6 for the case of dam with fixed support and in figure 7.7 for the case of dam with foundation; these modes are similar to those presented in figure 7.2 (similar in shapes only). Values of these sloshing frequencies are summarized in Table 7.3.

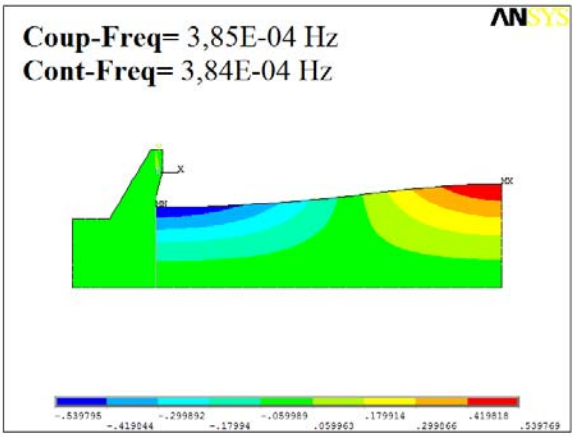

1st sloshing mode shape

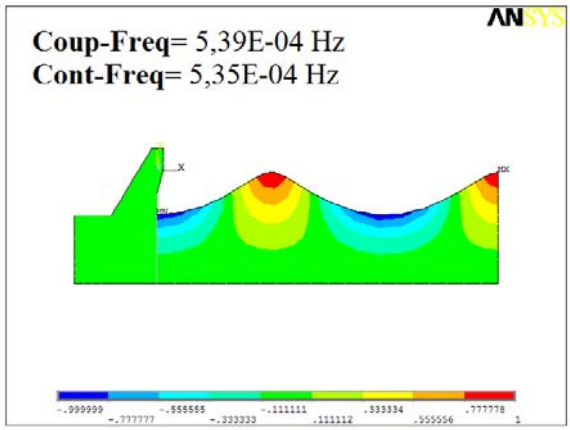

2nd sloshing mode shape

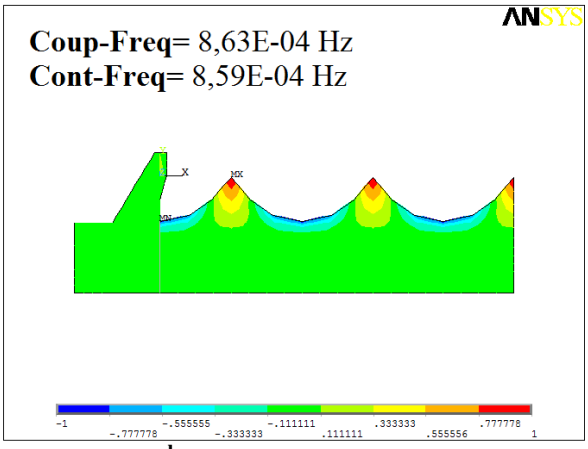

3rd sloshing mode shape

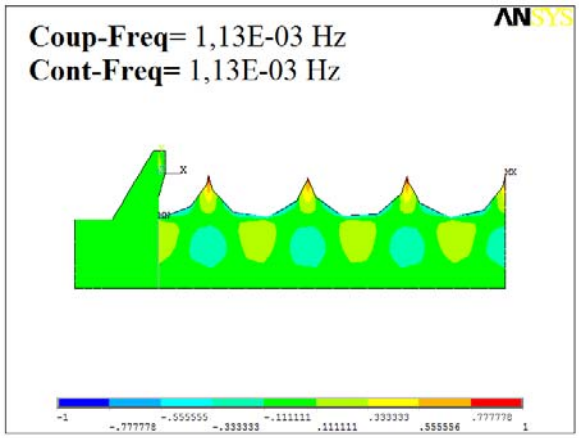

4th sloshing mode shape

Figure 7.6: The first four sloshing mode shapes for the case of dam with fixed support.

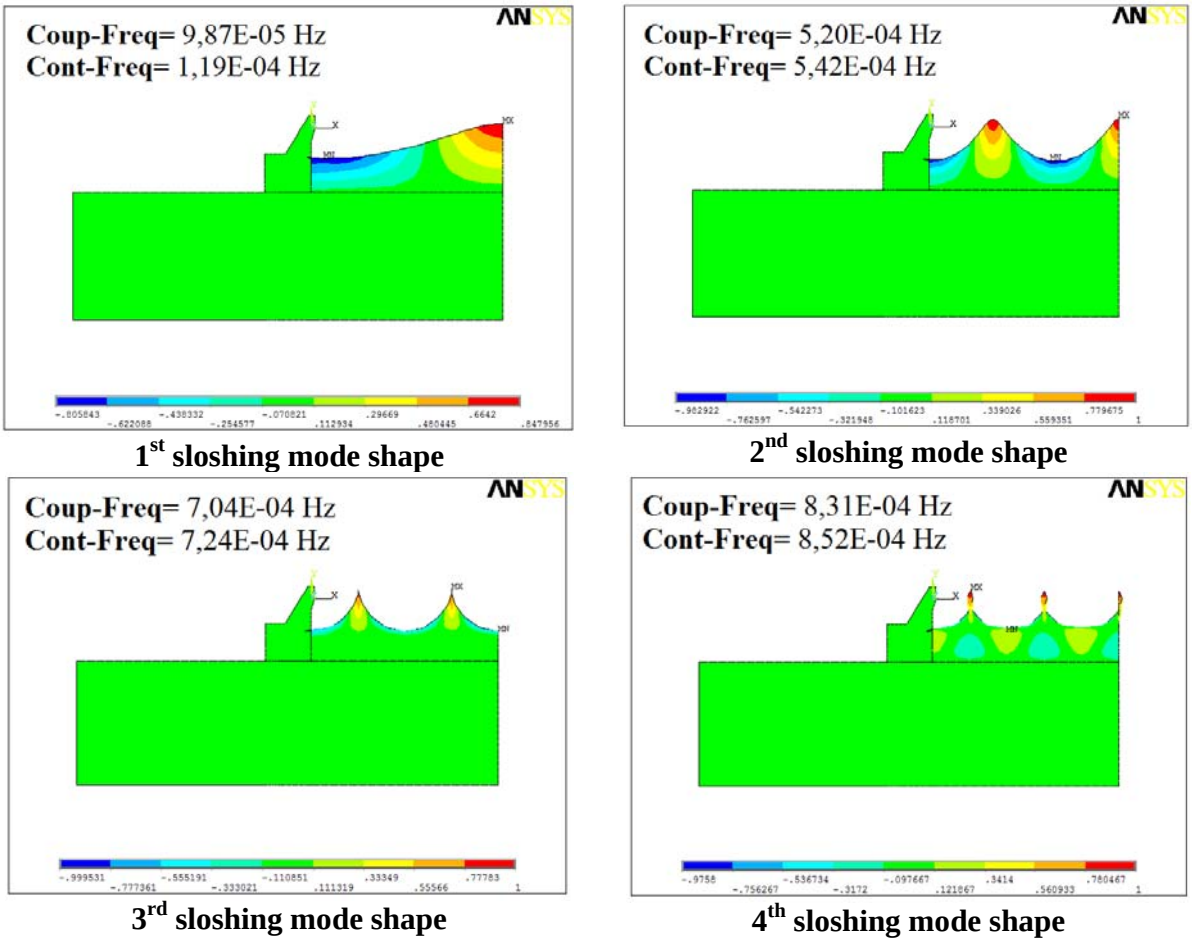

Figure 7.7: The first four sloshing mode shapes for the case of dam with mass foundation.

Table 7.3 shows that using coupling equations or contact elements to model fluid - dam and fluid-foundation interfaces gives the same sloshing frequencies values.

Mode Number	Fixed-coupling		Fixed- contact	
	Frequency (Hz)	Ratio	Frequency (Hz)	Ratio
1	3,85E-04	1	3,84E-04	1
2	5,39E-04	0,247756	5,35E-04	0,235694
3	8,63E-04	0,104371	8,59E-04	0,100223
4	1,13E-03	0,049275	1,13E-03	0,049275

Table 7.3: The first four sloshing modal frequencies values for the case of dam with fixed supports.

Mode Number	Massless-coupling		Massless - contact	
	Frequency (Hz)	Ratio	Frequency (Hz)	Ratio
1	9,87E-05	1	1,19E-04	1
2	5,20E-04	0,223915	5,42E-04	0,251464
3	7,04E-04	0,003701	7,24E-04	0,012851
4	8,31E-04	0,086763	8,52E-04	0,110919

Table 7.4: The first four sloshing modal frequencies values for the case of dam with massless foundation.

Mode Number	Mass-coupling		Mass - contact	
	Frequency (Hz)	Ratio	Frequency (Hz)	Ratio
1	9,87E-05	0,505445	1,19E-04	0,383475
2	5,20E-04	0,113177	5,42E-04	0,09643
3	7,04E-04	0,001871	7,24E-04	0,004928
4	8,31E-04	0,043854	8,52E-04	0,042535

Table 7.5: The first four sloshing modal frequencies values for the case of dam with mass foundation.

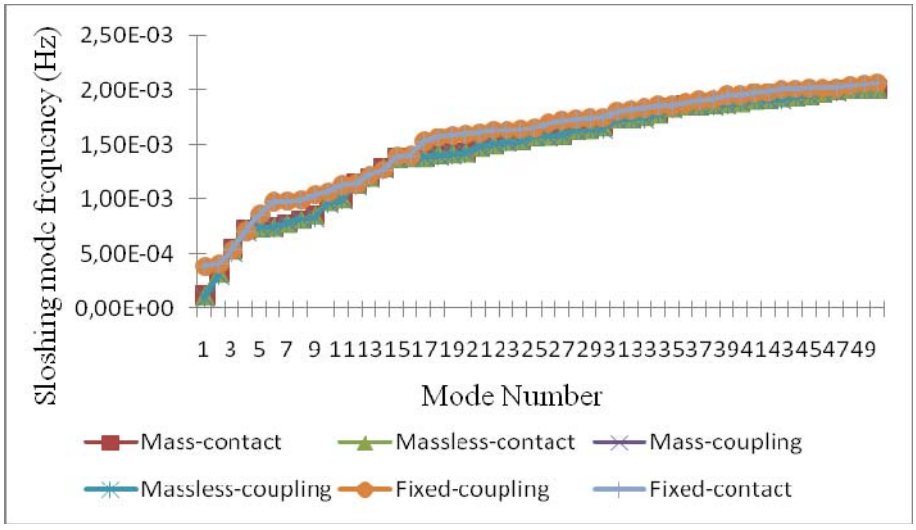

Figure 7.8: Effect of foundation-dam interaction and fluid-dam and fluid-foundation interface modeling on fluid sloshing frequencies values.

Table 7.3 and figure 7.8 show also that fluid sloshing frequencies values are independent on the foundation inertia; but little influenced by the system boundary condition.

7.5.2 Coupled mode frequencies of dam-fluid-foundation systems

The first four coupled mode shapes for the dam-fluid-foundation system are sketched in figure 7.9 for the case of dam with fixed support and in figure 7.10 for the case of dam with foundation support.

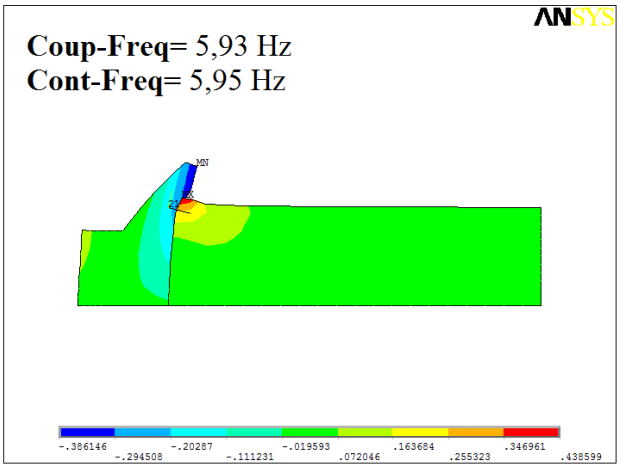

1st coupled mode shape

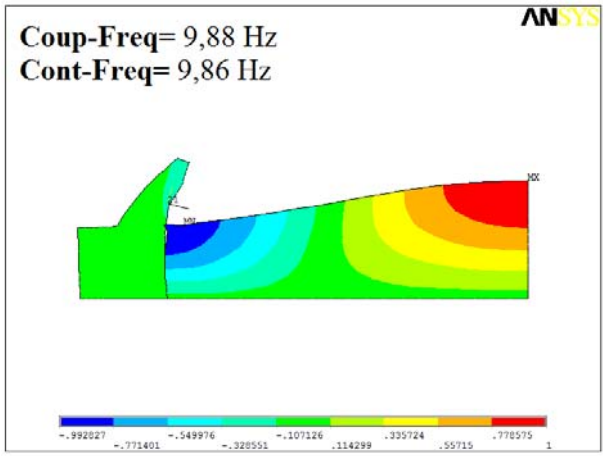

2nd coupled mode shape

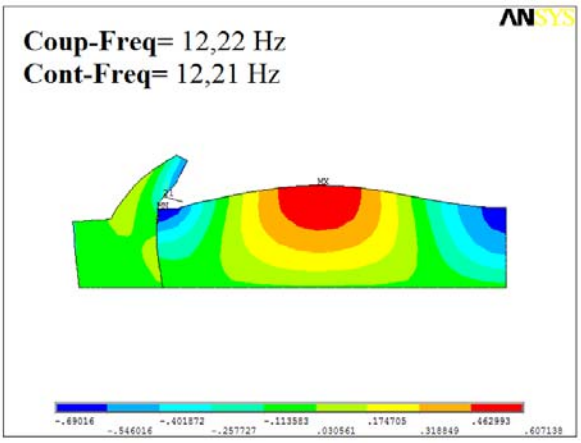

3rd coupled mode shape

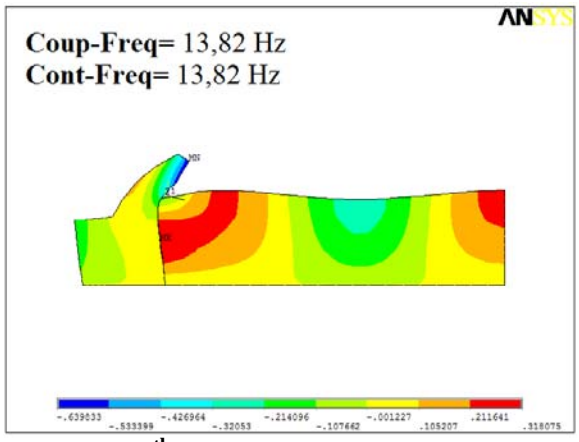

4th coupled mode shape

Figure 7.9 The first four coupling mode shapes for the case of dam with fixed support.

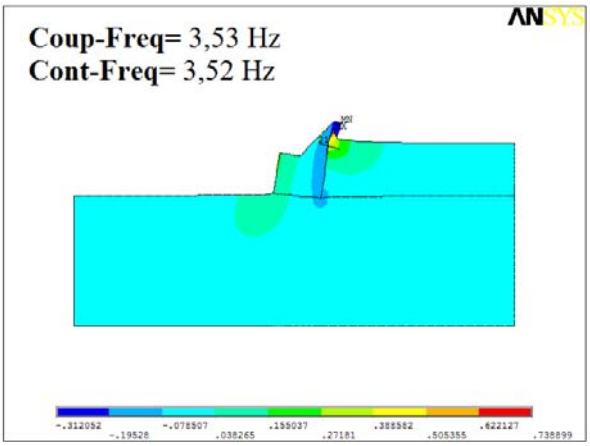

1st coupled mode shape

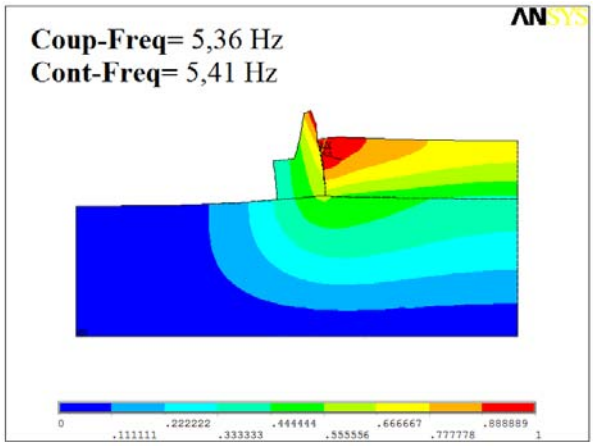

2nd coupled mode shape

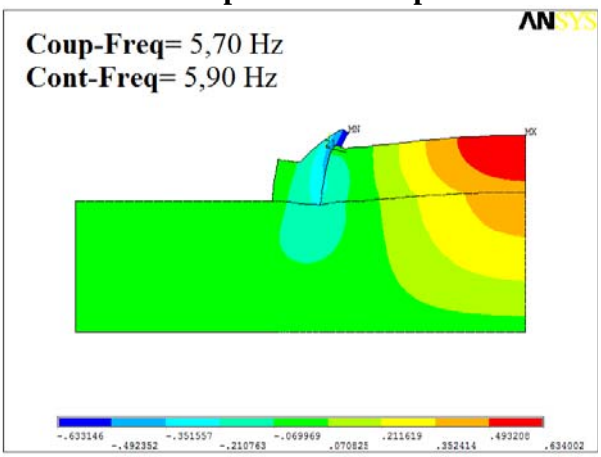

3rd coupled mode shape

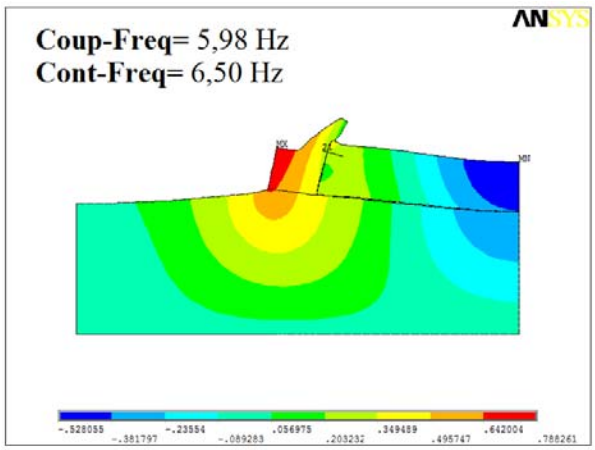

4th coupled mode shape

Figure 7.10: The first four coupling mode shapes for the case of dam with mass foundation.

From figure 7.9 and figure 7.10 it is clear that coupled mode shapes (shapes of modes) are independent on whether the foundation is presented or not (modelized by fixed support).

7.5.2.1 Effect of water reservoir and interface modeling on the modal coupled frequencies of dam-fluid-foundation system

a. Case of fixed support foundation model

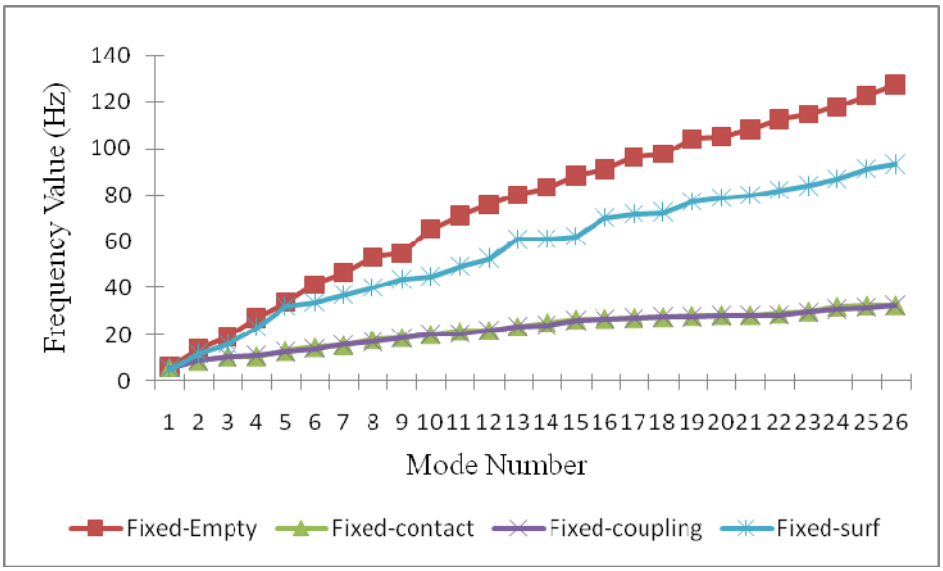

Figure 7.11: Combined effect of reservoir water and fluid-dam and fluid-foundation modeling on the modal frequencies of the dam-fluid-foundation system for the case of fixed support foundation model

The Figure 7.11 represents for the case of fixed support foundation the effect of the reservoir water presence and the interface modeling on modal frequencies of the dam object of this study. As mentioned above, the Fixed- Empty, the Fixed-contact, the Fixed-coupling and the Fixed-surf cases represent respectively for the fixed foundation model the system without water effect, the system with full reservoir and interfaces modeled by contact elements, the system with full reservoir and interfaces modeled by coupling equations and finally the case of the system with full reservoir modeled as added masses.

It is clear from this figure that the presence of water leads to a decrease of the modal frequencies of the dam and that modeling the interface fluid structure by coupling equations or using contact elements give the same results, however the added masses approach overestimate the frequencies modes values.

By modeling the reservoir water, the total mass of the system increases which leads to a decrease of system frequencies. For the two fluid modeling approaches the same quantity of water is added to the dam- foundation system, but the application manner is different. By fluid finite element, the water effect is transmitted to the structure (dam) as displacements (view § 4.5.2), while by modeling the fluid using surface element, the water effect is applied as uniform masses at the upstream dam face which increases the system stiffness. For this reason the frequencies obtained using surf elements are much greater than those obtained using fluid finite elements.

b. Case of massless foundation model

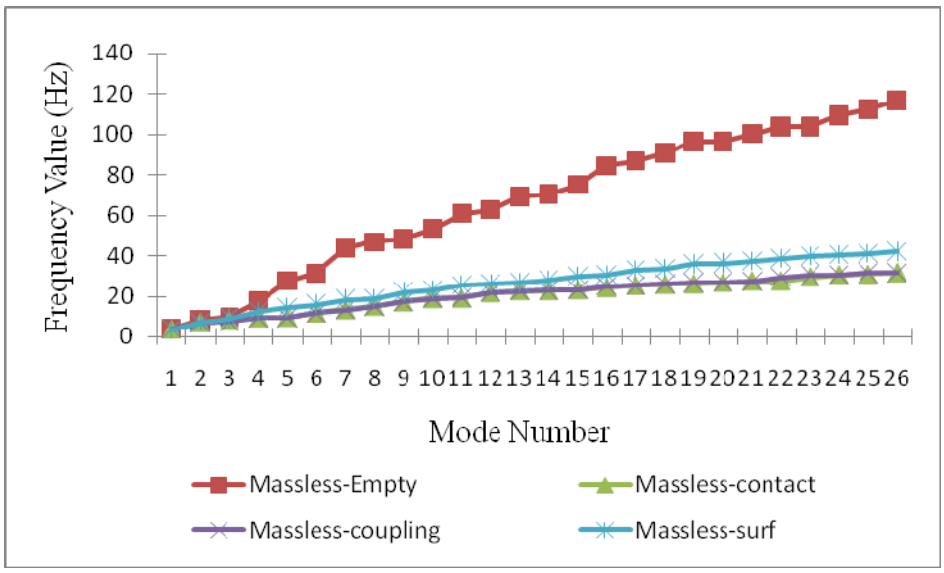

Figure 7.12: Combined effect of reservoir water and fluid dam/or foundation modeling on the modal frequencies of the foundation-dam-fluid system for the case of massless foundation model

The Figure 7.12 represents for the case of massless foundation the effect of the reservoir water presence and the interface modeling on modal frequencies of the dam object of this study.

As mentioned above, the Massless- Empty, the Massless -contact, the Massless -coupling and the Massless-surf cases represent respectively for massless foundation model the system without water effect, the system with full reservoir and interfaces modeled by contact element, the system with full reservoir and interfaces modeled by coupling equations and finally the case of the system with full reservoir modeled as added masses.

It is clear that the presence of water leads to a decrease of the modal frequencies of the dam and that modeling the interface fluid-dam by coupling equations or using contact elements give the same results, however the added masses approach overestimate the frequencies modes values, but the rate of this overestimation is less than that obtained for the case where the dam foundation is clamped. This is due to the fact that the stiffness added by the uniform masses applied at the upstream dam face is loosed by taking into account the massless foundation (the massless foundation model is more flexible than the fixed foundation one).

c. Case of mass foundation model

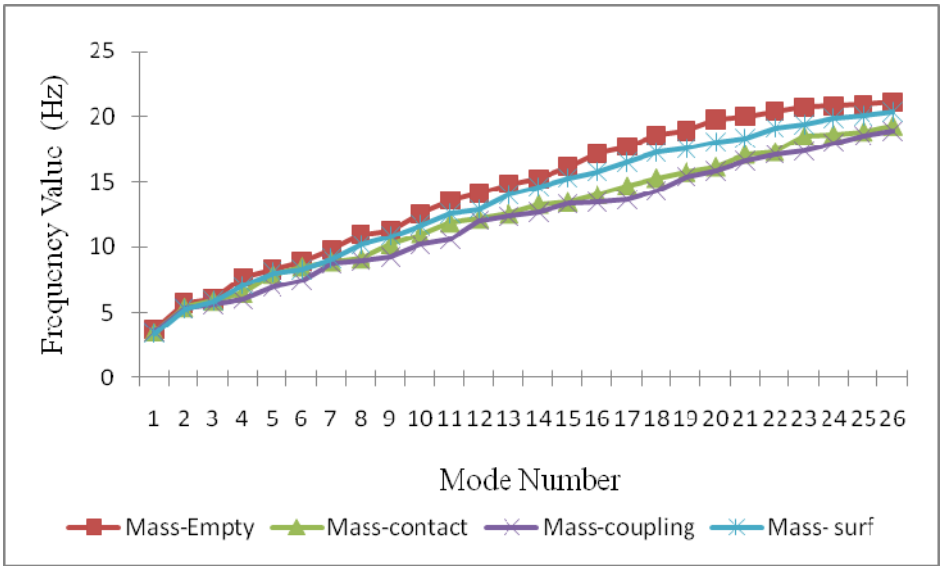

Figure 7.13: Combined effect of reservoir water and fluid dam/or foundation modeling on the modal frequencies of the foundation-dam-fluid system for the case of mass foundation model

The Figure 7.13 represents for the case of mass foundation the effect of the reservoir water presence and the interface modeling on modal frequencies of the dam object of this study.

As mentioned above, the Mass-Empty, the Mass-contact, the Mass-coupling and the Mass -surf cases represent respectively for mass foundation model the system without water effect, the system with full reservoir and interfaces modeled by contact element, the system with full reservoir and interfaces modeled by coupling equations and finally the case of the system with full reservoir modeled as added masses.

In this case the presence of water leads to a little decrease of the modal frequencies of the dam-reservoir-foundation system. The added masses approach using *surf elements* overestimate these frequencies, but this overestimation is neglected compared with that founds in the case of clamped foundation and massless foundation.

7.5.2.2 Effect of dam-foundation interaction modeling on the modal coupled frequencies of dam -fluid-foundation system

a. Empty reservoir case

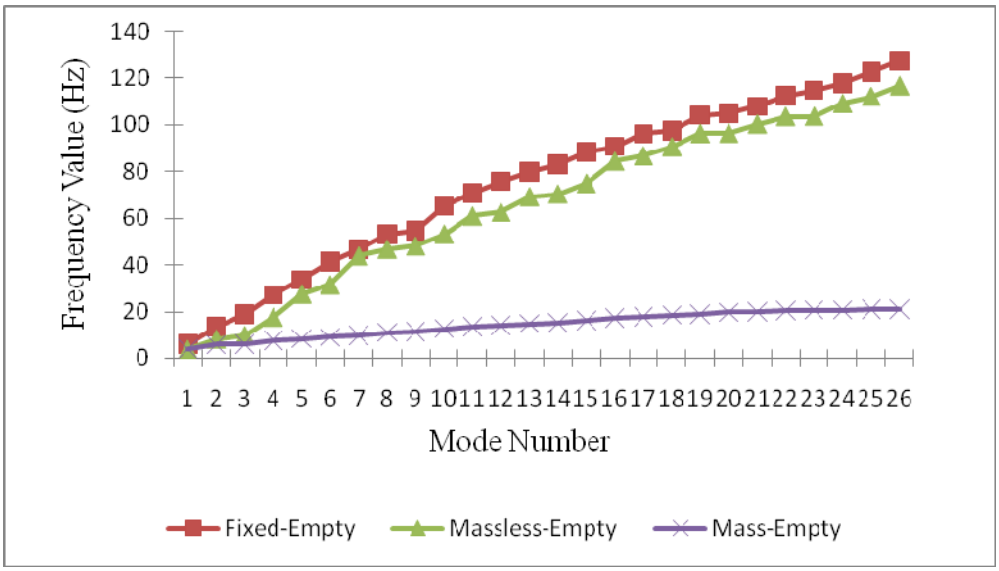

Figure 7.14: Effect of foundation structure interaction modeling on the modal frequencies of the dam-foundation system.

Figure 7.14 represents the modal frequencies for Fixed-Empty, Massless-Empty and Mass-Empty case which represent respectively the case of dam with fixed support with empty reservoir, the case of dam with massless foundation with empty reservoir and the case of dam with mass foundation with empty reservoir.

The Figure 7.14 shows that adding foundation to dam in the modeling which means taking into account the foundation structure interaction effect leads to a decrease in the modal frequencies values furthermore for the mass foundation model. Adding foundation to dam structure leads to a decrease in its stiffness and consequently a decrease in frequencies values furthermore when taking into account the mass of the added foundation, because this leads to an increase in the mass system and since this later is situated at the denominator in the frequency formula, the obtained value is smaller.

b. Full reservoir case (fluid dam/or foundation interface modeled by contact element)

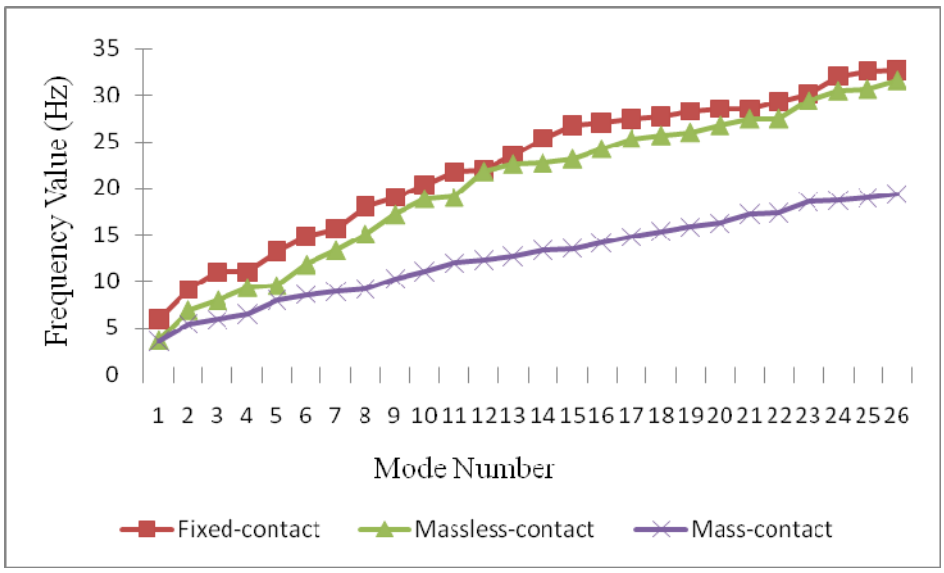

Figure 7.15: Effect of foundation structure interaction modeling on the modal frequencies of the dam-foundation-fluid system (interfaces modeled by contact elements).

Figure 7.15 represents the modal frequencies for Fixed-contact, Massless-contact and Mass-contact cases which represent respectively the case of dam with fixed support, the case of dam with massless foundation and the case of dam with mass foundation with fluid dam and fluid foundation interface modeled by contact elements. As previously, the figure 7.11 shows that adding foundation to dam structure decreases the system frequencies.

c. Full reservoir case (fluid dam/or foundation interface modeled by coupling equations)

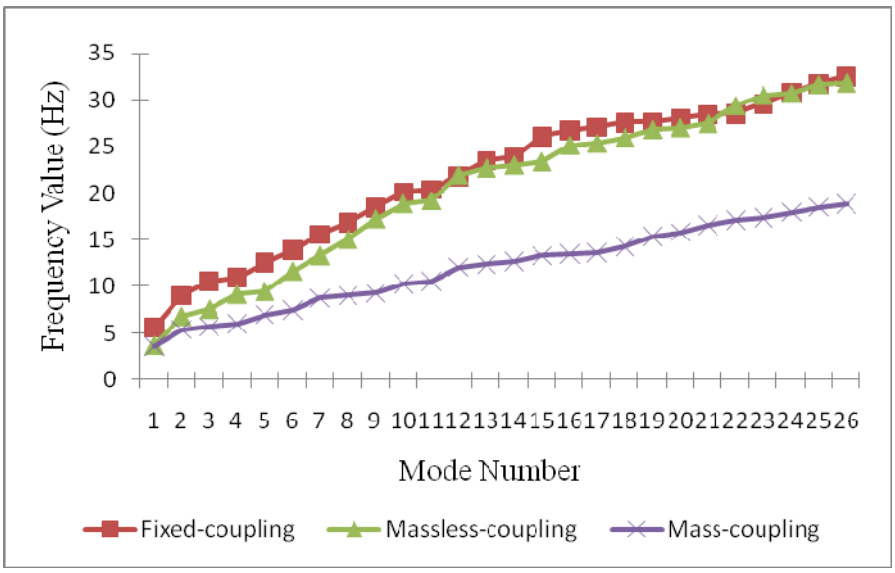

Figure 7.16: Effect of foundation structure interaction modeling on the modal frequencies of the dam-foundation-fluid system (interfaces modeled by coupling equations).

Figure 7.16 represents the modal frequencies for Fixed-coupling, Massless-coupling and Mass-coupling cases which represent respectively the case of dam with fixed support, the case of dam with massless foundation and the case of dam with mass foundation with fluid dam and fluid foundation interface modeled by coupling equations.

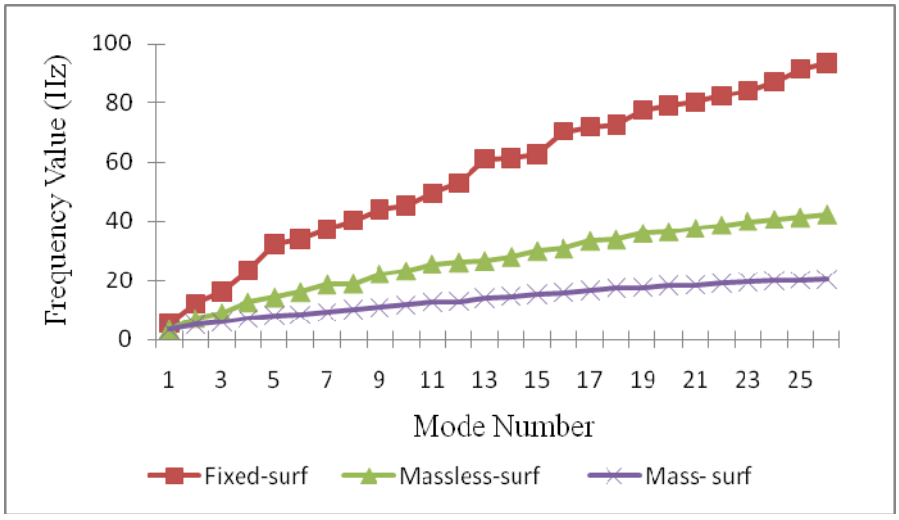

Figure 7.17: Effect of foundation structure interaction modeling on the modal frequencies of the dam-foundation-fluid system (Fluid modeled as added masses).

Figure 7.17 represents the modal frequencies for Fixed-surf, Massless- surf and Mass-surf cases which represent respectively the case of dam with fixed support, the case of dam with

massless foundation and the case of dam with mass foundation with fluid modeled by surf element representing the added masses approach.

From Figure 7.14, Figure 7.15, Figure 7.16 and Figure 7.17 it's clear that dam-foundation interaction modeling has the same effect on the modal frequencies for both cases of interfaces and fluid modeling; which means that taking into account the foundation structure interaction effect leads to a decrease in the modal frequencies even if the reservoir water is modeled (either by fluid finite element or added masses) or not (Empty case) and even if the fluid-dam and fluid-foundation interfaces are modeled by contact element or by coupling equations.

7.5.2.3 Reservoir water level effect on the modal coupled dam-fluid-foundation system frequencies

To expand the study, the effect of water level on the dynamic characteristics of the dam and consequently on its dynamic behaviour is examined. This is achieved for different foundation models and for the two assumptions of interface modeling; coupling equations and contact elements.

Considering the great importance of natural vibration modes, 27 first frequencies of dam-reservoir-foundation system in six different water levels for Brezina dam body were extracted (from figure 7.18 to figure 7.21).

In this paragraph the "H_W" denotes the water level height, and the "Hc" denote the concrete dam height which is about 60 m.

a. Interface modeled using coupling equations and foundation modeled as mass foundation

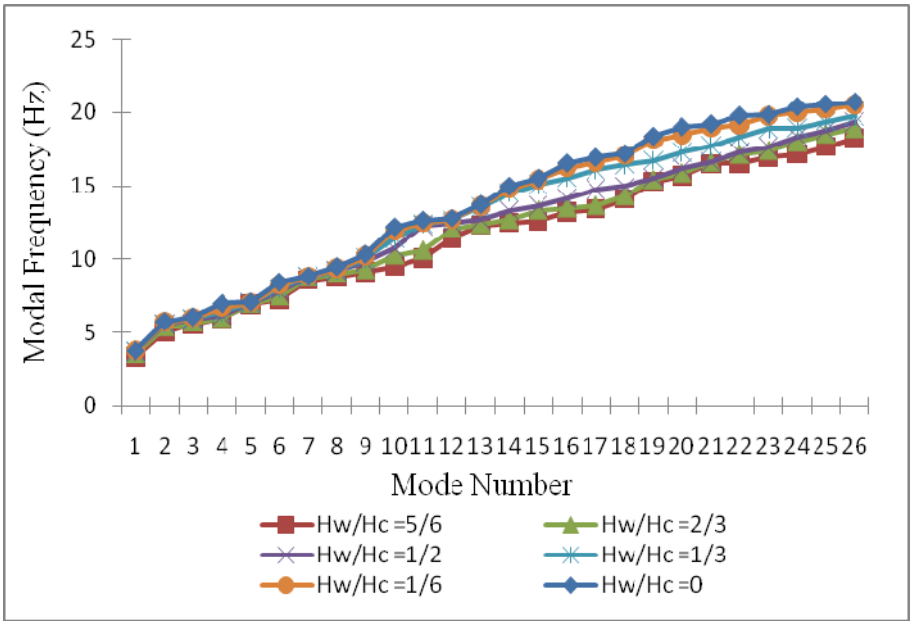

Figure 7.18: Reservoir water level effect on the modal frequencies of dam-fluid-foundation system for the case where the foundation is modeled as mass foundation and the interfaces modeled using coupling equations.

b. Interface modeled using coupling equations and foundation modeled as massless foundation

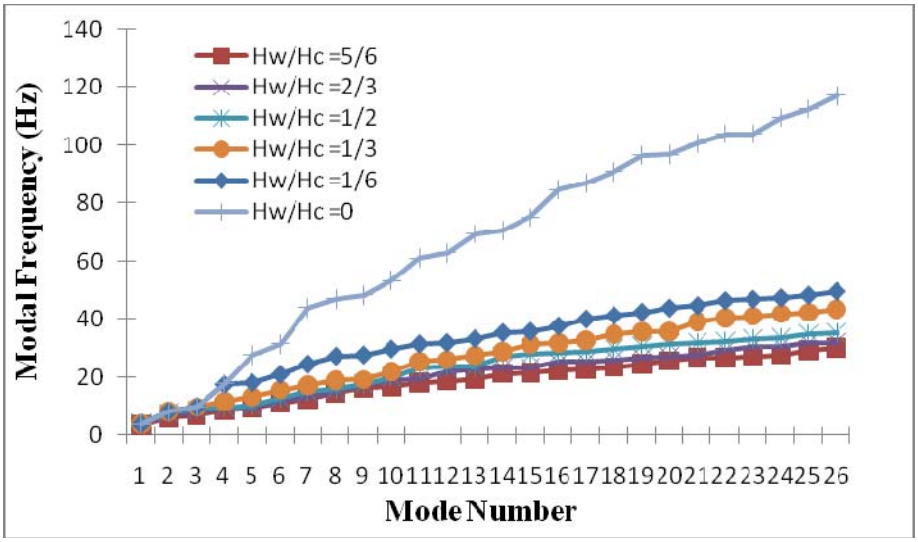

Figure 7.19: Reservoir water level effect on the modal frequencies of dam fluid foundation system for the case where the foundation is modeled as massless foundation and the interfaces modeled using coupling equations.

c. Interface modeled using contact elements and foundation modeled as mass foundation

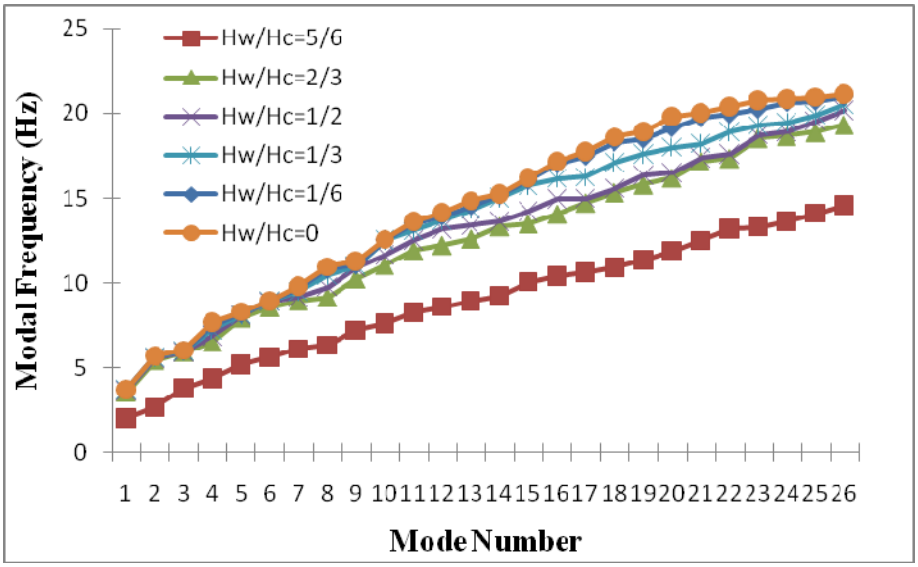

Figure 7.20: Reservoir water level effect on the modal frequencies of dam fluid foundation system for the case where the foundation is modeled as mass foundation and the interfaces modeled using contact elements.

d. Interface modeled using contact elements and foundation modeled as massless foundation

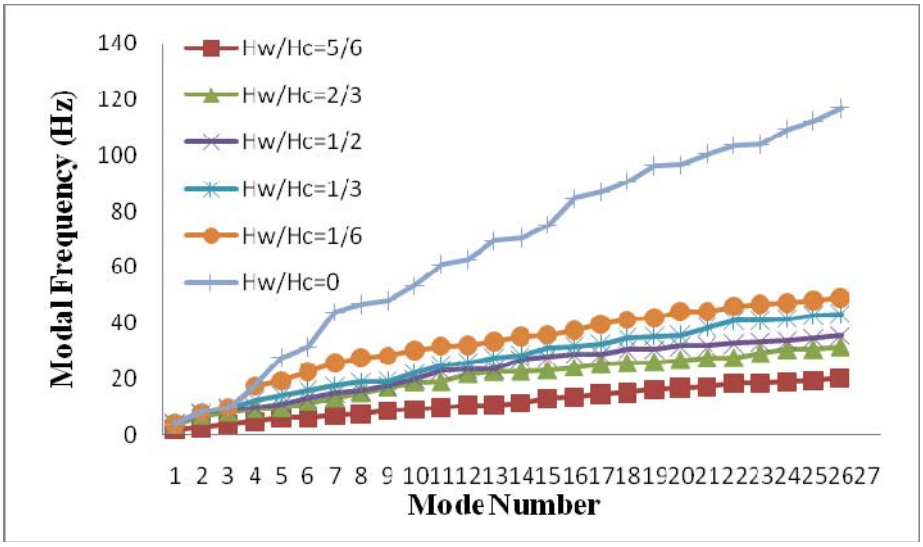

Figure 7.21: Reservoir water level effect on the modal frequencies of dam fluid foundation system for the case where the foundation is modeled as massless foundation and the interfaces modeled using contact elements.

Figure 7.18, Figure 7.19, Figure 7.20 and Figure 7.21 show that modal frequencies are inversely proportional with the reservoir water level; which means that frequencies decrease when water level increase (the amount of period grows with arising reservoir water level which is because of increasing total mass of the system and differences are meaningful for ten first modes). The same conclusion is obtained for "DEZ" high double curvature arch dam by M.A Hariri et al in 2011.

It is also shown that this decrease is more pronounced for the massless foundation case than it for the mass foundation case, this is due to the fact that for the same reservoir water level, the report of water mass with respect to the massless foundation system mass is more important than the report of the same water mass with respect to the mass of mass foundation system.

7.6 Two dimensional transient analysis of dam- foundation –reservoir interaction

In this part of the chapter, transient Analyses are performed for the same system presented previously (Brezina dam-foundation-reservoir system).

The system is excited at the foundation boundaries using the generated synthetic earthquake record having random number initializer of 17962 (view chapter 5).

The material properties and the same finite element model of Brezina dam-reservoir-foundation system; used for the previous modal analyses, were conserved for these transient studies using already Ansys, which can perform linear dynamic analyses using standard Rayleigh material damping (which takes into account a mass-proportional component and a stiffness-proportional component). The Rayleigh damping constants were adjusted so that the overall model had critical hysteretic damping ratio equal to ξ=5% for the whole frequency range considered.

From literature review (M.A Hariri et al in 2011), it has been confirmed that the worst case for high arch dams occurs in low water levels, for this reason in the present study the water reservoir level is taken about 30 m height which represents the half of the total dam height.

Inasmuch as from the modal analyses it has been concluded that modeling the dam-reservoir and foundation-reservoir using coupling equations or contact elements leads to the same system Eigen frequencies values, here in this application (transient study) only the coupling approach has been performed.

7.6.1 Reservoir water behaviour

Starting by water behaviour, two nodes located at the reservoir surface are chosen to represent water displacements, velocities and accelerations time histories, these nodes are “Node N1” and “Node N2” presented in figure 7.22.

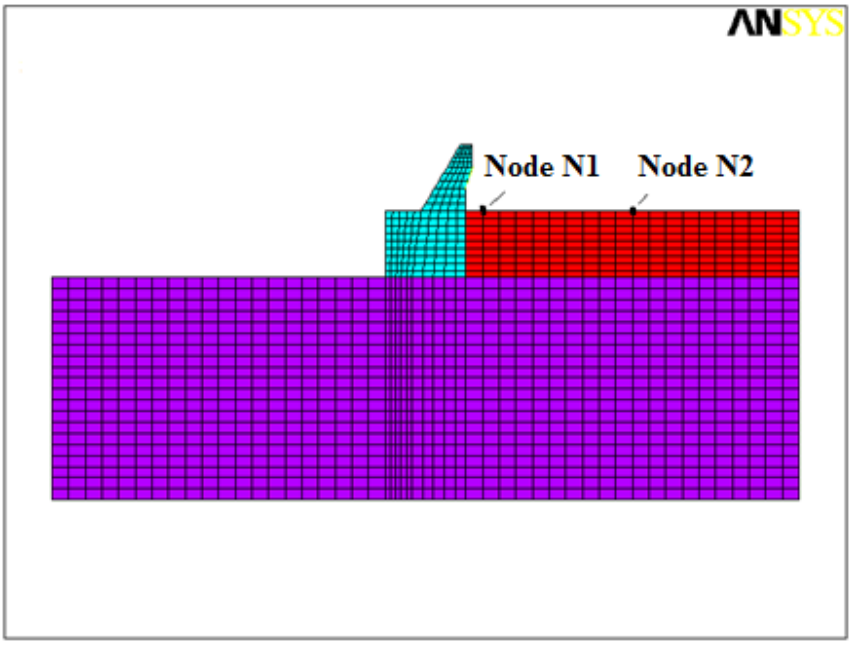

Figure 7.22: Location of nodes where results about water reservoir transient behaviour are presented

7.6.1.1 Water behaviour at node N1

a. Displacement in x direction at node N1

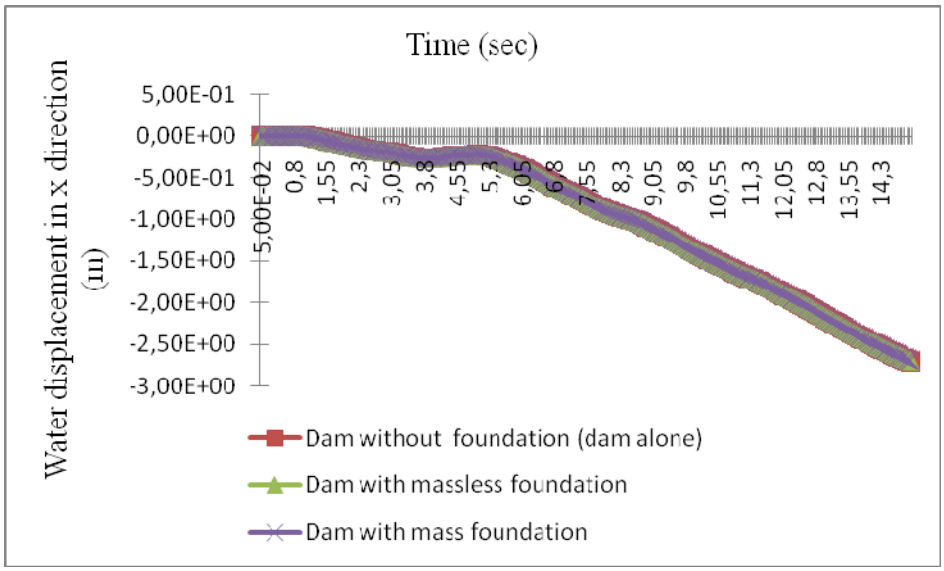

Figure 7.23: Water displacement in x direction at "Node N1"

b. Velocity in x direction at node N1

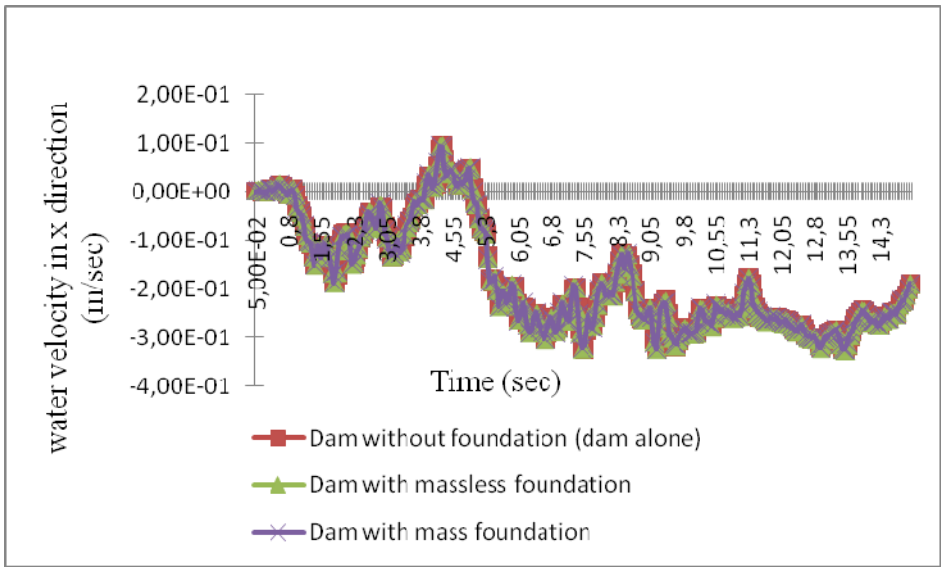

Figure 7.24: Water velocity in x direction at "Node N1"

c. Acceleration in x direction at node N1

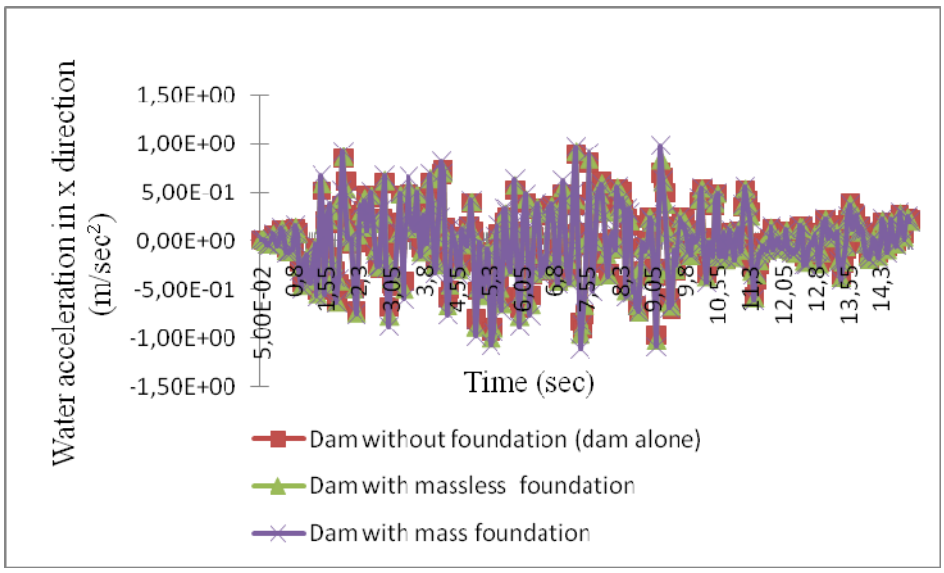

Figure 7.25: Water acceleration in x direction at "Node N1"

d. Displacement in y direction at node N1

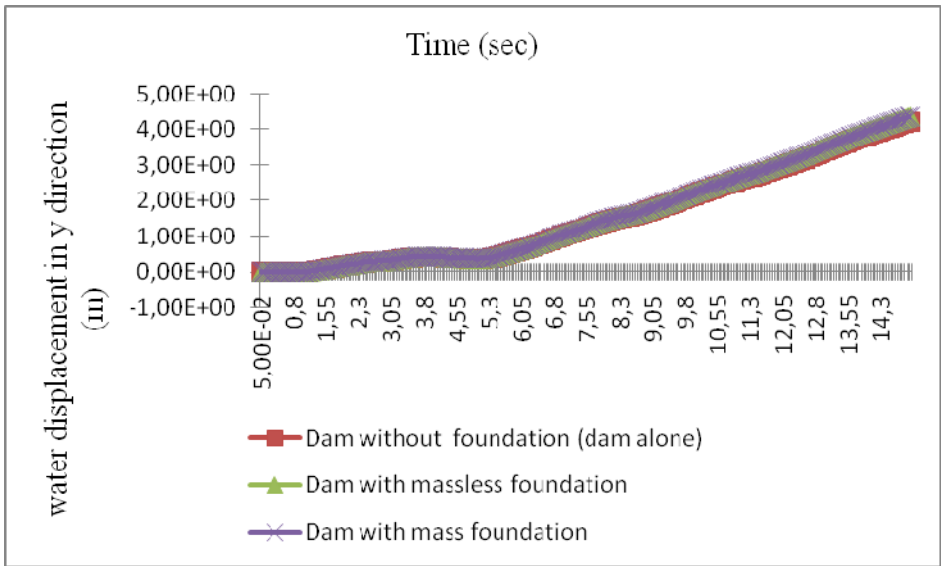

Figure 7.26: Water displacement in y direction at "Node N1"

e. Velocity in y direction at node N1

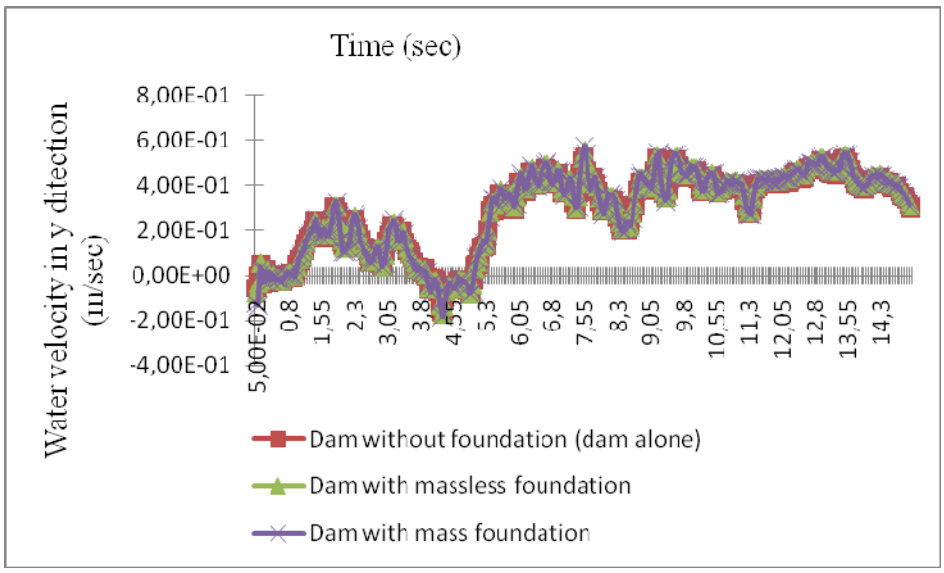

Figure 7.27: Water velocity in y direction at "Node N1"

f. Acceleration in y direction at node N1

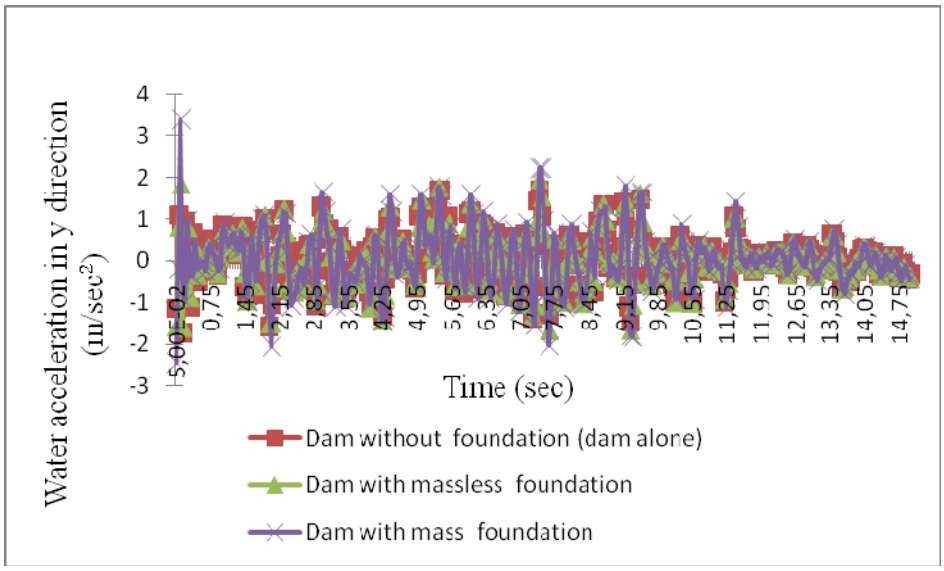

Figure 7.28: Water acceleration in y direction at "Node N1"

Figure 7.23 to figure 7.28 show that near to the concrete dam body, reservoir water transient behaviour in x and y direction is independent on the foundation-dam interaction modeling. This is due to the fact that in this location (next to dam body), water is more influenced by the dam body behaviour then the total system (dam-reservoir foundation system) behaviour.

7.6.1.2 Water behaviour at node N2

a. Displacement in x direction at node N2

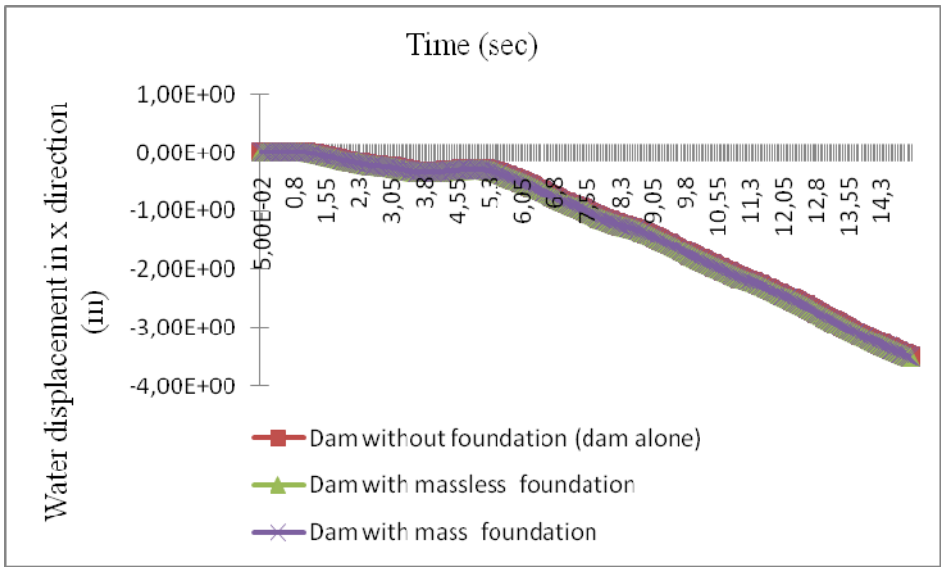

Figure 7.29: Water displacement in x direction at "Node N2"

b. Velocity in x direction at node N2

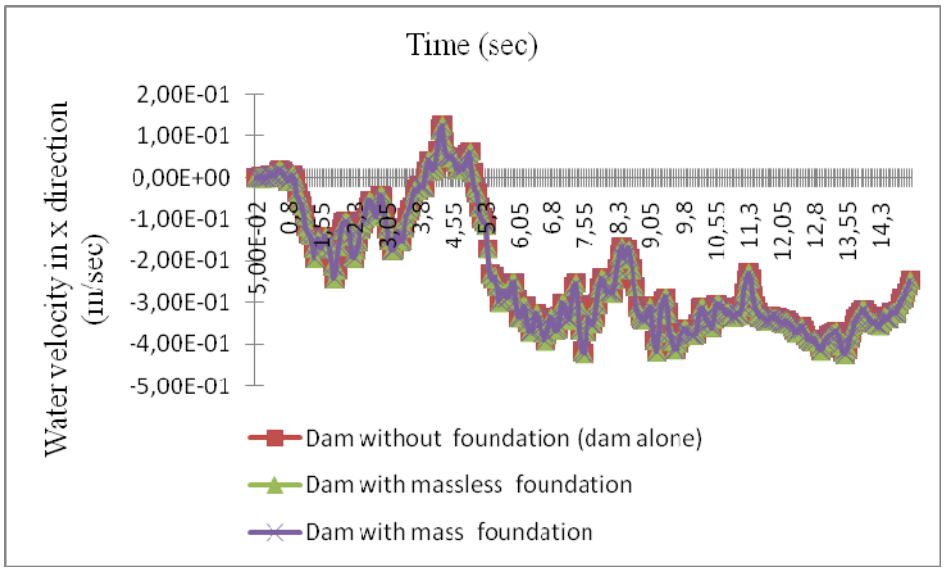

Figure 7.30: Water velocity in x direction at "Node N2"

c. Acceleration in x direction at node N2

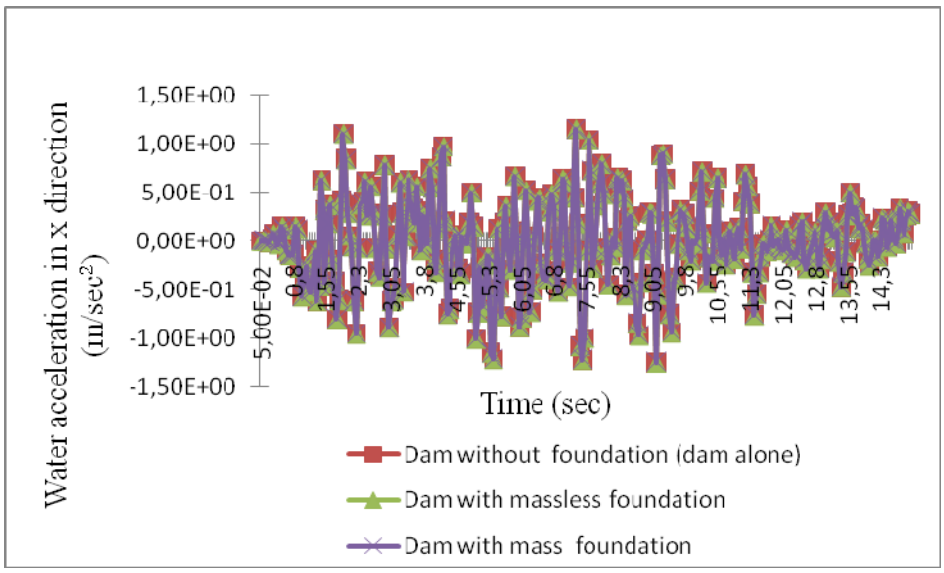

Figure 7.31: Water acceleration in x direction at "Node N2"

Figure 7.29 to figure 7.31 show also that far from concrete dam body, reservoir water transient behaviour in x direction is independent on the foundation-dam interaction modeling, the same displacement, velocity and acceleration time history are found for the three approaches of dam-foundation interaction modeling.

To interpret this result it is imperative to review the water boundary conditions applied to the model; as explained in section 7.4 of this chapter and for the coupled approach of dam-reservoir interface modeling, nodes representing the two reservoir extremities are coupled with dam body face nodes in the normal direction in one side and constrained in x direction and free to displace in the vertical direction in the extreme side. For this reason, in x direction reservoir motion is independent on the dam-foundation modelling.

d. Displacement in y direction at node N2

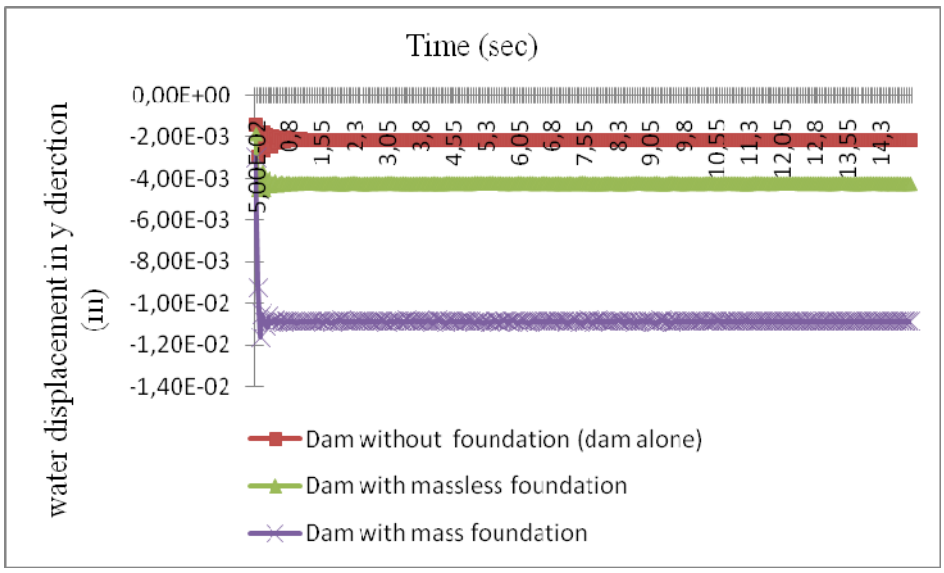

Figure 7.32: Water displacement in y direction at "Node N2"

e. Velocity in y direction at node N2

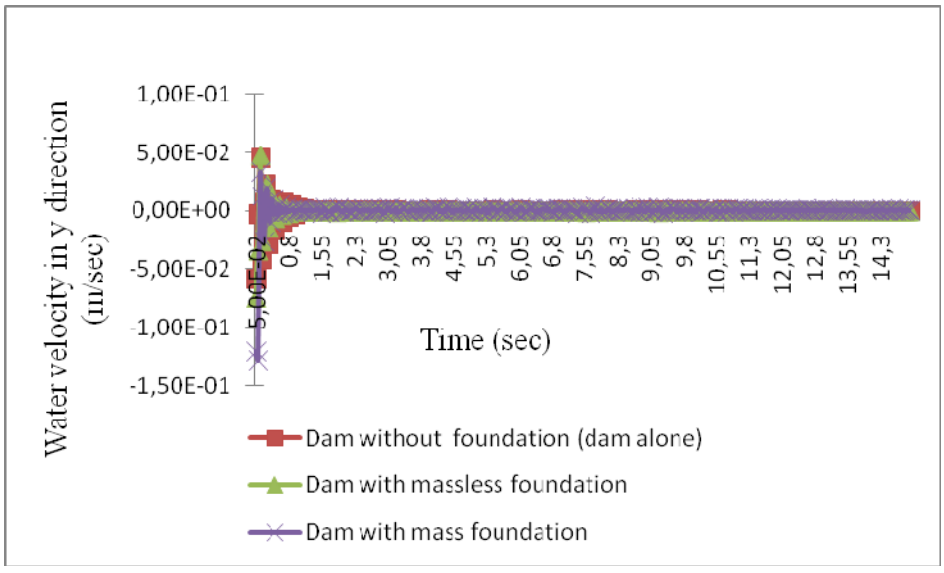

Figure 7.33: Water velocity in y direction at "Node N2"

f. Acceleration in y direction at node N2

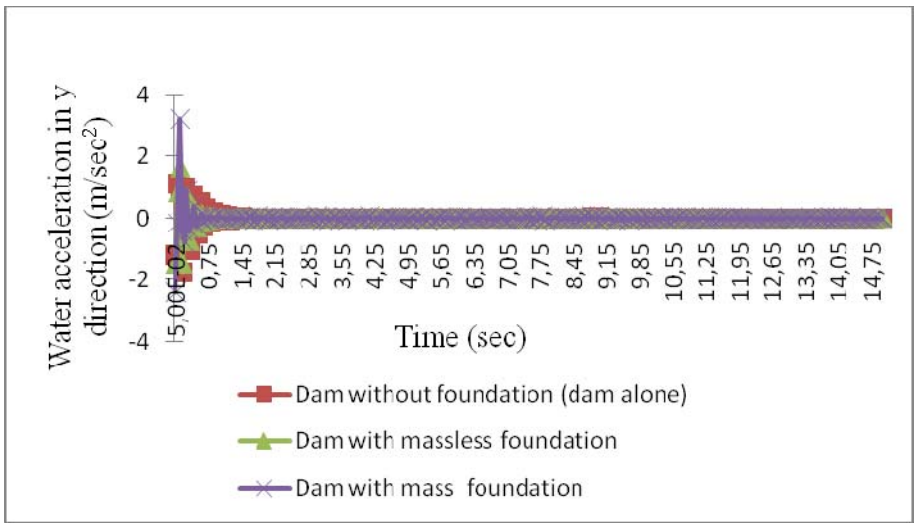

Figure 7.34: Water acceleration in y direction at "Node N2"

Figure 7.32, 7.33 and figure 7.34 show that far from the dam upstream face (node N2), for the case of dam with foundation, water reservoir is more excited in y direction (in terms of displacement, velocity and acceleration) than the case where the foundation is modeled as fixed support furthermore when the foundation is modeled as mass foundation model. This is due to the fact that far from the concrete dam body, reservoir water displacement in y direction depends on the total behaviour of the all dam-reservoir-foundation system and it has been well demonstrated in chapter 5 that the worst case occur when the foundation dam support is modelled as mass foundation model.

7.6.1.3 Comparison of water behaviour between N1 and N2

a. Water displacement in x direction for the case of dam with mass foundation

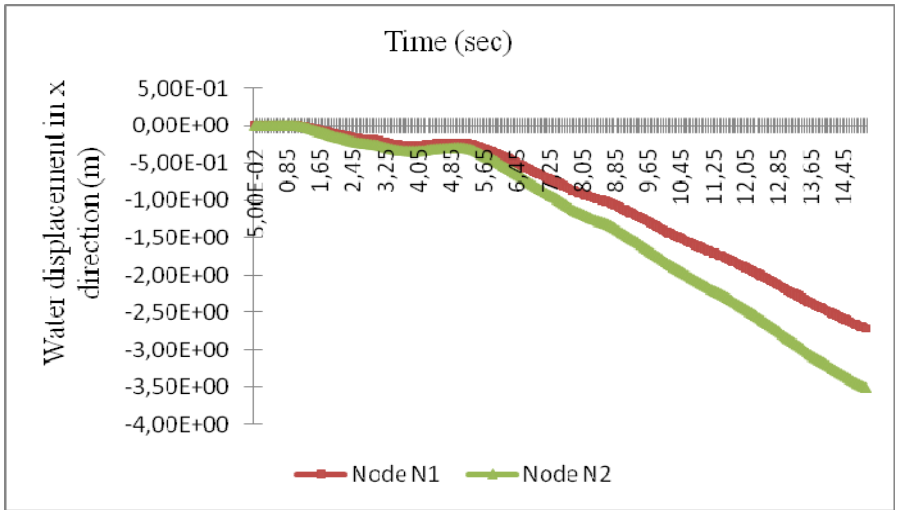

Figure 7.35: comparison of water displacement in x direction between node N1 and node N2 for the case of dam with mass foundation

b. Water velocity in x direction for the case of dam with mass foundation

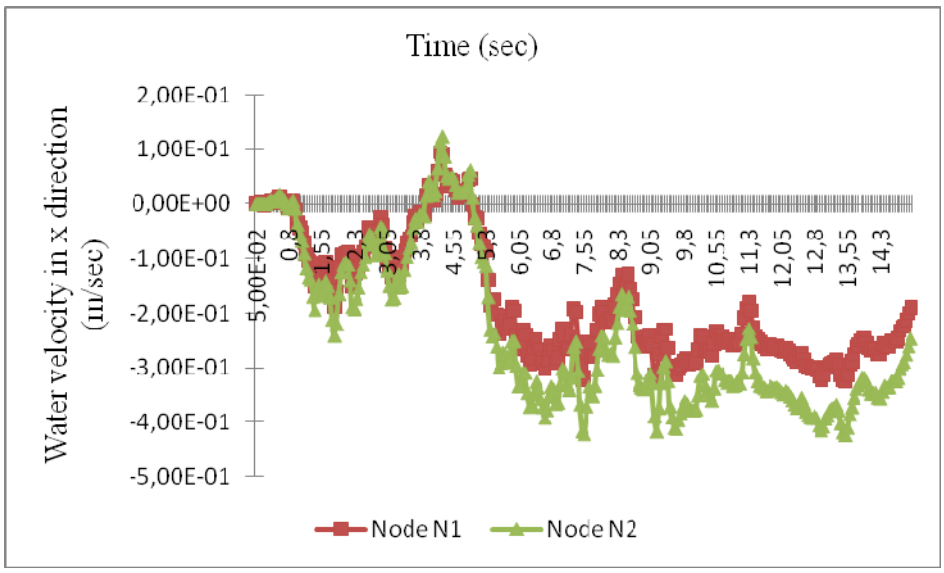

Figure 7.36: comparison of water velocity in x direction between node N1 and node N2 for the case of dam with mass foundation

c. Water acceleration in x direction for the case of dam with mass foundation

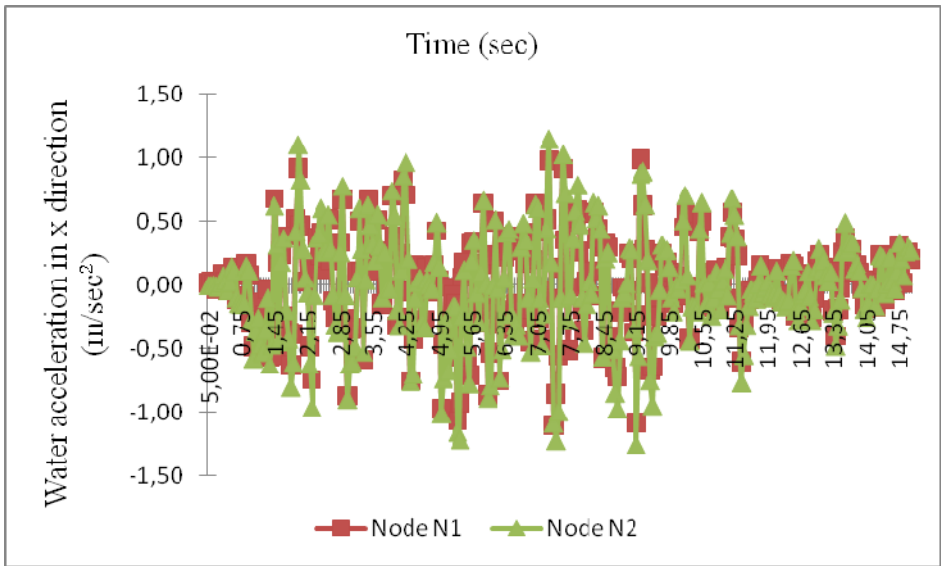

Figure 7.37: comparison of water acceleration in x direction between node N1 and node N2 for the case of dam with mass foundation

Figure 7.35, figure 7.36 and figure 7.37 sketch a comparison of water displacement, velocity and acceleration in x direction between nodes N1 and N2 for the case of dam with mass foundation model. It is shown that node N2 situated far from the dam body is more excited in x direction than node N1.

d. Water displacement in y direction for the case of dam with mass foundation

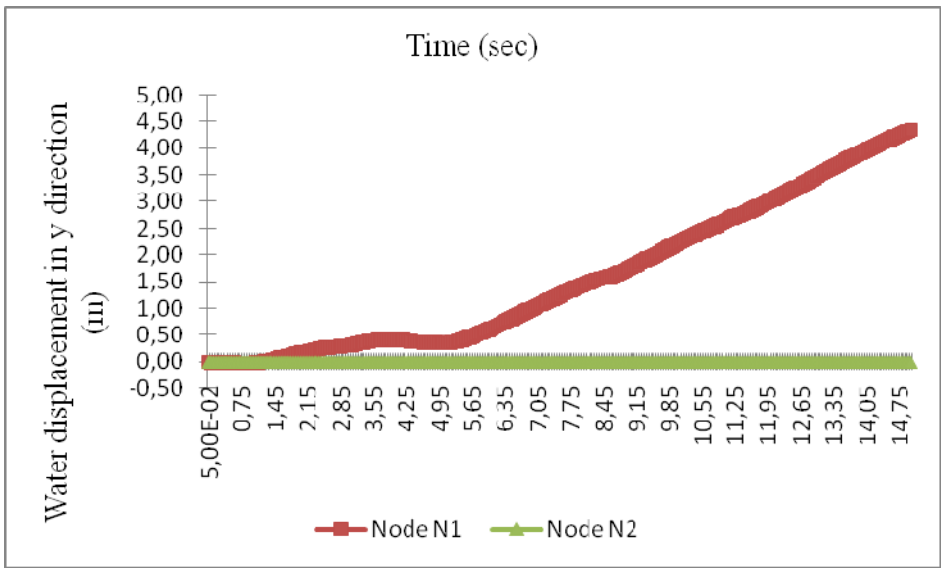

Figure 7.38: comparison of water displacement in y direction between node N1 and node N2 for the case of dam with mass foundation

e.Water velocity in y direction for the case of dam with mass foundation

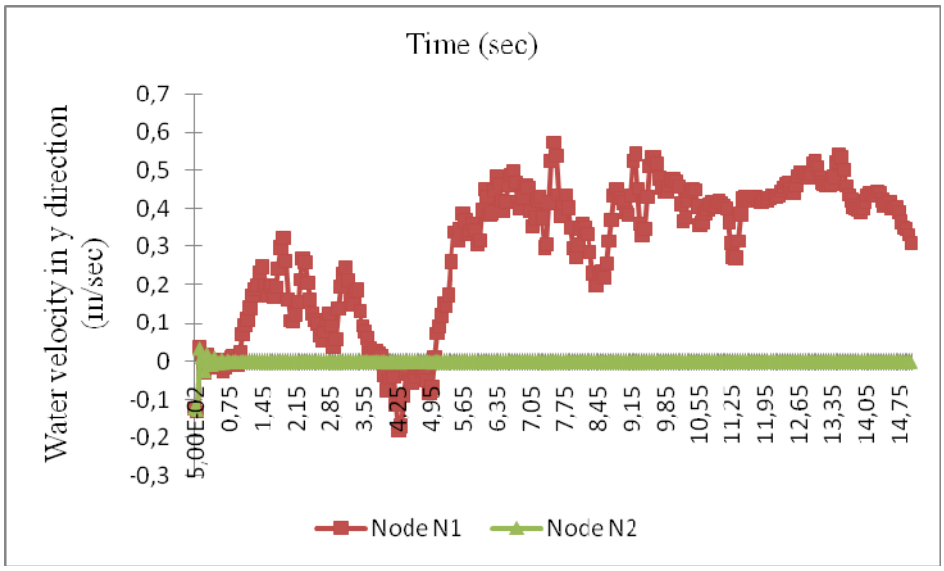

Figure 7.39: comparison of water velocity in y direction between node N1 and node N2 for the case of dam with mass foundation

f. Water acceleration in y direction for the case of dam with mass foundation

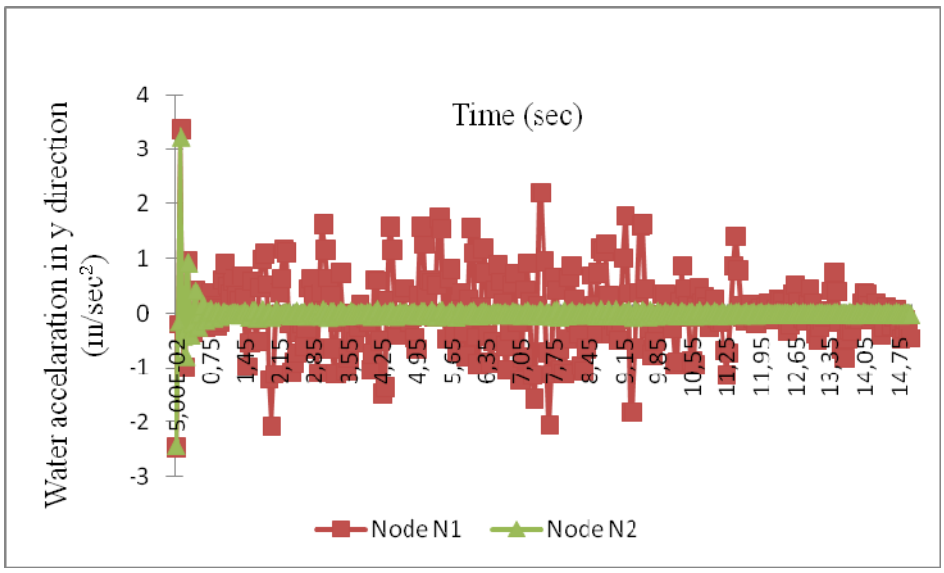

Figure 7.40: comparison of water acceleration in y direction between node N1 and node N2 for the case of dam with mass foundation

Figure 7.38, figure 7.39 and figure 7.40 sketch a comparison of water displacement, velocity and acceleration in y direction between nodes N1 and N2 for the case of dam with mass foundation model. Unlike water behaviour in x direction between the two mentioned nodes, in y direction it is node N1 which is more excited than node N2. When seismic record is applied to at dam-reservoir-foundation system base, foundation is the first part of the system which displace then the dam body and then the water reservoir, and after that interaction phenomena take place, for this reason motions in y direction for nodes located next to dam body (as node N1) are more important than motions for those located far from dam body (as node N2), which is the principle of wave propagation along a cord excited in one side.

7.6.2 Crest time history behavior for the three studied cases

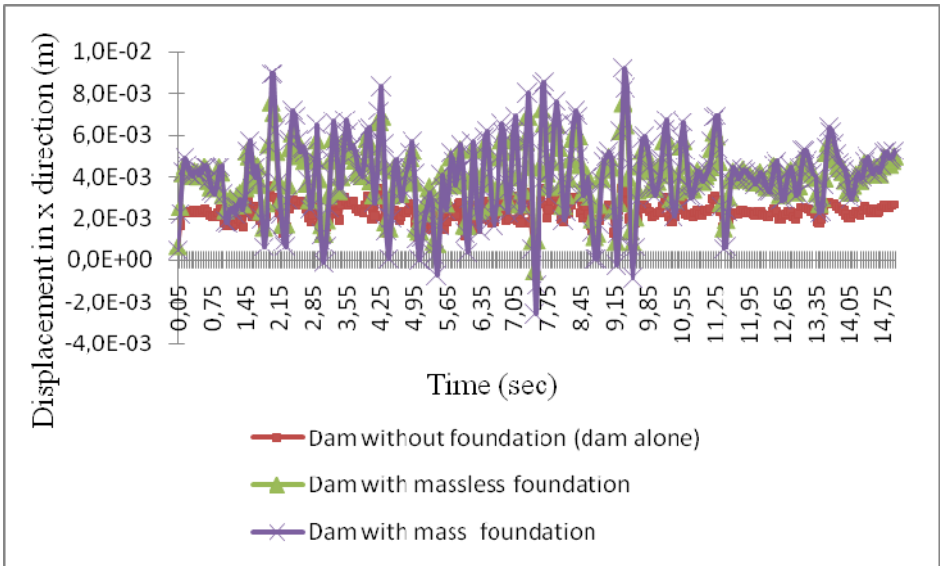

Figure 7.41: Crest displacement in x direction for the three studied cases

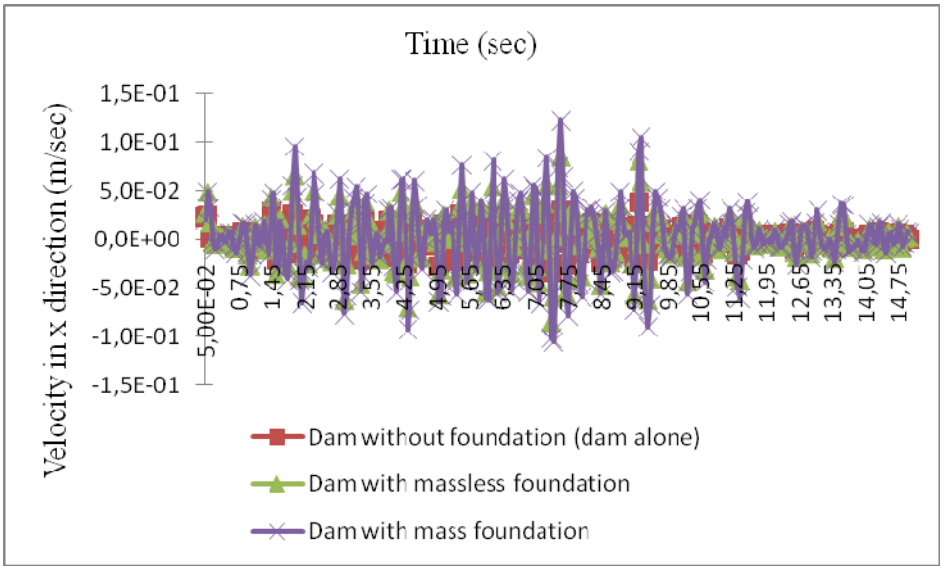

Figure 7.42: Crest velocity in x direction for the three studied cases

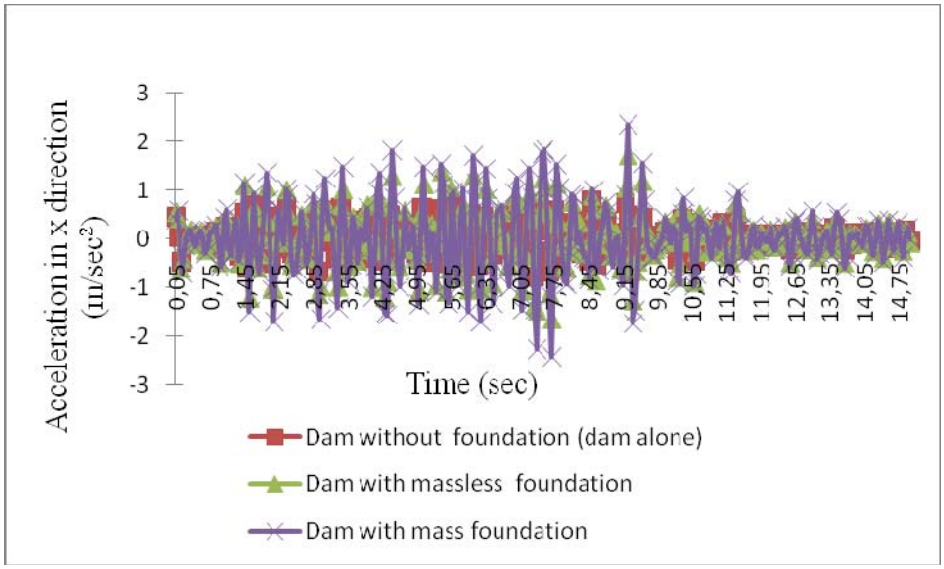

Figure 7.43: Crest acceleration in x direction for the three studied cases

Figure 7.41, 7.42 and 7.43 show that the crest displacement, velocity and acceleration time history are more pronounced for the case of dam with mass foundation, which means that foundation inertia force affect the dam behavior either if the water reservoir is present or not (case of Empty Reservoir) (results of chapter 5).

7.6.3 Time history behavior variation along the dam-foundation height

In this section, the variation of the time history behavior along the dam-foundation height is examined, for this reason; different points are chosen to represent the results. Figure 7.46 sketches these points.

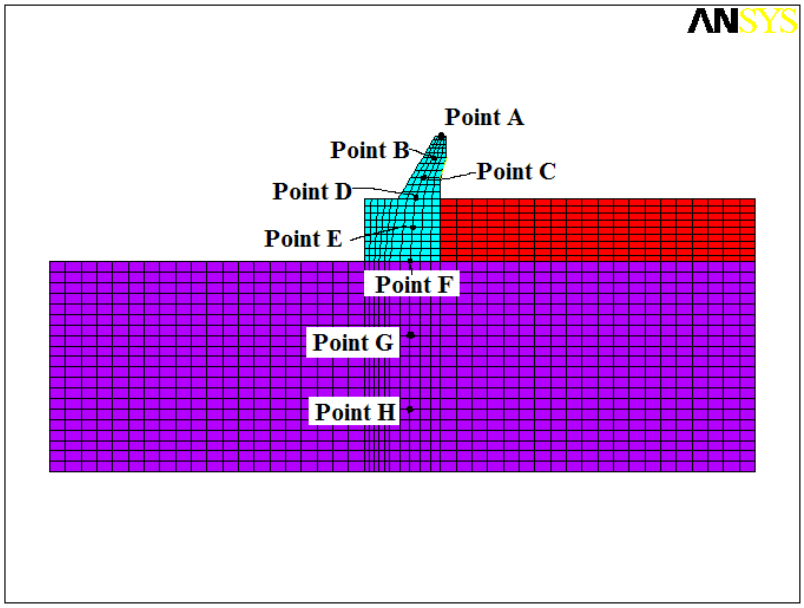

Figure 7.44: Location of nodes where results about dam and/or foundation transient behaviour are presented

a. Displacement variation in x direction along dam height for dam without foundation case

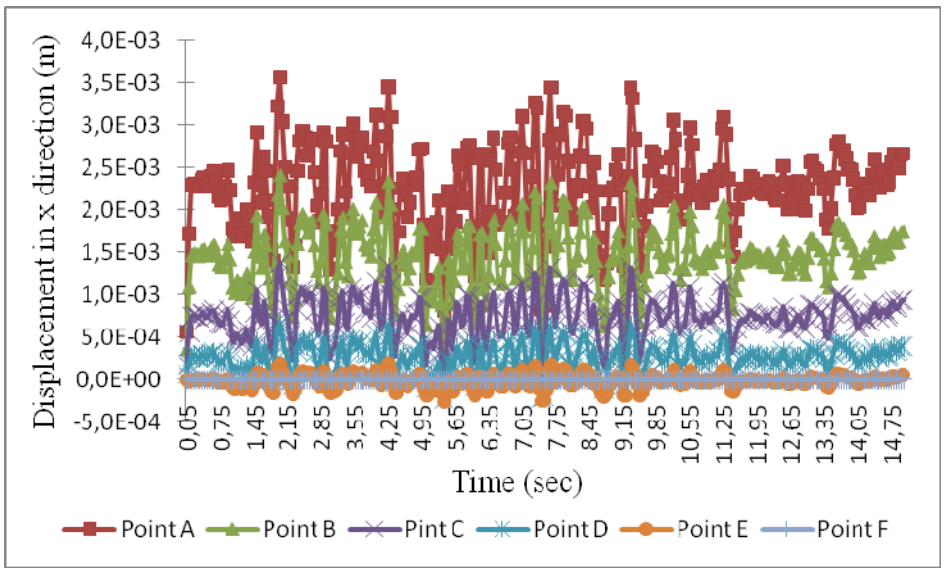

Figure 7.45: Variation of displacement in x direction for the case of dam without foundation

b. Stress variation in x direction along dam height for dam without foundation case

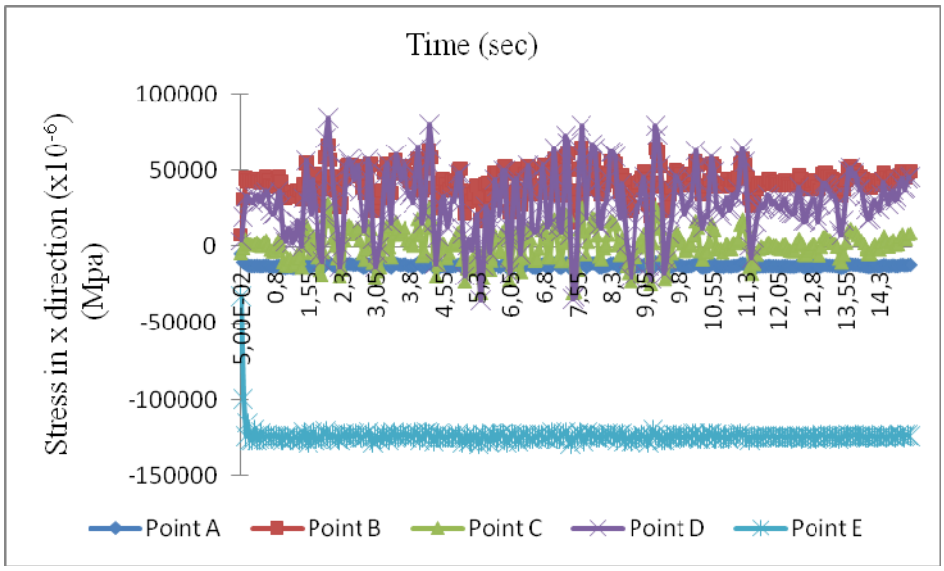

Figure 7.46: Variation of stress in x direction for the case of dam without foundation

c. Stress variation in y direction along dam height for dam without foundation case

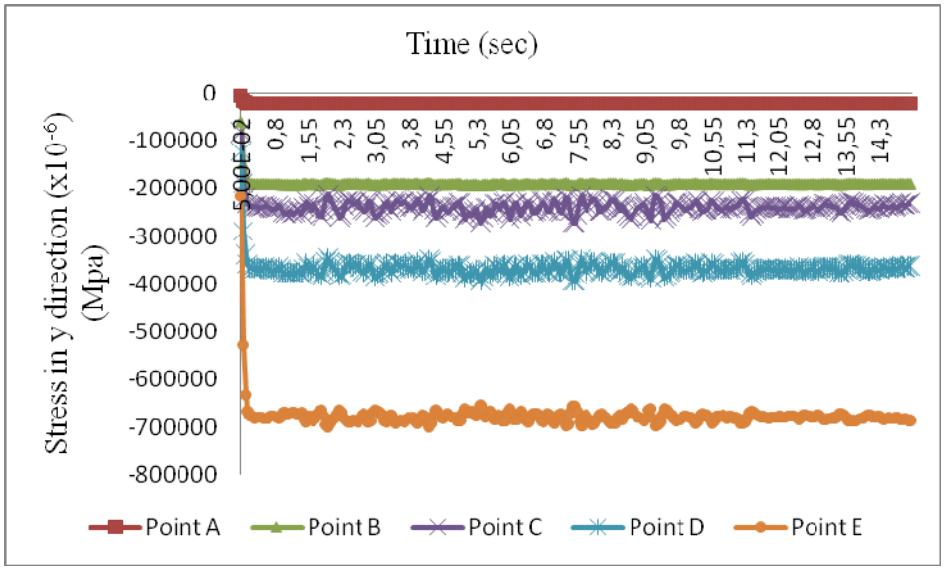

Figure 7.47: Variation of stress in y direction for the case of dam without foundation

d. Von Mises stress variation along dam height for dam without foundation case

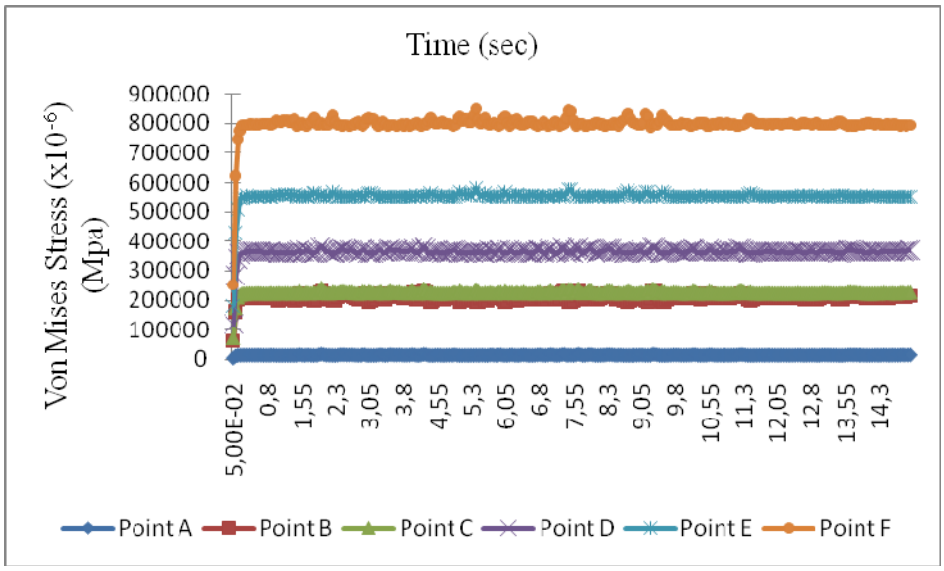

Figure 7.48: Variation of Von Mises stress for the case of dam without foundation

Figure 7.45, Figure 7.46, Figure 7.47 and Figure 7.48 represent respectively time history variation of displacement in x direction, stress in x direction, stress in y direction and von mises stress along dam height for the case of dam without foundation case. From this figure it is shown that displacements are more important at the dam top where stresses are negligible; however at the dam bottom, these displacements are negligible and stresses are important which is in perfect agreement with the reality.

e. Displacement variation in x direction along dam height for dam with massless foundation case

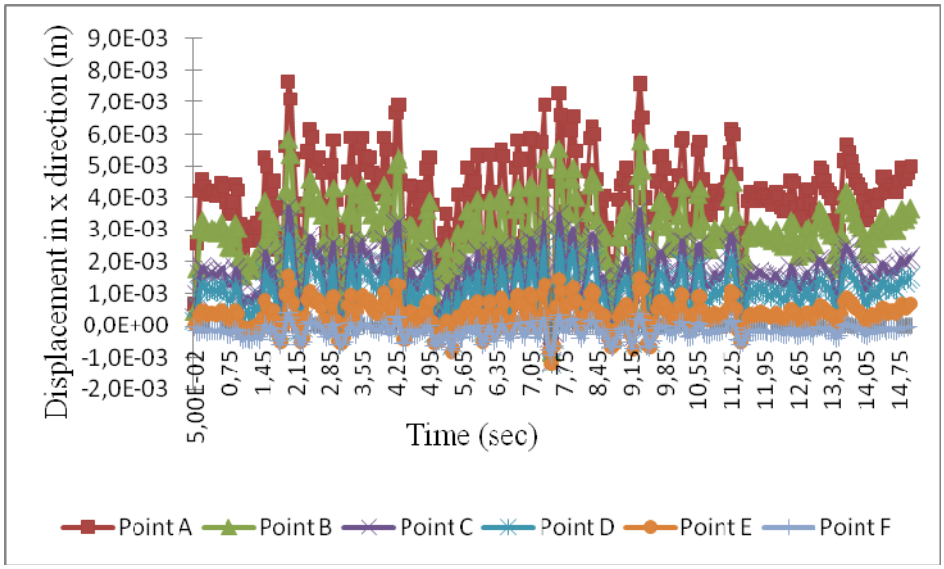

Figure 7.49: Variation of displacement in x direction for the case of dam with massless foundation

f. Stress variation in x direction along dam height for dam with massless foundation case

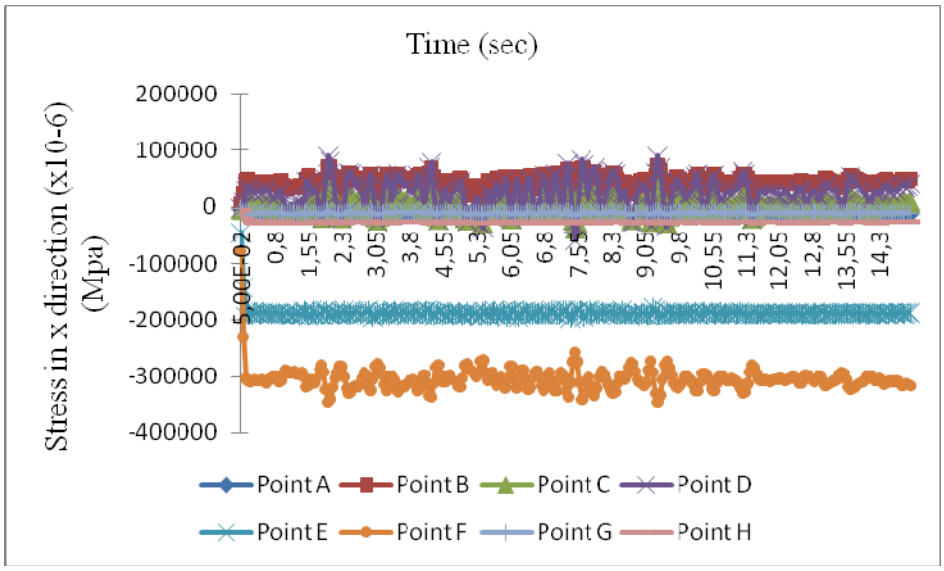

Figure 7.50: Variation of stress in x direction for the case of dam with massless foundation

g. Stress variation in y direction along dam height for dam with massless foundation case

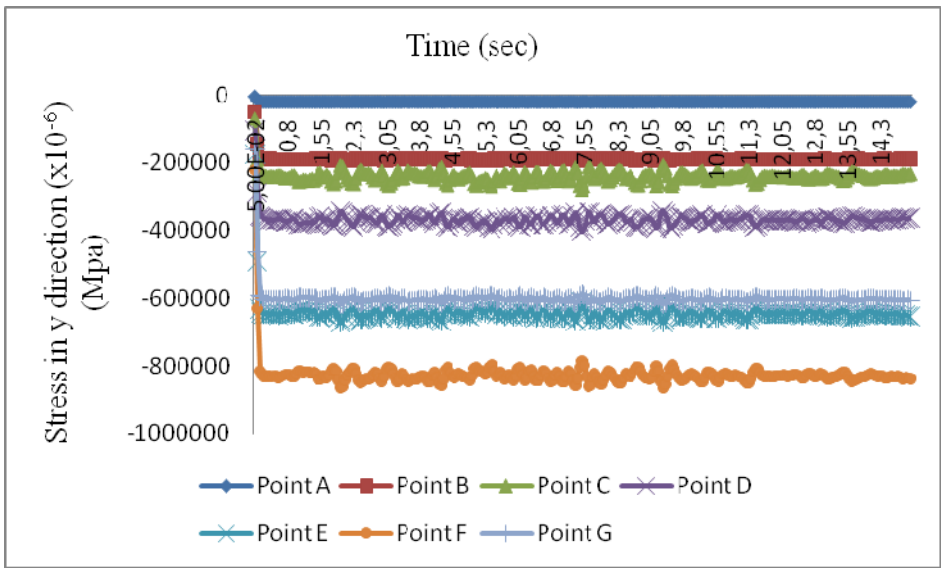

Figure 7.51: Variation of stress in y direction for the case of dam with massless foundation

h. Von Mises stress variation along dam height for dam with massless foundation case

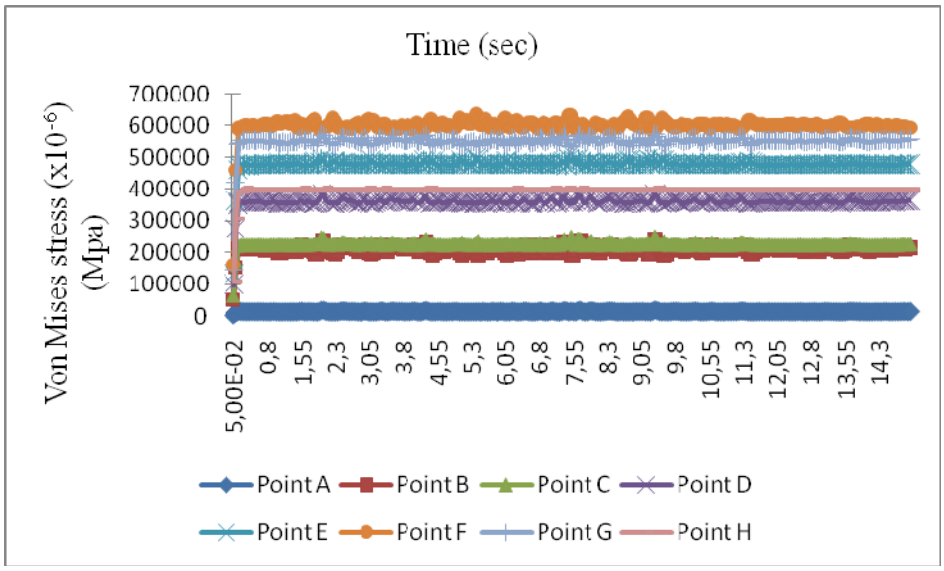

Figure 7.52: Variation of Von Mises stress for the case of dam with massless foundation

Figure 7.49, Figure 7.50, Figure 7.51 and Figure 7.52 represent respectively time history variation of displacement in x direction, stress in x direction, stress in y direction and von mises stress along dam height for the case of dam with massless foundation case. From this figure it is shown that displacements are more important at the dam-foundation top where stresses are negligible; however at the dam-foundation bottom, these displacements are negligible and stresses are important.

i. Displacement variation in x direction along dam height for dam with mass foundation case

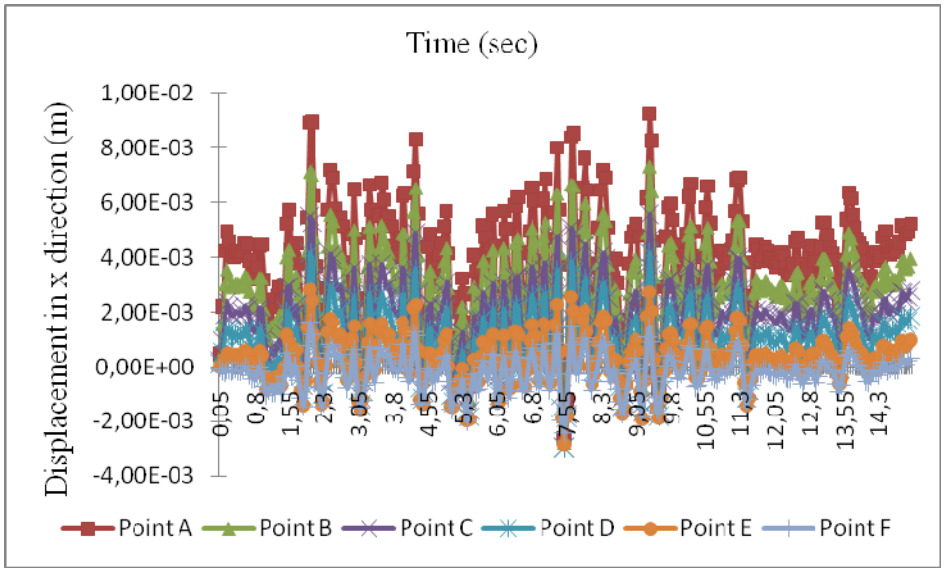

Figure 7.53: Variation of displacement in x direction for the case of dam with mass foundation

j. Stress variation in x direction along dam height for dam with mass foundation case

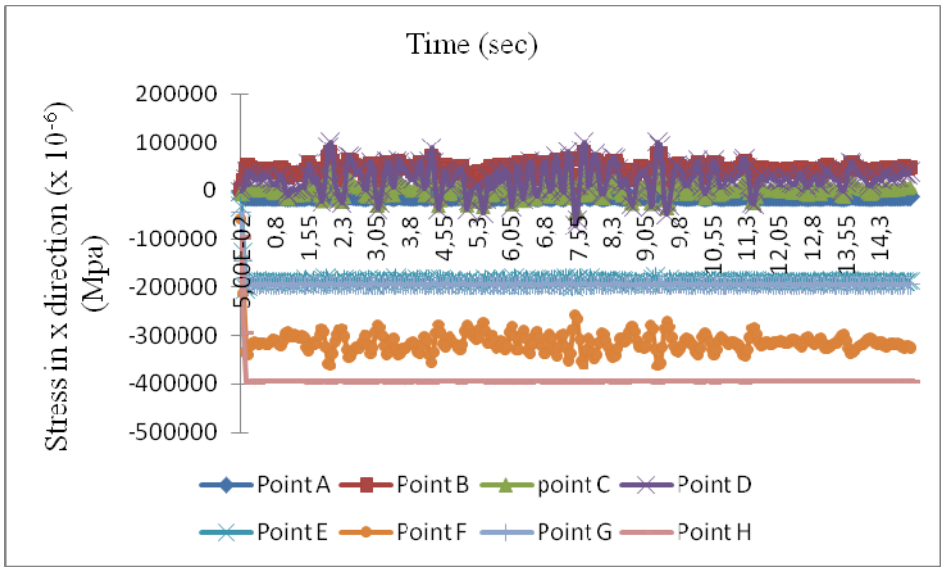

Figure 7.54: Variation of stress in x direction for the case of dam with mass foundation

k. Stress variation in y direction along dam height for dam with mass foundation case

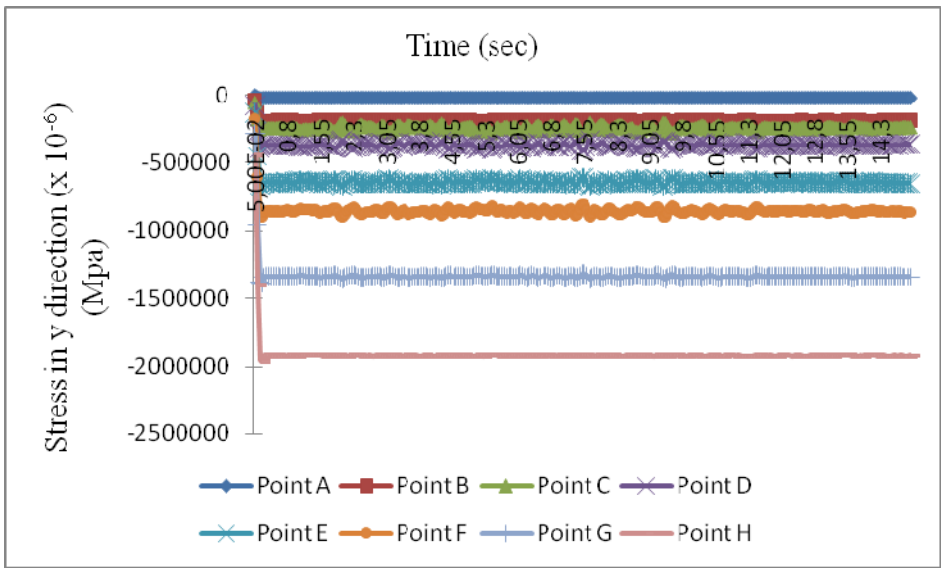

Figure 7.55: Variation of stress in y direction for the case of dam with mass foundation

l. Von Mises stress variation in y direction along dam height for dam with mass foundation case

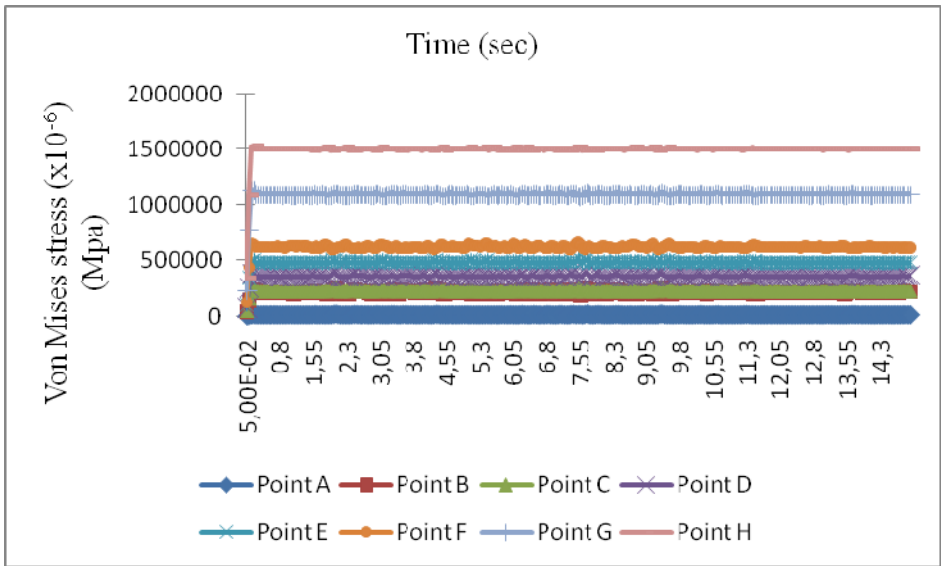

Figure 7.56: Variation of Von Mises stress for the case of dam with mass foundation

Figure 7.53, Figure 7.54, Figure 7.55 and Figure 7.56 represent respectively time history variation of displacement in x direction, stress in x direction, stress in y direction and von mises stress along dam height for the case of dam with mass foundation case. From this figure it is shown that displacements are more important at the dam-foundation system top where stresses are negligible; however at the dam-foundation bottom, these displacements are negligible and stresses are important.

7.6.4 Variation of concrete dam behaviour between the upstream and downstream dam faces

In this section the transfert of dam-reservoir-foundation system behaviour between the upstream and downstream dam faces is studied. Figure 7.59 sketches the upstream and downstream paths where the results are presented

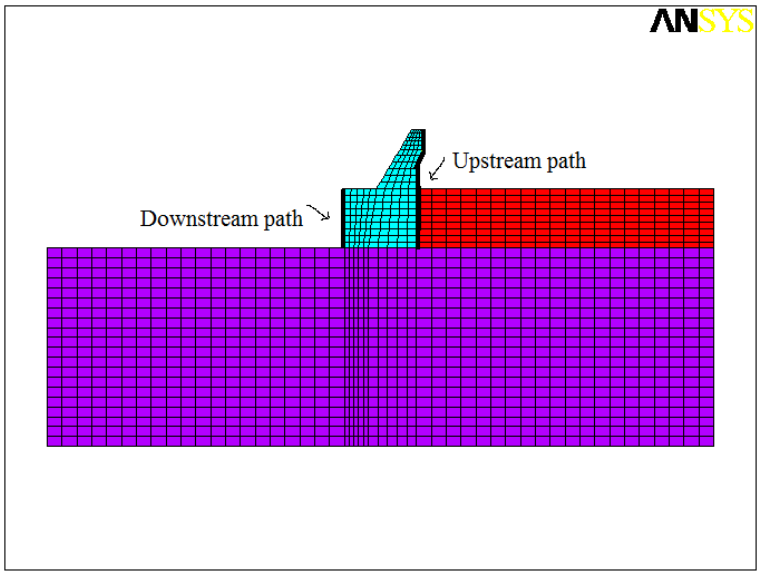

Figure 7.57: Location of upstream and downstream paths for the case of dam with foundation

7.6.4.1 Variation of dam behaviour between the upstream and downstream dam faces for the case of dam without foundation (dam alone)

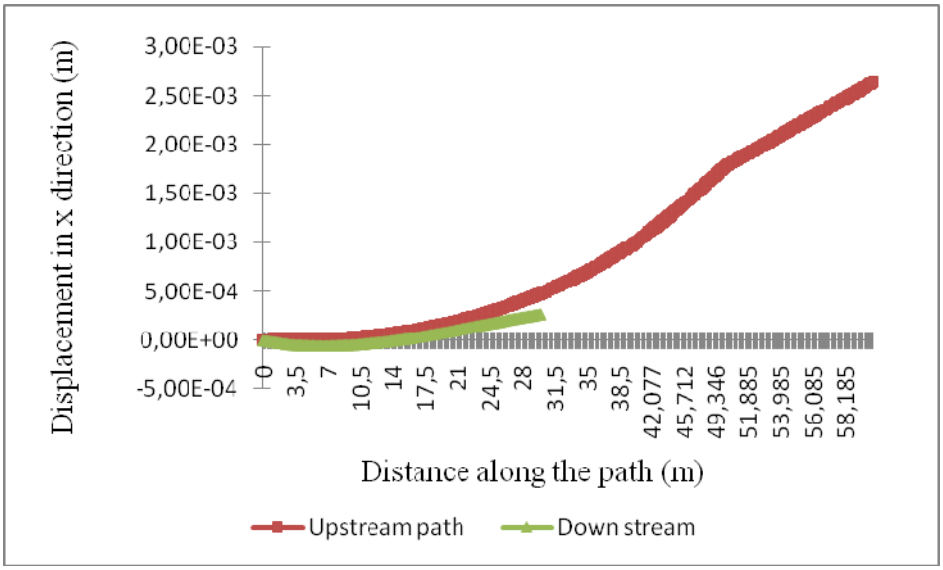

Figure 7.58: Variation of displacement in x direction between the upstream and downstream dam faces for the case of dam without foundation (dam alone)

a. Variation of stress in x direction between the upstream and downstream dam faces for the case of dam without foundation (dam alone)

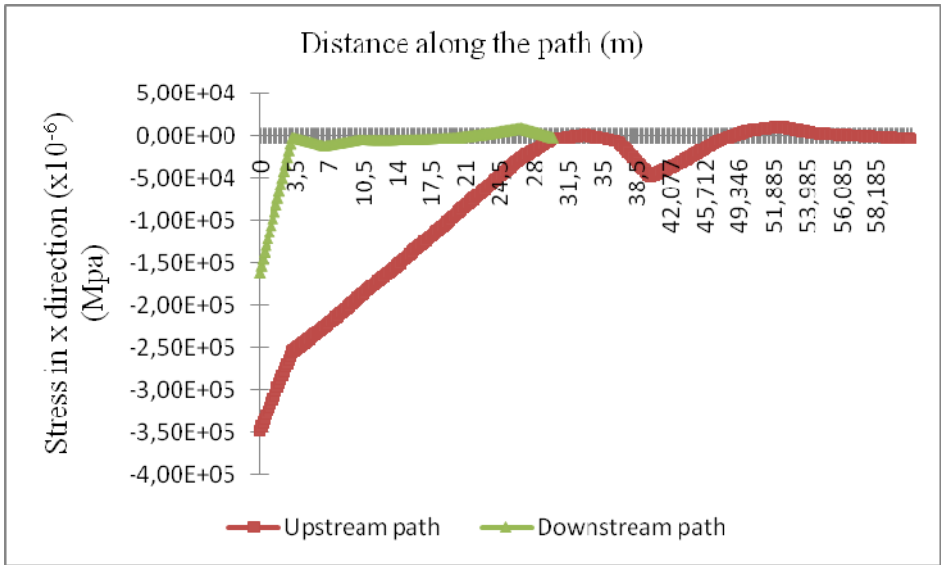

Figure 7.59: Variation of stress in x direction between the upstream and downstream dam faces for the case of dam without foundation (dam alone)

b. Variation of stress in y direction between the upstream and downstream dam faces for the case of dam without foundation (dam alone)

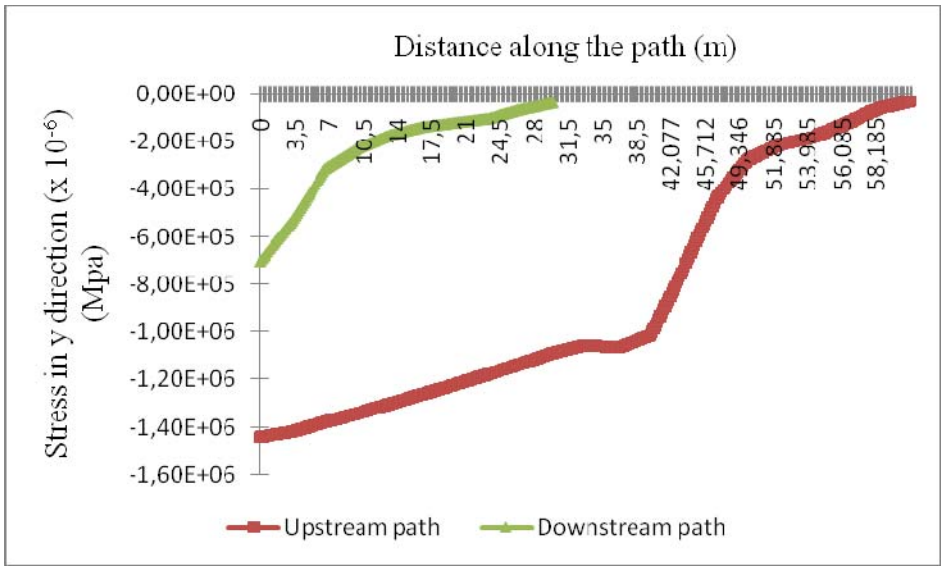

Figure 7.60: Variation of stress in y direction between the upstream and downstream dam faces for the case of dam without foundation (dam alone)

c. Variation of Von Mises stress between the upstream and downstream dam faces for the case of dam without foundation (dam alone)

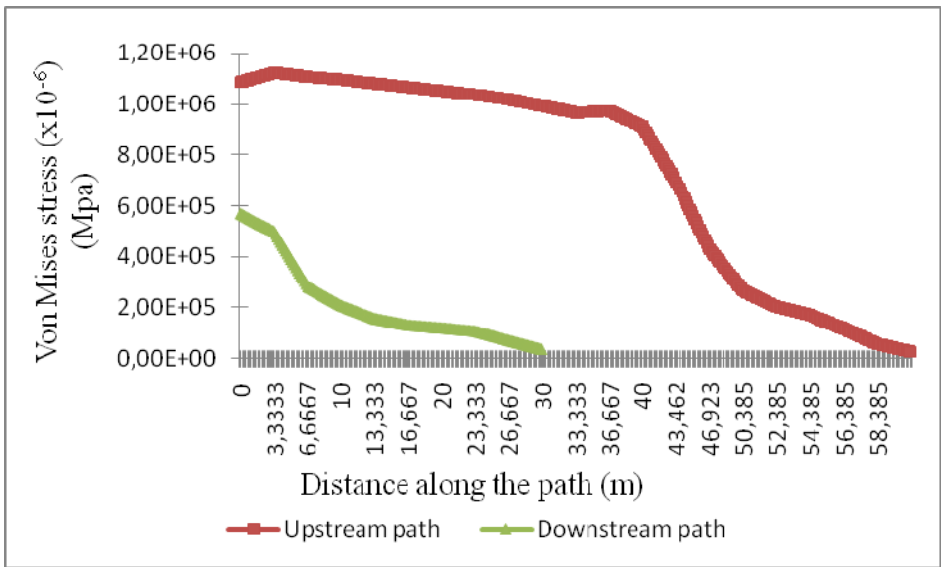

Figure 7.61: Variation of Von Mises stress between the upstream and downstream dam faces for the case of dam without foundation (dam alone)

Figure 7.58, Figure 7.59, Figure 7.60 and Figure 7.61 show respectively for the case of dam alone (with clamped foundation) the transfer of displacement in x direction, stress in x direction, stress in y direction and Von Mises stress between the upstream and downstream dam paths. It is shown that these stresses are important along the upstream path than along the downstream one.

7.6.4.2 Variation of dam behaviour between the upstream and downstream dam faces for the case of dam with mass foundation

a. Variation of displacement in x direction between the upstream and downstream dam faces for the case of dam with mass foundation

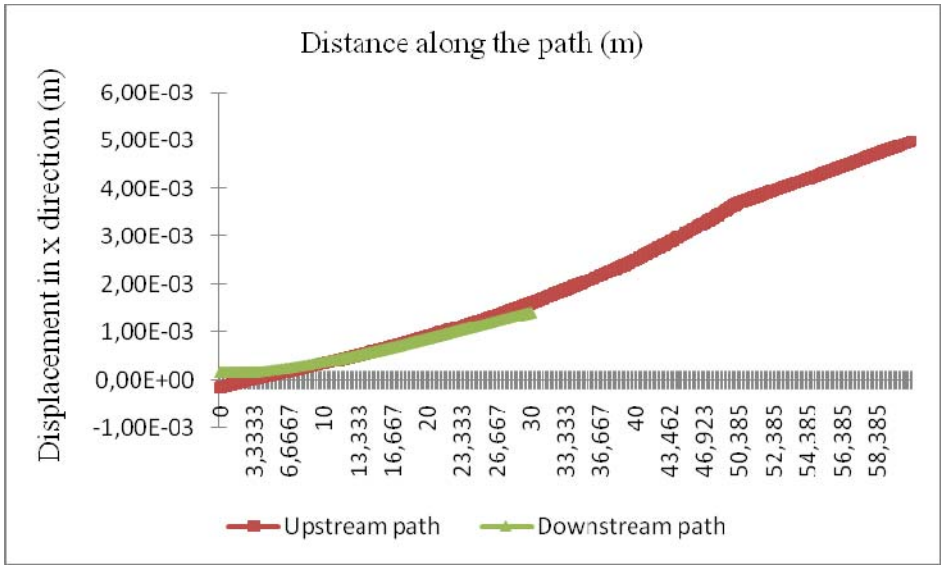

Figure 7.62: Variation of displacement in x direction between the upstream and downstream dam faces for the case of dam with mass foundation

b. Variation of stress in x direction between the upstream and downstream dam faces for the case of dam with mass foundation

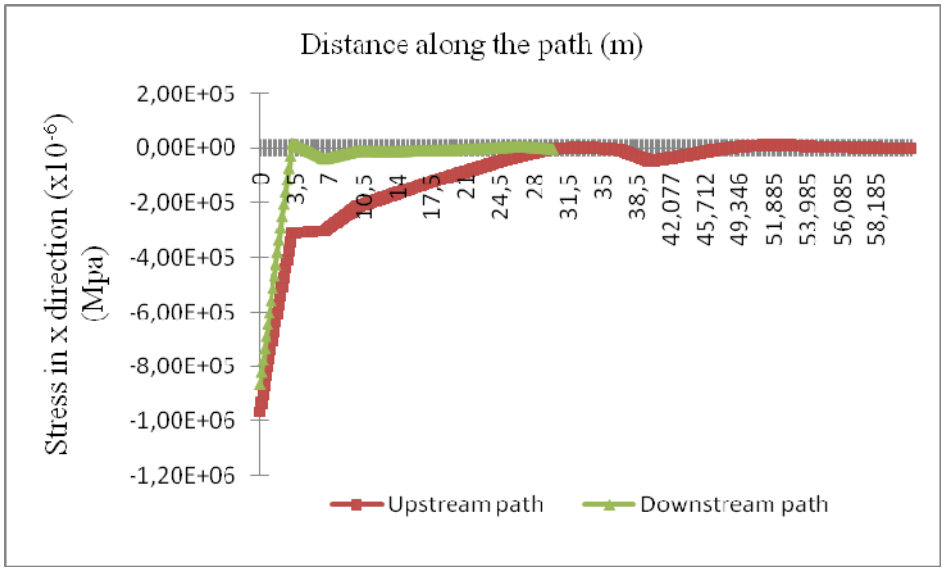

Figure 7.63: Variation of stress in x direction between the upstream and downstream dam faces for the case of dam with mass foundation

c. Variation of stress in y direction between the upstream and downstream dam faces for the case of dam with mass foundation

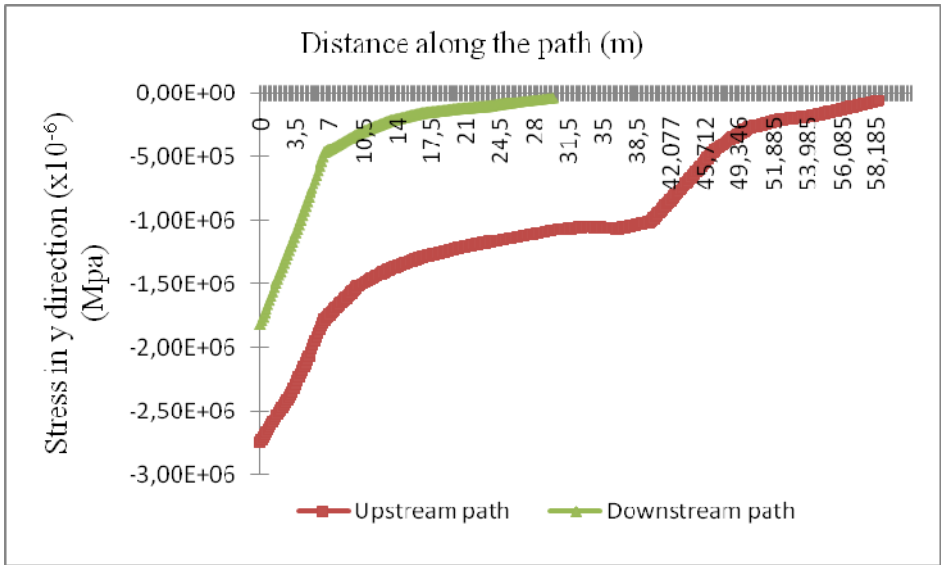

Figure 7.64: Variation of stress in y direction between the upstream and downstream dam faces for the case of dam with mass foundation

d. Variation of Von Mises stress between the upstream and downstream dam faces for the case of dam with mass foundation

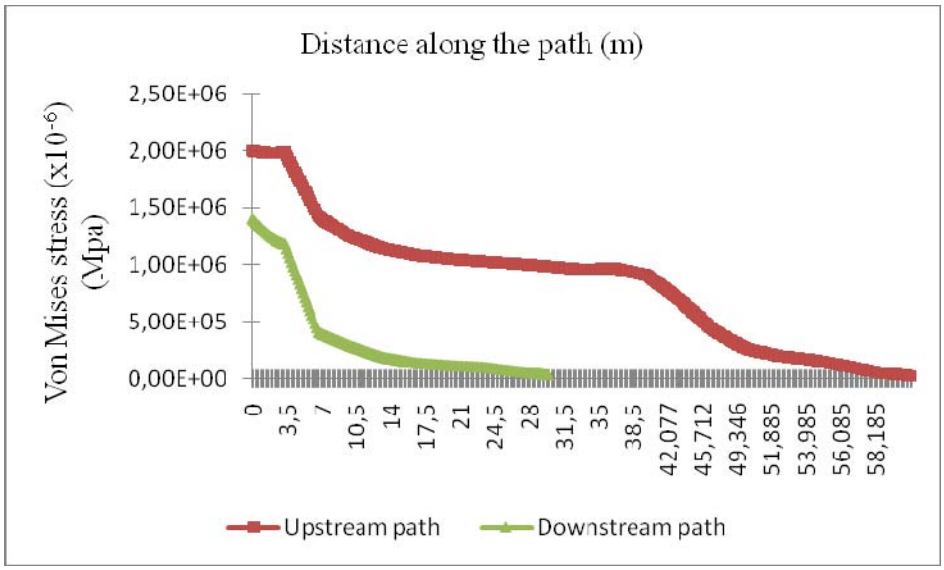

Figure 7.65: Variation of Von Mises stress between the upstream and downstream dam faces for the case of dam with mass foundation

Figure 7.62, Figure 7.63, Figure 7.64 and Figure 7.65 show respectively for the case of dam with mass foundation the transfer of displacement in x direction, stress in x direction, stress in y direction and Von Mises stress between the upstream and downstream dam paths. Already it

is shown that these stresses are important along the upstream path than along the downstream one.

Comparing figure 7.58, figure 7.62 which represent the variation of displacement in x direction between the upstream and downstream dam faces for dam alone and dam with mass foundation respectively, it is clear that the x displacement of the two dam face is independent on foundation modeling (displacement rate transfer is important). However comparing figure 7.59, figure 7.63 (representing the variation of stress in x direction between the upstream and downstream dam faces for dam alone dam with mass foundation respectively) lead to conclude that the difference of stresses in x direction between the upstream and downstream dam faces is more important for the case of dam with fixed support than the other two cases, otherwise, the rate of stress transfer between the two dam faces is more pronounced when the foundation dam is modelled. The same observation is made for the variation of stresses in y direction and the variation of Von Mises stresses already between the two dam faces.

7.7 Conclusions

A parametric study is performed in the present work to investigate the combined effect of foundation, water reservoir presence and fluid-dam / fluid-foundation interfaces modeling on the modal behaviour of Brezina concrete dam.

The study has shown that reservoir water presence and foundation modeling have the same effect on the modal frequencies results which means on the modal behaviour of the concrete dam; they decrease the frequencies values.

Two assumptions are adopted in this study in the subject of the interface fluid-dam and fluid-foundation modeling: the contact elements and coupling equations.

From modal analysis, it is shown that:

- ✓ Modeling the interfaces by contact elements or by coupling equations gives the same results.
- ✓ *Surface finite elements* available in Ansys library are a good and practical tool to represent the fluid using the added masses approach.
- ✓ The coupling approach is more complicated in the modeling but it takes a little run time, however the contact approach is very simple in the modeling phase; but it take more run time because of the contact elements added to the model, for this reason the contact approach is more desired practical than the coupling equation one.

From the transient analysis, the study shows that:

- ✓ Even if reservoir water is present, the worst case of the concrete dam object of the present study already occurs when the foundation is modeled as mass foundation model.
- ✓ Near to the upstream concrete dam face, reservoir water transient behaviour (water displacement in x and y direction) is independent on the foundation-dam interaction modelling, however far from the sloshing amplitude time history is more important for the dam with mass foundation case.
- ✓ The transfer of stresses between the upstream and the downstream dam faces is more pronounced for the dam with mass foundation then the dam with fixed support.

CHAPTER 8

Three Dimensional Modal Behaviour of Dam Reservoir Foundation System using ANSYS

CHAPTER 8

Three Dimensional Modal Behaviour of Dam Reservoir Foundation System using ANSYS

8.1 Introduction

A parametric study is performed in the present chapter to view the combined effect of foundation, fluid-dam and fluid-foundation interfaces modeling on the three dimensional (3D) modal behaviour of "Brezina" concrete dam situated at Algeria.

As natural frequencies and mode shapes are important parameters in design for dynamic loading conditions, it is very important to use modal analysis for determining the vibration characteristics (natural frequencies and mode shapes) of any system. For this reason modal analyses are adopted for the dam object of this study for two assumptions of dam-fluid and foundation- fluid interfaces modeling: the contact elements and the coupling equation, also for the three approaches of foundation-dam interaction modeling: the fixed support foundation, the massless foundation and the mass foundation. *Added masses approach* takes a place in this chapter by using *surf finite element* available in Ansys library.

8.2 Ansys Validation

The model is to be developed from the elements available in the ANSYS software. To ensure the validity of Ansys models, modal analysis is performed, and results are compared with the available theory approximate analytical solutions for flexible tank of fixed support conditions.

For the purpose of comparison with other analysis solutions, linear elastic material properties are assumed. Water properties are given by Table 4.3 however for the tank is characterized by an elastic modulus of 2e+11N/m^2, a Poisson's ratio of 0.3 and a Density about 7830 kg/ m^3. 1848 FLUID79 finite elements are used to model the fluid container; however, 492 SHELL181 finite elements are used to model the container itself. This later is constrained (fixed) at its base. Because of the system symmetry, one half of the tank is modeled. The finite element model and geometrical properties of the cylindrical liquid container is sketched in Figure 8.1.

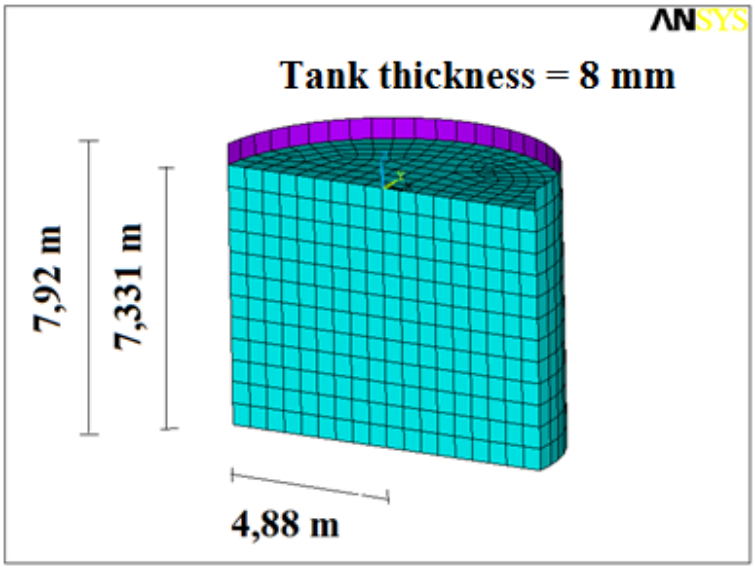

Figure 8.1: cylindrical reservoir finite element model

As for the two dimensional analyses explained in the previous chapter, two approaches are supposed for the fluid-container interfaces modeling:

First: The content is represented as three-dimensional contained fluid elements which are not attached to the shell elements at the wall boundary, but have separate coincident nodes that are coupled only in the direction normal to the interface. The relative movements in the tangential and vertical directions are allowed to occur. The fluid element nodes at the base are allowed to move horizontally, while the shell wall is fixed around the perimeter.

Second: The same model as the first one, but by the use of contact elements available in Ansys code library instead the coupling equations, considering the container as target elements (TARGE 170) and water as contact elements (CONTA 174) (view figure 4.10).

The added masses approach takes also a place in the current three dimensional (3D) study, by modeling tank water using *surface* finite element instead the *fluid* finite elements already available in Ansys code Library. The water mass is applied uniformly on the tank faces plus the hydrostatic pressure, the surface finite element "SURF 154" is characterized by its length and its thickness, these two properties depends on both water level and the contact length between the fluid and the container.

From the linear wave theory, the fundamental natural sloshing frequency is given by this formula (Robert D. Blevins 2001):

$$f_j = \frac{1}{2\pi}\sqrt{\frac{\lambda_j.g}{R}\tanh\frac{\lambda_j.h}{R}} \tag{8.1}$$

Where:

f_j : Sloshing frequency (Hz);

h: Fluid height (m)

g= Acceleration due to gravity (m/sec^2);

R= Radius of the plane form of the cylindrical container (m);

$\lambda_j = j^{th}$ zero root of the first derivative of the first order Bessel function of 1st kind. The first four values of λ are: 1.8412, 5.3314, 8.5363 and 11.7060.

However the coupled vibrations are expressed as (Robert D. Blevins 2001):

$$f_j = \frac{1}{2\pi}\sqrt{\frac{E.t}{\rho.R^3}.\Gamma_j.\frac{I_1(\Gamma_j)}{I_0(\Gamma_j)}} \tag{8.2}$$

Where:

E: tank material modulus of elasticity (N/m^2)

t: thank thickness (m)

ρ : Fluid density (kg/m^3)

I_0 and I_1 are the modified Bessel functions of the first kind, zero and 1st order, respectively (given from figure 8.2).

And:

$$\Gamma_j = \left(j - \frac{1}{2}\right)\pi\frac{R}{H} \tag{8.3}$$

Where:

H: the tank height (m)

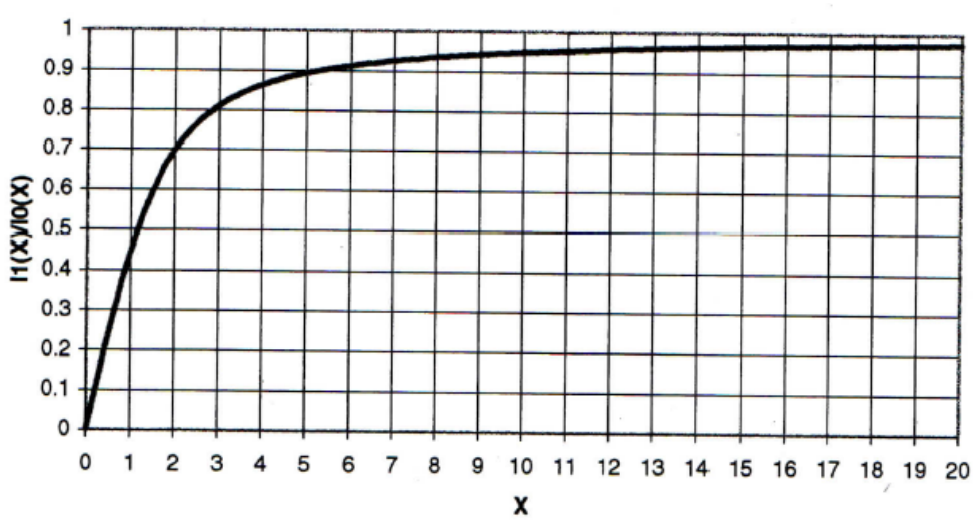

Figure 8.2: $I_1(x) / I_0(x)$ values (Robert D. Blevins 2001)

Table 8.1 lists the first four analytical tank sloshing frequencies and the Ansys frequencies (extracted using *Block Lanczos* method) for the case where the fluid-tank interface is modeled by coupling equations and for the case where this interface is modeled using contact elements. It is shown that Ansys results are in perfect agreement with the theoretical ones.

Frequency number	Approximate Analytical Results (Hz)	Interface fluid-container modeled using *coupling equations*	Interface fluid-container modeled using *contact elements*
1	0,306	0.306	0.273
2	0,526	0.510	0.497
3	0,665	0.625	0.644
4	0,779	0.770	0.673

Table 8.1: Fundamental mode value given

Figure 8.3 sketched the first four sloshing modes of the cylindrical tank for the two approaches of tank-fluid modeling.

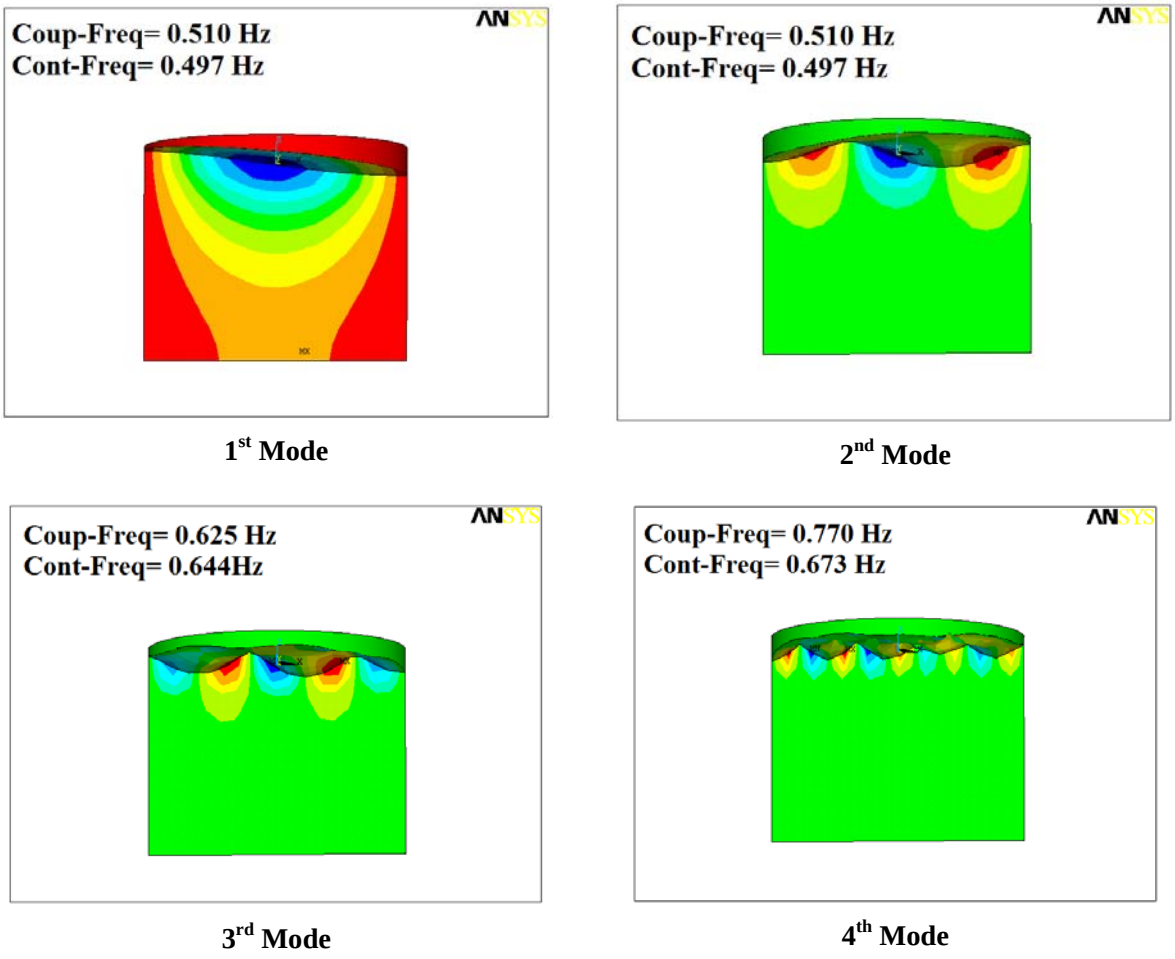

Figure 8.3: The first four sloshing mode shapes

Table 8.3 lists the first four analytical coupled frequencies and the Ansys frequencies obtained for the case where the fluid-tank interface is modeled by coupling equations and for the case where this interface is modeled using contact elements. Frequencies extracted for the case where the fluid container is modeled using added masses approach are also listed in table 8.2. It is shown that Ansys results are in perfect agreement with the theoretical ones for the two cases of fluid-tank interface modeling, however, frequencies are over-estimated for the added masses approach using *surf finite element*.

Frequency number	Approximate Analytical Results (Hz)	Interface fluid-container modeled using *coupling equations* (Hz)	Interface fluid-container modeled using *contact elements* (Hz)	Added masses approach using *Surf-elements* (Hz)
1	11,762	11.647	11.861	13.895
2	28,99	28.508	28.716	30.01
3	39,95	39.779	39.948	41.33
4	47,276	47.869	47.163	49.02

Table 8.2: Fundamental mode value for the three fluid modeling assumptions

Figure 8.4 sketched the first two coupled modes of the cylindrical tank for the two approaches of tank-fluid modeling.

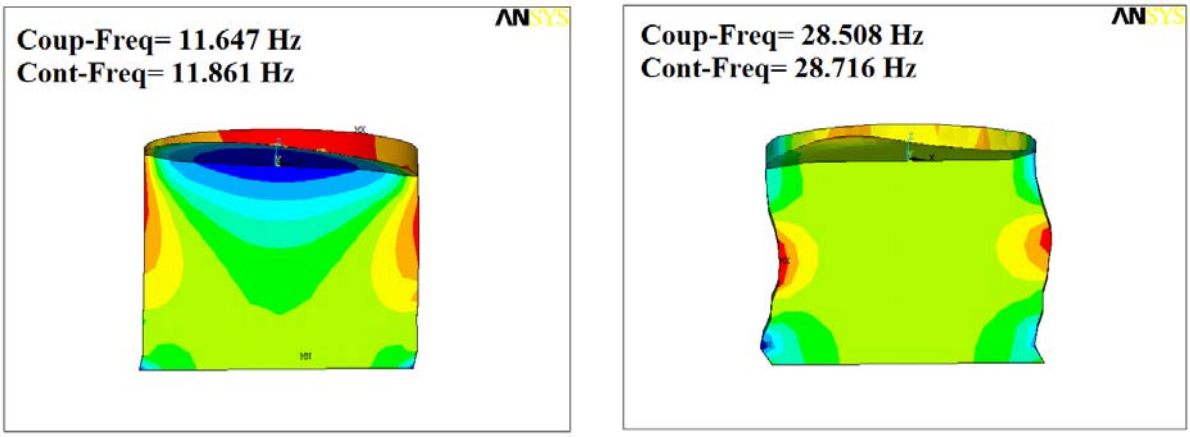

Figure 8.4: The first two coupling mode shapes

8.3 Three dimensional (3D) modeling of Brezina concrete arch dam

Using conclusion of chapter 5 and chapter 7 about the fact that the case of dam with foundation is more conservative then the dam with fixed support (dam only), in this chapter only the dam with foundation will be studied for the two discussed approaches of dam-fluid and fluid-foundation interfaces modeling and for the added masses approach.

The dam-fluid-foundation system is investigated using three 3D finite element models. The first model or dam-fluid-massless foundation model represents the dam and the adjacent foundation but the foundation's mass is neglected. The second model or fluid-dam-mass foundation is similar to the first one, except that the mass of the foundation is taken into account. These finite elements models are created using the finite element commercial package, ANSYS,

with a mapped meshing (Ansys theory manual, 2007). The finesse of the mesh has been determined by performing a convergence analysis (mesh sensitivity).

For the two models, 23790 quadratic solid elements (SOLID185) (view figure 4.6) are used to model both dam body and foundation rock, whereas 3000 FLUID 80 (view figure 4.10) finite element are used to represent water reservoir for the two approaches of fluid-dam and fluid-foundation interface modeling, however for the added masses approach using 600 SURF154 finite elements are used (view figure 4.8).

The length and width of the foundation, along the global X and Y axis, respectively, are taken to be 150 m, while its depth, along the Z direction, is taken to be 100 m. These sizes are chosen so that the applied boundary condition will not affect the modal responses of the dam. For the two models, water reservoir is taken about 50 m height (Figure 8.5).

For boundary conditions, foundation is clamped at its base. Nodes at water reservoir extremity which is neither in contact with dam body nor foundation, are constrained in X direction only and they are left free in Y and Z directions, however at the interfaces water-dam and water-foundation:

For coupling equation approach: The coincident nodes at the common areas between the fluid element (representing the fluid reservoir) and the quadratic elements (representing either the dam or the foundation system) are attached in the normal direction; this is achieved by rotating coincident nodes in local coordinate system of the common area and attaching them in the normal direction.

For coupling contact elements approach: By relating the common areas between the fluid element (representing the fluid reservoir) and the quadratic elements (representing either the dam or the foundation system) using contact elements. In this case CONTA 174 is used to represent water and TARGE170 is used for either dam or foundation.

For added masses approach: water reservoir is modeled as small masses applied uniformly at each water-dam and water-foundation interface using SURF154 finite element without forgetting the application of the hydrostatic pressure on these interfaces. The thickness of SURF154 is obtained by a simple arithmetical operation:

$$\text{SURF Thickness (m)} = \frac{\text{Reservoir water volume } (\text{m}^3)}{\text{interfaces water - dam and water foundation areas } (\text{m}^2)} * \text{water density}(\text{kg/m}^3)$$

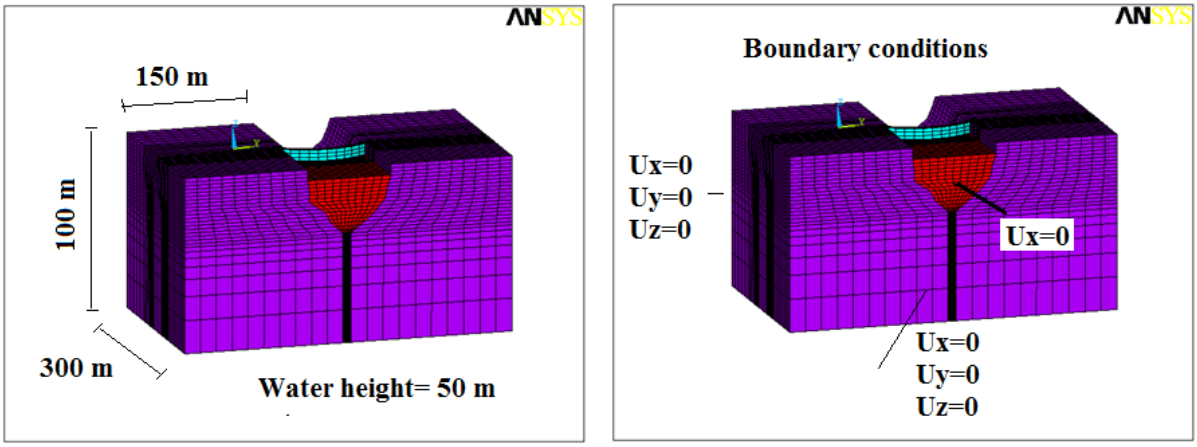

Figure 8.5: 3D finite element model of Brezina arch dam with water reservoir and adjacent foundation and boundary conditions.

The first four sloshing mode frequencies are sketched in figure 8.6 for the case of dam-water-mass foundation model for the two approaches of water-dam and water-foundation interfaces modeling.

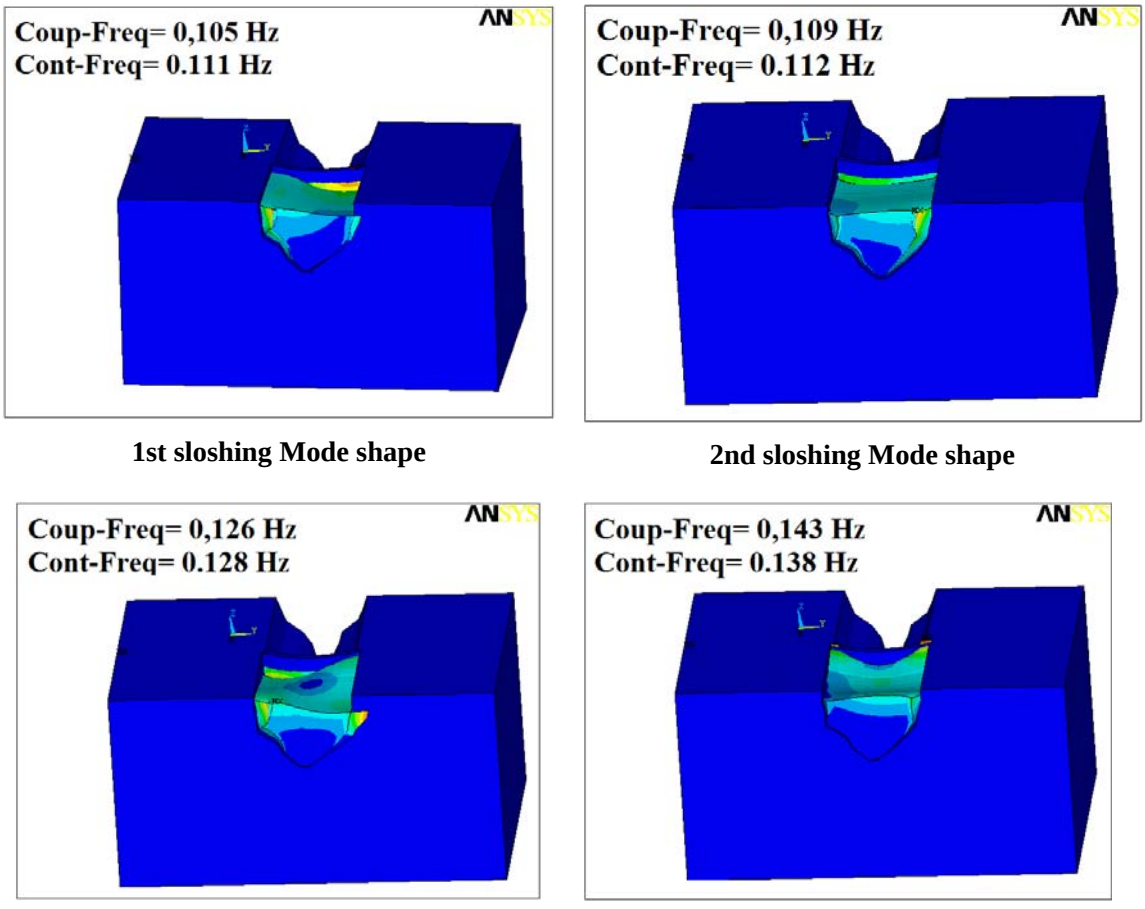

1st sloshing Mode shape

2nd sloshing Mode shape

3rd sloshing Mode shape

4th sloshing Mode shape

Figure 8.6: The first four sloshing mode shapes of the dam-fluid-mass foundation model

8.4 Effect of water-dam and water- foundation interfaces modeling on the sloshing mode values of dam-reservoir-foundation system

The effect of water-dam and water- foundation interfaces modeling on sloshing modes frequencies is examined in this paragraph for the two studied cases; dam with massless foundation and dam with mass foundation.

8.4.1 Dam with massless foundation

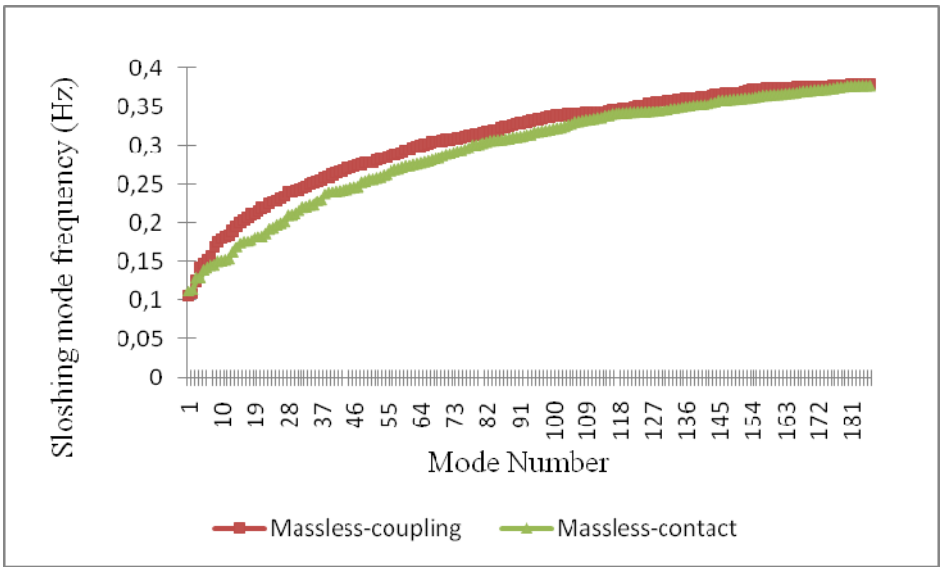

Figure 8.7: Effect of interface modeling on the reservoir sloshing modes frequencies for the case of dam with massless foundation

Figure 8.7 sketches the effect of dam-reservoir and foundation-reservoir interface modeling on the dam-water- massless foundation system mode frequencies values; it is also shown that there is a small difference between sloshing mode frequencies values for the two studied cases of the interface modeling (using coupling equations or contact elements).

8.4.2 Dam with mass foundation

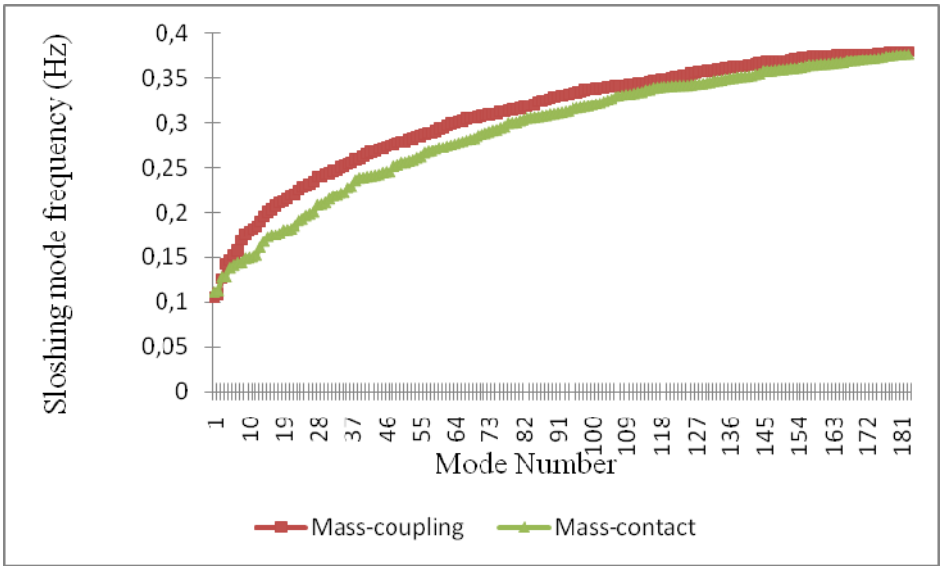

Figure 8.8: Effect of interface modeling on the reservoir sloshing modes frequencies for the case of dam with mass foundation

Figure 8.8 sketches the effect of dam-reservoir and foundation-reservoir interface modeling on the dam-water- mass foundation system mode frequencies values; it is also shown that there is a small difference between sloshing mode frequencies values for the two studied cases of the interface modeling (using coupling equations or contact elements).

From figure 8.7 and figure 8.8 we can say that that modeling the interface fluid-dam and fluid-foundation by coupling equations or by contact elements give the same results in term of sloshing mode frequencies.

8.5 Foundation-dam interaction modeling effect on the reservoir sloshing modes

The effect of foundation-dam interaction modeling on the sloshing modes of dam-reservoir-foundation system is presented here.

8.5.1 Interfaces modeled using coupling equations

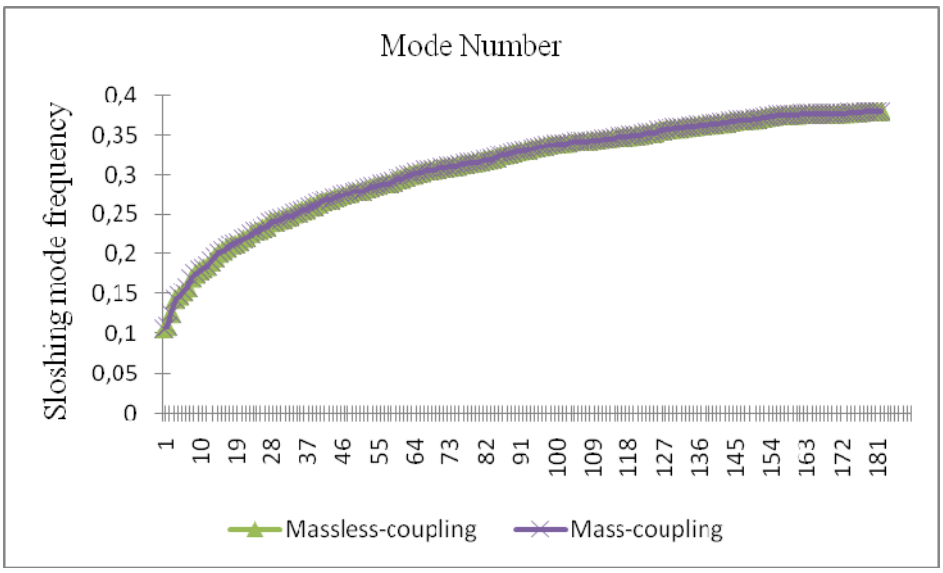

Figure 8.9: Foundation-dam interaction modeling effect on the reservoir sloshing modes for the case where interfaces are modeled using coupling equations

Figure 8.9 sketches the effect of foundation-dam interaction modeling on the sloshing modes of dam-reservoir-foundation system for the case where water-foundation interfaces and water-dam interfaces are modeled using coupling equations. It is shown that sloshing modes frequencies are independent on the foundation-dam interaction modeling.

8.5.2 Interfaces modeled using contact elements

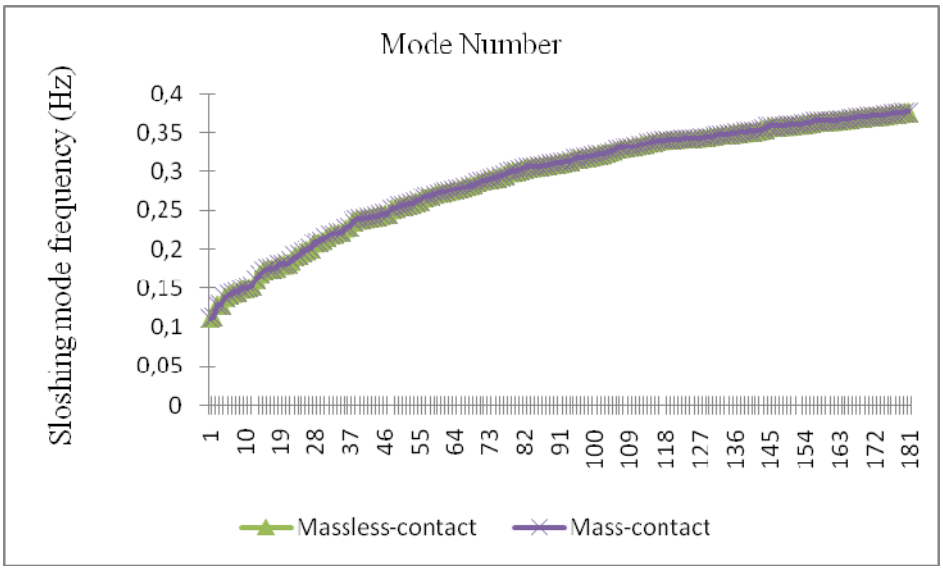

Figure 8.10: Foundation-dam interaction modeling effect on the reservoir sloshing modes for the case where interfaces are modeled using contact elements

Figure 8.10 sketches the effect of foundation-dam interaction modeling on the sloshing modes of dam-reservoir-foundation system for the case where water-foundation interfaces and water-dam interfaces are modeled using contact elements.

From figure 8.9 and figure 8.10 we can conclude that reservoir water sloshing mode frequencies are independent on the foundation-dam interaction modeling, which is the conclusion founded also in chapter 7 section 7.5.1 for the two dimensional modal analyses of the same dam.

8.6 Effect of water-foundation and water-dam interfaces modeling on the coupled mode values of dam-reservoir-foundation system

In this section and due to coupled frequencies shift between the two approaches of interface modeling, only the fundamental modes are presented and compared. Since this shift of frequencies is not found for the cylindrical container studied above, we can conclude that it (shift of frequencies) is due to the irregular geometry of the water-dam and water-foundation interfaces.

Figure 8.11 sketches the fundamental mode shape for dam-water-mass foundation system for the case where water-dam and water-foundation is modeled using coupling equations and for the case where these interfaces are modeled using contact elements.

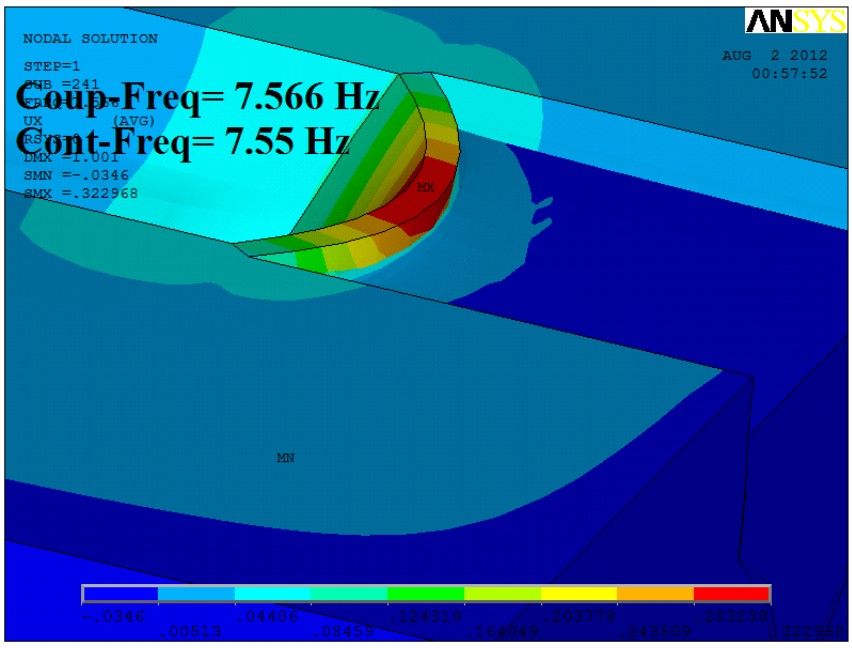

Figure 8.11: The fundamental coupling mode shapes of the dam-water-mass foundation system

8.6.1 Dam with massless foundation

The effect of water-dam and water-foundation interfaces modeling on the fundamental coupled modes frequencies is examined in this paragraph for dam-water-massless foundation case. Results are summarized in table 8.3 for the two approaches of interfaces modeling and also for the added masses approach.

Table 8.3 show a perfect agreement between the frequencies obtained for interfaces modeled by coupling equations and by contact elements, however for the added masses approach using surf finite elements, fundamental frequency is more important than those found for the two other approaches.

Mode Number	Massless-coupling		Massless -contact		Massless -surf	
	Frequency (Hz)	Ratio	Frequency (Hz)	Ratio	Frequency (Hz)	Ratio
Fondamental Mode	8.80	1	8.79	1	12.22	1

Table 8.3: Effect of water-dam and water-foundation interfaces modeling on the fundamental coupled mode for dam with massless foundation case

8.6.2 Dam with mass foundation

As discussed in the previous section (8.6.1), the effect of water-dam and water-foundation interfaces modeling on the fundamental coupled modes frequencies is examined in this paragraph for dam-water-mass foundation case. Results are summarized in table 8.4 for the two approaches of interfaces modeling and also for the added masses approach.

Table 8.4 show a perfect agreement between the frequencies obtained for interfaces modeled by coupling equations and by contact elements, however for the added masses approach using surf finite elements, fundamental frequency is overestimated compared with those found for the two other approaches.

Mode Number	Mass-coupling		Mass -contact		Mass -surf	
	Frequency (Hz)	Ratio	Frequency (Hz)	Ratio	Frequency (Hz)	Ratio
Fondamental Mode	7.566	1	7.55	1	8.31	1

Table 8.4: Effect of water-dam and water-foundation interfaces modeling on the fundamental coupled mode for dam with mass foundation case

8.7 Conclusion

In this chapter three dimensional modal analyses are performed for Brezina concrete arch dam-foundation system for:

- ✓ The two approaches of reservoir-dam and reservoir-foundation interfaces modeling ;
- ✓ The added masses approach case for reservoir water representation.

In this chapter only the fundamental frequencies are presented due to the shift of frequencies between the two approaches of interface modeling cited above, this shift of frequencies is caused by the irregular water-dam and water-foundation interfaces.

The study shows that:

- ✓ the results where interfaces are modeled using coupling equations are similar to results where interfaces are modeled using contact elements, which in the same conclusion founded on the last chapter for the two dimensional analyses.

- ✓ Water modeled using surf-element overestimates the frequencies values; this is because this modeling method represents "added masses" approach which is an approach that overestimates the analyses results.
- ✓ *Surface* finite elements available in Ansys library are practical tools to modelize reservoir water using added masses approach.

Conclusion

Conclusion

This work adds a contribution to the use of the finite elements commercial packages ANSYS for dynamic foundation-fluid-structure interaction problems and especially for concrete dams.

At first, a dynamic foundation-structure interaction has been performed for “Brezina” concrete arch dam using the direct method already with ANSYS code, and assuming different foundation modeling assumptions (clamped foundation, mass foundation and massless foundation). It has been shown that adding the foundation to the dam leads to a change in the system dynamic properties (natural frequencies) and therefore a change in its total response, all the more if the foundation is modeled as mass foundation.

Later on, a parametric study of the viscous damping in Rayleigh form has been conducted for the same dam. It has been found that the natural frequencies of either undamped or damped modes obtained from the dam-foundation with foundation mass model are drastically lower compared to that of the “dam alone” model, and are significantly lower than those obtained from the dam-massless foundation model. Likewise, similar comparisons have been observed for the damping quantities, in absolute values, between the three models. An in-depth review of the literature reveals that the study carried out herein constitutes several elements of originality as only very few similar works have been undertaken.

The third application consists in incorporating the hydrodynamic effect of reservoir water assuming different levels’ values. A special emphasis was done on modeling the fluid-foundation and also the fluid-dam upstream face interfaces. Two assumptions were adopted to model the interfaces; the coupling equations and the contact elements available in ANSYS finite elements code. An important application takes place in the present work, regarding the modeling of water reservoir by “*added mass approach*” using “*Surf Element*” available in ANSYS library. The study has shown that reservoir water presence and foundation modeling have the same effect on the modal frequencies results. In other words, regarding the modal behavior of the concrete dam, they decrease the frequencies’ values and modeling the interfaces by contact elements or coupling equations gives the same results for the two-dimensional analysis. However, for three-dimensional one, the results are slightly different due to the irregular interfaces (water-dam and water-foundation) geometry of the system being object of the present study. Also, the *surf* element is a good tool that can be used to model the “*added mass approach*”.

All the results obtained in this work are in perfect agreement with the theory, which means that the ANSYS code is good software for solving dynamic foundation-fluid-structure interaction problems.

References

References

A. Bayraktar and T. Turker and M. Akkose and S. Ates. “The Effect Of Reservoir Length On Seismic Performance Of Gravity Dams To Near and Far Fault Ground Motions”. Springer, Nat Hazards (2010) 52:257-275.

A. Bayraktar, Ebru Hancer, Mehmet Akkose. “Influence of base-rock characteristics on the stochastic dynamic response of dam-reservoir-foundation systems”. Elsevier, (2005).

A. Mansouri and R. Rezaei. “Considering Dynamic Analysis Results of Interactions between Concrete Dams and Reservoirs in Time Domain and Frequency Domain for Choosing the Optimimal Model”. European Journal of Scientific Research, Vol. 46 No 4 (2010), pp. 604-615.

A. Seghir. “Contribution à la Modélisation Numérique de la Réponse Sismique des Ouvrages avec Interaction Sol Structure et Interaction Fluide Structure“. Thèse de Doctorat, Université de Béjaia et Université de Paris-Est, Marne-La-Vallée, (convention de co-tutelle) (2011).

A.A. Shabana. “Theory of Vibration – An Introduction“. Mechanical Engineering Series, 2nd ed., Springer, (1995)

A.T Nicolas. “Modélisation de l’impact hydrodynamique par un couplage fluide-structure“. Thèse de Doctorat, Université des Sciences et Technologies de Lille, (2004).

Akköse M., Adanur S., Bayraktar A. and Dumanoğlu A. A. “Elasto-plastic earthquake response of arch dams including fluid–structure interaction by the Lagrangian approach”. Applied Mathematical Modelling, 32: 2396-2412 (2008).

Akköse M., Bayraktar A. and Dumanoğlu A. A. “Reservoir water level effects on nonlinear dynamic response of arch dams”, Journal of Fluids and Structures, 24: 418-435 (2008).

Amina Tahar Berrabah , Nazzal Armouti, Mohamed Belharizi and Abdelmalek Bekkouche. Dynamic Soil Structure Interaction Study. Jordan Journal of Civil Engineering, Volume 6, No. 2, (2012).

Amina Tahar Berrabah, Belharizi. M, Bekkouche. A. “Modal Behavior of Dam Reservoir Foundation System“. Ejge journal, Vol. 16, Bund. T (2011).

Amina Tahar Berrabah, Mohamed Belharizi, André Laulusa & Abdelmalek Bekkouche. “Three-Dimensional Modal Analysis of Brezina Concrete Arch Dam, Algeria“.Earth Science Research; Vol. 1, No. 2; (2012).

ANSYS. ANSYS User’s Manual, “ANSYS Theory Manual”. Version 11.0, (2007).

Arabshahi H. and Lotfi V. “Earthquake response of concrete gravity dams including dam–foundation interface nonlinearities”, Engineering Structures, 30: 3065–3073 (2008).

References

A. Bayraktar and T. Turker and M. Akkose and S. Ates. “The Effect Of Reservoir Length On Seismic Performance Of Gravity Dams To Near and Far Fault Ground Motions”. Springer, Nat Hazards (2010) 52:257-275.

A. Bayraktar, Ebru Hancer, Mehmet Akkose. “Influence of base-rock characteristics on the stochastic dynamic response of dam-reservoir-foundation systems”. Elsevier, (2005).

A. Mansouri and R. Rezaei. “Considering Dynamic Analysis Results of Interactions between Concrete Dams and Reservoirs in Time Domain and Frequency Domain for Choosing the Optimimal Model”. European Journal of Scientific Research, Vol. 46 No 4 (2010), pp. 604-615.

A. Seghir. “Contribution à la Modélisation Numérique de la Réponse Sismique des Ouvrages avec Interaction Sol Structure et Interaction Fluide Structure“. Thèse de Doctorat, Université de Béjaia et Université de Paris-Est, Marne-La-Vallée, (convention de co-tutelle) (2011).

A.A. Shabana. “Theory of Vibration – An Introduction“. Mechanical Engineering Series, 2nd ed., Springer, (1995)

A.T Nicolas. “Modélisation de l’impact hydrodynamique par un couplage fluide-structure“. Thèse de Doctorat, Université des Sciences et Technologies de Lille, (2004).

Akköse M., Adanur S., Bayraktar A. and Dumanoğlu A. A. “Elasto-plastic earthquake response of arch dams including fluid–structure interaction by the Lagrangian approach”. Applied Mathematical Modelling, 32: 2396-2412 (2008).

Akköse M., Bayraktar A. and Dumanoğlu A. A. “Reservoir water level effects on nonlinear dynamic response of arch dams”, Journal of Fluids and Structures, 24: 418-435 (2008).

Amina Tahar Berrabah , Nazzal Armouti, Mohamed Belharizi and Abdelmalek Bekkouche. Dynamic Soil Structure Interaction Study. Jordan Journal of Civil Engineering, Volume 6, No. 2, (2012).

Amina Tahar Berrabah, Belharizi. M, Bekkouche. A. “Modal Behavior of Dam Reservoir Foundation System“. Ejge journal, Vol. 16, Bund. T (2011).

Amina Tahar Berrabah, Mohamed Belharizi, André Laulusa & Abdelmalek Bekkouche. “Three-Dimensional Modal Analysis of Brezina Concrete Arch Dam, Algeria“.Earth Science Research; Vol. 1, No. 2; (2012).

ANSYS. ANSYS User’s Manual, “ANSYS Theory Manual”. Version 11.0, (2007).

Arabshahi H. and Lotfi V. “Earthquake response of concrete gravity dams including dam–foundation interface nonlinearities”, Engineering Structures, 30: 3065–3073 (2008).

Arabshahi H. and Lotfi V. “Earthquake response of concrete gravity dams including dam–foundation interface nonlinearities”, Engineering Structures, 30: 3065–3073 (2008).

Armouti, N. S. “Evaluation of Structural Response Subjected to Synthetic Earthquake Excitation“. Journal of Structural Engineering Vol. 31, 175-180 (2004)..

Armouti, N.S. “Computer program “RESSPEC” “. Department of Civil Engineering, University of Jordan. Amman (2004).

Armouti, N.S. “Computer program “GNREQ” “. Department of Civil Engineering. University of Jordan. Amman (2004).

Armouti, N.S. “Earthquake Engineering, Theory and Implementation,Department of Civil Engineering“. University of Jordan (First edition). Amman (2004).

Aznárez J. J., Maeso O. and Domínguez J.“BE analysis of bottom sediments in dynamic fluid-structure interaction problems”, Engineering Analysis with Boundary Elements, 30: 124-136 (2006).

B. F. Chen. “Nonlinear Hydrodynamic Effects On Concrete Dam”. Engineering Structures, Vol 18, No. 3, pp. 201-212, (1996).

B. Poursartip and V.Lotfi. “Modal analysis of concrete arch dams in time domain including dam-reservoir interaction”. The 14th world conference on Earthquake Engineering, October 12-17. Beijing, China,(2008).

B. Tiliouine and A. Seghir. “Fluid-Structure Models For Dynamic Studies of Dam-Water Systems”, 11th European Conference on Earthquake Engineering. Balkema, Rotterdam, (1998).

B.F Chen, “Nonlinear hydrodynamic effects on concrete dam”, Engineering structures, Vol. 18, No. 3, pp 201-212. Elsevier science (1996).

Bilici Y., Bayraktar A., Soyluk K., Haciefendioğlu K., Ateş Ş. and Adanur S. “Stochastic dynamic response of dam–reservoir–foundation systems to spatially varying earthquake ground motions”, Soil Dynamics and Earthquake Engineering, 29: 444-458 (2009).

C. Houqun and D. Xiuli and H. Shunzai. “Application of Transmitting Boundaries to Non Linear Dynamic Analysis of an Arch Dam Foundation Reservoir System“. Elsevier, (1998).

C.C. Spyrakos and C. Xu. “Seismic soil–structure interaction of massive flexible strip-foundations embedded in layered soils by hybrid BEM–FEM“. Soil Dynamics and Earthquake Engineering 23 pp 383–389 (2003).

C.C. Spyrakos and Ch.A. Maniatakis, I.A. Koutromanos. “Soil_structure interaction effects on base-isolated buildings founded on soil stratum“. Engineering Structures 31 pp 729-737 (2009).

Chavez J. W. and Fenves G. L. “Earthquake response of concrete gravity dams including base sliding”, ASCE Journal of Structural Engineering, 121(5): 865–875 (1995).

Cheng Hsing Chen and Shang Yi Hsu. “Using a simple model to investigate the effects of soil structure interaction”. The sixteenth KKCNN symposium on civil engineering, Korea (2003).

Chopra A. K. and Zhang L. “Earthquake-induced base sliding of concrete gravity dams”, ASCE Journal of Structural Engineering, 117(12): 3698–3719 (1991).

Clough R. W. and Penzien J. “Dynamics of Structures“. Second ed., McGraw-Hill, Singapore, (1993).

D. Maity and Bhattacharyya S. K. “A parametric study on fluid–structure interaction problems”. Journal of Sound and Vibration 263: 917–935 (2003).

D. Maity and Bhattacharyya S. K. “Time-domain analysis of infinite reservoir by finite element method using a novel far-boundary condition”. Finite Elements in Analysis and Design, 32: 85-96 (1999).

D. Maity. “A novel far-boundary condition for the finite element analysis of infinite reservoir”. Applied Mathematics and Computation, 170: 1314–1328 (2005).

D. Maity. “Coupled Hydrodynamic Response Of Dam- Reservoir Systems“, IE (I) Journal, Vol 85, (2004).

D. Pitilakis, M. Dietz, D.M. Wood, D. Clouteau, A. Modaressi. “Numerical simulation of dynamic soil-structure interaction in shaking table testing“. Soil dynamics and earthquake Engineering, 28:453-467, (2008).

Danay A. and Adeghe L. N. “Seismic-induced slip of concrete gravity dams”, ASCE Journal of Structural Engineering, 119(1): 108–129 (1993).

Donlon W. P. and Hall J. F. “Shaking table study of concrete gravity dam monoliths”. Earthquake Engineering and Structural Dynamics, 20: 769-786 (1991).

Du X., Zhang Y. and Zhang B. “Nonlinear seismic response analysis of arch dam-foundation systems- part I dam-foundation rock interaction”. Bulletin of Earthquake Engineering, 5: 105–119 (2007).

E. Kausel. “Early history of soil–structure interaction“. Soil Dynamics and Earthquake Engineering, (2009).

Erke Wang and Thomas Nelson, course entitled “Structural Dynamic Capabilities of Ansys”, CADFEM GmbH, Munich, Germany (2001)

F. Guan and I. D. Moore. “New techniques for modelling reservoir-dam and foundation-dam interaction“, Soil Dynamics and Earthquake Engineering 16 285-293 (1997).

F. Javanmardi and P. Leger and R. Tinawi, “Seismic Structural Stability Of Concrete Gravity Dams Considering Transient Uplift Pressures in cracks“. Engineering structures 27 616-628 (2005).

Fan S. C. and Li S. M. “Boundary finite-element method coupling finite element method for steady-state analyses of dam-reservoir systems”. ASCE Journal of Engineering Mechanics, 134(2): 133-142 (2008).

Fenves G. L. and Chopra A. K. “Earthquake analysis of concrete gravity dams including reservoir bottom absorption and dam-water-foundation rock interaction”, Earthquake Engineering and Structural Dynamics, 12: 663-680 (1984).

G. Haboussa. “Contribution à La Validation des Méthodes Numériques Pour Les Problèmes Dynamiques Couplés Fluide-Structure“. Thèse de doctorat, Academie de Lille, Université de Valenciennes et du Hainaut Hambresis, (2008).

Ghaemian M. and Ghobarah A. “Nonlinear seismic response of concrete gravity dams with dam–reservoir interaction”. Engineering Structures, 21: 306–315 (1999).

Ghaemian M. and Ghobarah A. “Staggered solution schemes for dam reservoir interaction”, Journal of Fluids and Structures, 12: 933-948 (1998).

Ghobarah A., El-Nady A. and Aziz T. “Simplified dynamic analysis for gravity dams”, ASCE Journal of Structural Engineering, 120(9): 2697-2716, September (1994).

Glauco Feltrin, Doctorate thesis. “Absorbing Boundaries for the Time-Domain Analysis of Dam-Reservoir-Foundation Systems”. Institute of Structural Engineering Swiss Federal Institute of Technology Zurich (1997).

Gogoi I. and Maity D. “Influence of sediment layers on dynamic behavior of aged concrete dams”. ASCE Journal of Engineering Mechanics, 133(4): 400-413 (2007).

H. Arabshahi and V. Lotfi. “Earthquake Response of Gravity Dams Including Dam-Foundation Interface Nonlinearities“. Engineering Structures 30 pp 3065-3073 (2008).

H. Shariatmadar, Adel Mirhaj. “Modal response of dam reservoir foundation interaction”. 8th International congress on Civil Engineering. Shiraz University, Shiraz, Iran. May 11-13, (2009).

Higdon R. L. “Radiation boundary condition for dispersive waves”. SIAM Journal on Numerical Analysis, 31: 64–100 (1994).

I.I.Johnson and Associates Alamo, CA, Earthquake Engineering Hand Book, chapter 10: Soil Structure Interaction, CRC Press LLC, 2003.

Ismail M. Ismail, Chris Mullen. “Soil structure interaction issues for three dimensional computational simulations of nonlinear seismic response”. ASCE 14th Engineering Mechanics Conference (EM2000). Austin, TX. May 21-24, (2000).

J. M. Llambias. “Validation of Seismic Soil Structure Interaction (SSI) Methodology for A UK PWR Nuclear Power Station“. SMiRT-12, Elsevier (1993).

J. Nasserzare and Y. Lei and F. Zeigler. “Inverse Identification of Dam Reservoir Interaction Including the Effect of Reservoir Bottom Absorption“. Asian Journal Of Civil Engineering Vol. 4, Nos 2-4 pp 101-113 (2003).

J. P. Wolf “Soil Structure Interaction Analysis In Time Domain“. Prentice Hall, Englewood Cliffs, New Jersey (1988).

J.N. Reddy. “Energy Principles and Variational Methods in Applied Mechanics“. 2nd ed., John Wiley & Sons, New York, (2002).

J.Rajasankar and N. Riyer and B.Swamy and N.Gopalakrishnan and P.Chellapandi, “SSI analysis of a massive concrete structure based on a novel convolution/deconvolution technique“. Sadhana Vol. 32, pp. 215–234 (2007).

J.V. Lemos, S. Oliveira and P. Mendes. “Analysis of The Dynamic Behaviour Of Cabril Dam Considering The Influence Of Contraction Joints., 7th European conference on Structural Dynamics, EUROYN 2008, Southampton (2008).

Javanmardi F., Léger P. and Tinawi R. “Seismic water pressure in cracked concrete gravity dams: experimental study and theoretical modeling”. ASCE Journal of Structural Engineering, 131(1): 139–150 (2005).

K. Hatami. “Effect of Reservoir Boundaries on The Seismic response of Gravity Dams“. PhD Thesis, (1997).

K. J. Bathe and E. L. Wilson. “Numerical Methods in Finite Element Analysis“. Prentice Hall Inc., (1983).

K. J. Bathe. “Finite Element Procedures“. Prentice Hall Inc., N.J., (1996).

K.J. Dreher. “Seismic analysis and design considerations for Concrete dams“. Proceeding of a Conference on Dams and Earthquake held at the Institution of Civil Engineers. London, October, (1980).

Küçükarslan S. “An exact truncation boundary condition for incompressible–unbounded infinite fluid domains”, Applied Mathematics and Computation, 163: 61–69 (2005).

Küçükarslan S. “Dam-reservoir interaction for incompressible-unbounded fluid domains using an exact truncation boundary condition”. Proceedings of 16th ASCE Engineering Mechanics Conference, July 16-18. University of Washington, Seattle (2003).

Küçükarslan S., Coşkun S. B. and Taşkın B. “Transient analysis of dam– reservoir interaction including the reservoir bottom effects”. Journal of Fluids and Structures, 20: 1073-1084 (2005).

L. Hu and J. Pu. “Testing and Modeling Of Soil Structure Interface“. Journal of Geotechnical and Geoenvironmental Engineering. Vol. 130 No. 8 (2004).

L. Jingbo and L. Yandong. “A Direct Method for Analysis of Dynamic Soil Structure Interaction Based on Interface Idea“. Elsevier, (1998).

L. Menglin and W. Jingning. “Effects of Soil Structure Interaction on Structural Vibration Control“. Elsevier, (1998).

L.E. Garcia and A. Sozen. “Multiple degrees of freedom structural dynamics. Purdue University. Earthquake Engineering (2003).

Lee J. and Fenves G. L. “A plastic-damage concrete model for earthquake analysis of dams”. Earthquake Engineering and Structural Dynamics, 27: 937-956 (1998).

Li X., Romo M. P. O. and Aviles J. L. “Finite element analysis of dam reservoir systems using an exact far-boundary condition”. Computers & Structures, 60(5): 751-762 (1996).

M. A. Ghorbani and M. P. Khiavi. “Hydrodynamic Modeling of Infinite Reservoir using Finite Element Method“. World Academy of Science. Engineering and Technology 80, (2011).

M. A. Hariri-Ardebili, H. Mirzabozorg. “Reservoir Fluctuation Effects on Seismic Response of High Concrete Arch Dams Considering Material Nonlinearity“.Journal of Civil Engineering Research 1(1): 9-20 (2011).

M. A. L. Yaghin and M.A. Hesari. “Dynamic Analysis of The Arch Concrete Dam Under Earthquake Force With ABAQUS“. Journal on AppliedSciences 8 (15): 2648-2658, (2008).

M. Akkose and A. Bayraktar and A.A. Dumanoglu. “Reservoir Water Level Effects On Nonlinear Dynamic Response Of Arch Dam“. Journal of Fluids And Structures 24 pp 418-435 (2008).

M. Akkose, A. A. Dumanoglu and M. E. Tuna. “Investigation of Hydrodynamic Effects on Linear and Nonlinear Earthquake response of Arch Dams By The Lagrangian Approach“. Turkish J. Eng. Env. Sci. 28 pp 25-40 (2004).

M. Anghileri and L. M. L. Castelletti and M. Tirelli. “Fluid Structure Interaction of Water Filled Tanks During the Impact With the Ground“. International Journal of Impact Engineering 31 pp 235-254 (2005).

M. H. aminfar and H. Mafi-Kandi and H. Ahmadi. “Improving The Seismic Performance of Aarch Dams Using Segmentation -A Case Study of Karun 4 Arch Dam, Iran“. Journal of Engineering Science and Technology Vol. 6, No. 4 pp 397 – 410 (2011).

M. Kutanis and M. Elmas. “Non Linear Seismic Soil Structure Interaction Analysis Based On The Substructure Method In The Time Domaine“. Turk Journal Engin Environ Sci 25 pp 617-626 (2001).

M. Srbulov. “Geotechnical Earthquake Engineering“. Springer Science Business Media B.V. (2008).

M. Yahyai and M.Mirtaheri and M. Mahoutian and A. S. Daryan and M. A. Assareh. “Soil Structure Interaction between Two Adjacent Buildings under Earthquake Load“. American J. of Engineering and Applied Sciences 1 (2): 121-125, (2008).

M.A. Saadeghvaziri and A.R. Yazdani-Motlagh and S. Rashidi. “Effects of soil structure interaction on longitudinal seismic response of MSSS bridges“. Soil Dynamics and Earthquake Engineering 20 pp 231-242 (2000).

M.R.Kianoush and H. Mirzabozorg and M. Ghaemian. “Dynamic Analysis of Rectangular Liquid Containers In Three Dimensional Space“. Can. J. Civ. Eng. 33:501-507 (2006).

Matthias Preisig. “Nonlinear Finite Element Analysis of Dynamic Soil-Foundation-Structure Interaction“. Master thesis, University of California, Davis, (2005).

Mir R. A. and Taylor C. A. “An experimental investigation into earthquake induced failure of medium to low height concrete gravity dams”. Earthquake Engineering and Structural Dynamics, 24: pp 373-393 (1995).

Mir R. A. and Taylor C. A. “An investigation into the base sliding response of rigid concrete gravity dams to dynamic loading”. Earthquake Engineering and Structural Dynamics, 25 pp 79-98 (1996).

N. Bouaanani and P. Paultre and J. Proulx. “Dynamic Response of a Concrete Dam Impounding an Ice – Covered Reservoir: Part II. Parametric and Numerical Study“. Can. J. Civ. Eng. 31 pp 965-976 (2004).

O. A. Pekau and C. Yuzhu. “Failure Analysis of Fractured Dams During Earthquakes By DEM“. Engineering structures 26 pp 1483-1502 (2004).

O.C. Zienkiewicz and R.L. Taylor, The Finite Element Method, McGraw-Hill Co., London, 1989.

P. Leger, M. Boughoufalah. “Earthquake input mechanisms for time domain analysis of dam-foundation systems“. Engineering Structures, 11 pp 37-46, (1989).

P. M. V Riberio and C. A. E Melo and L. J. Pedroeo. “Semi- Analytical Solution of Dam Reservoir Interaction In The Fundamental Mode Shape, Mechanics Of Solids in Brazil“. ISBN 978-85-85769-43-7 (2009).

P. Marcelo Vieira Ribeiro, Carlos Augusto Elias Melo and Lineu José Pedroso, “Semi-analytical solution of dam-resevoir interaction in the fundamental mode shape”. Brazilian Society of Mechanical Sciences and Engineering, ISBN 978-85-85769-43-7 (2009).

Parrinello F. & Borino G. “Lagrangian finite element modelling of dam–fluid interaction: Accurate absorbing boundary conditions”. Computers and Structures, 85 pp 932–943 (2007).

Plizzari G., Waggoner F. and Saouma V. E. “Centrifuge modeling and analysis of concrete gravity dams”. Journal of Structural Engineering, 121(10): 1471-1479 (1991).

R. J. Allemang and D. L. Brown. Chapter 21. “Experimental Modal Analysis“. Harris’ Shock and Vibration Handbook, (2009).

R. Livaoglu and A. Dogangun. “Simplified Seismic Analysis Procedures For Elevated Tanks Considereing Fluid Structure Soil Interaction“. Journal of Fluids And Structures 22 421-439 (2006).

R. Livaoglua and A. Dogangun. “Effect of foundation embedment on seismic behavior of elevated tanks considering fluid–structure-soil interaction“. Soil Dynamics and Earthquake Engineering 27 pp 855–863 (2007).

R. Priscu, A. Popovici, D. Stematiu, C. Stere. “Earthquake Engineering for Large Dams“. 2nd revised ed., Editura Academiei and John Wiley & Sons, (1985).

R. W. Clough and J. Penzien. “Dynamics of Structures“, McGraw Hill, Ic, (1993).

Robert D. Blevins. “Formulas for natural frequency and mode shape”. Van Nostrand reinhold Company, New York, Book (2001).

S. Adhikari. “Damping Models for Structural Vibration“. PhD thesis, Trinity College, Cambridge, (2000).

S. Grange. “Modélisation simplifiée 3D de l’interaction sol-structure : application au génie parasismique“. Thèse de doctorat, Institut Polytechnique de Grenoble, (2008).

S. L Kramer. “Geotechnical Earthquake Engineering“. Prentice- Hall International Series In Civil Engineering and Engineering Mechanics, (1996).

S. Mitra and K.P. Sinhamahapatra. “2D Simulation Of Fluid Structure Interaction Using Finite Element Method“. Elsevier, Finite Elements in Analysis and Design 45 pp 52-59 (2008).

S. Sezer. “An Evaluation of ANSYS Contact Elements“. Master thesis. Louisiana State University and Agricultural and Mechanical College, (2005).

Saeed Moaveni. “Finite Element Analysis, theory and application with Ansys”. second edition, IE prentice hall, Book (1999).

Saini S. S., Bettess P. and Zienkiewicz O. C. “Coupled hydrodynamic response of concrete gravity dams using finite and infinite elements”. Earthquake Engineering and Structural Dynamics, 6: 363-374 (1978).

Sharan S. K. “Finite element analysis of unbounded and incompressible fluid domains”. International Journal for Numerical Methods in Engineering, 21: 1659-1669 (1985).

T. O. Florin, G. Sunai. “Evaluation of damping in dynamic analysis of structures“. International journal of mathematical models and methods in applied sciences, 2(4), (2010).

Taylor R. E. “A review of hydrodynamic load analysis for submerged structures excited by earthquakes”. Engineering Structures, 3: 131-139 (1981).

Tsai C. S. and Lee G. C. “Time-domain analyses of dam-reservoir system. II: Substructure method”. Journal of Engineering Mechanics, 117(9): 2007-2026 (1991).

V. Lotfi and R. Espandar. “An Investigation of Joints Behavior In Seismic Response of Arch Dams“. Electronic Journal of Structural Engineering, 1 (2002).

V. Lotfi. “Seismic Analysis of Concrete Gravity Dams By Decoupled Modal Approach In Time Domain“. Electronic Journal of Structural Engineering, 3 (2003).

V. Saouma, “MERLIN Theory Manual“, March 5, (2006).

W. Schutz and S. Wang. “Soil Structure Interaction Analysis In Frequency Domain Using Fixed Base Eigenvalues“. Elsevier, (1993).

W. Shiming and G. Gang. “Dynamic Soil Structure Interaction for High Rise Building“. Elsevier, (1998).

Wang Jiachun. “Influence of different boundary conditions on analysis of SSI” .18th International Conference on Structural Mechanics in Reactor Technology (SMiRT 18) Beijing, China, August 7-12, (2005).

Westergaard H. M. “Water pressure on dams during earthquakes”, ASCE Transactions, 98, 418-433(1931).

X. Zhixin and L. Heshan. “Dynamic Soil Structure Interaction on Layered Strata under Seismic Wave Incidence“. Elsevier, (1998).

Y. Kim and C. Yun. “A Spurious Free Four-node Displacement-Based Fluid Element For Fluid-Structure Interaction Analysis“. Engineering Structure, Vol 19, No 8, PP. 665-679, (1997).

Z. Chongbin. “Applications of Infinite Elements to Dynamic Soil Structure Interaction Problems“. Elsevier, (1998).

Z. Chuhan and W. Guanglun and C. Xinfeng. “A Coupling Model of FE-BE-IE-IBE for Nonlinear Layered Soil Structure Interactions“. Elsevier, (1998).

Z. Chuhan and X. Yanjie and J. Feng. “Effects of Soil Structure Interaction on Nonlinear Response of Arch Dams“. Elsevier, (1998).

Z. Chuhan and X. Yanjie and W. Guanglun and J. Feng. “Non Linear Seismic Response of Arch Dams With Contraction Joint Opening and Joint Reinforcement“. Earthquake Engineering and Structural Dynamics, 29: 1547-1566 (2000).